

**CREEP MODELLING OF GAS TURBINE BLADES USING  
THETA PROJECTION METHOD  
THROUGH  
ABAQUS USER SUBROUTINES**

**THESIS REPORT**

*Submitted by*

**CB.EN.P2DTE21018 - VARADHAYAMUNAN KK**

*In partial fulfillment for the award of the degree of*

**MASTER OF TECHNOLOGY IN  
DEFENCE TECHNOLOGY  
(AEROSPACE TECHNOLOGY)**

*Under the guidance of*

**Dr. A. R. SRIKRISHNAN**  
Vice Chairperson & Professor



**AMRITA SCHOOL OF ENGINEERING, COIMBATORE  
AMRITA VISHWA VIDYAPEETHAM  
COIMBATORE  
JUNE 2023**

**AMRITA VISHWA VIDYAPEETHAM**  
**AMRITA SCHOOL OF ENGINEERING, COIMBATORE 641112**

**BONAFIDE CERTIFICATE**

This is to certify that the thesis entitled '**CREEP MODELLING OF GAS TURBINE BLADES USING THETA PROJECTION METHOD THROUGH ABAQUS USER SUBROUTINES**' submitted by **VARADHAYAMUNAN KK** (CB.EN.P2DTE21018) in partial fulfilment of requirements for the award of the degree of Master of Technology in Defence Technology (specialized in Aerospace Technology), is a bonafide record of the work carried out under my internal supervision at the Amrita School of Engineering, Amritanagar, Coimbatore.

**Dr. A. R. SRIKRISHNAN**  
Vice Chairperson & Professor  
Department of Aerospace Engineering,  
Amrita School of Engineering,  
Amritanagar, Coimbatore.

This project was evaluated by us on:

INTERNAL EXAMINER

EXTERNAL EXAMINER

**AMRITA VISHWA VIDYAPEETHAM**  
**AMRITA SCHOOL OF ENGINEERING, COIMBATORE 641112**  
**DEPARTMENT OF AEROSPACE ENGINEERING**

**DECLARATION**

I, VaradhaYamunan KK (CB.EN.P2DTE21018), hereby declare that this project report entitled, **CREEP MODELLING OF GAS TURBINE BLADES USING THETA PROJECTION METHOD THROUGH ABAQUS USER SUBROUTINES**, is a record of original work done by us under the guidance of, Dr. A. R. Srikrishnan, Vice Chairperson & Professor, Department of Aerospace Engineering, Amrita School of Engineering, Coimbatore. This work has not formed the basis of any degree/diploma/fellowship or a similar award to any candidate in any university, to the best of our knowledge.

VaradhaYamunan KK : :

Place: Coimbatore

Date:

**COUNTERSIGNED**

**Dr. A. R Srikrishnan**

Vice Chairperson & Professor,  
Department of Aerospace Engineering,  
Amrita School of Engineering,  
Amritanagar, Coimbatore - 641112

**Dr. V. Sivakumar,**

Chairperson & Professor,  
Department of Aerospace Engineering,  
Amrita School of Engineering,  
Amrita Nagar, Coimbatore - 641112

## **I. ACKNOWLEDGEMENT**

I would like to express my gratitude to my parent institution - Amrita Vishwa Vidyapeetham, Coimbatore and Gas Turbine Research Establishment (GTRE), Bengaluru for providing me an opportunity to do this project as a part of my master's degree dissertation work.

I am very much indebted to the academic guidance of Dr. A. R. Srikrishnan, Department of Aerospace, Amrita Vishwa Vidyapeetham and the technical guidance of Shri Rajesh Kumar, Sc – F, Structure Integrated Mechanics (SIMA), GTRE who not only emphasized the scope & importance of the work but also constantly mentored and motivated me throughout the entire span of project.

This endeavor would not have been possible without the professional guidance of Shri Ranjith Gopi, Dassault Systems Simulia Corp. whose inputs on Abaqus & finite element analysis techniques were very resourceful towards executing the project.

Words cannot express my gratitude to my beloved wife Sujana for providing me with constant emotional support as well as technical support in compiling & debugging the Fortran code time to time. My sincere thanks to my parents and all my friends whose goodwill indirectly added values to the project.

## II. TABLE OF CONTENTS

<b>I. ACKNOWLEDGEMENT .....</b>	<b>3</b>
<b>II. TABLE OF CONTENTS .....</b>	<b>4</b>
<b>III. LIST OF FIGURES .....</b>	<b>8</b>
<b>IV. LIST OF GRAPHS.....</b>	<b>9</b>
<b>V. LIST OF TABLES .....</b>	<b>11</b>
<b>VI. ABSTRACT .....</b>	<b>12</b>
<b>VII. CHAPTERS.....</b>	<b>13</b>
1. PROJECT BACKGROUND .....	13
1.1. GAS TURBINE FAILURE MODES .....	13
2. INTRODUCTION TO CREEP .....	15
2.1. CREEP CURVE & STAGES OF CREEP .....	15
2.2. CREEP BEHAVIOR OF ENGINEERING MATERIALS .....	16
2.2.1. TYPES OF CREEP CURVES .....	16
2.3. FACTORS AFFECTING CREEP .....	17
2.3.1. EFFECT OF STRESS & TEMPERATURE.....	18
2.3.2. EFFECT OF MICROSTRUCTURE.....	18
2.4. MICRO-MECHANISMS OF CREEP .....	18
2.4.1. DIFFUSION.....	19
2.4.2. DISLOCATION .....	19
2.5. BARRIERS TO DISLOCATION MOTION.....	21
2.6. DISLOCATION HARDENING .....	21
2.7. RECOVERY (or) SOFTENING.....	22
2.8. DAMAGE .....	22
2.9. CREEP STRAIN RATE .....	23
2.10. CREEP RATE CONTROLLING MECHANISMS.....	25
2.10.1. NABARRO – HERRING CREEP MECHANISM.....	26
2.10.2. COBLE CREEP MECHANISM.....	26
2.10.3. HARPER DORN CREEP MECHANISM.....	27
2.10.4. GRAIN BOUNDARY SLIDING MECHANISM .....	27
2.10.5. VISCOUS GLIDE CREEP MECHANISM.....	27
2.10.6. POWER LAW CREEP MECHANISM .....	28
2.10.7. POWER LAW BREAKDOWN MECHANISM .....	28
2.11. TRANSITIONS IN CREEP MECHANISMS .....	28
2.11.1. ARRHENIUS PLOT .....	30
2.11.2. MECHANISMS IN SERIES & PARALLEL .....	31

2.12. CREEP BEHAVIOUR OF SUPERALLOYS .....	31
2.12.1. PARTICLE STRENGHTENED ALLOYS .....	33
2.12.2. SINGLE CRYSTAL SUPERALLOYS .....	33
3. CREEP LIFE ESTIMATION .....	35
3.1. EXPERIMENTAL CREEP TEST .....	35
3.2. CREEP LIFE EXTRAPOLATION METHODS .....	37
3.2.1. STEADY STATE CREEP LIFE APPROACH .....	37
3.2.2. LARSON MILLER METHOD .....	38
3.2.3. MONKMAN GRANT APPROACH .....	38
4. CREEP MODELS .....	40
4.1. BASIC CREEP MODELS .....	40
4.1.1. NORTON'S POWER LAW MODEL .....	40
4.1.2. NORTON BAILEY'S TIME HARDENING MODEL .....	41
4.1.3. NORTON BAILEY'S STRAIN HARDENING MODEL .....	41
4.1.4. HYPERBOLIC SINE LAW MODEL .....	41
4.2. CONTINUUM DAMAGE MECHANICS MODELS .....	42
4.2.1. KACHANOV-RABOTNOV MODEL .....	42
4.2.2. OMEGA METHOD .....	43
4.2.3. LIU – MURAKAMI MODEL .....	44
4.2.4. DYSON MODEL .....	44
4.2.5. THETA PROJECTION METHOD .....	45
4.3. VISCOPLASTICITY MODELS .....	46
4.3.1. CHABOCHE UNIFIED VISCO-PLASTICITY MODEL .....	46
4.4. CREEP MODELS IN CAE TOOLS .....	47
5. LITERATURE REVIEW .....	48
5.1. LITERATURE REVIEW - SUMMARY .....	51
6. PROJECT SCOPE & OBJECTIVES .....	53
6.1. AIM .....	53
6.2. OBJECTIVES .....	53
6.3. SCOPE .....	53
7. REFERENCE MATERIAL .....	54
7.1. MATERIAL PROPERTIES .....	54
7.2. EXPERIMENTAL CREEP DATA .....	54
8. REVIEW OF POWER LAW CREEP .....	57
8.1. POWER LAW CONSTANTS CALCULATION .....	57
8.1.2. POWER LAW CREEP - ANALYSIS .....	60
8.2. POWER LAW CREEP - RESULTS .....	61
8.2.1. POWER LAW CREEP ANALYSIS - INFERENCE .....	61
9. THETA PROJECTION METHOD .....	63

9.1. THETA COEFFICIENTS CALCULATION .....	63
9.1.1. GOODNESS OF FIT .....	65
9.1.2. THETA COEFFICIENT RESULTS .....	65
9.2. MATERIAL CONSTANTS CALCULATION .....	66
9.2.1. UNIQUE SOLUTION .....	67
9.2.2. LEAST SQUARE REGRESSION SOLUTION .....	68
9.2.3. MATERIAL CONSTANT RESULTS .....	70
9.3. FRACTURE STRAIN FORMULATION .....	71
9.3.1. FRACTURE STRAIN CONSTANT CALCULATION .....	71
9.3.2. FRACTURE STRAIN CONSTANT RESULTS .....	71
9.4. CONSTITUTIVE EQUATIONS .....	72
9.5. ABAQUS USER SUBROUTINE.....	76
9.5.1. SUBROUTINE TERMINOLOGIES .....	78
9.5.2. EQUATIONS FOR SUBROUTINE .....	82
9.5.3. SUBROUTINE – FORTRAN CODE .....	84
9.5.4. SUBROUTINE – EXPLANATION .....	87
<b>VIII. RESULTS AND DISCUSSION.....</b>	<b>95</b>
10. CODE VALIDATION – TEST CASES .....	95
10.1. TEST CASE 1 - RECTANGULAR PLATE .....	95
10.1.1. TEST CASE 1 – ANALYSIS DATA .....	95
10.1.2. TEST CASE 1 – RESULTS.....	97
10.1.3. COMPARISON WITH POWER LAW CREEP.....	100
10.2. TEST CASE 2 – PROCEDURE VALIDATION .....	101
10.2.1. VERIFICATION OF THETA COEFFICIENTS:.....	102
10.2.2. TEST CASE 2 – ANALYSIS DATA .....	102
10.2.3. TEST CASE 2 – RESULTS.....	103
10.3. TEST CASE 3 - RECTANGULAR BAR .....	104
10.3.1. TEST CASE 3 – ANALYSIS DATA .....	104
10.3.2. TEST CASE 3 – RESULTS.....	104
10.4. TEST CASE 4 – SECTOR .....	107
10.4.1. TEST CASE 4 – ANALYSIS DATA .....	107
10.4.2. BOUNDS FOR APPLIED LOAD .....	108
10.4.3. TEST CASE 4 – RESULTS.....	109
10.5. TEST CASE 5 – SECTOR + TEMPERATURE FIELD.....	116
10.5.1. TEST CASE 5 – ANALYSIS DATA .....	116
10.5.2. TEST CASE 5 – RESULTS.....	116
10.6. TEST CASE 6 – TURBINE BLISK .....	120
10.6.1. TEST CASE 6 – ANALYSIS DATA .....	120
10.6.2. TEST CASE 6 – RESULTS – 10,000 RPM .....	124

10.6.3. CREEP LIFE ESTIMATION – CASE 1 .....	129
10.7. TEST CASE 7 – TURBINE BLISK CASE 2.....	131
10.7.1. TEST CASE 7 – ANALYSIS DATA .....	132
10.7.2. TEST CASE 7 – RESULTS – 10,000 RPM .....	135
10.7.3. CREEP LIFE ESTIMATION – CASE 2 .....	140
11. ACCURACY & ROBUSTNESS OF MODEL.....	142
11.1. ERRORS IN CREEP PREDICTION.....	142
11.2. ANALYSIS OF VARIANCES.....	143
11.2.1. AUTOCORRELATION .....	143
11.3. ROBUST CURVE FITTING.....	144
11.3.1. ROBUST CURVE FITTING – MATLAB CODE .....	146
11.3.2. ROBUST CURVE FITTING - RESULTS .....	147
11.4. IMPROVING RANGE OF ANALYSIS .....	148
11.5. ROBUST WEIGHTING SCHEME.....	149
11.5.1. ROBUST WEIGHTING – MATLAB CODE .....	152
11.5.2. ROBUST WEIGHTING - RESULTS .....	152
11.6. ACCURACY – MATERIAL CONSTANTS .....	152
11.6.1. ACCURACY – UNIQUE SOLUTION .....	153
11.6.2. ACCURACY – LEAST SQUARE SOLUTION .....	153
11.6.3. ACCURACY – ROBUST SOLUTION .....	154
11.7. ACCURACY – CREEP PREDICTION .....	154
11.7.1. ACCURACY AT DESIGN POINTS.....	154
11.7.2. ACCURACY AT INTERPOLATED LOADS .....	155
11.7.3. ACCURACY AT EXTRAPOLATED LOADS .....	155
11.8. EFFECT OF TIME INCREMENT ON ACCURACY .....	157
<b>IX. FUTURE WORK.....</b>	<b>157</b>
<b>X. CONCLUSION.....</b>	<b>158</b>
<b>XI. REFERENCES .....</b>	<b>159</b>

### III. LIST OF FIGURES

Figure 1.1.1 - Creep failure in LPT stage 1 blades of a CFM-56 Engine.....	13
Figure 2.4.1 - Schematic of diffusion processes .....	19
Figure 2.4.2 - Schematic of dislocation glide process .....	20
Figure 2.4.3 - Schematic of dislocation climb process .....	20
Figure 2.6.1 - Internal stress field around dislocation .....	21
Figure 2.7.1 - Annihilation of dislocation.....	22
Figure 2.7.2 - Recrystallization and grain growth .....	22
Figure 2.8.1 - Schematic of damage micro-mechanisms .....	23
Figure 2.8.2 - Crack formation & propagation in HK30 cast steel.....	23
Figure 2.10.1 - Nabarro - Herring Creep & Coble Creep Mechanisms.....	26
Figure 2.10.2 - Grain switching .....	27
Figure 2.10.3 - Schematic of grain boundary sliding.....	27
Figure 2.11.1 - Ashby map of pure nickel .....	29
Figure 2.11.2 - Ashby map of MAR-M200 superalloy .....	30
Figure 3.1.1 - Schematic of Uniaxial Tensile Creep Test.....	36
Figure 7.1.1 - MAR-247 Superalloy composition .....	54
Figure 8.1.1 - Conventional creep test specimen .....	60
Figure 8.1.2 - Test specimen Mesh & Quality metrics .....	60
Figure 8.1.3 - Creep test specimen - Boundary conditions.....	60
Figure 8.2.1 - Power law results - Von Mises Stress at 130 hrs .....	61
Figure 8.2.2 - Power law results - Equivalent creep strain at 130 hrs .....	61
Figure 9.1.1 - MATLAB CurveFit Tool .....	64
Figure 9.1.2 - CurveFit results .....	65
Figure 9.2.1 - MATLAB Code - Unique solution .....	68
Figure 9.2.2 - MATLAB Code - Least square solution .....	69
Figure 9.3.1 - MATLAB code for fracture strain constants .....	72
Figure 9.5.1 - Abaqus User Subroutine Flow .....	78
Figure 10.1.1 - Mesh - Test case 1 .....	95
Figure 10.1.2 - Boundary condition - Test case 1 .....	96
Figure 10.1.3 - Von Mises Stress - Rectangular Plate - 800 degC & 550 MPa.....	97
Figure 10.1.4 – Equiv. creep strain - Rectangular Plate - 800 degC & 550 MPa.....	98
Figure 10.3.1 - Boundary conditions - Test case - 3 .....	104
Figure 10.3.2 - Mesh - Test case - 3 .....	104
Figure 10.3.3 - Von Mises Stress - Test case 3 - Rectangular bar.....	105
Figure 10.3.4 - Equivalent creep strain – Rectangular bar - 800degC & 550MPa.....	105
Figure 10.4.1 - Boundary conditions and Mesh - Test case 4 - Sector .....	107
Figure 10.4.2 - Radial and hoop stress components in a hollow disc .....	108
Figure 10.4.3 - Von Mises Stress - Test case - 4 - Sector.....	109
Figure 10.4.4 - Stress components before creep - Test case 4 - Sector .....	109
Figure 10.4.5 - Stress components after creep - Test case 4 - Sector .....	110
Figure 10.4.6 - Equivalent creep strain – Sector - 800 degC & 10,000 RPM .....	111
Figure 10.4.7 - Creep Strain Components - Sector - 800 degC & 10,000 RPM .....	111
Figure 10.4.8 - Damage - Element deletion exceeding fracture strain .....	115
Figure 10.5.1 - Temperature field for test case 5 .....	116
Figure 10.5.2 - Von Mises Stress distribution - Test case 5 .....	117

Figure 10.5.3 - Creep strain distribution - 5000 & 6000 RPM .....	117
Figure 10.5.4 - Creep strain distribution - 8000 & 10000 RPM .....	117
Figure 10.6.1 - Turbine blisk Geometry & Partition for meshing .....	120
Figure 10.6.2 - Boundary conditions - Turbine blisk.....	121
Figure 10.6.3 - Mesh - Turbine blisk .....	121
Figure 10.6.4 - Mesh quality metrics - Turbine blisk .....	121
Figure 10.6.5 - Material properties - inputs in Abaqus.....	122
Figure 10.6.6 - Creep analysis - solution settings.....	123
Figure 10.6.7 - Field output settings .....	123
Figure 10.6.8 - Job settings .....	123
Figure 10.6.9 - Von Mises Stress distribution - Turbine blisk - 10,000 RPM.....	124
Figure 10.6.10 - Stress components before & after creep damage .....	124
Figure 10.6.11 - Deformation before and after creep damage .....	126
Figure 10.6.12 - Equivalent creep strain - 10,000 RPM - 19 hours.....	127
Figure 10.6.13 - Creep strain components - 10,000 RPM – 19 hours .....	127
Figure 10.6.14 - Stress & Creep strain - at different RPMs.....	129
Figure 10.6.15 - Result showing only 2% creep strain elements - 10,000 RPM.....	131
Figure 10.7.1 - Temperature field - Test case 7 .....	132
Figure 10.7.2 - Mesh - Test case 7.....	132
Figure 10.7.3 - Quality metrics - Test case 7 .....	132
Figure 10.7.4 - Material Properties - Test case 7 .....	133
Figure 10.7.5 - Creep analysis - solution settings.....	133
Figure 10.7.6 - Field output settings .....	133
Figure 10.7.7 - Job settings - Test case 7 .....	134
Figure 10.7.8 - Von Mises Stress - Test case 7.....	135
Figure 10.7.9 - Stress components - Test case 7 .....	135
Figure 10.7.10 - Deformation before & after creep damage.....	137
Figure 10.7.11 - Equivalent creep strain - 10,000 RPM – 10.6 hours .....	138
Figure 10.7.12 - Creep strain components - 10,000 RPM – 11 hours .....	138
Figure 10.7.13 - Stress & Creep strain - at different RPMs.....	140
Figure 11.3.1 - MATLAB code for Robust curve fitting.....	146
Figure 11.3.2 - Robust CurveFit output from MATLAB code.....	147
Figure 11.5.1 - MATLAB code for Robust weighted regression .....	152

## IV. LIST OF GRAPHS

Graph 2.1.1 - Typical creep curve .....	15
Graph 2.2.1 - Types of Creep curves .....	17
Graph 2.3.1 - Effect of Temperature & Stress on creep .....	18
Graph 2.9.1 - Creep rate curve at constant stress & temperature .....	24
Graph 2.9.2 - Exhaustion or Logarithmic creep .....	25
Graph 2.10.1 - Viscous glide mechanism .....	28
Graph 2.11.1 - Arrhenius plot.....	31
Graph 2.12.1 - Yield strength anomaly in MAR-M200.....	33
Graph 3.1.1 - Typical Experimental Creep Test data .....	36
Graph 3.2.1 - Steady state creep rate projection .....	37
Graph 3.2.2 - LMP Master Curve and LMP Vs Stress for Astroloy .....	38

Graph 3.2.3 - Monkman - Grant Ductility criteria.....	39
Graph 7.1.1 - MAR-247 Young's modulus Vs. Temperature .....	54
Graph 7.2.1 - Experimental Creep Curves of MAR-247 .....	55
Graph 7.2.2 - MAR-247 - Min creep rate & time to fracture Vs Applied stress .....	56
Graph 8.1.1 - Creep strain rate Vs Stress – 800 degC .....	58
Graph 8.2.1 - Creep Strain Vs Time - Power law Vs Experimental Results .....	62
Graph 8.2.1 - Physical interpretation of Theta coefficients .....	63
Graph 9.2.1 - Variation of Theta Coefficients with applied uniaxial stress .....	66
Graph 9.3.1 - Time to fracture Vs Stress & Temperature.....	71
Graph 10.1.1 - Stress Vs Time - Rectangular Plate - 800 degC & 550 MPa.....	97
Graph 10.1.2 - Creep strain Vs Time - Rectangular Plate - 800 degC & 550 MPa.....	98
Graph 10.1.3 - Hardening - Rectangular Plate - 800 degC & 550 MPa .....	99
Graph 10.1.4 - Recovery - Rectangular Plate - 800 degC & 550 MPa.....	99
Graph 10.1.5 - Damage - Rectangular Plate - 800 degC & 550 MPa.....	99
Graph 10.1.6 - Creep Strain Result - Comparison with power law .....	100
Graph 10.2.1 - Experimental Creep Curves - GH-4169 .....	101
Graph 10.2.2 - Creep curve - GH-4169 - Experimental Vs Theta projection results .....	103
Graph 10.3.1 - Stress History - Test case - 3 - Rectangular Bar.....	105
Graph 10.3.2 - Creep strain Vs Time - Rectangular Bar - 800 degC & 550 MPa .....	106
Graph 10.3.3 - Hardening - Rectangular bar - 800 degC & 550 MPa .....	106
Graph 10.3.4 - Recovery - Rectangular bar - 800 degC & 550 MPa.....	106
Graph 10.3.5 - Damage - Rectangular bar - 800 degC & 550 MPa.....	107
Graph 10.4.1 - Stress components Vs Time - on high strain element .....	110
Graph 10.4.2 - Stress components Vs Time - on low strain element.....	111
Graph 10.4.3 - Sector - Creep strain components Vs time – High strain element.....	112
Graph 10.4.4 - Creep strain components Vs time – Low strain element .....	112
Graph 10.4.5 - Creep curve result - Elements on outer & inner faces .....	113
Graph 10.4.6 - Hardening behaviour - Element on inner & outer faces .....	113
Graph 10.4.7 - Recovery behaviour - Element on inner & outer faces .....	114
Graph 10.4.8 - Damage behaviour - Elements on inner & outer faces .....	114
Graph 10.4.9 - Creep Strain Vs RPM - Sector.....	115
Graph 10.5.1 - Creep strain Vs Time - Sector - 10000 RPM.....	118
Graph 10.5.2 - Creep strain Vs Time - Sector - 8000 RPM.....	118
Graph 10.5.3 - Creep strain Vs Time - Sector - 6000 RPM.....	119
Graph 10.5.4 - Creep strain Vs Time - Sector - 5000 RPM.....	119
Graph 10.6.1 - Von Mises Stress - Time history .....	125
Graph 10.6.2 - Creep curve results - 10,000 RPM.....	127
Graph 10.6.3 - Hardening curve - Turbine blisk - 10,000 RPM – 19 hours .....	128
Graph 10.6.4 - Recovery curve - Turbine blisk - 10,000 RPM – 19 hours.....	128
Graph 10.6.5 - Damage curve - Turbine blisk - 10,000 RPM – 19 hours.....	129
Graph 10.6.6 - Creep Life Vs RPM .....	130
Graph 10.7.1 - Time history of Von Mises Stress .....	136
Graph 10.7.2 - Creep curve results - 10,000 RPM.....	138
Graph 10.7.3 - Time history of creep components .....	139
Graph 10.7.4 - Hardening curve .....	139
Graph 10.7.5 - Recovery curve .....	139

Graph 10.7.6 - Damage curve .....	139
Graph 10.7.7 - Creep Life Vs RPM - Test case 7 .....	140
Graph 11.2.1 - Variances Vs Time .....	143
Graph 11.2.2 - Auto-correlation of errors .....	144
Graph 11.4.1 - Theta coefficients Vs Stress at 800 degC .....	148
Graph 11.4.2 - Theta coefficients Vs Stress at 900 and 950 degC .....	149
Graph 11.7.1 - Accuracy at design points.....	155
Graph 11.7.2 - Accuracy at interpolated loads .....	155
Graph 11.7.3 - Accuracy for short time extrapolation .....	156
Graph 11.7.4 - Accuracy for long time extrapolation.....	156
Graph 11.8.1 - Effect of time increment size on accuracy.....	157

## V. LIST OF TABLES

Table 2.10.1 - Rate controlling mechanisms in creep.....	26
Table 2.12.1 - Superalloy - Typical composition .....	31
Table 4.4.1 - Creep models in commercial CAE tools .....	47
Table 7.2.1 - MAR-247 Experimental data on min creep rate & fracture .....	55
Table 8.1.1 - Power law time hardening constant results .....	59
Table 8.1.2 - Power law Strain hardening constant results.....	59
Table 9.1.1 - Theta coefficient results .....	65
Table 9.2.1 - Material constants - Unique solution.....	70
Table 9.2.2 - Material constants - Least Square solution.....	70
Table 9.3.1 - Fracture strain constants results.....	72
Table 10.2.1 - Mechanical Properties - GH-4169.....	101
Table 10.2.2 - Material constant results - GH-4169 .....	102
Table 10.2.3 - Material constants verification summary .....	102
Table 10.4.1 - Stresses in hollow rotating disc Vs RPM .....	108
Table 11.3.1 - Robust curve fitting results.....	147
Table 11.5.1 - Weights, weighted stress & temperature for 11 load cases .....	151
Table 11.5.2 - Variances & weights for 11 load cases.....	151
Table 11.5.3 - Material constants - Robust weighted .....	152
Table 11.6.1 - Accuracy - Unique solution.....	153
Table 11.6.2 - Accuracy - Least square solution .....	153
Table 11.6.3 - Accuracy - Robust weighting .....	154

## VI. ABSTRACT

Creep is one of the most significant failure modes in gas turbine components where the working temperature and stresses are high for prolonged period of time. Existing creep models in commercial analysis softwares like Abaqus are not adequate to model all stages of creep namely – primary, secondary and tertiary stages. ‘*Theta projection method*’ is a convenient method proven to predict all stages of creep, especially tertiary stage where strain rates are high leading to internal damage and fracture.

The aim of the project is to develop a user subroutine for Abaqus to model creep in gas turbine components using Theta projection method

The constitutive model for Theta projection method based on accumulation of internal state variables such as hardening, recovery and damage developed by (R.W.Evans, 1984) is adopted to compile a Fortran code for the user subroutine. The user subroutine is validated through several test cases and comparing the results with experimental creep data (Marie Kvapilova, 2018). Creep analysis of a sample gas turbine blade is then performed in Abaqus through the user subroutine and the results are interpreted.

Results of test cases validate the accuracy of Theta Projection Method in predicting all primary, secondary and tertiary stages of creep than existing creep models in Abaqus. Results at interpolated & extrapolated stress & temperature conditions with robust weighted least square regression material constants show the convenience in creep modelling with less input data than existing models. Results of creep analysis in sample gas turbine blade not only predicted the creep life but also indicated the internal damage accumulation.

Thus, creep modelling of gas turbine components through the user subroutine at different load conditions could lead us to more reliable creep life predictions and also indicate the regions of high creep strain for improvements in the early stages of design.

**Keywords:** Creep, Theta Projection Method, Creep damage, Creep fracture, Gas turbine blade, Creep life, MAR-247 superalloy, Abaqus, Creep modelling, power law creep, user subroutine, R.W.Evans.

## VII. CHAPTERS

### 1. PROJECT BACKGROUND

Gas turbine blades are the most critical components of turbojet or turbofan engines. Nearly 50% of jet engine failures are attributed to damage in turbine blades and discs<sup>1</sup> as they operate at highest stress & temperature conditions.

#### 1.1. GAS TURBINE FAILURE MODES

In a typical gas turbine blade, the maximum centrifugal stresses are near the root. However, several practical instances show failures occurring at other regions of blade where the stresses are less, well below the yield stress due to thermo-mechanical phenomena such as creep and fatigue. One such creep failure is shown in Figure 1.1.1. (Reference: ATSB investigation AO-2009-069).



*Figure 1.1.1 - Creep failure in LPT stage 1 blades of a CFM-56 Engine*

Most common failure modes<sup>2</sup> of gas turbine blades are as follows:

1. Creep
2. High & Low cycle fatigue
3. Oxidation / Erosion / Corrosion
4. Fluid – Structure interaction / acoustics
5. Foreign object damage, icing, blade-off, etc.

Out of all the failure modes, ‘Thermo-mechanical fracture’ phenomena such as Creep and fatigue are more significant for hot section of gas turbine engine as they operate at very high temperature & stresses for prolonged period of time.

Yet, there is a need for military jet engines to operate at highest possible turbine entry temperature (TET) to improve performance parameters like ‘Thrust-to-weight ratio’ and ‘isentropic efficiency’. However,

---

<sup>1</sup> R. K. Mishra et. al., “Investigation of HP Turbine Blade Failure in a Military Turbofan Engine” - International Journal of Turbo Jet Engine - 2015

<sup>2</sup> Poppy Puspitasari et. al. 2021 IOP Conf. Ser.: Mater. Sci. Eng. 1034 012156

increasing the operating temperature results in decrease in mechanical strength of the gas turbine blade material and the requirement of special temperature resistant alloys arises.

Nickel based ‘superalloys’ are proven to maintain exceptional mechanical properties like strength, toughness and resistance to corrosive degradation at higher temperatures. A lot of metallurgical & manufacturing advancements like directional solidification, single crystal casting technology, ceramic matrix composite technology, etc. has enabled us to maintain higher turbine entry temperature without significant loss of mechanical strength.

Turbine entry temperature of our indigenous Kaveri engine is around 1700 K<sup>3</sup>. Pratt & Whitney F135 which is a fourth-generation military turbofan engine has its turbine entry temperature of around 1850 – 1950 K which is very close to the melting point of super alloys<sup>4</sup>. Also, with recent advancements in cooling technologies like thermal barrier coating (TBC), turbine entry temperatures could reach as high as 2000K. With this trend of increasing turbine entry temperatures & engine RPMs, accurate prediction of creep life of gas turbine components becomes very essential.

The use of computer aided analysis software enables us to model creep life of gas turbine components in its early stages of development leading to better design life and reliability. This project aims to develop a reliable technique to predict creep life of gas turbine blades using commercial analysis software.

---

<sup>3</sup> Bulletin of Defence Research and Development Organization, October 2009, Vol. 17 No. 5 p.2

<sup>4</sup> Xu, L.; Sun, Z.; Ruan, Q.; Xi, L.; Gao, J.; Li, Y. Development Trend of Cooling Technology for Turbine Blades at Super-High Temperature of above 2000 K. Energies 2023, 16, 668.

## 2. INTRODUCTION TO CREEP

Creep is defined as the time-dependent progressive plastic deformation of a material when subjected to stress at elevated temperatures.

Creep phenomenon is significant when the operating temperature of the material is more than 40% of melting point of the material<sup>5</sup>. This ratio of operating temperature to melting point ( $T_m$ ) in absolute scale is called ‘homologous temperature’.

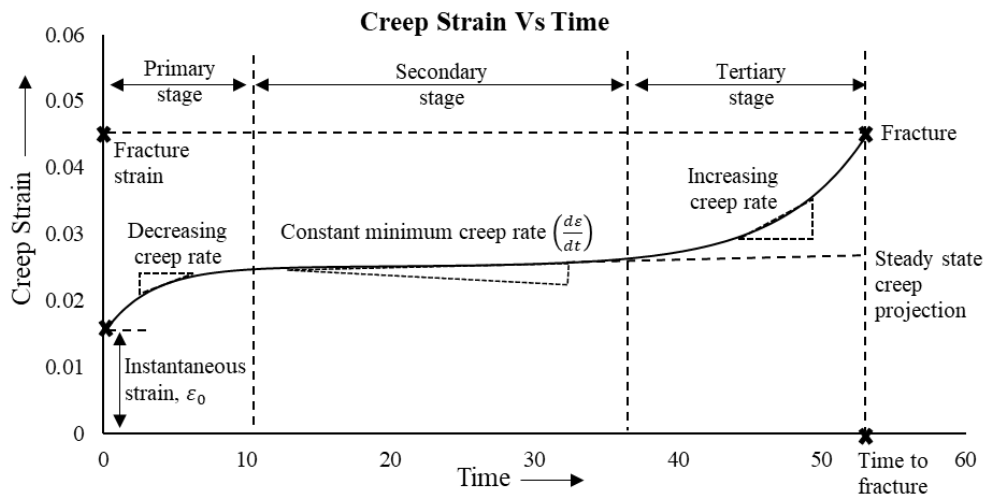
Whenever load is applied, materials undergo elastic deformation resulting in “initial strain” or “instantaneous strain”. At elevated temperatures, even at constant stress much lower than the yield strength, materials undergo plastic deformation due to microstructural changes resulting in plastic strain called “creep strain”. Rate of change of creep strain with respect to time is called “creep rate” ( $\dot{\epsilon}$ ). A graph of creep strain with respect to time is called a ‘creep curve’ as shown in Graph 2.1.1

### 2.1. CREEP CURVE & STAGES OF CREEP

In metals and alloys, creep curve is characterized by three stages namely,

1. Primary (or) Transient creep
2. Secondary (or) Steady state creep
3. Tertiary creep

Primary creep stage is the short initial stage characterized by decreasing creep rate. Secondary creep stage is longer with almost constant and minimum creep rate. Tertiary creep stage is relatively shorter characterized by steep increasing creep rate leading to ‘creep rupture’ or fracture.



Graph 2.1.1 - Typical creep curve

<sup>5</sup> N. Eswara Prasad and R.J.H. Wanhill (eds.), “Aerospace Materials and Material Technologies, Indian Institute of Metals Series”, DOI 10.1007/978-981-10-2143-5\_10, Springer, 2017

Strain value at fracture condition is called ‘fracture strain’ and time taken for fracture to occur is called ‘time to creep rupture’ or ‘time to fracture’. Instantaneous strain  $\varepsilon_0$  is almost elastic where creep strain  $\varepsilon_{cr}$  has both plastic and anelastic strain components. The anelastic creep strain component is recoverable where plastic strain component is permanently set in the material.

For most static applications like high temperature piping, power plant structures and pressure vessels where stresses are relatively low & constant with time, secondary (or) steady state creep stage is predominantly longer and time to reach fracture is very high to compute experimentally. In such cases, required creep life can be easily computed by projecting steady state creep slope linearly with time.

For dynamic applications like gas turbine components, tertiary stage is crucial as the strain rates increase steeply accelerating to damage and fracture. Consideration should be given in design of such components to make sure that creep does not reach the tertiary stage.

## 2.2. CREEP BEHAVIOR OF ENGINEERING MATERIALS

### 2.2.1. TYPES OF CREEP CURVES

Different materials show different creep behavior. Engineering materials are classified based on creep behaviour as two major types namely,

- Class I or Class A – Alloy type creep behavior
- Class II or Class M – Pure & annealed metal type creep behavior

Creep behaviour with time can be studied through the shape of creep curves which depends on the mechanism of creep exhibited in the material.

Four types of creep behaviour can be witnessed in engineering materials namely, Type A, Type B, Type C and Type D which are explained briefly below.

#### TYPE - A CURVE

- Typical creep curve with defined primary, secondary & tertiary stages
- Exhibited by class II or Class M alloys and annealed metals

#### TYPE - B CURVE

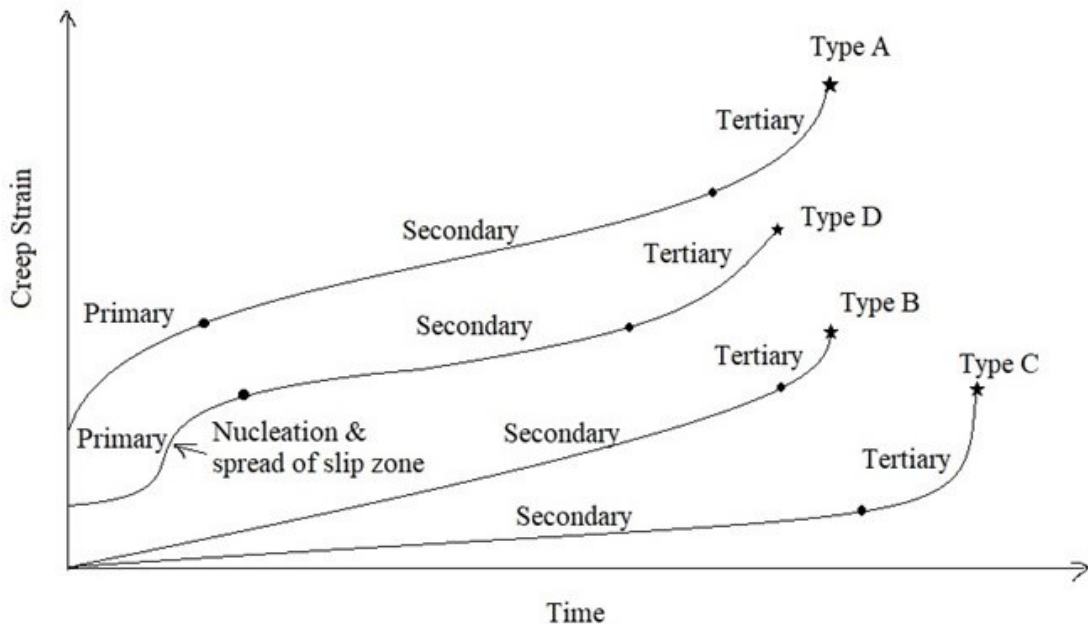
- Primary stage is insignificant
- Material reaches steady state very soon and secondary stage is longer
- Exhibited by Class I or Class A alloys

## TYPE - C CURVE

- Material is already in steady state and reaches tertiary slowly
- Primary stage is insignificant
- Exhibited by materials that are already crept at higher stress

## TYPE - D CURVE

- Sigmoid curve with sudden change in creep rates
- Nucleation and spread of slip zones in primary stage is observed
- Exhibited in dispersed phase alloys



Graph 2.2.1 - Types of Creep curves

## 2.3. FACTORS AFFECTING CREEP

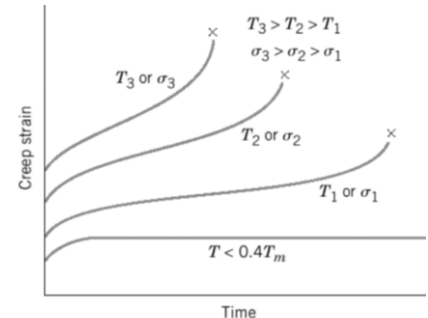
Most significant factors affecting creep in Class – I or Class – M materials (pure metals & alloys) are as follows:

- Temperature
- Applied stress
- Time
- Grain size, grain boundary characteristics, etc.
- Microstructure, dislocation density, stacking faults, etc.
- Concentration, relative size, interparticle spacing & atomic bonding between different phases and constituents in an alloy

### 2.3.1. EFFECT OF STRESS & TEMPERATURE

Creep strain follows exponential function of applied stress and temperature. With increase in temperature or stress, curve gets steeper and also following changes are observed:

- Instantaneous strain increases
- Steady state creep rate increases
- Time to failure decreases



**Graph 2.3.1 - Effect of Temperature & Stress on creep**

### 2.3.2. EFFECT OF MICROSTRUCTURE

Whenever an external stress is applied on a material, internal stresses are developed in the material. In an ideal material, internal stress is equal to the applied stress. In practical cases, due to the presence of grain boundaries, internal stresses are not equal to the applied stresses or flow stresses.

This effect of grain size on internal stresses is given by the ‘Hall-Petch equation’ which defines that internal stresses are inversely proportional to the square root of grain size. Generally plastic deformation rate increases with larger grain size.

However, at temperatures greater than ‘equicohesive temperature’ grain boundaries become weaker and Hall-Petch relation does not hold good.

Since creep phenomenon usually occurs at temperatures greater than equicohesive temperatures, creep strain rate is inversely proportional to the grain size.

Hence, larger grains (single crystal casting) are preferred over finer grain materials for better creep resistance.

## 2.4. MICRO-MECHANISMS OF CREEP

To understand creep better, it is necessary to have basic knowledge of crystal imperfections & associated micro-mechanisms in materials which are very briefly discussed in this section.

Creep behaviour is a result of interaction between three major microstructural phenomena namely,

1. Dislocation hardening (strain hardening)
2. Recovery (or) Softening
3. Damage

These phenomena occur due to two fundamental processes in a microstructure namely,

1. Diffusion
2. Dislocation

#### 2.4.1. DIFFUSION

Diffusion is the movement of atoms from their original lattice position to vacant spaces called “voids”. In the process, material is plastically deformed.

In pure metals and alloys with constituent atoms of similar size, when external stress is applied, atoms move and occupy any vacant site in the lattice called as vacancy diffusion.

In alloys when the relative sizes of constituent atoms differ, smaller atoms move and occupy the space between two lattices upon application of stress. This is called as interstitial diffusion.

An atom needs some external energy to break the chemical bonds with neighboring atoms and move across lattice which is called as “activation energy”.

This is provided by the kinetic temperature of the material. Externally applied stresses also generate stronger stress fields around vacancy sites which provide the activation energy for diffusion of atoms towards vacant or interstitial sites.

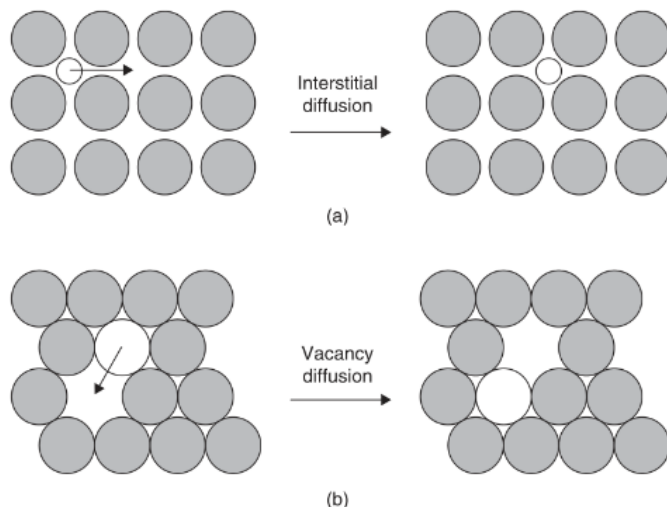


**Figure 2.4.1 - Schematic of diffusion processes**

Diffusion process is significant only at low applied stresses and high temperatures. Once the atoms diffuse and occupy more convenient sites, internal stress fields are minimized which reduces the rate of diffusion further. As a result, creep strain rate is low with linear stress dependance at constant high temperatures ( $\dot{\varepsilon} \propto \sigma$ ).

#### 2.4.2. DISLOCATION

Dislocations are line defects in which a half row of atoms are missing from their regular lattice position. Motion of dislocation across crystal lattice is called “slip”.

Dislocations tend to move across to more convenient lattice positions so as to minimize the internal stress field created due to externally applied stresses. In the process, material is plastically deformed. Dislocation motion along the direction of applied stress is called “glide”.

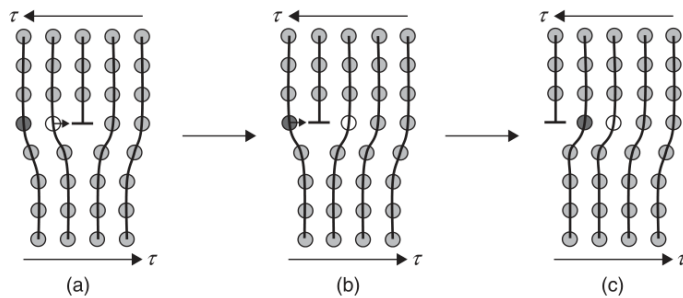


**Figure 2.4.2 - Schematic of dislocation glide process**

- External stress causes internal stress field around the dislocation in the middle
- Dislocation moves to adjacent row due to external applied stress
- Dislocation reaches grain periphery and cannot glide further. Surface crack forms

Dislocation motion normal to the direction of applied stress is called “climb”.

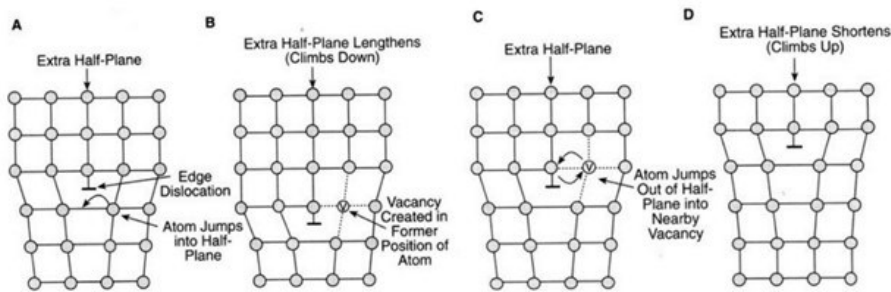


**Figure 2.4.3 - Schematic of dislocation climb process**

A & B - Atom from the row adjacent to dislocation jumps to dislocation row further lengthening the dislocation. Vacancy is created at the original site of jumped atom.

C & D - Atom from the dislocation row jumps to vacant site in the adjacent row further shortening the dislocation. Internal stress fields are reduced by this process.

Dislocation glide requires lesser activation energy than dislocation climb. Also strain rates are relatively lower and temperature assisted. Dislocation climb process requires more activation energy. The strain rates are relatively higher and stress assisted. Both the dislocation processes are significant at higher stresses and temperatures and are characterized by higher creep strain rates compared to diffusion processes.

Only those dislocations that are free to move will contribute towards strain rate and plastic deformation. Number of dislocations per unit volume is called ‘dislocation density’. Strain rate is directly proportional to the dislocation density of the material. Larger grain size will result in smaller dislocation density and smaller creep strain rate.

In the initial state, dislocation density is small and upon application of external stress, new dislocation sites are formed and the dislocation density increases increasing the creep strain rate exponentially. Hence,

creep strain rate increases exponentially with applied stress during dislocation process ( $\dot{\varepsilon} \propto \sigma^n$ , where  $n \sim 3$  to 10)

## 2.5. BARRIERS TO DISLOCATION MOTION

Dislocations cannot move freely to any position in the lattice due to the presence of ‘barriers’ such as,

- Vacancies & solutes in interstitial positions
- Dislocation intersection – jog & kink
- Stress fields of other dislocations
- Different orientation of grains across the grain boundary
- Presence of solute atoms
- Massive second phase particles
- Large incoherent precipitates, etc.

Energy required to overcome such barriers is called ‘dislocation energy’ which is provided by the kinetic temperature and applied external stress. Dislocation energy for motion within grains is lesser than motion across the grain boundaries.

As a result of the above micro-mechanisms, phenomena such as dislocation hardening, recovery and damage arise which are explained below.

## 2.6. DISLOCATION HARDENING

Dislocation hardening or strain hardening is the result of increase in resistance to dislocation motion.

Every dislocation has an internal stress field around it which is compressive around the extra half pair of atoms and tensile around the vacant half row in the lattice as shown in Figure 2.6.1.

This internal stress field around dislocation interact with any externally applied stress causing dislocation motion or slip towards convenient positions in the lattice like grain boundaries so as to create equilibrium and minimize or nullify the internal stress. The material is plastically strained during this process.

Once dislocations move to minimum energy levels, more and more activation energy is required to cause further dislocation motion. Dislocations at grain boundaries resist free movement of grains. Also, these dislocations have to overcome the barriers for further plastic deformation. These phenomena resist plastic deformation resulting in “strain hardening” or “dislocation hardening”

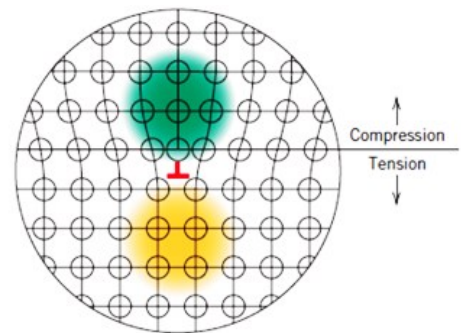


**Figure 2.6.1 - Internal stress field around dislocation**

## 2.7. RECOVERY (or) SOFTENING

Recovery is the process where material properties like which increased during strain hardening stage are recovered back to initial state.

Recovery happens due to rearrangement of atoms to minimum energy state. During hardening stage, material reaches a state where no more dislocation movement is possible without any external energy. Soon after this state, with some activation energy, dislocations are able to overcome the barriers and atoms start to rearrange across grain to lower strain energy positions. Recovery happens due to,

- Thermal diffusion of dislocated atoms to vacant sites
- Annihilation by movement of positive edge dislocation towards a negative edge dislocation site as illustrated in Figure 2.7.1.

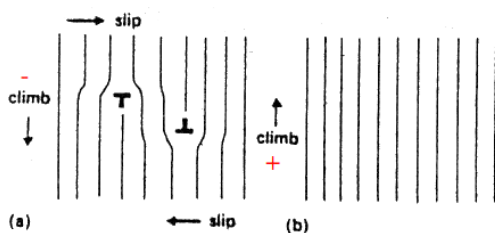


Figure 2.7.1 - Annihilation of dislocation

- Recrystallization - Rearrangement and formation of new strain free sub-grains and grain growth with reduced dislocation density as illustrated in Figure 2.7.2.

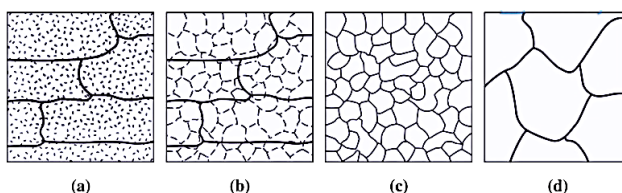


Figure 2.7.2 - Recrystallization and grain growth

- Grain Boundary Sliding (GBS) – Relative motion of grains along common boundaries along narrow zone to resist formation of voids at grain boundaries.

As a result of the above phenomena, dislocation density decreases, internal stress fields are minimized and the material properties are recovered. The material becomes soft and allows further plastic deformation.

## 2.8. DAMAGE

Damage is the process of progressive plastic deformation due to degradation of material properties, formation and growth of creep voids or cavities within the microstructure. Location of these voids are often observed to be at the junction of three or more grains and at non-metallic inclusions or precipitates.

Creep voids or cavitation develops on grain boundaries at low stresses and can nucleate at both grain boundaries and within the grains at high stresses.

The rate of void nucleation is strain dependent while growth rate due to diffusion or grain boundary sliding is governed by applied stress and concentration of precipitates.

Increasing dislocation density on the grain boundaries will lead to coalescence of smaller grain boundary cracks to form multiple boundary length cracks which will eventually cause failure as explained in Figure 2.8.2<sup>6</sup> and illustrated in a practical case of HK30 cast steel bar as shown in Figure 2.8.1<sup>7</sup>.

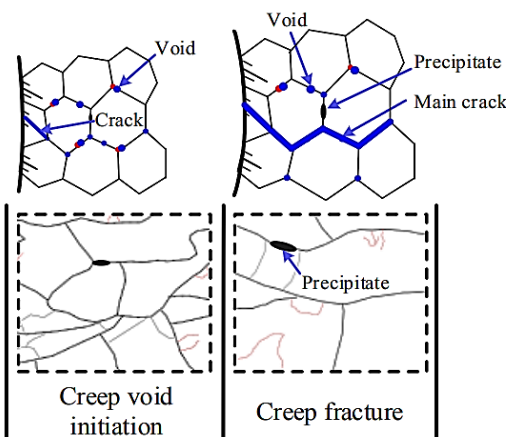


**Figure 2.8.2 - Schematic of damage micro-mechanisms**

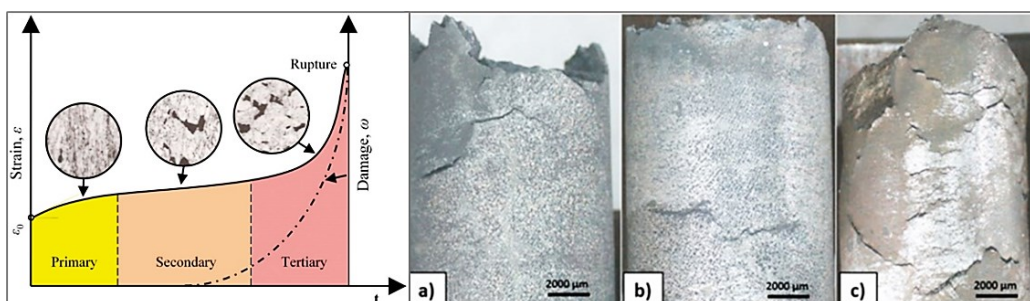


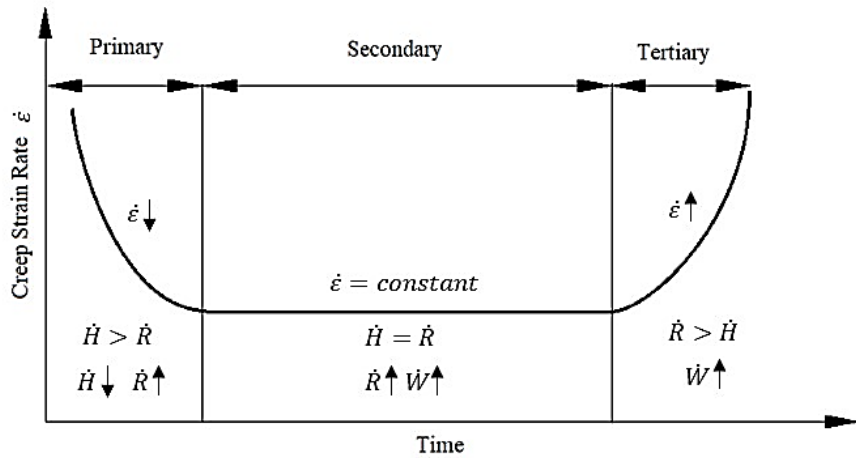
**Figure 2.8.1 - Crack formation & propagation in HK30 cast steel**

## 2.9. CREEP STRAIN RATE

Rate of change of creep strain with respect to time is controlled by the micro-mechanisms discussed in the previous section. Creep strain rate behaviour at different stages of creep with respect to these micro-mechanisms is illustrated in Graph 2.9.1.

<sup>6</sup> Wei Zhang et. al., “Microstructural damage mechanics-based model for creep fracture of 9%Cr steel under prior fatigue loading” Theoretical and Applied Fracture Mechanics, Volume 103, 2019

<sup>7</sup> Christian Öberg, Baohua Zhu, Stefan Jonsson, “Creep behaviour, creep damage and precipitation in the austenitic cast steel HK30 at 750 °C”



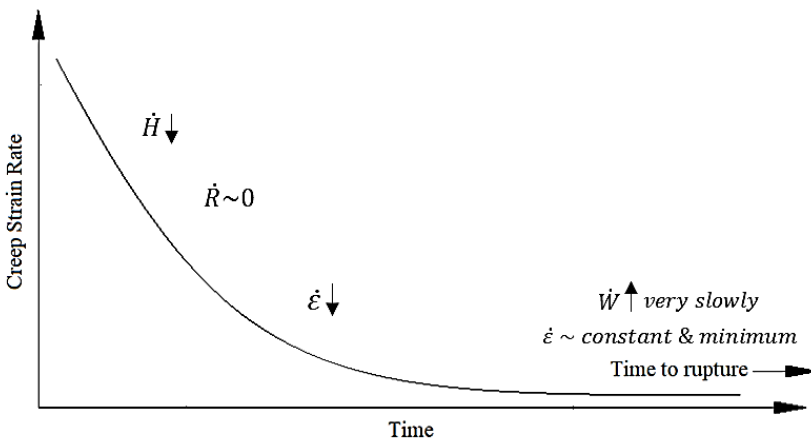
**Graph 2.9.1 - Creep rate curve at constant stress & temperature**

In the primary stage of creep, material is strained due to the presence of voids for diffusion & dislocation. As time progresses, motion of dislocation to minimum energy state enables the material to resist further deformation (harden) by allowing some plastic strain. As a result of this, creep strain rate gradually decreases to reach a minimum constant rate (steady state) during the secondary stage. Rate of hardening  $\dot{H}$  is directly proportional to the rate of straining whereas rate of recovery  $\dot{R}$  is bound only by microstructural properties and independent of strain. During the primary stage, rate of hardening is more than rate of recovery.

In the secondary stage, as the chances of further dislocation motion are reduced, a steady state is reached as rate of hardening  $\dot{H}$  becomes equal to the rate of recovery  $\dot{R}$  towards the end of primary stage. Hence creep strain rate is also minimum as the material is in minimum strain energy state and higher activation energies are required to cause plastic deformation in this steady state. But, with recrystallization and grain growth, voids & microcracks are also formed at some portion of the material as discussed in the previous section which accounts for damage initiation. Even though hardening rates and recovery rates are at equilibrium, damage is still accumulated very gradually in the material till the onset of tertiary stage.

In the tertiary stage, damage is the most dominant factor. Tertiary stage is characterized by lower rate of hardening and higher rate of recovery & damage. At the onset of tertiary stage, dislocation density at the grain boundaries is higher leading to grain boundary cracks due to processes such as grain boundary sliding. These micro-cracks coalesce together quickly resulting in increasing rate of damage which in turn results in increasing rate of creep strain leading to fracture.

At low temperatures, the activation energy for recovery is low. Material can still harden due to the applied stress as it strains. At constant applied stress, there comes a state where the applied stresses and the internal stress fields are almost in equilibrium and the material can no longer strain unless the temperature is increased. Failure is only due to damage which is accumulated very gradually. Time to creep fracture is very long as explained in Graph 2.9.2. This is called ‘Exhaustion creep’ or ‘Logarithmic creep’.



*Graph 2.9.2 - Exhaustion or Logarithmic creep*

## 2.10. CREEP RATE CONTROLLING MECHANISMS

Several formulations for creep strain rate have been developed based on the micro-mechanisms controlling creep, microstructural behaviour of materials and activation mechanisms. Notable formulations are the Andrade creep equation, Garofalo equation, extended Garofalo equation and logarithmic creep equation.

The formulation considering the most significant factors is as follows:

$$\dot{\epsilon} = Ad^{-p}\sigma^n e^{-\left(\frac{Q}{RT}\right)}$$

where,

$A$  – Proportionality constant

$d$  – Grain size

$p$  – Grain size exponent

$\sigma$  – Applied stress

$n$  – Stress exponent

$Q$  – Activation energy

$R$  – Universal gas constant

$T$  – Temperature in absolute scale

The values of  $p$ ,  $n$  and  $Q$  decide the rate controlling mechanism in creep. Most significant rate controlling mechanisms are listed in Table 2.10.1.

*Table 2.10.1 - Rate controlling mechanisms in creep*

S. No	Creep Mechanism	Stress exponent, n	Grain size exponent, p
1	Nabarro – Herring creep	1	2
2	Coble creep	1	3
3	Harper – Dorn creep	1	0
4	Grain Boundary Sliding	2	2
5	Viscous glide creep	3	0
6	Power law creep	4 - 7	0
7	Power law breakdown	> 7	-

Basics of each creep mechanism & its applicability is briefly explained in next section.

### 2.10.1. NABARRO – HERRING CREEP MECHANISM

Creep rate governing mechanism is the diffusion of vacancies upon application of externally applied stress from grain boundaries perpendicular to the direction of applied stress to grain boundaries parallel to the direction of applied stress, through the lattice. Direction of motion of atoms can be assumed to be opposite to the direction of motion of the vacancies.

Grains are elongated due to the motion of atoms towards boundaries perpendicular to applied stress as shown in Figure 2.10.1 (left). Finer grains will have more boundaries. Creep strain rate varies linearly with applied stress and varies inversely with the grain size. This mechanism is favored at high temperature & low stress condition.

### 2.10.2. COBLE CREEP MECHANISM

Coble creep mechanism is similar to Nabarro – Herring mechanism except that the movement of vacancies is across the grain boundaries as shown in Figure 2.10.1 (right). Activation energy for grain boundary diffusion is usually lesser than that of lattice diffusion. Hence coble creep is more sensitive to grain size.

This mechanism is favored at high temperature, low applied stress and finer grain sizes.

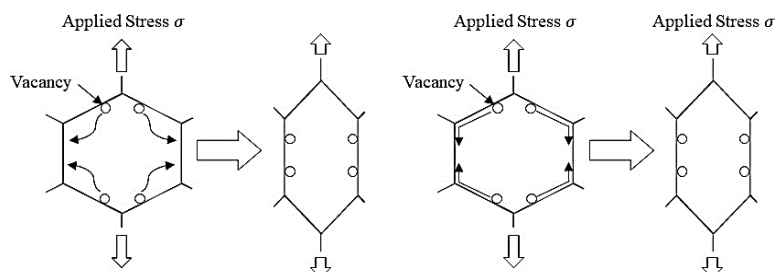


*Figure 2.10.1 - Nabarro - Herring Creep & Coble Creep Mechanisms*

### 2.10.3. HARPER DORN CREEP MECHANISM

In highly pure materials with large grain size, the dislocation density is very low initially. In such cases, creep strain rate is independent of grain size due to the lack of dislocations & grain boundaries. Creep strain varies linearly with applied stress.

This mechanism is favored at very high temperatures ( $T > 0.99 T_m$ ), low applied stress and large grain size.

### 2.10.4. GRAIN BOUNDARY SLIDING MECHANISM

Grain boundary sliding is the process of relative motion of grains along common boundaries. This is significantly observed in high angle grains where misorientation angle is greater than  $15^\circ$ . According to ‘Gifkin’s model’, all deformation occurs only in the mantle of grain and not in the core. Upon application of external stresses, as the material strains, voids are formed at grain boundaries. To minimize the stress field created by these voids, grain boundaries slide across and accommodate to low strain energy levels.

Accommodation by diffusion is explained by Lifshitz’s theory where grain neighbors switch to accommodate straining as explained in Figure 2.10.2. In the initial state, grain 1 and 4 are neighbors and after straining, grain 2 and 3 become neighbors.

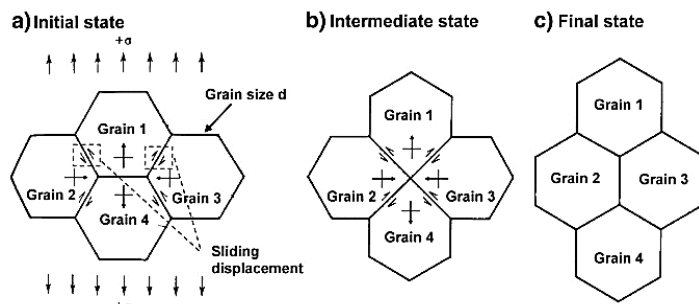


Figure 2.10.2 - Grain switching

Accommodation by glide and climb is explained by Rachinger’s theory where dislocations glide and climb across grain boundaries to avoid void formation at grain boundaries as explained in Figure 2.10.3.

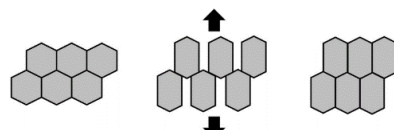


Figure 2.10.3 - Schematic of grain boundary sliding

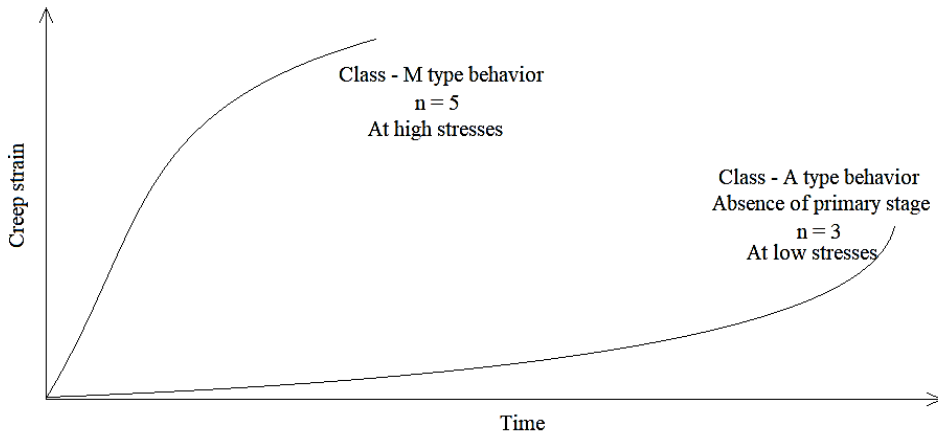
### 2.10.5. VISCOUS GLIDE CREEP MECHANISM

Viscous glide creep mechanism governs the creep rate in Class A type material (alloys) especially when the relative sizes of constituent atoms are different. Larger precipitates or solute atoms act as barrier and impede dislocation motion. Activation energy to overcome this barrier comes from “break-away stress” – minimum stress at which dislocations could break away from an impeding solute atom’s stress field.

For applied stress less than the break-away stress, the dislocations are impeded by solutes and the material shows Class-A (alloy) type behavior. Stress exponent is 3.

For applied stress greater than the break-away stress, the dislocations have enough activation energy to overcome the solute barrier and the material shows Class-M (pure metal) type behavior. Stress exponent, n becomes 5. This behavior also comes under power law creep regime.

This characteristic feature of this mechanism is the absence of primary creep stage as rate of hardening is very low due to the presence of solutes impeding dislocation motion.



*Graph 2.10.1 - Viscous glide mechanism*

#### 2.10.6. POWER LAW CREEP MECHANISM

At significantly higher stresses, both glide and climb processes occur and contribute to the total plastic deformation. Dislocation glide process governs the extent of strain( $\varepsilon$ ) whereas dislocation climb process governs the rate of strain( $\dot{\varepsilon}$ ). At such high stresses, creep rate becomes independent of grain size ( $p = 0$ ). This mechanism is applicable to Class – M type materials at considerably higher stresses.

#### 2.10.7. POWER LAW BREAKDOWN MECHANISM

Stress exponent ‘n’ increases with increase in applied stress. At very high applied stresses, the activation energy for dislocation to overcome barriers is readily available. In such cases, creep strain rate is only stress dependent.

### 2.11. TRANSITIONS IN CREEP MECHANISMS

Creep behaviour of materials differ with time due to transitions in different creep mechanisms operating at different conditions of stress, temperature and grain sizes. To understand the creep behavior of materials and infer reasonably from the creep curves, it is necessary to understand ‘Deformation Mechanism Map’ or ‘Ashby Map’ which is a plot of applied stress ( $\sigma$ ) normalized with shear strength (G) Vs homologous temperature ( $T/T_m$ ).

For illustration how different mechanisms operate at different temperature and stress conditions, Ashby maps<sup>8</sup> of pure nickel (Class – M) with 100  $\mu\text{m}$  grain size and MAR - M200 (Class – A) superalloy are illustrated below:

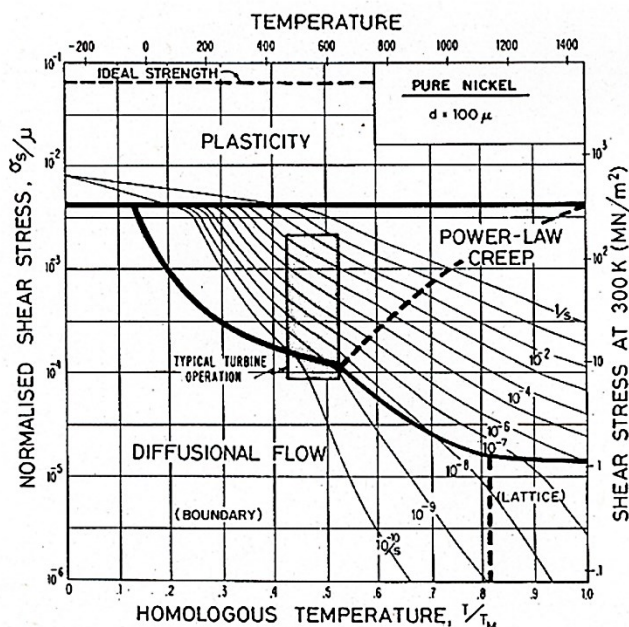


Figure 2.11.1 - Ashby map of pure nickel

At low stress & low temperature conditions, deformation starts from being elastic towards plastic deformation due to boundary diffusion creep with very low creep strain rate of the order  $10^{-10}/\text{s}$ . At low stress & high temperatures, the mechanism transits to lattice diffusion with increase in creep strain rate.

As both temperature and stress increases, the mechanism transits to power law with increasing strain rate and more stress dependence as dislocation processes take dominance.

Deformation mechanism map of nickel-based superalloy MAR-M200 of same grain size as pure nickel is illustrated in Figure 2.11.1.

Even though, the mechanisms are similar at low temperature and stress conditions, the superalloy exhibits lower creep rates relatively. Also, the envelope of power law creep regime is also reduced significantly to high temperature and high stress conditions than pure nickel. This indicates better creep resistance of superalloy.

Also, in Figure 2.11.2, on the right is the Ashby map of same superalloy with much larger grain size (1 cm). We can clearly see that creep rates are extremely low for considerable range of temperature and stress. This is due to the effect of reduced grain boundaries in larger grains which limit the extent of dislocation motion. It is clear empirically that larger the grain size, lower the creep rate.

---

<sup>8</sup>Ashby maps referenced from “Case study: Creep of a superalloy turbine blade”, url: [https://defmech.engineering.dartmouth.edu/Chapter\\_19.htm](https://defmech.engineering.dartmouth.edu/Chapter_19.htm)

This is also the basis of going for directionally solidified castings (DS) or single crystal technology (CM-SX) for improved creep resistance.

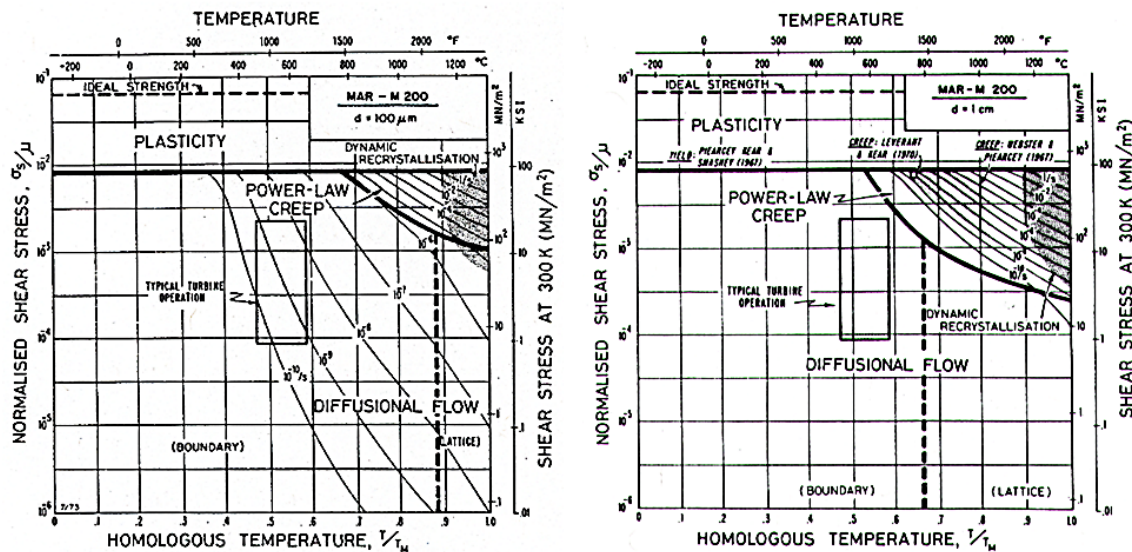


Figure 2.11.2 - Ashby map of MAR-M200 superalloy

Other notable means of studying creep transitions are through Bird-Mukherjee-Dorn or BMD plot, Arrhenius plot and Mohamad-Langdon map.

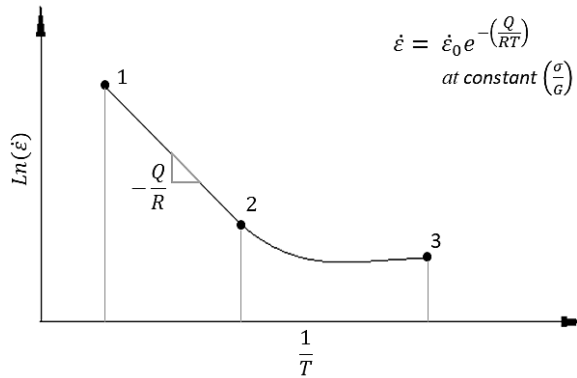
### 2.11.1. ARRHENIUS PLOT

A plot of natural logarithm of creep strain rate Vs. reciprocal of temperature at constant stress condition is called “Arrhenius Plot”. Slope of such a curve gives the ratio of activation energy to universal gas constant.

Stress ( $\sigma$ ) is often normalized with shear modulus ( $G$ ) as the internal flow stresses are not exactly the same as applied external stresses and they depend on shear modulus ( $G$ ). The slope describes ‘apparent’ activation energy if applied stress is considered and ‘true’ activation energy if normalized stress is considered.

In Graph 2.11.1, we can see that as temperature increase from 2 to 1, the curve is linear. This signifies that only one mechanism of creep is present in that temperature range. As we further reduce temperature from 2 to 3, strain rate decreases non-linearly. This shows the presence of two or more creep mechanisms in that range of temperatures.

Also, we can see that  $Q_1 > Q_2 > Q_3$ , since low temperature mechanisms (2-3) can step in with less activation energy and high temperature mechanisms (1-2) require more activation energy.



**Graph 2.11.1 - Arrhenius plot**

## 2.11.2. MECHANISMS IN SERIES & PARALLEL

If two or more mechanisms are transiting in series, time of every mechanism is additive. Slower process contributes to creep rate while faster process affects the total creep strain. If mechanisms occur in parallel, faster process is rate controlling.

## 2.12. CREEP BEHAVIOUR OF SUPERALLOYS<sup>9</sup>

Superalloys are the nickel-based alloy class of engineering materials which are particularly known for their exceptional creep resistance and use in high temperature applications like gas turbine components. Even though titanium-based alloys are preferred for their strength to weight ratio, they have the disadvantage of low oxidation strength at temperatures beyond 800°C where superalloys perform relatively better.

Super alloys can be primarily classified based on their strengthening process which highly affect their creep properties, namely solution-hardened alloys, oxide dispersed strengthened (ODS) alloys, particle precipitation hardened alloys, etc., and also by their crystal grain structure namely polycrystalline alloys (EA), directionally solidified (DS) alloys and single crystal (SX) alloys. Directionally solidified and single crystal alloys show anisotropic properties which invoke more complexity for creep modelling using finite element methods.

While generations of single crystal superalloys like SRR99, CMSX-4 and RR3000 are being used for turbine blade applications, polycrystalline superalloys like Inconel, Hastelloy, Waspaloy, MA754, MAR247, etc. are still being used for blades, disc and other components for their creep superiority over other materials.

Basic composition & purpose of each alloyed element is explained in Table 7.2.1.

**Table 2.12.1 - Superalloy - Typical composition**

---

<sup>9</sup> Reference: Roger C. Reed., “The Superalloys – Fundamentals and Applications”, 2006, Cambridge Publications, isbn-13 978-0-511-24546-6

S.No.	Element	Composition (% by weight)	Purpose
1	Ni	40 – 60 %	Base matrix $\gamma$ phase
2	Co	5 – 20%	Corrosion resistance Improving solubility of phases
3	Cr	5 – 20%	Corrosion resistance through $Cr_2O_3$
4	Al	0.5 – 6 %	Forms the $\gamma'$ phase; Oxidation resistance through $Al_2O_3$
5	Ti	1 – 4 %	Forms the $\gamma'$ phase;
6	Re, W, Hf, Mo, Ta	1 – 10%	Solid solution strengthening Higher melting point
7	Nb	0 – 5 %	Forms $\gamma''$ , for low temperatures
8	C	0.05 – 0.2 %	Forms carbide for strengthening

## STRENGTHENING PHASES

Nickel based superalloys exhibit three major phases namely,

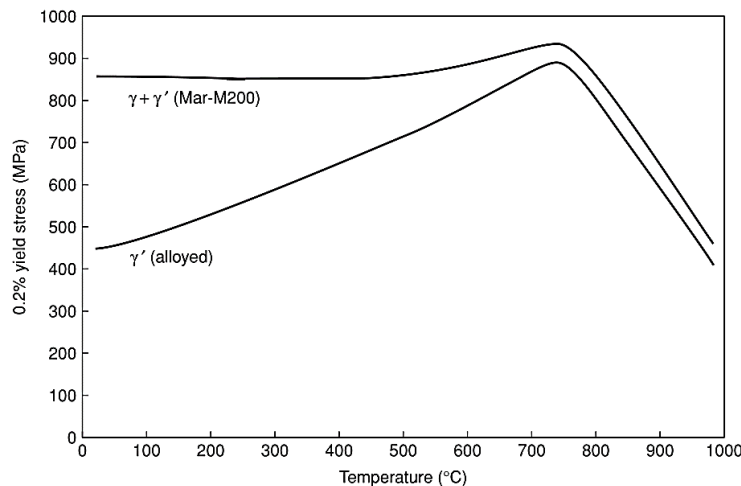
- $\gamma$  phase – Matrix with disordered FCC structure
- $\gamma'$  phase – Strengthening phase with ordered FCC structure
- Carbide phase – Dispersion strengthening & grain boundary stabilization phase with FCC structure

Majority of creep strength comes from the fact that a dislocation travelling in  $\gamma$  cannot enter the  $\gamma'$  phase without the formation of an anti-phase boundary (APB). The material requires an anti-phase boundary energy,  $\gamma_{APB}$  which acts as a barrier to dislocation motion and reduces strain rate considerably.

## YIELD STRENGTH ANOMALY

As for common materials, yield strength decreases with temperature. However, in the case of superalloys, yield strength increases with temperature up to 800°C due to metallurgical strengthening effects of  $\gamma'$  phase and then decreases quickly over 800°C. MAR-M200 alloy has about 60% of  $\gamma'$  phase and the anomaly of increasing yield strength with temperature as illustrated in Graph 2.12.1.

The underlying microstructural phenomenon is cross-slipping of anti-phase boundaries during plastic deformation leading to microstructural locks that resists deformation known as ‘Kear–Wilsdorf lock’.



**Graph 2.12.1 - Yield strength anomaly in MAR-M200**

### 2.12.1. PARTICLE STRENGTHENED ALLOYS

In particle strengthened alloys, the presence of the  $\gamma'$  phase, which is promoted by alloying with Al, Ti and Ta, has a profound influence on the creep resistance of the nickel alloys. It is observed that upon addition of these solute atoms, strength of the materials is increased and this increase is directly proportional to the difference in atomic sizes between the solute & the solvent (Ni) atoms. Also, increased concentration of these solutes (which increases the fraction of the  $\gamma'$  phase) increases the creep strength of the material. Grain size also has significance in creep rate.

Creep behavior of Class-A alloys exhibit power law stress dependence with exponent  $n \sim 3$  and do not have distinguishable primary creep stage where as Class-M alloys show stress exponent of about 5 and have a significant primary creep stage. This difference in Class-A and Class-M behaviour is found to be due to the misfit in atomic size of the primary constituents.

Care should be taken to identify the stress & temperature range for which creep behaviour is distinct so that finite element modelling can predict with good accuracy.

### 2.12.2. SINGLE CRYSTAL SUPERALLOYS

Creep behavior of single crystal superalloys is significantly different from other superalloys due to the absence of grain boundaries for creep cavitation that plays a vital role in onset of tertiary stage. As a result, creep curve of single crystal superalloys does not show significant secondary stage, but shows a progressive increase in creep rate with time. Also, since the activation energies are much higher, the stress exponent values go as high as 8 (Power law breakdown regime). Single crystal alloys show progressive increase in dislocation density with time which is still lower than other alloy types.

One more interesting property of single crystal alloys is that pre-straining reduces their creep strength while other alloys show improved creep strength with strain hardening.

Due to the anisotropic behaviour of columnar grain or single crystal superalloys, finite element creep modelling requires special considerations, which are no in the scope of this project.

### 3. CREEP LIFE ESTIMATION

Creep life of materials can be expressed in two major forms namely,

- Strength life
- Stiffness life

Strength life refers to the time taken for total loss of strength due to creep rupture. Deformation & percentage elongation at creep rupture can be relatively higher.

Strength life is suitable for applications that allow considerable deformation like high temperature thin structures, pressurized pipes, thin pressure vessels, etc. where even small cracks are not tolerable.

Stiffness life refers to the time taken for attaining a prescribed amount of strain which is usually 1% to 5% creep strain. Stiffness life is suitable for applications that do not allow considerable deformation like high precision fit components. These systems can even allow some minute cracks that relieves creep strain but cannot tolerate excess deformation (strain) that will cause mechanical failure due to change in fit and tolerances. A typical example is gas turbine blade which has a very small tip clearance. Small cracks on blade tip does not affect the functionality whereas axial elongation more than the specified tip clearance will cause tip rubbing on the casing and may lead to a catastrophic failure.

<sup>10</sup>Safe stress levels are usually prescribed for a rupture life of > 1,00,000 hours or when the total nominal strain is within 0.1% or 0.2% in its service level.

#### 3.1. EXPERIMENTAL CREEP TEST

Creep behaviour of engineering materials are studied and validated through uniaxial tensile creep tests. Standard test methods and procedures for creep testing of metals and alloys are described in detail by ASTM E-139 standard<sup>11</sup>.

Test method is by measuring the amount of deformation (creep strain) as function of time with extensometer at constant applied tensile stress and temperature conditions as described in Figure 3.1.1. For a typical creep test, testing is done for a prescribed time or until a prescribed strain value is reached. For creep rupture test, the test is carried out until fracture and time to rupture is also measured. Creep test gives the stiffness for the material at test loads whereas stress rupture test gives the ultimate creep strength at test loads.

---

<sup>10</sup> R.K.Penny, D.L.Marriot, “Design for creep”, 2<sup>nd</sup> ed., Chapman and Hall, 1995.

<sup>11</sup> “Standard Test Methods for Conducting Creep, Creep-rupture and Stress-rupture Tests of Metallic materials” – ASTM E139 - Rev.11, 2018

The test specimen is usually standard stepped cylindrical tensile test specimen as described in ASTM Test Methods E-8 with marked test section in the middle and plain or threaded sections on one or both sides for clamping in the extensometer. Testing on notched specimens are described in ASTM - 292

A typical creep test data is illustrated in Graph 3.1.1. Data points of uniaxial strain values measured by the extensometer are marked at different times till creep rupture which is characterized by sudden & significant loss of applied load.

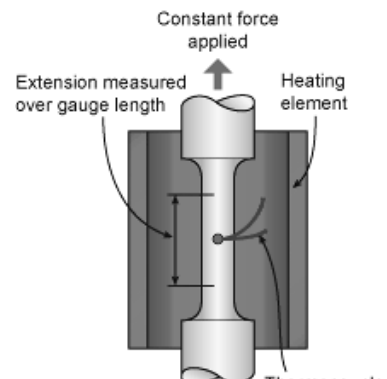
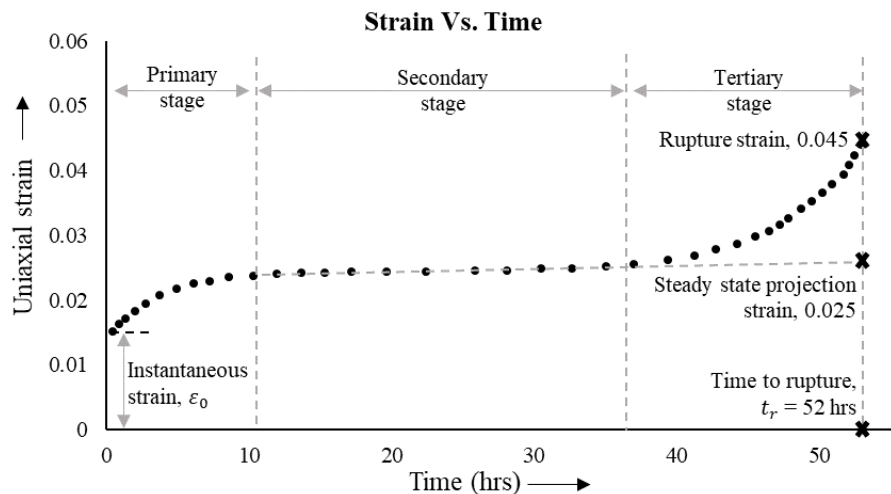


Figure 3.1.1 - Schematic of Uniaxial Tensile Creep Test



Graph 3.1.1 - Typical Experimental Creep Test data

It is to be noted that the data starts with an instantaneous strain  $\epsilon_0$  of 0.015 at time  $t = 0$  which is the elastic strain component. For calculations & analysis purposes, only plastic component of creep strain is significant and it is necessary to subtract this elastic component of strain from every data point ( $\epsilon_{cr} = \epsilon - \epsilon_0$ ) after which the curve shifts to origin with strain value of  $\epsilon = 0$  at time  $t = 0$ . A curve can be regressed and fit over the data points and any outlier data which may be due to errors in measurement are omitted. Different stages of creep can be identified by marked change in slope of the curve.

Creep strain at rupture and time at which creep rupture occurs are noted. Sometimes, at low applied stresses, material may take a very long time for rupture to be practically measured. In such cases, slope of steady state creep can be projected till it crosses a prescribed strain value (usually 1% to 5% creep strain) and corresponding time value can be assumed as its creep life.

This process is repeated for different stress, temperature and grain size of the material. Creep curves at different load conditions can be plotted together to visualize the creep behavior of material at different conditions. Any unusual creep behavior at certain load conditions depicts the change in microstructural properties or rate controlling mechanisms in that temperature or stress range.

## 3.2. CREEP LIFE EXTRAPOLATION METHODS

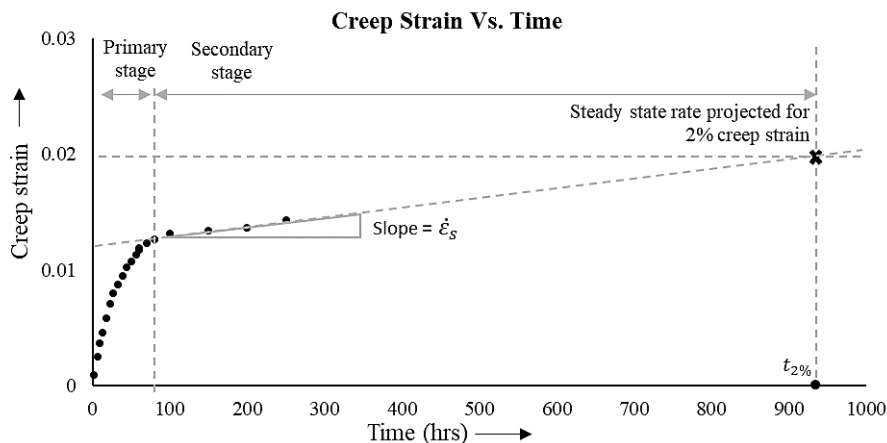
In many applications, materials operate at complex non-uniform stress states and temperatures. But experimental creep data gives the creep behaviour at constant and uniform uniaxial stress state at constant temperatures. It is impractical to obtain experimental creep data at every possible temperature and stress states. Also, there is a commercial need to conduct creep test for durations as short as possible. Hence, there is a need for reasonable interpolation and extrapolation of creep data at different stresses and temperatures wherever experimental data is not available. This can be carried out by using different creep life estimation techniques such as,

- Steady state creep rate approach
- Larson Miller Parameter (LMP) method
- Monkman – Grant approach

Other parametric creep life extrapolation techniques include Orr-Sherby-Dorn (OSD) parameter, Manson – Haferd parameter, Manson – Brown parameter, Minimum commitment method, etc. which may not be pertinent to the scope of the project.

### 3.2.1. STEADY STATE CREEP LIFE APPROACH

When time to rupture is so long for the creep test to complete till rupture, steady state creep rate  $\dot{\varepsilon}_s$  can be projected to intercept a prescribed creep strain value and corresponding time can be obtained.



Graph 3.2.1 - Steady state creep rate projection

As illustrated above, creep strain does not increase significantly after 200 hours and takes about 40 days to even reach 2% creep strain. Instead, the experiment can be stopped at considerably lesser time after steady state has been established, ( $\sim 300$  hrs). Time taken for  $k$  % creep strain can be simply calculated as,  $t_{k\%} = \dot{\varepsilon}_s \times \frac{k}{100}$

This method does not take in account of creep rate change after onset of tertiary and is less accurate. But it is useful when time to rupture is very large.

### 3.2.2. LARSON MILLER METHOD

This method involves a representation of time to failure ' $t_r$ ' and temperature 'T' in terms of "Larson-Miller Parameter" or LMP and plotting it against stress ' $\sigma$ '. This method assumes that the mechanism controlling activation is constant throughout the range of stress and temperature studied.

$$LMP = T \times (k + \ln(t_r))$$

where,

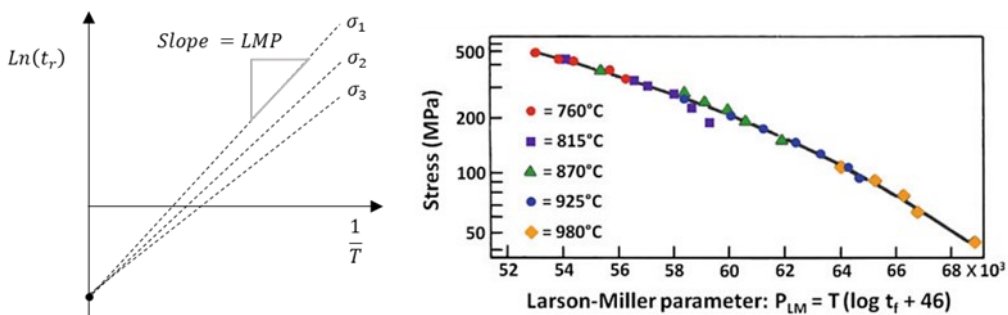
$T$  – Temperature in kelvin

$t_r$  – Time to creep rupture

$c$  – Constant ( $\sim 46$ )

Larson Miller parameter (LMP) is the slope of curve plotted of ' $\ln(t_r)$ ' against  $\frac{1}{T}$  as shown in Graph

3.2.2. LMP is constant for given stress and decreases with increase in stress.



Graph 3.2.2 - LMP Master Curve and LMP Vs Stress for Astroloy

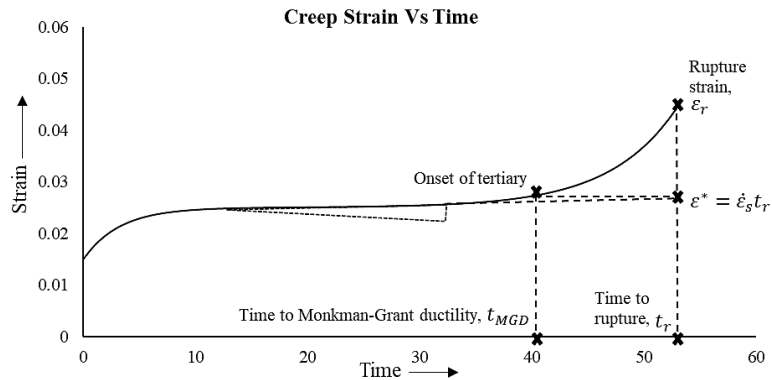
After calculating LMP values for different temperature and rupture times for different stress conditions, the LMP values are again plotted against stress known as a 'master curve'. Significance of this master curve is that LMP follows linear or quasi-linear relationship with stress as shown in a sample master curve in Graph 3.2.2.

Using LMP values for known stresses, value of LMP can be calculated by interpolation or extrapolation, in-turn time to rupture for any given temperature can be calculated approximately.

### 3.2.3. MONKMAN GRANT APPROACH

In many engineering applications, it is necessary to maintain safe stress level such that tertiary creep stage does not occur in its service life. To estimate the time to onset of tertiary creep, Monkman-Grant approach is used.

Upon extrapolating the steady state creep rate to rupture time( $t_r$ ), we get a value of creep strain called ‘Uniform creep ductility strain ( $\varepsilon^*$ )’. If a line is drawn parallel to time axis at this uniform creep ductility strain, it intersects the creep curve at a point whose ordinate is called ‘Time to Monkman-Grant ductility’ ( $t_{MGD}$ ).



*Graph 3.2.3 - Monkman - Grant Ductility criteria*

## 4. CREEP MODELS

There are many creep models formulated to describe creep behaviour of different kinds of materials. They can be classified as follows:

- Basic creep models
  - Norton's power law model
  - Norton – Bailey's Time hardening model
  - Norton – Bailey's Strain hardening model
  - Hyperbolic sine law model
- Continuum Damage Mechanics (CDM) models
  - Kachanov-Rabotnov Model
  - MPC Omega method
  - Liu – Murakami model
  - Dyson Model
  - Theta projection method
- Visco-plasticity Models

### 4.1. BASIC CREEP MODELS

#### 4.1.1. NORTON'S POWER LAW MODEL

The most common and basic creep model for describing the steady state (secondary) creep rate ( $\dot{\varepsilon}_{min}$ ) is the Norton's power law model which describes a power relationship between creep strain and stress as below:

$$\dot{\varepsilon}_{min} = A\sigma^n$$

Where,

$A$  – Hardening Coefficient based on Arrhenius rate equation,  $A = Be^{-\frac{Q_c}{RT}}$

$\sigma$  – Applied stress

$n$  – stress exponent

$B$  – material constant

$Q_c$  – Activation energy for creep

$R$  – Universal gas constant

$T$  – Applied temperature

Norton's power law equation can be directly applied to constant stress and constant temperature creep processes to find the minimum (steady state) creep rate. To apply this to different stress and temperature conditions, experimental data is required at each temperature and stress for which creep rate has to be

calculated. This is because the hardening coefficient ‘A’ is dependent on temperature and activation energy and also, the stress exponent ‘n’ varies for different temperature range due to different creep rate controlling mechanisms taking dominance at different temperature ranges.

#### 4.1.2. NORTON BAILEY’S TIME HARDENING MODEL

Norton’s power law expressed in its time – integrated form is the Norton – Bailey’s time hardening model as shown below:

$$\dot{\varepsilon}_{cr} = A\sigma^n t^m$$

Where,

$\dot{\varepsilon}_{cr}$  – Creep strain rate at time ‘t’

$t$  – Time

$m$  – Time exponent

#### 4.1.3. NORTON BAILEY’S STRAIN HARDENING MODEL

Norton Bailey’s Time hardening creep equation where the time term replaced with creep strain is called Norton – Bailey’s strain hardening model.

$$\dot{\varepsilon}_{cr} = [A\sigma^n \{(m + 1)\varepsilon_{cr}\}^m]^{\frac{1}{m+1}}$$

Where,

$\varepsilon_{cr}$  – Creep strain at time ‘t’

Strain hardening form is more accurate than time hardening model as creep strain rate is controlled by current creep strain instead of time.

In all the power law models, the time exponent ‘m’, the stress exponent ‘n’ and hardening coefficient ‘A’ are functions of temperature. Hence, this form is only valid for constant temperature. Experimental data is required at different temperature / stress conditions to find constants A, n and m.

Since there is only one power term in the creep equation, both power law equations do not describe all stages of creep. Power law models can only predict steady state creep at constant temperature.

#### 4.1.4. HYPERBOLIC SINE LAW MODEL

Hyperbolic sine law model is based on Garofalo’s creep equation augmented by Arrhenius rate equation as follows:

$$\dot{\varepsilon}_{cr} = A(\sinh B\sigma)^n e^{-\frac{Q_c}{RT}}$$

Where A, B and n are material constants.

Hyperbolic sine law model is effective for moderate to high stress conditions and describes tertiary creep behaviour. The constants ‘A’ and ‘B’ are functions of temperature and the stress exponent ‘n’ varies for different range of temperatures.

## 4.2. CONTINUUM DAMAGE MECHANICS MODELS

The basic models discussed in the above section do not describe all stages of creep effectively. Also, they require estimation of constants for different temperature and stress conditions. The constitutive equations of these basic models do not involve creep damage accumulation which is a good indicator for effective creep life.

Continuum Damage Mechanics (CDM) based models effectively describe the creep behaviour of materials in terms of internal state variables that govern the underlying creep mechanism and accumulates damage due to creep which can be an indicator of creep fracture. Common CDM based creep models are discussed here.

### 4.2.1. KACHANOV-RABOTNOV MODEL

Kachanov & Rabotnov proposed a new model by incorporating a damage variable ' $\omega$ ' to Norton's power law equation and its uniaxial form is given below:

$$\dot{\varepsilon}_{cr} = A \left( \frac{\sigma}{1 - \omega} \right)^n t^m$$

Where, ‘A’ and ‘n’ are hardening coefficient and stress exponent respectively

This damage variable  $\omega$  is zero initially for virgin material and accumulates with creep strain over time. The effect of damage variable is to accelerate the creep strain rate to model the tertiary creep behaviour.

Rate of creep damage,  $\dot{\omega}$  can be calculated as,

$$\dot{\omega} = \frac{M\sigma^\chi}{(1 - \omega)^\phi}$$

Where,  $M, \chi$  and  $\phi$  are tertiary creep damage constants and can be calculated by regressing the integral form of above equations to experimental creep data with constraint equations. Detailed description of the procedure is explained by (Calvin M. Stewart, 2010).

Since the power law based Kachanov – Rabotnov formulation does not account for strain hardening during primary creep, care should be taken to set damage variable to zero till secondary creep stage (minimum creep rate) for the regressing equations while calculating material constants.

A lot of literature has been found incorporating this Kachanov-Rabotnov damage variable to other advanced creep models as well in creep rupture formulations and have good correlation to experimental data on creep behaviour of many engineering materials.

#### 4.2.2. OMEGA METHOD

Omega method was proposed by Prager in 1995 and subsequently developed & validated by Materials Properties Council (MPC) and American Petroleum institute which relies on life fraction parameter ' $\omega$ ' defined as the ratio of current time to rupture time for given stress and temperature. This life fraction parameter is related to creep strain rate as,

$$\omega = \frac{t}{t_r} = \frac{\dot{\varepsilon}_{cr}\Omega t}{1 + \dot{\varepsilon}_{cr}\Omega t}$$

Where,

$t$  – Time from the end of primary stage

$t_r$  – Time to rupture from the end of primary stage

$\Omega$  – Material creep damage constant

As the time ' $t$ ' progresses and nears rupture time ' $t_r$ ', damage variable  $\omega$  becomes 1 and the equation collapses. In such cases, Prager suggested the following equation could be used,

$$1 - \dot{\varepsilon}_0\Omega t = \frac{1}{e^{\Omega\varepsilon_{cr}}}$$

Where,

$\dot{\varepsilon}_0$  – Strain rate at the end of primary stage

$\varepsilon_{cr}$  – Accumulated creep strain from primary stage

Time to rupture can be calculated by setting creep strain rate to infinity, as follows:

$$t_r = \frac{1}{\dot{\varepsilon}_0\Omega}$$

The creep strain equation can be simplified in the below form which says that the creep strain rate is proportional to the exponent of the accumulated creep strain.

$$\dot{\varepsilon}_{cr} = \dot{\varepsilon}_0 e^{\Omega\varepsilon_{cr}}$$

Initial strain rate  $\dot{\varepsilon}_0$  and the damage variable  $\Omega$  are functions of stress and temperature and can be expressed in terms of Power law – Arrhenius form as below:

$$\dot{\varepsilon}_0 = A_0 \sigma^{n_0} e^{-\frac{Q_0}{RT}}$$

$$\Omega = A_\Omega \sigma^{n_\Omega} e^{-\frac{Q_\Omega}{RT}}$$

Where,

$A_0, A_\Omega$  – Hardening coefficients

$n_0, n_\Omega$  – Stress exponents

$Q_0, Q_\Omega$  – Apparent activation energy

### $Q_\Omega$ – Temperature dependence of $\Omega$

The material constants can be determined by regressing the above equation with experimental creep data.

The purpose of Omega method is to find the remaining useful creep life of materials and it does not account for primary creep in itself and should be augmented for complete creep curve predictions.

#### 4.2.3. LIU – MURAKAMI MODEL

To avoid computational difficulties of determining fracture at high strain rates close to infinity, Liu and Murakami developed a damage evolution-based model based on power law type creep relationship as below:

$$\dot{\varepsilon}_{cr} = B\sigma^n e^{\left[ \frac{2(n+1)}{\pi\sqrt{1+\left(\frac{3}{n}\right)}} \right] \omega^2}$$

Rate of damage ( $\dot{\omega}$ ) can be calculated as below:

$$\dot{\omega} = \frac{A(1 - e^{-q})}{q} \sigma^p e^{q\omega}$$

Where,

$A, B$  and  $q$  – Material constants

$n, p$  – Stress exponents

$\omega$  – Damage variable

The material constants can be determined by regressing the integral form of above equation applying boundary constraints with experimental creep data.

#### 4.2.4. DYSON MODEL

Dyson formulated a hyperbolic sine relation for creep in terms of internal variables such as strain hardening variable ( $H$ ), ageing damage parameter ( $\phi$ ) and cavitation damage parameter ( $\omega$ ) as given below:

$$\dot{\varepsilon}_{cr} = A \sinh \left[ \frac{B\sigma(1-H)}{(1-\omega)(1-\phi)} \right]$$

Rate of hardening is given by,

$$\dot{H} = \frac{h}{\sigma} \frac{A}{(1-\omega)^n} \sinh \left[ \frac{B\sigma(1-H)}{(1-\phi)} \right] \left[ 1 - \frac{H^*}{H} \right]$$

Where,

$h$  – constant, (product of Young's modulus and volume fraction)

$H^*$  – Saturation value of hardening variable

Rate of ageing damage and cavitation damage are given by,

$$\dot{\phi} = \frac{K_c}{3}(1 - \phi)^4$$

$$\dot{\omega} = DA \sinh \left[ \frac{B\sigma(1 - H)}{(1 - \omega)(1 - \phi)} \right]$$

Where,

$K_c$  – Constant based on grain geometry

$D$  – Material constant

Dyson's model describes all stages of creep. The hardening rate that will be dominant in the primary stage slowly decreases and will reach the saturation  $H^*$  towards the start of secondary stage and the rate of hardening will become minimum, close to zero. The damage variables  $\omega$  and  $\phi$  start to increase after primary stage and amplifies the effective stress to further increase the damage rate and creep strain rate exponentially.

Since Dyson's model is based on microstructural damage mechanisms and generation of back stresses, it is suitable for materials with a good proportion of second phase constituent. An approach to modelling creep using Dyson's creep model for superalloys has been developed by (Ramkumar Oruganti, 2012).

#### 4.2.5. THETA PROJECTION METHOD

Evans and Wilshire developed the Theta projection method which is widely accepted as a full curve creep prediction and extrapolation method which expresses creep strain as an exponential function of four  $\theta$  coefficients and time as below:

$$\varepsilon_{cr} = \theta_1(1 - e^{-\theta_2 t}) + \theta_3(e^{\theta_4 t} - 1)$$

The first term in the above equation represents the primary creep and the second term represents the tertiary creep. Secondary creep will be the continuum curve connecting the primary and tertiary creep terms. Hence it models all stages of creep. The four theta coefficients are related to stress, temperature and stress – temperature interaction by an exponential relationship as shown below:

$$\ln(\theta_i) = a_i + b_i\sigma + c_iT + d_i\sigma T$$

Where,  $a, b, c$  and  $d$  are material constants and are independent of stress and temperature. This method is discussed in detail in the later sections.

## 4.3. VISCOPLASTICITY MODELS

Viscoplasticity models are used for high stress cases where creep is accompanied by plasticity and cyclic loading. The application may include creep fatigue interaction, high temperature & high strain rate plastic deformation, stress relaxation and dynamic recovery of materials.

### 4.3.1. CHABOCHE UNIFIED VISCO-PLASTICITY MODEL

Chaboche's unified visco-plasticity model is a widely accepted visco-plasticity model which can substantially model wide range of elastic and inelastic mechanisms occurring in material such as yield, kinematic hardening, isotropic hardening and time dependent plastic deformation such as creep and stress relaxation. According to Chaboche's formulation, total strain rate in material is decomposed to elastic and inelastic strain rate terms as below:

$$\dot{\varepsilon} = \dot{\varepsilon}_e + \dot{\varepsilon}_p$$

While the elastic strain rate can be modelled with Hooke's law based-formulation ( $\sigma = E\varepsilon_e$ ), the evolution of the inelastic strain is defined as a function of accumulated plastic strain increment  $\dot{p}$ , external stress  $\sigma$  and kinematic back stress  $\chi$  developed in the material.

$$\dot{\varepsilon}_p = \dot{p} \operatorname{sgn}(\sigma - \chi)$$

$$\text{Where, } \dot{p} = \langle \frac{f}{Z} \rangle^n$$

The yield criterion  $f$  is given by,

$$f = |\sigma - \chi| - R - k$$

Where,

$R$  – Isotropic hardening variable

$k$  – True elastic strain limit (Initial yield strength)

The elastic domain is defined by  $f \leq 0$  and the inelastic domain by  $f > 0$ .

$$\operatorname{sgn} \text{ denotes the sign function defined as, } \operatorname{sgn}(x) = \begin{cases} 1, & x > 1 \\ 0, & x = 0 \\ -1, & x < 1 \end{cases}$$

$$\text{McCauley brackets defined as, } \langle x \rangle = \begin{cases} x, & x > 0 \\ 0, & x \leq 0 \end{cases}$$

$Z$  is the viscous parameter based on isotropic hardening variable  $R$ .

Isotropic hardening variable  $R$  describe directionally independent effects such as change in yield surface during cyclic loading as for the cyclic hardening or for the cyclic softening. whose rate is given by,

$$R = \sum R_i \text{ and } \dot{R}_i = b_i(Q_i - R_i)\dot{p}$$

Where,

$b$  – Scale factor for isotropic hardening

$Q$  – Saturation value of isotropic hardening

Kinematic hardening variable  $\chi$  is used to describe direction dependent effects such as Bauschinger effect due to plastic flow under cyclic loading. Kinematic hardening rate  $\dot{\chi}$  is a sum of linear hardening, static and dynamic recovery as given below:

$$\chi = \sum \chi_i \text{ and } \dot{\chi}_i = C_i \dot{\varepsilon}_p - \gamma_i \chi_i \dot{p} - \beta_i |\chi_i|^{r_i-1} \chi_i$$

While the linear hardening and dynamic recovery term govern the overall hysteresis loop shape, the static recovery term allows for stress relaxation.

The viscous overstress  $\sigma_v$  function describes the rate dependency of the stress in Norton's power law form as given below:

$$\sigma_v = Z \dot{p}^{\frac{1}{n}}$$

Stress at each moment is given by,

$$\sigma = \chi + v(R + k + \sigma_v)$$

Where,  $v = \operatorname{sgn}(\sigma - \chi) = \pm 1$ , according to the direction of flow.

Chaboche's model is widely accepted for modelling combined creep and time dependent plastic behaviour, but requires a lot of experimental data and complex procedures for estimation of constants and numerical calculations in CAE environment.

#### 4.4. CREEP MODELS IN CAE TOOLS

Creep analysis of gas turbine components using Computer Aided Engineering (CAE) tools proves to be an excellent opportunity to assess and improve the design of components in developmental stages. These softwares have creep models inbuilt in them so that components can be analyzed if we have the input data. Even though accuracy of the CAE results highly depends upon the accuracy of input data, creep analysis using these tools provides a good estimate of creep behaviour of components. Creep models inbuilt in common analysis softwares are listed in Table 4.4.1.

Table 4.4.1 - Creep models in commercial CAE tools

S.No	CAE Software	Creep model	Remarks
1	ANSYS	Strain Hardening	
2		Time Hardening	

3		Generalized exponential	Almost all of the models do not predict all stages of creep and requires material constants which are specific to stress & temperature
4		Generalized Graham	
5		Generalized Blackburn	
6		Modified time hardening	
7		Modified strain hardening	
8		Generalized Garofalo	
9		Exponential form	
10		Norton	
11		Combined time hardening	
1	ABAQUS	Time hardening	Does not predict tertiary creep
2		Strain hardening	
3		Hyperbolic sine law	Only for tertiary creep analysis & requires activation energy data
4		Double law	
5		Darveau law	
6		Anand model	For solder alloys

Aforesaid models are for generalized creep analysis and have the following disadvantages for gas turbine applications:

- All stages of creep cannot be predicted together
- Damage accumulation is not modelled
- Material constants are specific to stress & temperature and require a lot of experimental data
- Changes in creep behaviour due to change in rate controlling mechanism at certain temperature or stress ranges cannot be modelled

## 5. LITERATURE REVIEW

There are advanced creep models available in the literature out of which the suitability for gas turbine applications and convenience for mathematical modelling are taken as the base criteria in selecting the appropriate model for CAE implementation. Also considering the inadequacies in existing models mentioned in the previous section, advanced creep models such as the Kachanov-Rabotnov model, Omega method, Liu-Murakami method, Dyson model, Theta projection method are considered.

All the above models can directly or with modifications, predict all stages of creep behaviour and also accounts for damage accumulation. However, there are no ‘inbuilt’ models in CAE tools based on these advanced methods. Unified Viscoplasticity models, though advanced and capable of modelling creep & plasticity effects, are too advanced for the scope of the project and require complex procedures for determining material constants and numerical calculation. Hence there is a need to develop a user subroutine based on one of these CDM methods which when integrated with CAE tools, would predict creep better than the inbuilt models for gas turbine applications.

Several literatures based on modifications to these base models have also been considered for implementation and some important research papers are reviewed here.

A comparative analysis of hyperbolic sin model and Kachanov-Rabotnov creep damage model done by (Mohammad Shafinul Haque, 2019) on stainless steel clearly shows the inadequacy of Kachanov-Rabotnov model to capture the sigmoid bend in double log scale creep curves. A similar analysis has been done by (J.P. Rouse, 2013) establishes the superiority of hyperbolic-sine based models like Dyson's model over power law-based models such as "Liu-Murakami model" and "Kachanov-Rabotnov model".

A new constitutive relationship loosely based on Theta projection method developed by (Mingchen Huoa, 2021), establishes two different forms for creep constitutive equation below and above a critical time around which there is a change in nature of creep rate. While the method claims improved accuracy in creep prediction with the estimation of 'glass strain' and 'critical creep time creep', in addition to estimating material constants, 4-parameter Theta projection equation proves a good start for us as we are trying to develop more generalized & simpler form for CAE integration.

A new empirical model for predicting full creep curve for a wide range of materials using a power-based stress – strain - time relationship suggested by (Veronica Gray, 2015) proves promising in predicting full creep curve for different materials as stress normalized with yield strength of the material is considered. The model is empirical and do not adopt any physical constitutive equations for creep and hence implementation for CAE simulations needs further development.

A novel and accurate method for interpolation and extrapolation of creep curves using piecewise exponential interpolating functions for Theta projection method suggested by (Peng Yu, 2020) shows a very good accuracy over traditional method and could be useful if enough experimental creep curves are available as input.

The modified theta projection method proposed by (Ming Song, 2018) takes into account of the micro-mechanisms and their activation energies but the number of material constants and the procedure to estimate the same along with the ease of CAE implementation has to be explored.

The modified Theta projection method with second order relationship for primary theta coefficient with material constants suggested by (Bong Min Song, 2007) validates the accuracy of Theta Projection Method over Omega method through comparative analysis and the proposed model will be useful for better primary creep characterization.

The model proposed by (Seongin Moon, 2021) based on Theta Projection Method is very valuable in estimation of constants and coefficients when constant load creep test data is available instead of constant stress creep test data. The hardening rule proposed is specific to the micro-mechanisms of steam generation tube materials like alloy 690 and generalization needs further investigation.

A modified Theta projection method proposed by (W David Day, 2014) discusses the material property degradation when the applied stress and temperature reaches near yield stress and melting temperature of the material. The use of LMP as internal state variable and the use of effective time for creep

strain calculation best describes the practical cases where stress is removed for a period of time. The proposed model seems to best suit for varying stress cases and the use of life fraction may be of good practical use for designers. But the use of 8 Theta coefficients, 32 material constants and calculation of life fraction and time to tertiary creep as variables makes it little complex for CAE implementation. Efficiency of this model over the original Theta projection model by Evans and its constitutive equations has to be investigated further.

“C-Project” concept developed by (Li, 1996) based on Theta projection method, relates the coefficients to the dimensions of the geometry being analyzed and the software “Creep Life Predictor” designed based on the same proves to be good fit for piping applications especially for predicting residual creep life. However, such a method may not be a good fit for turbine blade applications and our scope of work.

Constitutive physical model for creep deformation based on CDM approach developed by (D.R. Hayhurst\*, 2003) describes creep in SS-316 alloy in terms of hardening and softening as the internal variables expressed in terms of hyperbolic sine relation with stress, time and damage variable. The effect of pre-strain was also studied in the paper which may be of great use for forming simulations. However, the constitutive equations do not involve the temperature dependence of material constants and has been proven to hold good only for long term creep at almost constant temperature, which cannot be applied to gas turbine applications.

(Donghuan Liu, 2014) have presented their work on numerical simulation of power law-based creep relation along with creep damage evolution based on modified Lemaitre-Chaboche model. The procedure seems to be great on visualizing the damage, but the damage variable is related to only to the Young’s modulus of the material and the effect of damage on creep strain rate needs further validation.

Creep prediction using LMP and damage variable taking into account of nature of creep recovery mechanism (tensile or compressive healing) has been suggested by (Domen Sergua, 2010) could be useful for creep – fatigue interaction simulations.

While the new constitutive model suggested by (Ramkumar Oruganti, 2012) expresses creep rate of superalloys in terms of temperature, activation energy, applied stress and back stresses, the results have been shown to hold good for directionally solidified and composites where the volume fraction of second phase particle is high. The model seems to be valuable in gas turbine material point of view if its applicability for FE modelling & ease of deriving and validating the constants have been well established.

An improved CDM based model suggested by (Xiao-feng Guo a, 2022) takes into account of damage due to two dominant mechanisms namely particle coarsening and intergranular cavitation pertaining to austenitic stainless steel which may not be the best fit for our scope as we are concerned on developing generalized model for superalloys.

## **5.1. LITERATURE REVIEW - SUMMARY**

Among the advanced creep models, “Theta Projection Method” proves to be the best model for finite element analysis because of the following advantages over other models:

- Mathematically simpler for coding
- Requires fewer material constants & experimental data
- Material constants hold good for a range of stress & temperature
- Availability of literature with proven data for comparison & validation

Hence “Theta Projection Method” is chosen as the base model for creep prediction.

Procedure to estimate material constants and fracture strain using Theta projection method has been described by (S G R Brown, 1984) and has been adopted. The constitutive model for Theta Projection Method developed by (R.W.Evans, 1984) which relates the Theta coefficients to hardening, recovery and damage as internal state variables is adopted for developing the user-subroutine.

Accuracy of procedure for creep prediction using Theta Projection Model has been statistically established by (Evans R. W., 1988). The procedure for determination of material constants has been given by (Evans.M, 2011) using ordinary and robust weighted least square regression methods has been adopted in the project and executed through MATLAB code. Similar methodology for prediction of creep curves has been followed by (C.M.Omprakash, 2013) whose scope was limited to generation of creep curves.

Towards improving the range and accuracy of the method, robust weighting scheme suggested by (Evans M. , 2002) has also been adopted and a MATLAB code has been developed that relies upon including robust weights for material constants estimation based on the variances of curve fitted Theta coefficients. The improved results of robust weighted least square regression method have also been compared with ordinary least square method.

The methodology for developing user subroutine for Theta Projection Method has been explained by (Harrison, 2007) and provides useful insights to this project.

The superalloy CM-247 or MAR-247 has been chosen as the reference material for analysis and validation of the user subroutine. The reason for choosing this material is because, it is a common material used for gas turbine components and also a lot of reliable literature data is available its mechanical and creep properties. Data on mechanical properties at different temperatures of MAR-247 superalloy has been referenced from (K. Harris, 1984) and (R Rajendran, 2012) and (Agustín Jose Torroba, 2014)

Experimental creep curves of MAR-247 superalloy at different temperature and stress conditions from (Marie Kvapilova, 2018) has been taken as base for material constant calculation as well as for validation of analysis results. Experimental creep data of GH4169 superalloy provided in (Donghuan Liu, 2014) has been

utilized as an alternate material for reference, for validation of material constant calculation process and the analysis results.

For comparative study, power law creep is also studied in this project and the detailed procedure for estimation of material constants given by (D. L. May, 2013) and (M.I.M Ahmad, 2011) were very helpful.

## **6. PROJECT SCOPE & OBJECTIVES**

### **6.1. AIM**

Based on the background research & literature review, aim of the project has been arrived as “*to develop a user subroutine for Abaqus to model creep in gas turbine components using Theta projection method*”.

### **6.2. OBJECTIVES**

Considering the creep behaviour of superalloys and analysis requirement specific to gas turbine applications, following objectives have been arrived:

1. Identify & adopt constitutive equations for Theta Projection Model
2. Develop MATLAB codes for calculating Theta coefficients and material constants
3. Develop Fortran code for Abaqus user subroutine for Theta Projection Method
4. Test & validate the Fortran code with experimental data
5. Creep analysis of gas turbine blade using Theta Projection Method
6. Life prediction of gas turbine blade
7. Testing the accuracy & robustness for a range of stress & temperature

### **6.3. SCOPE**

As creep behaviour of engineering materials differ widely based on several factors, it is difficult to formulate one creep model that will hold good for every material at every load conditions. For example, single crystal alloys or composites show anisotropic properties and cannot be modelled with the same code developed for polycrystalline isotropic alloys. On that account, scope of the project has been narrowed down to creep analysis of gas turbine components limited to,

- Polycrystalline superalloys or alloys exhibiting isotropic material properties
- All stages of creep excluding fracture (necking) / visco-plasticity / cyclic loading
- Temperature & stress range where creep effects are significantly pronounced
- Creep mechanism is consistent in the analysis range of stress & temperature
- The dominant creep rate controlling mechanisms is dislocation climb
- Material is pure (virgin) and there are no creep effects before analysis
- Simulated model has the same grain size as that of material taken for creep test

## 7. REFERENCE MATERIAL

### 7.1. MATERIAL PROPERTIES

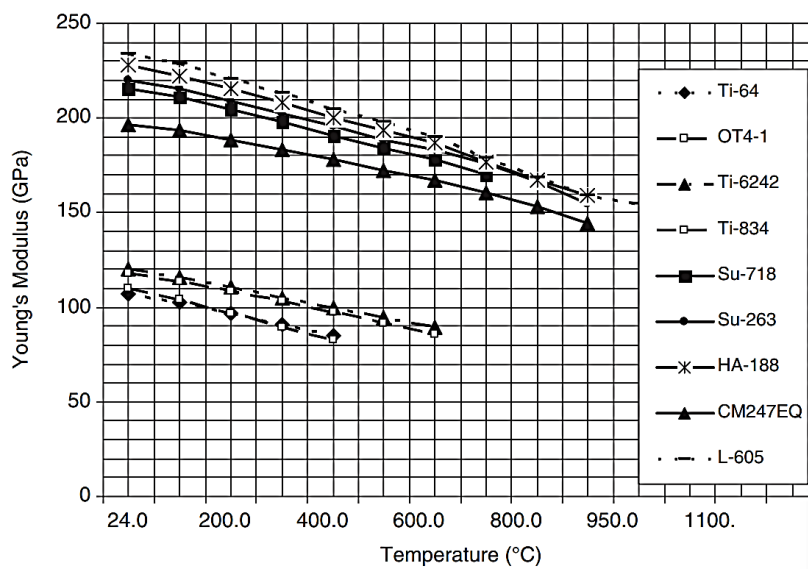
The reference material for study is the MAR-247 superalloy which has a density of  $8540 \text{ kg/m}^3$  and composition as referenced from (K. Harris, 1984) as shown in Figure 7.1.1.

It has a Poisson's ratio of 0.16 averaged for temperatures between  $25^\circ\text{C}$  to  $1000^\circ\text{C}$ . Variation of Young's modulus (E) with temperature has been described by (R Rajendran, 2012), as shown in Graph 7.1.1. These mechanical properties are used in the project for calculations & analyses.

MAR-M-247*		
NOMINAL COMPOSITION (wt. %)		
C	0.15	Al 5.5
Cr	8.4	Ti 1.0
Co	10.0	Hf 1.5
W	10.0	B 0.015
Mo	0.7	Zr 0.05
Ta	3.0	Ni Balance
Density-0.308 lbs/cu. in. (8.54 gms/cc)		

Figure 7.1.1 - MAR-247 Superalloy composition

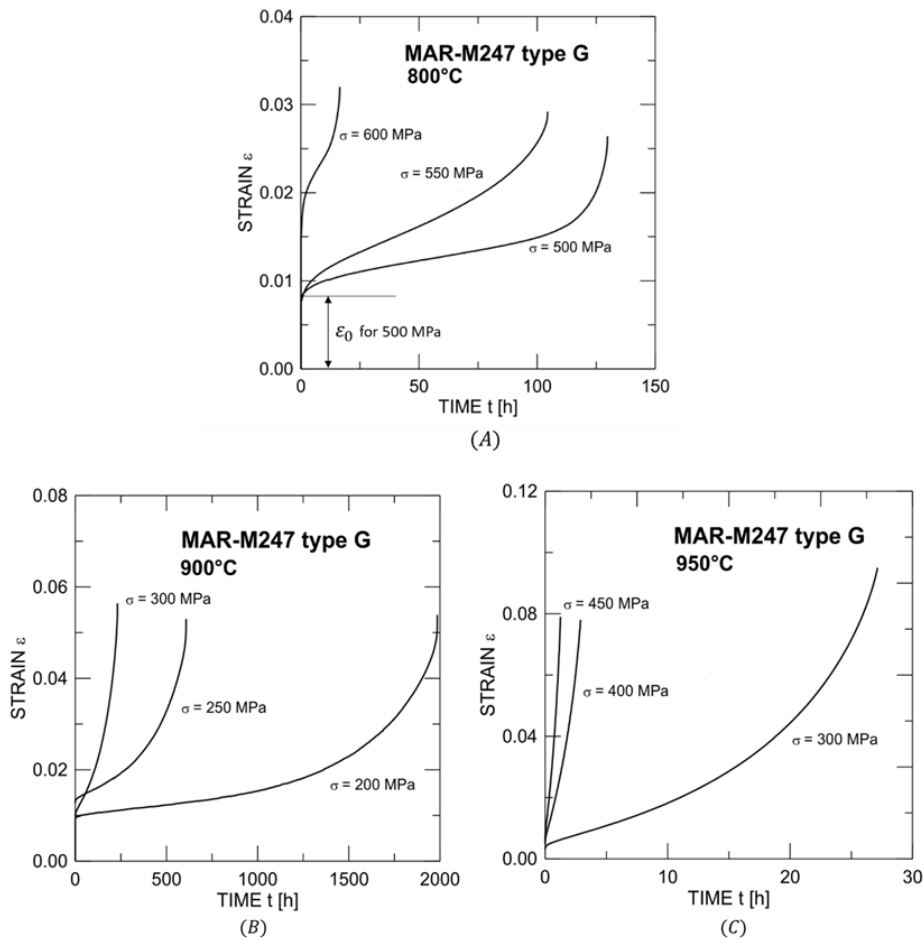
### 7.2. EXPERIMENTAL CREEP DATA



Graph 7.1.1 - MAR-247 Young's modulus Vs. Temperature

Uniaxial tensile creep tests of MAR-247 superalloy were conducted by (Marie Kvapilova, 2018) at three constant temperatures namely,  $800^\circ\text{C}$ ,  $900^\circ\text{C}$  and  $950^\circ\text{C}$  and at three different stresses for each temperature condition. Constant stress and constant temperature condition was maintained for each of these 9 creep tests.

The plots of strain vs time in ‘hours’ are as follows:



**Graph 7.2.1 - Experimental Creep Curves of MAR-247**

**Table 7.2.1 - MAR-247 Experimental data on min creep rate & fracture**

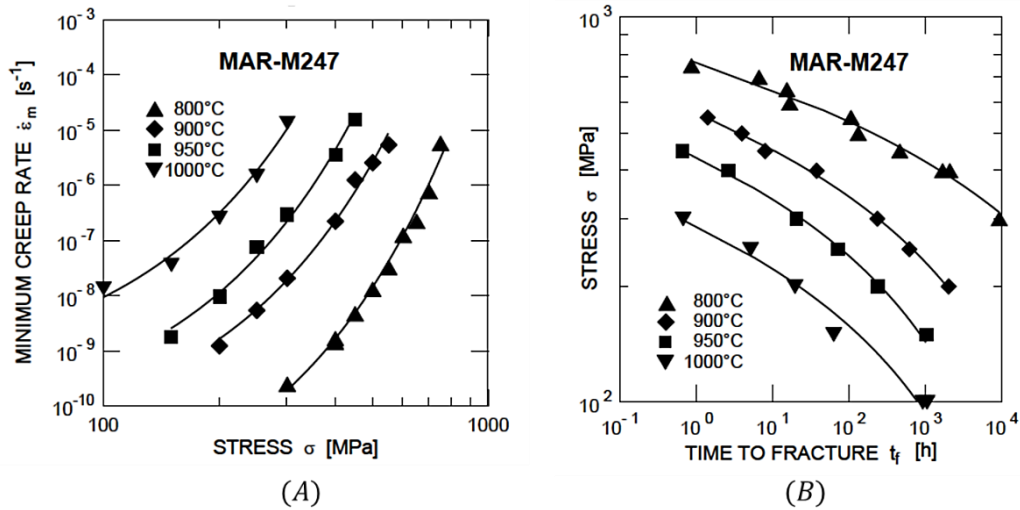
temperature T [°C]	applied stress $\sigma$ [MPa]	minimum creep rate $\dot{\epsilon}_m$ [s <sup>-1</sup> ]	time to fracture $t_f$ [h]	fracture elongation $\epsilon_f$ [%]
800	300	$2.5 \times 10^{-10}$	9131.1	4.1
	400	$1.4 \times 10^{-9}$	1655.3	2.9
	400	$1.6 \times 10^{-9}$	2053.41	
	450	$4.7 \times 10^{-9}$	454.535	
	500	$1.3 \times 10^{-8}$	129.79	2.6
	550	$3.2 \times 10^{-8}$	104.4	2.9
	600	$1.2 \times 10^{-7}$	16.44	3.2
	650	$2.2 \times 10^{-7}$	15.092	
	700	$7.8 \times 10^{-7}$	6.492	
	750	$5.8 \times 10^{-6}$	0.847	
900	200	$1.2 \times 10^{-9}$	1985.6	5.3
	250	$5.5 \times 10^{-9}$	607.3	5.4
	300	$2.1 \times 10^{-8}$	230.75	5.8
	400	$2.2 \times 10^{-7}$	37.05	7.7
	450	$1.2 \times 10^{-6}$	7.829	7.7
	500	$2.6 \times 10^{-6}$	3.88	7.0
	550	$5.5 \times 10^{-6}$	1.384	5.1
950	150	$1.8 \times 10^{-9}$	1013.9	6
	200	$9.8 \times 10^{-9}$	233.8	6.3
	200			
	250	$7.7 \times 10^{-8}$	69.8	5.5
	300	$3.0 \times 10^{-7}$	20	8.5
	400	$3.6 \times 10^{-6}$	2.569	7.8
	450	$1.6 \times 10^{-5}$	0.648	6.4

In addition to the creep curves, minimum creep rate or steady state creep rate ( $\dot{\varepsilon}_m$  or  $\dot{\varepsilon}_s$ ), time to fracture ( $t_f$ ) and percentage elongation till fracture ( $\epsilon_f$ ) at different load conditions has also been recorded in the experiment and the results are produced in Table 7.2.1.

Plot of minimum creep rate ( $\dot{\varepsilon}_m$  or  $\dot{\varepsilon}_s$ ) and time to fracture ( $t_f$ ) with respect to applied stress is shown in Graph 7.2.2.

The paper concludes that the apparent decrease of stress exponent at lower stresses indicates changes in the rate-controlling creep deformation mechanism and/or microstructural instability. Also, fracture strain value of 3% at 800°C and increase in fracture strain up to 8% with increase in temperature indicates the increase in ductility due to coarsening of  $\gamma'$  phase and microstructural instability due to dissolution of carbides  $M_{23}C_6$  at elevated temperatures.

These data will be useful in calculating power law creep constants as well as to compare and correlate the results of creep behaviour analyzed through Theta projection method.



*Graph 7.2.2 - MAR-247 - Min creep rate & time to fracture Vs Applied stress*

## 8. REVIEW OF POWER LAW CREEP

To effectively understand and demonstrate the inadequacy of power law creep model at tertiary creep stage, a sample analysis is performed and results are compared with experimental data.

Power law creep model defines creep strain rate as exponential functions of stress & time on at constant temperature. It has two major forms namely, time hardening & strain hardening. Time hardening form is directly derived from “Norton-Bailey” power relationship where as in strain hardening form, the factor ‘time’ is replaced in terms of creep strain. The constitutive equations for power law creep models are:

Where,

**Time hardening Creep model:**

$$\dot{\varepsilon}_{cr} = A\sigma^n t^m$$

**Strain hardening Creep model:**

$$\dot{\varepsilon}_{cr} = [A\sigma^n \{e(m+1)\}^m]^{\frac{1}{m+1}}$$

$\varepsilon_{cr}$  – Equivalent creep strain (no unit)

$\sigma$  – Equivalent stress (MPa)

$t$  – Time (hr)

$A$  – Hardening coefficient ( $MPa^{-n}hr^{-m-1}$ )

$n$  – Stress exponent (no unit)

$m$  – Time exponent (no unit)

It is also to be noted that,

- A, n and m are temperature dependent material constants
- A, n and m are independent of stress, but depend on mechanism of creep
- Time hardening creep model holds good only at constant stress & temperature
- Strain hardening creep model holds good at constant temperature only

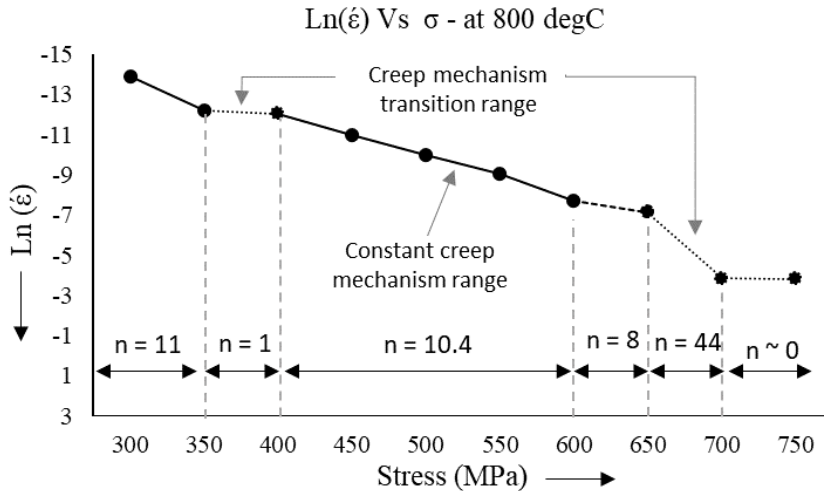
In time hardening form, since strain rates are dependent of time, analysis could be done only at constant stress & constant temperature. Any changes in stress will not affect the time exponent and hence analysis will be progressed with constant time exponent. In strain hardening form, any changes in stress will affect the creep strain which will affect the total creep strain rate. Hence, “strain-hardening form” is more accurate.

### 8.1. POWER LAW CONSTANTS CALCULATION

Detailed procedure for calculation of the power law constants for both time hardening & strain hardening creep models using power law regression has been laid out by (D. L. May, 2013).

To understand the stress dependence of creep rate,  $Ln(\dot{\varepsilon}_m)$  at different stress values ( $\sigma_i$ ) values taken from Table 7.2.1 are plotted as shown in Graph 8.1.1. Slope of the curve represents the stress exponent ‘n’. We can find from the graph that the stress exponent, ‘n’ is not constant throughout but varies for different range of stresses. This indicates the transition in rate controlling mechanism of creep. When dislocation glide process dominates, barriers are overcome thermally. For dislocation climb process, effect of applied stress in addition to temperature is required.

In both power law models, only primary & secondary creep data is considered and creep data from onset of tertiary stage is omitted for constant calculation.



Graph 8.1.1 - Creep strain rate Vs Stress – 800 degC

### 8.1.1.1. TIME HARDENING CONSTANTS

For every power law regression analysis, ‘n’ should be constant. So ‘n’ value should be calculated for every segment of the curve with constant slope (n). Using Bivariate regression, at constant temperature, for every stress range as indicated in Graph 8.1.1, stress exponent ‘n’ can be calculated as,

$$n = \frac{k \sum_{i=1}^k (\ln \sigma_i \ln \varepsilon_i) - \sum_{i=1}^k (\ln \sigma_i) \sum_{i=1}^k (\ln \varepsilon_i)}{k \sum_{i=1}^k (\ln \sigma_i)^2 - \left( \sum_{i=1}^k \ln \sigma_i \right)^2}$$

The result of stress exponent ‘n’ calculated at constant temperature of 800°C for different stress ranges is indicated in Graph 8.1.1.

Almost all the stress exponents are in power law breakdown regime ( $n > 7$ ) while creep mechanism transitions very low stress exponents are observed at stress ranges of 350 MPa – 400 MPa and at 600 MPa to 700 MPa.

Time exponent ‘m’ and constant ‘A’ for every given stress range (with constant stress exponent ‘n’) at constant temperature can be calculated as,

$$m = \frac{k \sum_{i=1}^k (\ln t_i \ln \varepsilon_i) - \sum_{i=1}^k (\ln t_i) \sum_{i=1}^k (\ln \varepsilon_i)}{k \sum_{i=1}^k (\ln t_i)^2 - \left( \sum_{i=1}^k \ln t_i \right)^2} \quad A = e^{\frac{\sum_{i=1}^k (\ln \varepsilon_i) - (1) \sum_{i=1}^k \ln(\sigma^n t^m)_i}{k}}$$

Using similar procedure, material constants for power law time hardening creep model at different temperatures for MAR-247 superalloy have been calculated and the results are shown in Table 8.1.1.

### 8.1.1.2. STRAIN HARDENING CONSTANTS

*Table 8.1.1 - Power law time hardening constant results*

Temperature (deg C)	800	900	950	1000
n	10.378	7.050	8.266	7.890
m	-0.352	-0.132	-0.060	-0.030
A	1.7318E-32	8.057E-22	4.0465E-24	3.907E-22

Procedure for calculation of strain hardening constants slightly different due to the expression of time component in terms of creep strain ' $\varepsilon'$ ' & stress exponent 'm'.

Time exponent 'm' can be found by regressing creep strain vs time data (excluding tertiary creep data) as,

$$m = \left[ \frac{\{(k \times \sum_{i=1}^k (\ln \varepsilon_i)^2) - (\sum_{i=1}^k \ln \varepsilon_i)^2\}}{(k \times \sum_{i=1}^k \{Ln(\varepsilon_i) \times Ln(t_i)\}) - \{\sum_{i=1}^k \ln(\varepsilon_i) \times \sum_{i=1}^k \ln(t_i)\}} \right] - 1$$

To calculate stress exponent 'n', the time (t) values for same creep strain ( $\varepsilon$ ) at different stresses are considered and regressed as,

$$n = -(m + 1) \times \left[ \frac{\{(k \times \sum_{i=1}^k \{(\ln \sigma_i) \times (\ln(t_i))\}) - (\{\sum_{i=1}^k \ln(\sigma_i)\} \times \{\sum_{i=1}^k \ln(t_i)\})\}}{\{(k \times \{\sum_{i=1}^k (\ln t_i)^2\}) - (\sum_{i=1}^k (\ln t_i))^2\}} \right]$$

With the same data, material constant A can be calculated as,

$$A = (m + 1) \times e^{-\frac{(k \times \left[ \left( \sum_{i=1}^k \ln(t_i) - \sum_{i=1}^k \left\{ \ln \left( \varepsilon_i^{\left(\frac{1}{m+1}\right)} \sigma_i^{-\left(\frac{n}{m+1}\right)} \right) \right\} \right])}{k}}}$$

Using similar procedure, material constants for power law strain hardening creep model at different temperatures for MAR-247 superalloy have been calculated and the results are shown in Table 8.1.2.

Using the above derived material constants, creep analysis using both power law creep models is performed in Abaqus on a sample creep test specimen as discussed in the next section.

*Table 8.1.2 - Power law Strain hardening constant results*

Temperature (degC)	800	900	950	1000
n	0.030	0.077	0.053	0.086
m	-0.357	-0.394	-0.457	-0.258
A	4.602E-04	1.011E-04	6.219E-03	1.480E-03

### 8.1.2. POWER LAW CREEP - ANALYSIS

Conventional creep test specimen has been modelled in Abaqus with the dimension as per (Tom H. Hyde, 2013) as shown in Figure 8.1.1. (Dimensions in mm).

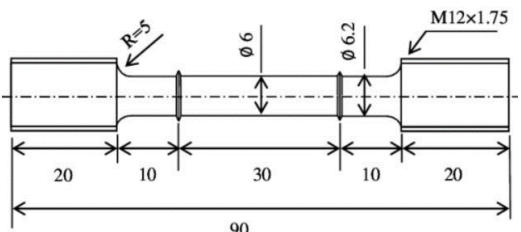


Figure 8.1.1 - Conventional creep test specimen

Threads are not modelled for simplicity and the geometry is meshed with 3D Linear (C3D6) wedge elements with global size of 1 mm and 0.75 mm on fillets. The mesh satisfies the basic quality metrics as below:

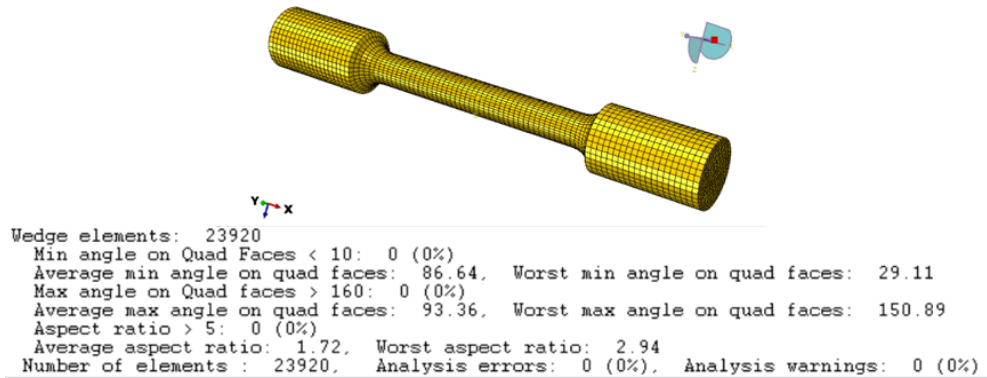


Figure 8.1.2 - Test specimen Mesh & Quality metrics

Boundary conditions are applied such that all degree of freedom (DOFs) is fixed on one of the end faces and a uniaxial tensile stress is applied on the opposite face such that uniform stress of 500 MPa is produced in the middle test section. Temperature of 800°C is applied on all the elements.

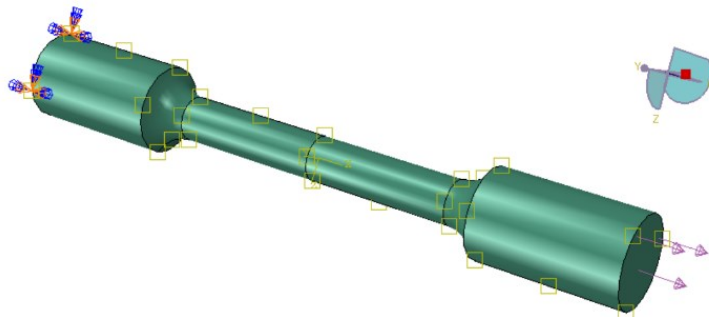


Figure 8.1.3 - Creep test specimen - Boundary conditions

The specimen is analyzed using power law time hardening & power law strain hardening creep models. Each analysis is carried out in two steps, a general static structural test for 0.001 hrs followed by visco step for 130 hrs with the applied load conditions with creep strain increment error tolerance (CETOL) of 0.001 and a time increment of 0.5 hrs.

## 8.2. POWER LAW CREEP - RESULTS

The results of the two analyses are compared. Contour plot of Von Mises equivalent stress at the end of creep step for both creep models is shown in Figure 8.2.1. Stress is almost uniform but not constant with respect to time in the test region. The small variation in Von Mises stress is due to progressive elemental area reduction during plastic (Creep) deformation leading to non-linearity.

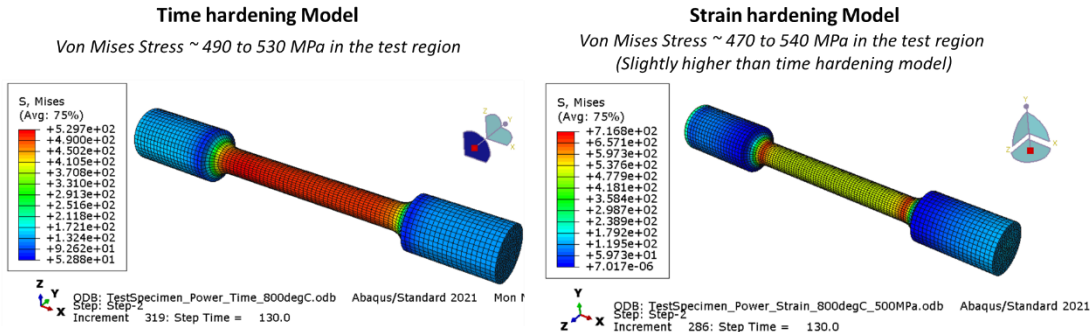


Figure 8.2.1 - Power law results - Von Mises Stress at 130 hrs

Contour plots of equivalent creep strain at the end of 130 hours for both the power law models are shown in Figure 8.2.2.

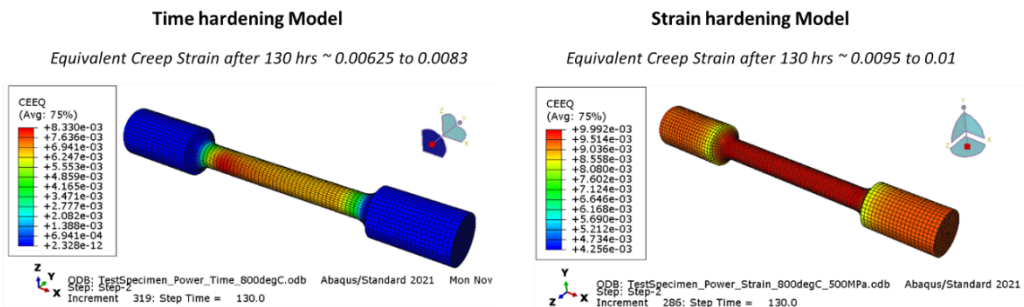


Figure 8.2.2 - Power law results - Equivalent creep strain at 130 hrs

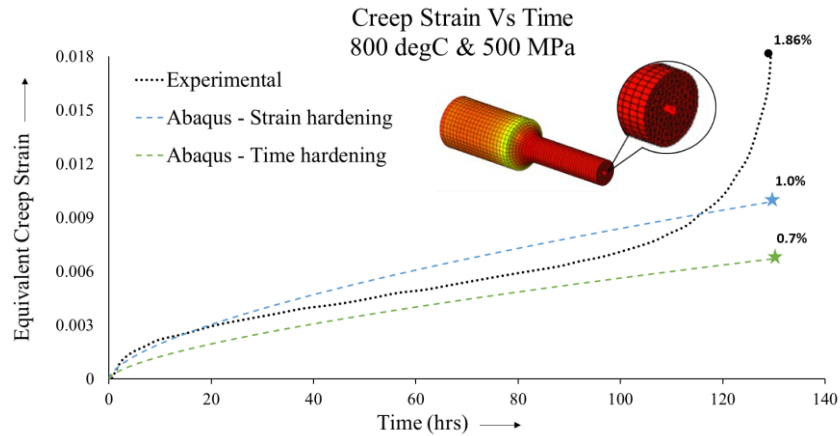
An element in the middle section is selected and evolution of equivalent creep strain with respect to time, ' $\varepsilon_{cr}$  vs  $t'$ ' is plotted for both power law models and compared with experimental creep data as shown in Graph 8.2.1.

### 8.2.1. POWER LAW CREEP ANALYSIS - INFERENCES

The following inferences can be drawn from the analysis results:

- Both the power law models predict fairly good result in the secondary creep stage, but predict lower values of tertiary creep
- Strain hardening model prediction is better than time hardening model

- Both Abaqus models do not indicate damage or time to creep rupture



**Graph 8.2.1 - Creep Strain Vs Time - Power law Vs Experimental Results**

This confirms the inadequacy of power law models for gas turbine application and validates the need for advanced models like Theta Projection Method.

## 9. THETA PROJECTION METHOD

Theta projection method is a mathematical method to describe all stages of creep, developed by (Evans R. W., 1982) and elaborated by (Evans & Wilshire, 1985). It was conceived as a mathematical method of interpolating and extrapolating creep properties of materials by expressing creep strain as a function of four different parameters called ‘Theta Coefficients’ as shown below:

$$\varepsilon_t = \theta_1(1 - e^{-\theta_2 t}) + \theta_3(e^{\theta_4 t} - 1) \quad (1)$$

where,

$\varepsilon_t$  – Creep Strain at time ‘t’

t – Time

$\theta_1$  – Primary creep strain scale factor

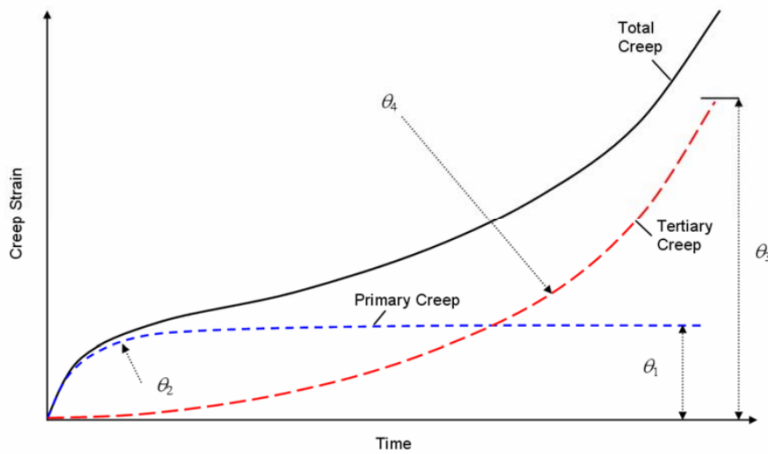
$\theta_2$  – Curvature of the primary creep

$\theta_3$  – Tertiary creep strain scale factor

$\theta_4$  – Curvature of tertiary creep

### 9.1. THETA COEFFICIENTS CALCULATION

$\theta_1$  represents the extent of primary creep while  $\theta_2$  represents the curvature or slope of primary creep.  $\theta_3$  decides the extent of tertiary creep while  $\theta_4$  controls the curvature of tertiary creep. By varying these Theta values, we can accurately describe the shape of any creep curve as shown in Graph 8.2.1.



Graph 8.2.1 - Physical interpretation of Theta coefficients

Theta coefficients are calculated by curve fitting creep strain Vs Time data obtained from uniaxial creep tests at different stress and temperature conditions. The statistical procedure for non-linear regression has been laid out by (Evans R. W., 1988) and validated further by (William Harrison, 2017). The method describes the use of a minimizing function  $\phi$  to minimize the Theta projection equation (1). Experimental creep strain ( $\varepsilon$ ) values at corresponding time (t) values are put in the equation along with assumed initial values of four Theta coefficients and the error between experimental strain value and the strain value

calculated through assumed initial Theta coefficients is calculated. The assumed Theta values are corrected based on the error values and the process is carried out at every data point (creep strain Vs time).

$$\phi^{n-1} = \sum_{i=1}^{n-1} [\varepsilon_i - \theta_1(1 - e^{-\theta_2 t_i}) + \theta_3(e^{\theta_4 t_i} - 1)]^2$$

By minimizing the sum of squares of error obtained from the minimizing function  $\phi$ , Theta coefficients for a given creep curve can be obtained.

The procedure can be simplified by using MATLAB ‘CurveFit’ tool which follows Least Square non-linear regression. Experimental data is usually obtained the form of strain vs time which has both elastic and plastic creep components. Instantaneous strain ( $\varepsilon_0$ ) which is the elastic component, is subtracted from all the strain values to get only the creep strain. Resulting data will start from creep strain value of 0 at time 0 as illustrated in Figure 9.1.1. It is found that Bisquare, Trust-Region algorithm gives better fit.

Time values are taken in “seconds” for more accurate results & to be consistent with Abaqus units.

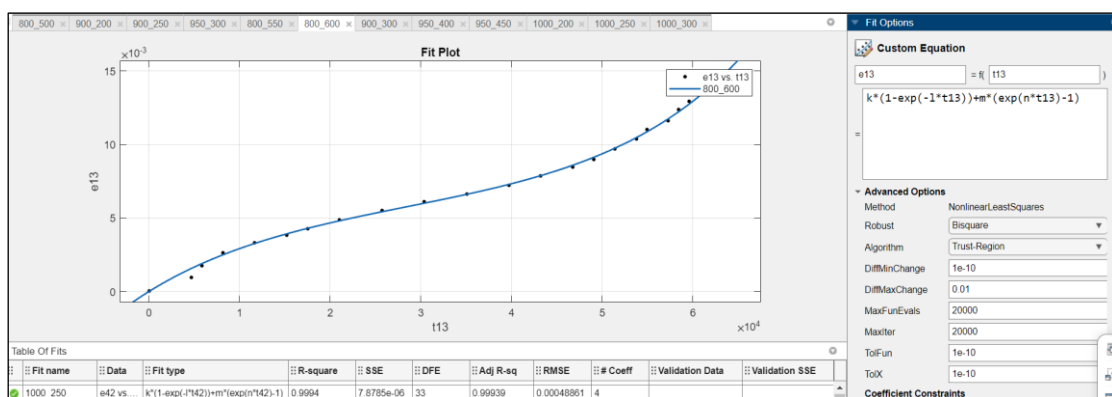


**Figure 9.1.1 - MATLAB CurveFit Tool**

Theta values taken from any reference literature is given as start point (initial guess) and lower bound is given as ‘0’ as theta values cannot be negative. Upper bound can also be given. Giving these bounds improves the fit. Theta projection equation is inputted as the regressing equation using the custom non-linear model in MATLAB CurveFit tool.<sup>12</sup>

<sup>12</sup> <https://www.mathworks.com/help/curvefit/custom-nonlinear-models.html>

### 9.1.1. GOODNESS OF FIT

A sample of results from curve fitting a creep curve of MAR-247 superalloy at  $800^{\circ}\text{C}$  and  $600 \text{ MPa}$  is illustrated in Figure 9.1.2. Goodness of fit can be seen visually by how accurately the curve covers all the data points.

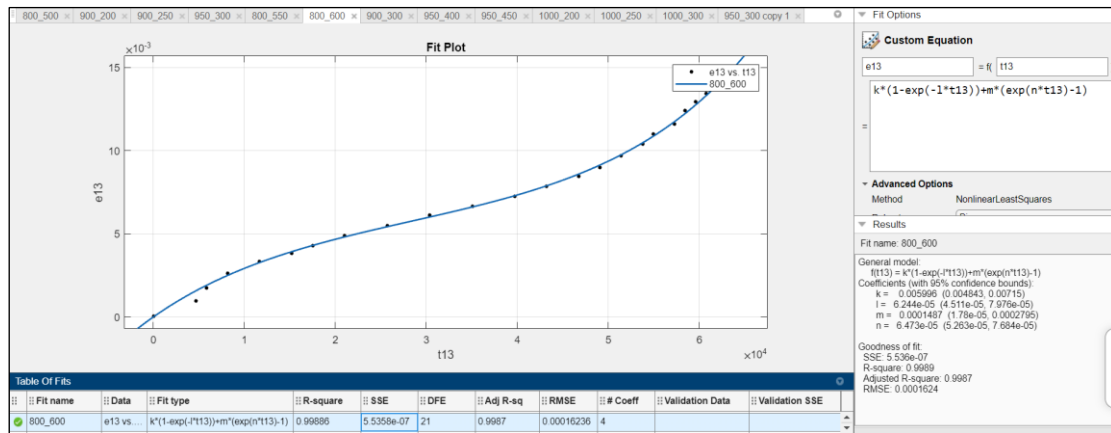


Figure 9.1.2 - CurveFit results

In addition, statistical parameters for goodness of fit are also displayed in the bottom right corner. Basic statistical guidelines for a good fit are as follows:

- Higher R-Square value (Close to 1) and lower SSE (close to 0) means a good fit.
- 95% confidence bounds of Theta coefficient values should be as close as possible.
- Infinity (displayed as 'inf') should not be a bound.
- Wider bounds indicate wider standard deviation and results will be inaccurate.

### 9.1.2. THETA COEFFICIENT RESULTS

By following similar procedure, curve fitting of creep curves of MAR-247 as displayed in Graph 7.2.1 at different temperature and stress conditions is done and the corresponding Theta coefficients are obtained from MATLAB CurveFit tool. Minimum of 6 significant figures of output Theta values should be obtained. The results are tabulated in Table 9.1.1.

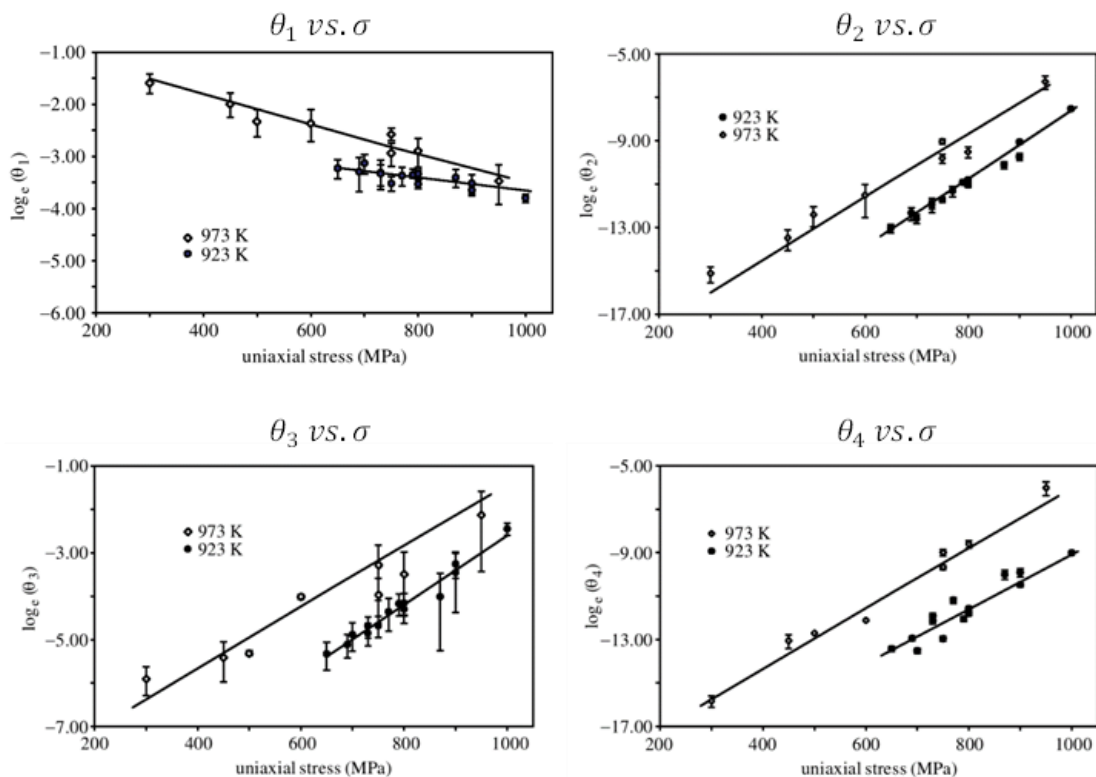
Table 9.1.1 - Theta coefficient results

Material	MAR-M247 EA	(From Matlab CurveFit Tool)				
		Last update	03rd March 2023	Theta 1	Theta 2	Theta 3
Temp (deg C)	Stress (MPa)					
800	500	6.480E-03	1.056E-05	1.942E-07	2.330E-05	
800	550	5.142E-03	3.673E-05	2.216E-03	5.440E-06	
800	600	7.190E-03	1.596E-04	2.659E-04	5.857E-05	
900	200	5.714E-01	4.402E-01	4.931E-09	3.540E-06	
900	250	8.146E-03	1.145E+00	7.672E-09	3.623E-06	
900	300	3.015E-03	4.800E-05	4.795E-03	2.629E-06	
950	300	6.044E-03	3.857E-04	5.305E-03	2.890E-05	
950	400	2.139E-02	1.638E-04	7.466E-03	2.021E-04	
950	450	9.411E-04	5.437E-02	2.722E-02	2.726E-04	

Accuracy of the arrived Theta coefficients is studied in later sections through analysis of variances and the Robust weighting scheme suggested by (Evans M. , 2002) has been adopted and proven to be better accurate as discussed in later sections.

## 9.2. MATERIAL CONSTANTS CALCULATION

By fitting experimental creep curve data with the Theta projection equation, the variation of four Theta coefficients with applied uniaxial stress at different temperatures was studied by (R.W.Evans, 1984) as illustrated in Graph 9.2.1. It was found that  $\ln(\theta)$  shows linear dependence with applied stress, temperature and product of stress & temperature. Also, it was found from biaxial creep tests that the tertiary Theta coefficients ( $\theta_3$  and  $\theta_4$ ) also depend on maximum principal stress ( $\sigma_1$ ) in addition to the applied uniaxial stress ( $\sigma$ ) when the mean stress ( $\sigma_m$ ) is positive. When mean stress is negative or zero, tertiary Theta coefficients are found to be independent of maximum principal stress.



*Graph 9.2.1 - Variation of Theta Coefficients with applied uniaxial stress*

This dependence of maximum principal stress can be neglected if we are dealing with uniaxial creep test data as,  $\sigma_1 = \sigma$ .

For uniaxial stress states, Theta coefficients can be expressed in terms of applied uniaxial stress and temperature as,

$$\begin{aligned}
 \ln(\theta_1) &= a_1 + b_1\sigma + c_1T + d_1\sigma T \\
 \ln(\theta_2) &= a_2 + b_2\sigma + c_2T + d_2\sigma T \\
 \ln(\theta_3) &= a_3 + b_3\sigma + c_3T + d_3\sigma T \\
 \ln(\theta_4) &= a_4 + b_4\sigma + c_4T + d_4\sigma T
 \end{aligned} \tag{2}$$

These material constants are independent of stress & temperature and can be used to interpolate or extrapolate creep data. For each Theta coefficient, there are four material constants and therefore with these 16 material constants, we can define creep properties of material at any temperature and stress conditions, neglecting microstructural effects or mechanism transitions.

### 9.2.1. UNIQUE SOLUTION

Each of the material constant equations (2) has 4 unknown constants (a, b, c & d). Theta values for different stress & temperature conditions arrived from curve fitting (Table 9.1.1) are the known variables. So, we need a minimum of 4 different creep curves (4 equation) to calculate the material constants algebraically by solving system of equations.

- There are ‘4 x 4’ theta values for ‘4’ different temp & stress conditions.
- There are 4 constants  $a_i$ ,  $b_i$ ,  $c_i$  and  $d_i$  for each Theta values ( $i=1$  to 4)
- The matrix equation is:

$$\begin{bmatrix} 1 & \sigma_1 & T_1 & \sigma_1 T_1 \\ 1 & \sigma_2 & T_2 & \sigma_2 T_2 \\ 1 & \sigma_3 & T_3 & \sigma_3 T_3 \\ 1 & \sigma_4 & T_4 & \sigma_4 T_4 \end{bmatrix}_{4 \times 4} \begin{bmatrix} a_1 \\ b_1 \\ c_1 \\ d_1 \end{bmatrix}_{4 \times 1} = \begin{bmatrix} \ln\theta_{11} \\ \ln\theta_{12} \\ \ln\theta_{13} \\ \ln\theta_{14} \end{bmatrix}_{4 \times 1}$$

- $\theta_{11}$  denotes  $\theta_1$  (primary scale factor) for test condition one (for  $\sigma_1$  and  $T_1$ )
- The 4 x 4 matrix is denoted as “y”

$$[y] \begin{bmatrix} a_i \\ b_i \\ c_i \\ d_i \end{bmatrix}_{i=1 \rightarrow 4} = \begin{bmatrix} \ln\theta_{i1} \\ \ln\theta_{i2} \\ \ln\theta_{i3} \\ \ln\theta_{i4} \end{bmatrix}_{i=1 \rightarrow 4}$$

- Taking the 4 x 4 matrix to the other is equivalent to taking inverse of matrix [y]

$$\begin{bmatrix} a_i \\ b_i \\ c_i \\ d_i \end{bmatrix}_{i=1 \rightarrow 4} = [y]^{-1} \begin{bmatrix} \ln\theta_{i1} \\ \ln\theta_{i2} \\ \ln\theta_{i3} \\ \ln\theta_{i4} \end{bmatrix}_{i=1 \rightarrow 4}$$

- Product of  $[y]^{-1}$  and  $[Ln\theta_{ii}]$  matrix gives the unique solution values of corresponding material constants  $a_i, b_i, c_i, d_i$

This calculation is done through a MATLAB code for as shown in Figure 9.2.1.

```

Current Folder
Name
Experiments
1
800degC_500MPa.txt
800degC_550MPa.txt
800degC_600MPa.txt
a1.m
createFit.m [a; b; c; d]
createFit1.m
Derivative.m
Material_constants_3d.m
Workspace
Name Value Size
k1 [-60.4423;0.0480;-0] 4x1
k2 [-124.9348;0.0919;-0] 4x1
k3 [308.8884;-0.2718;0] 4x1
k4 [-273.3360;0.2191;-0] 4x1

```

```

ln_th1=[-5.270368676; -4.935095887; -5.80403850; -6.968451787];
ln_th2=[-10.21180075; -8.742877077; -9.944369414; -2.911971994];
ln_th3=[-6.111913357; -8.232519834; -5.340194375; -3.603898897];
ln_th4=[-12.1217058; -9.745308587; -12.84901612; -8.207554773];

[y]=[1, 550000000, 1073, 5.9015E+11;
     1, 600000000, 1073, 6.438E+11;
     1, 300000000, 1173, 3.519E+11;
     1, 450000000, 1223, 5.5035E+11];

y_i=inv(y); ← Matrix inversion

k1=y_i*ln_th1;
k2=y_i*ln_th2;
k3=y_i*ln_th3;
k4=y_i*ln_th4; } Unique Solution

| Results

```

Figure 9.2.1 - MATLAB Code - Unique solution

## 9.2.2. LEAST SQUARE REGRESSION SOLUTION

We can also calculate 16 material constants with more than 4 equations (stress & temperature conditions) through linear regression methods. In such cases, analysis stress and temperature conditions should lie within the minimum and maximum stress and temperature values taken for material constant calculation. However, the solution is approximate and hence accuracy is less than that of a unique solution. Considering we have ‘n’ number of creep curves (n different load cases of stress & temperature). The corresponding matrix equation becomes,

$$\begin{bmatrix} 1 & \sigma_1 & T_1 & \sigma_1 T_1 \\ 1 & \sigma_2 & T_2 & \sigma_2 T_2 \\ \vdots & \vdots & \vdots & \vdots \\ 1 & \sigma_n & T_n & \sigma_n T_n \end{bmatrix}_{n \times 4} \begin{bmatrix} a_1 \\ b_1 \\ c_1 \\ d_1 \end{bmatrix}_{4 \times 1} = \begin{bmatrix} Ln\theta_{11} \\ Ln\theta_{12} \\ \vdots \\ Ln\theta_{1n} \end{bmatrix}_{n \times 1}$$

$$[y] \begin{bmatrix} a_i \\ b_i \\ c_i \\ d_i \end{bmatrix}_{i=1 \rightarrow 4} = \begin{bmatrix} Ln\theta_{i1} \\ Ln\theta_{i2} \\ Ln\theta_{i3} \\ Ln\theta_{i4} \end{bmatrix}_{i=1 \rightarrow 4}$$

Since this  $[y]_{n \times 4}$  matrix is not invertible as  $n > 4$ , unique solution cannot be obtained by matrix inversion. Instead, an approximate solution can be arrived for this over-determined system by using linear least square method as explained below:

- Consider the system of matrix equation, where  $[a]$  is the unknown

$$[y]_{n \times 4} [a]_{4 \times 1} = [t]_{n \times 1}$$

- It is assumed that there exists a column vector  $[k]_{n \times 1}$  such that

$$[a]_{4 \times 1} = [y]'_{4 \times n} [k]_{n \times 1}$$

- The matrix equation then becomes,

$$[y]_{n \times 4} ([y]'_{4 \times n} [k]_{n \times 1}) = [t]_{n \times 1}$$

- Changing the order of matrix multiplication,

$$([y]_{n \times 4} [y]'_{4 \times n}) [k]_{n \times 1} = [t]_{n \times 1}$$

- By doing so, the result of matrix product  $yy'$  becomes a square matrix of size  $n \times n$  and the system becomes invertible with unique solution.
- Initial solution of matrix  $[\hat{k}]$  is obtained by matrix inversion, as  $\hat{k} = (yy')^{-1}t$  and the initial guess solution of unknown constant matrix  $[\hat{a}]$  can be calculated as  $[\hat{a}] = [y]'[\hat{k}]$
- Error in this initial estimate is calculated as,  $\|t - y\hat{a}\|$
- Considering the magnitude and direction of error, the guess matrix  $[\hat{k}]$  is corrected and the procedure is repeated again.
- Considerably good solution is obtained by minimizing the sum of squares|

$$\text{Minimize} \|t - y\hat{a}\|^2 \rightarrow 0$$

This method is called ‘normalization’ and the corresponding function is called ‘norm’. There are other methods of solving overdetermined system of equations such as,

- QR decomposition
- Singular value decomposition (SVD)
- Eigen value decomposition, etc.

This procedure of solving system of overdetermined linear equations can be simplified by using the ‘/’ function in MATLAB as shown in Figure 9.2.2

```

Current Folder
Name
> Examples
  1
  800degC_500MPa.txt
  800degC_550MPa.txt
  800degC_600MPa.txt
  a1.m
  createFit.m
  [a1; b1; c1; d1]
  Material_constants_3d.m

Material_constants_U_MAR247.m x Material_constants_LS_MAR247.m x +
ln;
clear;

ln_th1=[ -5.270368676; -4.935095887; -5.80403850; -5.108752609; -3.844713325; -6.968451787];
ln_th2=[ -10.21180075; -8.742877077; -9.944369414; -7.860488104; -8.716692995; -2.911971994];
ln_th3=[ -6.111913357; -8.232519834; -5.340194375; -5.239049306; -4.897338012; -3.603898897];
ln_th4=[ -12.1217058; -9.745308587; -12.84901612; -10.45151334; -8.506599974; -8.207554773];

[y]=[1, 55000000, 1073, 5.9015E+11;
     1, 60000000, 1073, 6.438E+11;
     1, 30000000, 1173, 3.519E+11;
     1, 30000000, 1223, 3.669E+11;
     1, 40000000, 1223, 4.892E+11;
     1, 45000000, 1223, 5.5035E+11];

k1=y\ln_th1
k2=y\ln_th2
k3=y\ln_th3
k4=y\ln_th4

```

*ln( $\theta$ ) values*

*\ denotes solution by least square regression*

Results

Figure 9.2.2 - MATLAB Code - Least square solution

Material constants are very sensitive to stress and temperature values due to their exponential relation. Though unique solution of a, b, c and d theoretically works for all temperature and stress conditions, creep strain calculation in Abaqus may have convergence issues if strain rate goes high during extrapolation as the

error increases exponentially. Hence it is always recommended to calculate material constants using equations close to analysis stress & temperatures.

### 9.2.3. MATERIAL CONSTANT RESULTS

For calculations, unit of Temperature is taken as ‘K’ and that of stress is ‘ $N/m^2$ ’ and Time is ‘seconds’ The units of constants a, b, c and d are converted to be consistent for Abaqus system of units.

Material constants calculated through matrix inversion method (unique solution) by choosing 4 creep curves are shown in Table 9.2.1. Material constants calculated through linear least square regression (least square solution) by considering 6 creep curves are shown in Table 9.2.2.

It is found that the accuracy of creep calculations increases considering as much as precise values of the material constants as possible. Fortran alloys 17 digits in its double precision datatype including the sign and decimal point. At least 8 to 10 significant figures are recommended. Accuracy of the material constants has been studied in later sections and the Robust weighting scheme suggested by (Evans M. , 2002) has been adopted and proven to be better accurate as discussed in later sections.

**Table 9.2.1 - Material constants - Unique solution**

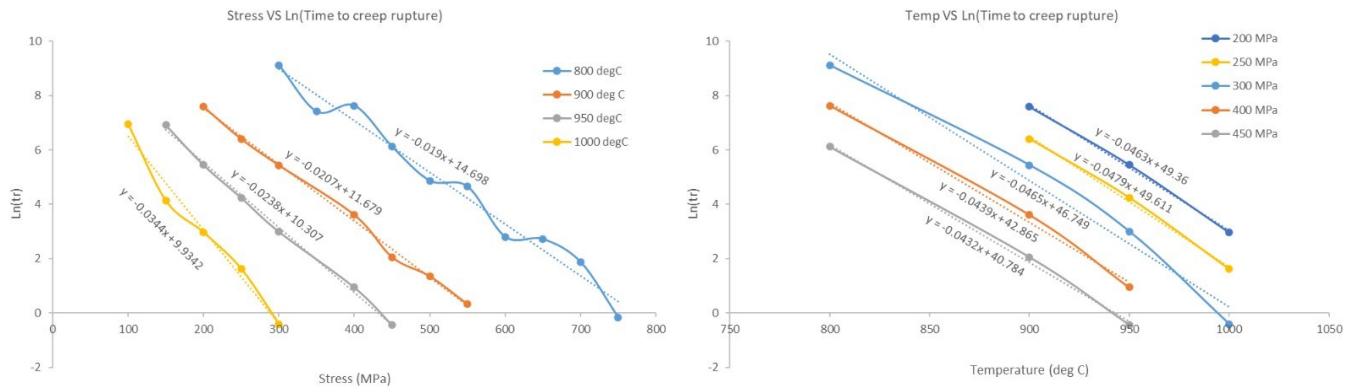
Material MAR-M247 EA Last update 03rd March 2023												
Material constants - Unique solution		(From Matlab CurveFit Tool)										
		Temp (deg C)	Stress (MPa)	Temp (K)	Stress (N/m <sup>2</sup> )	T*S (NK/m <sup>2</sup> )	Theta 1	Theta 2	Theta 3	Theta 4	Ln(Th1)	Ln(Th2)
		800	550	1073	550000000	5.902E+11	5.142E-03	3.673E-05	2.216E-03	5.440E-06	-5.270369	-10.2118
		800	600	1073	600000000	6.438E+11	7.190E-03	1.596E-04	2.659E-04	5.857E-05	-4.935096	-8.742877
		900	300	1173	300000000	3.519E+11	3.015E-03	4.800E-05	4.795E-03	2.629E-06	-5.804039	-9.944369
		950	450	1223	450000000	5.504E+11	9.411E-04	5.437E-02	2.722E-02	2.726E-04	-6.968452	-2.911972
			a				-6.04E+01	-1.25E+02	3.09E+02	-2.73E+02	-	
			b				1.37E-07	8.57E-08	-6.63E-07	4.32E-07	m <sup>2</sup> N <sup>-1</sup>	
			c				4.80E-02	9.19E-02	-2.72E-01	2.19E-01	K <sup>-1</sup>	
			d				-1.22E-10	-5.25E-11	5.78E-10	-3.58E-10	m <sup>2</sup> N <sup>-1</sup> K <sup>-1</sup>	
			a				-60.442330082	-124.93482160	308.88844321	-273.33598776	-	
			b				0.137448298	0.085670364	-0.663024438	0.432142084	mm <sup>2</sup> N <sup>-1</sup>	FOR FORTRAN CODE
			c				0.047981324	0.091859143	-0.271830089	0.219081000	K <sup>-1</sup>	
			d				-0.000121848	-0.000052462	0.000578390	-0.000358447	mm <sup>2</sup> N <sup>-1</sup> K <sup>-1</sup>	

**Table 9.2.2 - Material constants - Least Square solution**

Material MAR-M247 EA Last update 03rd March 2023												
Material constants -- Least square solution		(From Matlab CurveFit Tool)										
		Temp (deg C)	Stress (MPa)	Temp (K)	Stress (N/m <sup>2</sup> )	T*S (NK/m <sup>2</sup> )	Theta 1	Theta 2	Theta 3	Theta 4	Ln(Th1)	Ln(Th2)
		800	550	1073	550000000	5.902E+11	5.142E-03	3.673E-05	2.216E-03	5.440E-06	-5.2703687	-10.2118
		800	600	1073	600000000	6.438E+11	7.190E-03	1.596E-04	2.659E-04	5.857E-05	-4.9350959	-8.74288
		900	300	1173	300000000	3.519E+11	3.015E-03	4.800E-05	4.795E-03	2.629E-06	-5.8040385	-9.94437
		950	300	1223	300000000	3.669E+11	6.044E-03	3.857E-04	5.305E-03	2.890E-05	-5.1087526	-7.86049
		950	400	1223	400000000	4.892E+11	2.139E-02	1.638E-04	7.466E-03	2.021E-04	-3.8447133	-8.71669
		950	450	1223	450000000	5.504E+11	9.411E-04	5.437E-02	2.722E-02	2.726E-04	-6.9684518	-2.91197
			a				-7.703216E+01	-2.406420E+01	6.943288E+01	-1.214526E+02	-	
			b				1.480842E-07	-7.389613E-08	-1.932470E-07	1.343895E-07	m <sup>2</sup> N <sup>-1</sup>	
			c				6.132149E-02	6.240804E-03	-6.426105E-02	8.743329E-02	K <sup>-1</sup>	
			d				-1.280861E-10	8.171512E-11	1.675889E-10	-9.810599E-11	m <sup>2</sup> N <sup>-1</sup> K <sup>-1</sup>	
			a				-77.032158043600	-24.064196237154	69.432875938298	-121.45260933533	-	
			b				0.1480842073625	-0.0738961272302	-0.1932470047154	0.1343894895305	mm <sup>2</sup> N <sup>-1</sup>	FOR FORTRAN CODE
			c				0.0613214943858	0.0062408043698	-0.0642610486067	0.0874332920112	K <sup>-1</sup>	
			d				-0.0001280860924	0.0000817151245	0.0001675888950	-0.0000981059920	mm <sup>2</sup> N <sup>-1</sup> K <sup>-1</sup>	

### 9.3. FRACTURE STRAIN FORMULATION

Input data for time to creep fracture is obtained from uniaxial creep test. Rupture time for MAR-247 at different stresses and temperatures shows an exponential relation with stress and temperature. Natural logarithm of time to creep rupture shows linear relationship as shown below:



As per (Evans M. , 2002), creep strain at fracture can be modelled as an exponential function of stress, temperature and stress-temperature interaction similar to the material constants of Theta projection equation. For every test condition (stress & temperature), fracture strain  $\epsilon_f$  can be represented as,

$$\ln(\epsilon_f) = a_f + b_f \sigma + c_f T + d_f \sigma T$$

Where,  $a_f, b_f, c_f$  and  $d_f$  are the material constants for fracture strain.

Here, stress, temperature and creep strain at fracture are known from experimental data. With a minimum of four creep rupture data and initial guesses, the constants  $a_f, b_f, c_f$  and  $d_f$  are calculated by minimizing the below equation:

$$\min_{\sum \delta^2 \rightarrow 0} [a_f + b_f \sigma + c_f T + d_f \sigma T - \ln(\epsilon_f) + \delta]$$

This minimization problem can be simplified by using “least square regression” operator in MATLAB

#### 9.3.1. FRACTURE STRAIN CONSTANT CALCULATION

Fracture strain, stress & temperature for 9 creep test data are known from experimental data. Fracture strain constants  $a_f, b_f, c_f$  and  $d_f$  are calculated by least square regression by the MATLAB code as shown. Time to fracture data for 550 MPa has been modified to match with the rest of data assuming some error in that dataset.

#### 9.3.2. FRACTURE STRAIN CONSTANT RESULTS

Results of the MATLAB code for fracture strain constants are given below. The derived constants are found to predict fracture strain values with a reasonable accuracy.

**Table 9.3.1 - Fracture strain constants results**

Weights	Stress (MPa)	Temp (K)	T*S (kNK/mm <sup>2</sup> )	Time to Fracture (hrs) (Experimental)	Time to fracture (hrs) (Adjusted)	Time to fracture (s)	Fracture strain, (Experimental)	Ln(ef)	Fracture strain, (Calculated)	Deviation %
1	500	1073	536500	130	130	4.67E+05	0.018	-4.01738352	0.022	-20%
1	550	1073	590150	104	60	2.16E+05	0.026	-3.64965874	0.024	7%
1	600	1073	643800	16	16	5.92E+04	0.029	-3.54045945	0.027	7%
1	200	1173	234600	1986	1986	7.15E+06	0.053	-2.93746337	0.054	-3%
1	250	1173	293250	607	607	2.19E+06	0.054	-2.91877123	0.052	3%
1	300	1173	351900	231	231	8.31E+05	0.058	-2.84731227	0.050	16%
1	300	1223	366900	20	20	7.20E+04	0.085	-2.46510402	0.095	-12%
1	400	1223	489200	3	3	9.25E+03	0.078	-2.55104645	0.075	4%
1	450	1223	550350	1	1	2.33E+03	0.064	-2.7488722	0.066	-3%
	a <sub>f</sub>		<b>-2.88170858E+01</b>			-				
	b <sub>f</sub>		<b>3.57331943E-02</b>			MPa <sup>-1</sup>				
	c <sub>f</sub>		<b>2.22331983E-02</b>			K <sup>-1</sup>				
	d <sub>f</sub>		<b>-3.11971782E-05</b>			MPa <sup>-1</sup> K <sup>-1</sup>				

```

ln_ef=[-4.017383521
      -3.649658741
      -3.540459449
      -2.937463365
      -2.918771232
      -2.847312268
      -2.465104022
      -2.551046452
      -2.748872196];

[y]=[1 500 1073 536500
     1 550 1073 590150
     1 600 1073 643800
     1 200 1173 234600
     1 250 1173 293250
     1 300 1173 351900
     1 300 1223 366900
     1 400 1223 489200
     1 450 1223 550350];

k=[y\ln_ef];
format longG
k

```

**Figure 9.3.1 - MATLAB code for fracture constants**

Constants  $a_f$ ,  $b_f$ ,  $c_f$  and  $d_f$  can be used in Fortran code to calculate fracture strain for given stress and temperature to code for element deletion based on the calculated fracture strain.

## 9.4. CONSTITUTIVE EQUATIONS

Constitutive model of creep behaviour of particle hardened creep resistant alloys using Theta Projection Method was developed by (R.W.Evans, 1984) and is adopted as base of this project. As discussed previously in the sections 2.4. and 2.12., creep behavior of most superalloys can be modelled by considering the 3 underlying internal processes as internal variables namely,

- Dislocation hardening variable, H
- Softening or Recovery variable, R
- Damage variable, W

These internal processes may occur due to one or more micro mechanisms occurring in series or parallel and are functions of stress and temperature. The overall effect of each mechanism on these internal processes can be conceived as algebraic sum of the internal processes of each mechanism. The effect of these internal variables on creep strain rate of the material is given as,

$$\dot{\epsilon} = \dot{\epsilon}_0 [1 + H + R + W] \quad (3)$$

where,

$\dot{\epsilon}_0$  – Instantaneous (initial) creep strain rate

H – Hardening variable

R – Recovery variable

W – Damage variable

For a virgin material without any previous creep occurrence, the value of internal variables H, R and W are zero. Hence, the initial creep rate is unaffected and equal to the instantaneous or transient creep strain rate.

Hardening & damage are dynamic processes whereas recovery a static process. Rate of strain hardening  $\dot{H}$  and rate of damage  $\dot{W}$  are directly proportional to the creep strain rate  $\dot{\epsilon}$ . Rate of recovery is independent of creep strain rate. Hardening rate decreases with strain whereas rate of damage increases with strain.

Based on abovesaid behavior, expression for these internal variables in terms of creep strain rate can be given as follows:

$$\begin{aligned}\dot{H} &= -\hat{H}\dot{\epsilon} \\ \dot{R} &= \hat{R} \\ \dot{W} &= \hat{W}\dot{\epsilon}\end{aligned}\tag{4}$$

where,

$\hat{H}$  – Hardening coefficient

$\hat{R}$  – Recovery coefficient

$\hat{W}$  – Damage coefficient

These coefficients  $\hat{H}, \hat{R}$  and  $\hat{W}$  are proportionality constants and are positive values. They are constant for constant stress & temperature.

Effect of damage is to increase the creep strain rate. Since damage is insignificant in the primary stage, rate of change of creep strain rate can be given by differentiating equation (3) with respect to time as,

$$\ddot{\epsilon} = \dot{\epsilon}_0 [\dot{H} + \dot{R}] \tag{5}$$

From the equations (4),

$$\ddot{\epsilon} = \dot{\epsilon}_0 [-\hat{H}\dot{\epsilon} + \hat{R}]$$

Integrating the above equation with respect to creep strain rate from initial rate of  $\dot{\epsilon}_0$  to final creep rate of  $\dot{\epsilon}$ ,

$$\begin{aligned}\int_{\dot{\epsilon}_0}^{\dot{\epsilon}} \left( \frac{\ddot{\epsilon}}{[-\hat{H}\dot{\epsilon} + \hat{R}]} \right) d\dot{\epsilon} &= \int_0^t \dot{\epsilon}_0 dt \\ [Ln(-\hat{H}\dot{\epsilon} + \hat{R})]_{\dot{\epsilon}_0}^{\dot{\epsilon}} \times \left( \frac{1}{-\hat{H}} \right) &= \dot{\epsilon}_0 t \\ Ln \left[ \frac{-\hat{H}\dot{\epsilon} + \hat{R}}{-\hat{H}\dot{\epsilon}_0 + \hat{R}} \right] &= -\hat{H}\dot{\epsilon}_0 t \\ \frac{-\hat{H}\dot{\epsilon} + \hat{R}}{-\hat{H}\dot{\epsilon}_0 + \hat{R}} &= e^{-\hat{H}\dot{\epsilon}_0 t} \\ -\hat{H}\dot{\epsilon} + \hat{R} &= (-\hat{H}\dot{\epsilon}_0 + \hat{R}) \times e^{-\hat{H}\dot{\epsilon}_0 t} \\ -\hat{H}\dot{\epsilon} &= (-\hat{H}\dot{\epsilon}_0 + \hat{R}) \times e^{-\hat{H}\dot{\epsilon}_0 t} - \hat{R}\end{aligned}$$

$$\dot{\varepsilon} = \left[ \dot{\varepsilon}_0 - \frac{\hat{R}}{\hat{H}} \right] e^{-\hat{H}\dot{\varepsilon}_0 t} + \frac{\hat{R}}{\hat{H}} \quad (6)$$

In the expression for creep strain rate above, first term denotes the primary and steady state creep rate as it is time dependent whereas the second term  $\frac{\hat{R}}{\hat{H}}$  is constant for given stress and temperature and independent of time. Since hardening and softening are the dominant time dependent parameters in primary stage, this term  $\frac{\hat{R}}{\hat{H}}$  can be considered as small initial damage and will appear till the onset of tertiary stage after which damage becomes the significant rate controlling parameter and the creep rate derivation has to be corrected for damage term. Then equation (6) becomes,

$$\dot{\varepsilon} = \left[ \dot{\varepsilon}_0 - \frac{\hat{R}}{\hat{H}} \right] e^{-\hat{H}\dot{\varepsilon}_0 t} + \dot{\varepsilon}_t \quad (7)$$

where,  $\dot{\varepsilon}_t$  – Tertiary creep rate

Assume the constant term in equation (6) to be,  $\frac{\hat{R}}{\hat{H}} = \rho$  which is the damage at the onset of tertiary creep stage and will scale up the rate of tertiary creep rate.

Rate of change of tertiary creep rate depends on rate of damage  $\dot{W}$  scaled up by  $\rho$ .

$$\ddot{\varepsilon}_t = \rho \dot{W}$$

$$\frac{d\dot{\varepsilon}_t}{dt} = \rho \widehat{W} \dot{\varepsilon} \quad (\text{From equation (4)})$$

Integrating the above equation from initial value of  $\rho$  at onset of tertiary creep stage to tertiary creep rate  $\dot{\varepsilon}_t$ ,

$$\int_{\rho}^{\dot{\varepsilon}_t} \frac{d\dot{\varepsilon}_t}{\dot{\varepsilon}} = \int_0^t \rho \widehat{W} dt$$

$$\ln \left( \frac{\dot{\varepsilon}_t}{\rho} \right) = \rho \widehat{W} t$$

$$\dot{\varepsilon}_t = \rho e^{\rho \widehat{W} t}$$

Substituting the value of  $\rho$  back to  $\frac{\hat{R}}{\hat{H}}$ , we get the tertiary creep strain rate as,

$$\dot{\varepsilon}_t = \frac{\hat{R}}{\hat{H}} \times e^{\left( \frac{\hat{R} \widehat{W} t}{\hat{H}} \right)}$$

It has been observed that instantaneous creep strain rate  $\dot{\varepsilon}_0$  is not significant in the tertiary creep stage as tertiary creep strain rate  $\dot{\varepsilon}_t$  depends only on rate of damage  $\dot{W}$  and the damage at the onset of tertiary  $\frac{\hat{R}}{\hat{H}}$ . As we have derived the creep rate equations separately for primary-secondary and tertiary stages separately, equation (3) can be written as,

$$\dot{\varepsilon} = \dot{\varepsilon}_0 \left[ 1 + H + R + \frac{\hat{R}}{\hat{H}\dot{\varepsilon}_0} W \right] \quad (8)$$

Similarly, equation (6) which is the overall creep strain rate becomes,

$$\dot{\varepsilon} = \left[ \dot{\varepsilon}_0 - \frac{\hat{R}}{\hat{H}} \right] e^{-\hat{H}\dot{\varepsilon}_0 t} + \left[ \frac{\hat{R}}{\hat{H}} \right] e^{\left( \frac{\hat{R}\hat{W}}{\hat{H}} \right)t} \quad (9)$$

By integrating this creep rate equation from initial state to time ‘t’, creep strain can be expressed in terms of the internal variables as,

$$\varepsilon = \left[ \frac{\left( \dot{\varepsilon}_0 - \frac{\hat{R}}{\hat{H}} \right)}{\hat{H}\dot{\varepsilon}_0} \right] (1 - e^{-\hat{H}\dot{\varepsilon}_0 t}) + \left[ \frac{1}{\hat{W}} \right] \left( e^{\left( \frac{\hat{R}\hat{W}}{\hat{H}} \right)t} - 1 \right) \quad (10)$$

Comparing this with Theta projection equation, we get the expression for Theta coefficients in terms of internal variables as shown below.

$$\varepsilon_t = \theta_1 (1 - e^{-\theta_2 t}) + \theta_3 (e^{\theta_4 t} - 1)$$

$$\theta_1 = \frac{\left( \dot{\varepsilon}_0 - \frac{\hat{R}}{\hat{H}} \right)}{\hat{H}\dot{\varepsilon}_0}$$

$$\theta_2 = \hat{H}\dot{\varepsilon}_0$$

$$\theta_3 = \frac{1}{\hat{W}}$$

$$\theta_4 = \frac{\hat{R}\hat{W}}{\hat{H}}$$

By rearranging the above equations, expression for internal variables in terms of Theta coefficients are arrived as follow:

$$\dot{\varepsilon}_0 = \theta_1 \theta_2 + \theta_3 \theta_4$$

$$\hat{H} = \frac{\theta_2}{\theta_1 \theta_2 + \theta_3 \theta_4}$$

$$\hat{R} = \frac{\theta_2 \theta_3 \theta_4}{\theta_1 \theta_2 + \theta_3 \theta_4}$$

$$\hat{W} = \frac{1}{\theta_3} \quad (II)$$

Using the material constants derived in section 9.2.3., values of Theta coefficients can be calculated at any given stress and temperature values using equation (2). By using the calculated Theta values, instantaneous creep strain rate, hardening, recovery and damage coefficients can be calculated using equation (5) which in turn can be used to compute the hardening, recovery and damage rates using equation (4). Ultimately creep strain rate at any time ‘t’ can be computed by using equation (3) which upon integration gives the creep strain at any time ‘t’.

## 9.5. ABAQUS USER SUBROUTINE

Simulia ABAQUS is a computer aided engineering (CAE) software suite currently maintained by Dassault Systems, widely used for a variety of simulations such as static structural & thermal analysis, computational fluid dynamics and non-linear analysis like buckling, fatigue and creep.

Abaqus allows users to write their own “user-subroutines” to satisfy specific analysis requirements which cannot be satisfied by its inbuilt functions. User subroutines are written in C, C++ or Fortran language and usually compiled by ‘Intel Fortran compiler’ which is a part of ‘Microsoft Visual Studio development environment’. Input and output data of these subroutines are exchanged between Abaqus and the Fortran compiler through ‘Microsoft Incremental Linker’ which acts as an interface. Detailed procedure for preparing Abaqus to run user subroutines is explained well in the guide document.<sup>13</sup>

Abaqus has a set of predefined input & output arguments for time dependent viscoplastic deformation in its base subroutine “CREEP” which allows users to define creep behaviour in terms of input and output variables which are recognized by Abaqus so that data can be transferred in and out of Abaqus interactively. More information can be obtained from Abaqus documentation on writing subroutines<sup>14</sup>.

While performing a creep analysis in Abaqus, analysis is done in ‘increments’ and the solution is arrived in ‘iterations’ by the Abaqus inbuilt solver. Force equilibrium of the model may vary with time (iterations) due to the effect of nodal displacements (strain) caused by boundary conditions (loads). In explicit analysis, a ‘global stiffness matrix’ is formed in the beginning. In the successive iterations, solution is progressed by recalculating force equilibrium at the end of every iteration through forward or backward time integration. In implicit scheme, global stiffness matrix is also recalculated for every iteration.

In both cases, if the calculated residual force (error value of force equilibrium calculation) is within prescribed limits, the solution is said to be converged.

If solution did not converge, iteration is repeated with smaller and smaller time increment until convergence is obtained. If the solution is converged, analysis continues to the next iteration. Output is written for each iteration and can be visualized as contour plots.

The procedure for calculating creep strain using Theta Projection Method, laid out by (R.W.Evans, 1984) as discussed in the previous section is taken as the foundation for developing a Fortran code for user subroutine which could be used with Abaqus to analyse creep behaviour of gas turbine components.

The material constants derived from the creep curves are inputted in the Fortran subroutine. This subroutine is called by Abaqus at the start of increment at each integration point and theta values are calculated

---

<sup>13</sup> Ryan Enos, “Linking Abaqus 2022 & Intel oneAPI & Visual Studio in Windows 10 x64”,

<sup>14</sup> Abaqus documentation, “Writing User Subroutines with Abaqus”, 2022.

from the nodal stress & temperature values. The hardening, recovery and damage coefficients are calculated from the Theta values which will be used to calculate creep strain increment and stress gradient of creep strain increment. At the end of increment, internal state variables such as hardening, recovery and damage are updated and sent back to Abaqus and Abaqus solver is invoked once these output data is obtained on all integration points. Abaqus' inbuilt solver solves the force equilibrium at the end of increment after converting the strain values obtained from subroutine into nodal displacements. Convergence is checked and next iteration is proceeded. The results can be visualized by using Abaqus' visualization module as contour plots for each iteration. The process is continued till the end of all steps. This procedure is explained in Figure 9.5.1.

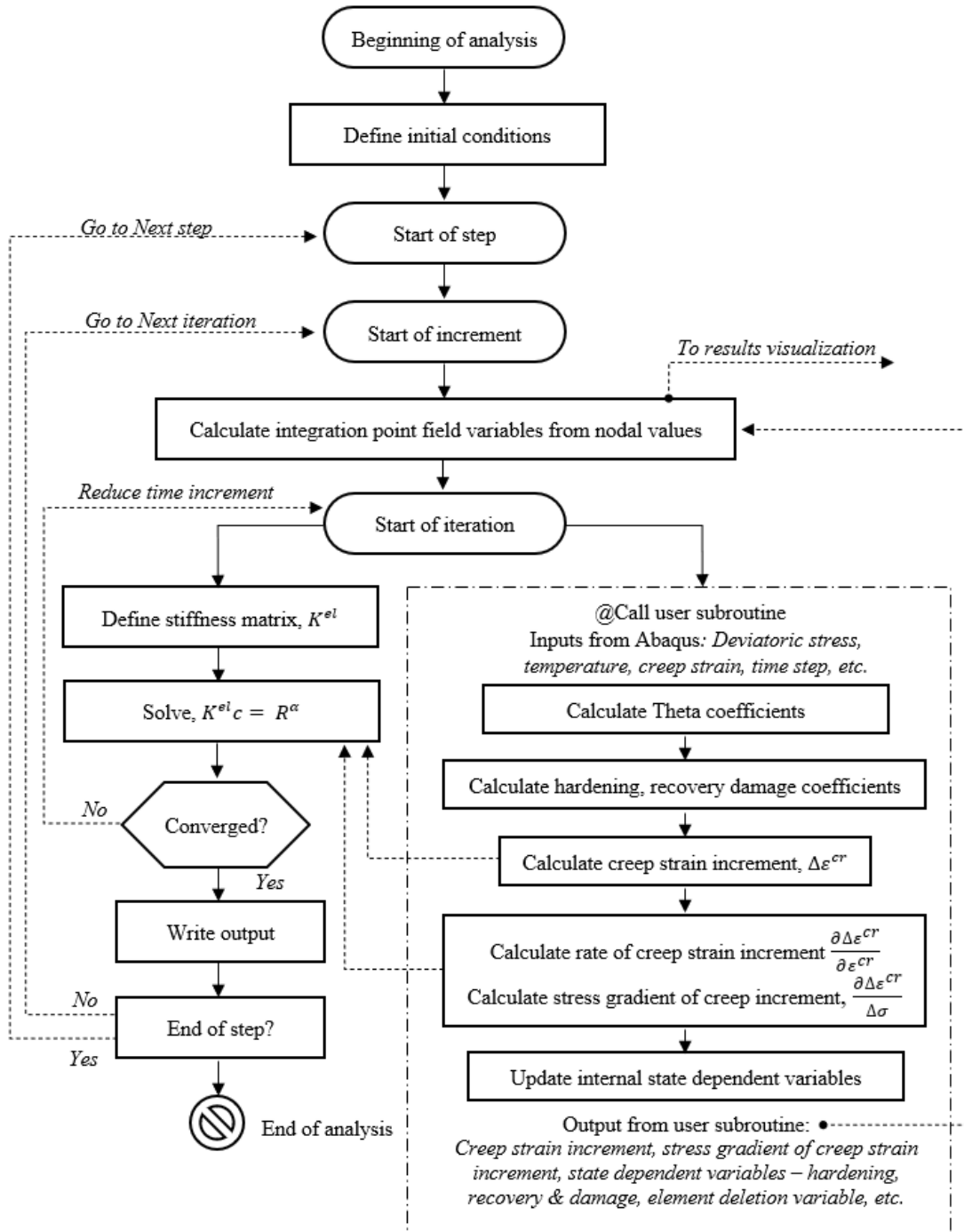


**Figure 9.5.1 - Abaqus User Subroutine Flow**

### 9.5.1. SUBROUTINE TERMINOLOGIES

Abaqus allows only prescribed input and output variables for subroutine. Important variables used in our subroutine are discussed in the section.

## QTILD

- Equivalent deviatoric stress (Mises),  $\tilde{q}$
- Deviatoric stress is the component of total stress responsible for plastic strain. Since creep is a plastic deformation phenomenon, volumetric swelling part of stress, called the hydrostatic or pressure stress has no effect. The second invariant of deviatoric stress component is the Von-Mises stress which is a scalar quantity.
- Creep behaviour is defined in subroutine as uniaxial equivalent “creep” strain rate,  $\dot{\bar{\varepsilon}}^{cr}$  as a function of time, Mises equivalent deviatoric stress,  $\tilde{q}$  and temperature.

## DECRA(1)

- Uniaxial equivalent of deviatoric (creep) strain increment,  $\Delta\bar{\varepsilon}^{cr}$
- Since experimental creep curve data corresponds to uniaxial stress and strain states, the creep strain value calculated by Theta projection method in the user subroutine in every time increment is the uniaxial equivalent of creep strain increment,  $\Delta\bar{\varepsilon}^{cr}$  which is addressed as DECRA(1).
- Abaqus converts this uniaxial equivalent creep strain to triaxial components of incremental creep strain as,  $\Delta\varepsilon^{cr} = n \times \Delta\bar{\varepsilon}^{cr}$   
‘n’ is the gradient of deviatoric stress potential  $(\partial\tilde{q}/\partial\sigma)$  at that integration point.
- This gradient ‘n’ converts the uniaxial equivalent stress and strain values into their components in triaxial state.

## DECRA(2)

- Rate of change of deviatoric creep strain increment with respect to deviatoric creep strain,  $\left(\frac{\partial\Delta\bar{\varepsilon}^{cr}}{\partial\bar{\varepsilon}^{cr}}\right)$
- Used in implicit creep integration where creep strain rates are to be controlled by using smaller time increments to avoid large displacements

## **DECRA(5)**

- Rate of change of deviatoric creep strain increment with respect to deviatoric Mises stress,  $\left(\frac{\partial \Delta \bar{\varepsilon}^{cr}}{\partial \tilde{q}}\right)$
- Used in implicit creep integration where creep strain rates are to be controlled by using smaller time increments to avoid large reduction in stress due to strain

## **EC(1)**

- Equivalent creep strain  $\bar{\varepsilon}^{cr}$  at the start of increment
- At the end of each increment, equivalent creep strain increment  $\Delta \bar{\varepsilon}^{cr}$  which is DECRA(1) is added to EC(1) to get the equivalent creep strain at the end of increment EC(2)

## **LEXIMP:**

- Flag for defining creep integration method
- Explicit integration scheme is used if LEXIMP = 0 and only DECRA(1) should to be defined. Subroutine is called both at the start and end of every iteration. Nodal creep calculations are done by Forward difference method. Faster method but faces convergence issues if strain rates are high or plasticity is present. By default, it automatically switches to implicit integration scheme when convergence issues are faced.
- Implicit integration scheme is used if LEXIMP = 1 and DECRA(1), DECRA(2) and DECRA(5) should to be defined. Subroutine is called only at the start of every iteration. Used backward integration and stiffness matrix is reformed every iteration. This process is slower by more stable than explicit scheme.

## **LEND:**

- Flag for defining when to call the subroutine
- Subroutine is called at the start of increment if LEND = 0
- Subroutine is called at the end of increment if LEND = 1 and any state variable must be updated in the subroutine

## **STATEV(\*):**

- Solution dependent state variable or SDV
- State variables are stored by Abaqus and are passed on to next increment
- State variables which are progressive with strain have to be updated in the subroutine itself otherwise they are passed on to next increment as such
- Number of solution dependent state variables is denoted as NSTATV
- We can define any number of state variables and the number inside bracket indicates the order. For example, STATEV(3) addresses the third state variable
- In our subroutine, we have defined hardening factor as STATEV(1), recovery factor as STATEV(2) and damage factor as STATEV(3).
- In addition, to visualize damage, a state variable ‘Z’ is defined whose value will be creep strain at the start of increment EC(1).
- When this creep strain crosses the fracture strain value (F) defined in subroutine, the element is deleted which helps to visualize damage

**TEMP** : Temperature at the end of increment

**DTIME** : Time increment

**TIME(1)** : Value of step time at the end of increment

**TIME(2)** : Value of total time at the end of increment

**TIME(3)** : Value of creep time at the end of increment

### 9.5.2. EQUATIONS FOR SUBROUTINE

In Abaqus, creep calculations are made in incremental basis and progressed with time. Hence it is necessary to rephrase the creep equations in incremental steps. Based on the above derivations, creep calculations in our user subroutine can be made as follows.

Creep strain rate as per equation (8) is given as,

$$\dot{\epsilon} = \dot{\epsilon}_0 \left[ 1 + H + R + \frac{\hat{R}}{\hat{H}\dot{\epsilon}_0} W \right]$$

For a small time increment  $\partial t$ , creep strain increment  $\Delta\epsilon$  can be calculated as,

$$\Delta\epsilon = \dot{\epsilon}_0 \left[ 1 + H + R + \frac{\hat{R}}{\hat{H}\dot{\epsilon}_0} W \right] \times \partial t \quad (12)$$

Above expression is used for DECRA(1).

State variables like hardening, recovery and damage can be calculated from the equation (4) as follows:

$$\begin{aligned} \dot{H} &= -\hat{H}\dot{\epsilon} \\ \dot{R} &= \hat{R} \\ \dot{W} &= \hat{W}\dot{\epsilon}_t \end{aligned}$$

where, creep strain rate is given as  $\dot{\epsilon} = \dot{\epsilon}_0[1 + H + R + W]$  from equation (3)

Since damage does not affect the rate of hardening, the damage term from equation (3) can be neglected for calculating rate of hardening as below:

$$\begin{aligned} \dot{H} &= -\hat{H}\dot{\epsilon}_0[1 + H + R] \\ \frac{\partial H}{\partial t} &= -\hat{H}\dot{\epsilon}_0[1 + H + R] \end{aligned}$$

For small time increment  $\partial t$ , expression for hardening at any time ' $t + \partial t$ ' is,

$$H_{t+\partial t} = H_t - (\hat{H}\dot{\epsilon}_0[1 + H + R]) \times \partial t \quad (13)$$

Rate of recovery from equation (4) can be written as,

$$\frac{\partial R}{\partial t} = \hat{R}$$

For small time increment  $\partial t$ , expression for recovery at any time ' $t + \partial t$ ' is,

$$R_{t+\partial t} = R_t + (\hat{R} \times \partial t) \quad (14)$$

Rate of damage is proportional to damage coefficient at tertiary creep strain rate.

$$\dot{W} = \hat{W} \dot{\epsilon}_t$$

This tertiary creep strain rate  $\dot{\epsilon}_t$  has a initial damage term  $\left(\frac{\hat{R}}{\hat{H}}\right)$  accumulated in the primary stage which is a constant till onset of tertiary as well as damage term 'W' which is again scaled up by this constant initial damage.

$$\dot{\epsilon}_t = \left(\frac{\hat{R}}{\hat{H}}\right) + \left(\frac{\hat{R}}{\hat{H}}\right) \times W$$

Hence rate of damage can be written as,

$$\frac{\partial W}{\partial t} = \hat{W} \times \left[ \left(\frac{\hat{R}}{\hat{H}}\right) + \left(\frac{\hat{R}}{\hat{H}}\right) \times W \right]$$

For small time increment  $\partial t$ , expression for damage at any time ' $t + \partial t$ ' is,

$$W_{t+\partial t} = W_t + \left[ \frac{\hat{W}\hat{R}}{\hat{H}} \times (1 + W_t) \right] \times \partial t \quad (15)$$

Equations (13), (14) and (15) are used for updating the state variables for every increment  $\partial t$ .

Derivatives of creep strain increment can be derived as follows:

DECRA(2) is the rate of change of creep strain increment with respect to creep strain. It can be written in terms of creep rate using chain rule as below:

$$\frac{\partial(\Delta\varepsilon)}{\partial\varepsilon} = \frac{\partial(\Delta\varepsilon)}{\partial t} \times \frac{\partial t}{\partial\varepsilon} = \frac{\partial(\Delta\varepsilon)}{\partial t} \times \frac{1}{\dot{\varepsilon}} \quad (16)$$

Creep strain rate  $\dot{\varepsilon}$  can be taken from equation (8) as,

$$\dot{\varepsilon} = \dot{\varepsilon}_0 \left[ 1 + H + R + \frac{\hat{R}}{\hat{H}\dot{\varepsilon}_0} W \right]$$

Creep strain increment as per equation (12) is,

$$\Delta\varepsilon = \dot{\varepsilon}_0 \left[ 1 + H + R + \frac{\hat{R}}{\hat{H}\dot{\varepsilon}_0} W \right] \times \partial t$$

where,  $\dot{\varepsilon}_0, \hat{R}$  and  $\hat{H}$  are constants with respect to time.

Differentiating with respect to time,

$$\frac{\partial(\Delta\varepsilon)}{\partial t} = \dot{\varepsilon}_0 \left[ \dot{H} + \dot{R} + \frac{\hat{R}}{\hat{H}\dot{\varepsilon}_0} \dot{W} \right] \times \partial t$$

Substituting the expressions for  $\dot{H}$ ,  $\dot{R}$  and  $\dot{W}$  from

$$\frac{\partial(\Delta\varepsilon)}{\partial t} = \dot{\varepsilon}_0 \left[ -\widehat{H}\dot{\varepsilon} + \widehat{R} + \left( \frac{\widehat{R}}{\widehat{H}\dot{\varepsilon}_0} \right) \widehat{W}\dot{\varepsilon} \right] \times \partial t$$

Rewriting  $\dot{\varepsilon}$  in terms of  $H$ ,  $R$  and  $W$ ,

$$\frac{\partial(\Delta\varepsilon)}{\partial t} = \dot{\varepsilon}_0 \left[ -\widehat{H}\dot{\varepsilon}_0[1+H+R+W] + \widehat{R} + \left( \frac{\widehat{R}}{\widehat{H}\dot{\varepsilon}_0} \right) \widehat{W}\dot{\varepsilon}_0 \left[ 1+H+R+\frac{\widehat{R}}{\widehat{H}\dot{\varepsilon}_0}W \right] \right] \times \partial t$$

Substituting  $\frac{\partial(\Delta\varepsilon)}{\partial t}$  and  $\dot{\varepsilon}$  back to equation (16),

$$\frac{\partial(\Delta\varepsilon)}{\partial\varepsilon} = \frac{\left( \dot{\varepsilon}_0 \left[ -\widehat{H}\dot{\varepsilon}_0[1+H+R+W] + \widehat{R} + \left( \frac{\widehat{R}\widehat{W}}{\widehat{H}} \right) \left[ 1+H+R+\frac{\widehat{R}}{\widehat{H}\dot{\varepsilon}_0}W \right] \right] \times \partial t \right)}{\dot{\varepsilon}_0 \left[ 1+H+R+\frac{\widehat{R}}{\widehat{H}\dot{\varepsilon}_0}W \right]}$$

Therefore, expression for DECRA(2) becomes,

$$\frac{\partial(\Delta\varepsilon)}{\partial\varepsilon} = \frac{\left[ -\widehat{H}\dot{\varepsilon}_0[1+H+R+W] + \widehat{R} + \left( \frac{\widehat{R}\widehat{W}}{\widehat{H}} \right) \left( 1+H+R+\frac{\widehat{R}}{\widehat{H}\dot{\varepsilon}_0}W \right) \right] \times \partial t}{1+H+R+\frac{\widehat{R}}{\widehat{H}\dot{\varepsilon}_0}W} \quad (17)$$

DECRA(5) is the rate of change of creep strain increment with respect to deviatoric Mises stress. Creep strain increment as per equation (12) is given as,

$$\Delta\varepsilon = \dot{\varepsilon}_0 \left[ 1+H+R+\frac{\widehat{R}}{\widehat{H}\dot{\varepsilon}_0}W \right] \times \partial t$$

Differentiating the above equation with respect to stress, we get,

$$\begin{aligned} \frac{\partial(\Delta\varepsilon)}{\partial\sigma} = & \left\{ [(b_1 + d_1T) + (b_2 + d_2T)\{1 + \ln(1+H+R)\}] \left( \dot{\varepsilon}_0 - \frac{\widehat{R}}{\widehat{H}} \right) (1+H+R) + [(b_3 + d_3T) + \right. \\ & \left. (b_4 + d_4T)\{1 + \ln(1+H+R+W)\}] \left( \frac{\widehat{R}}{\widehat{H}} \right) (1+H+R+W) \right\} \times \partial t \end{aligned} \quad (18)$$

The above expression is used for DECRA(5).

Fracture strain is calculated as.

$$\epsilon_f = e^{a_f + b_f\sigma + c_fT + d_f\sigma T}$$

### 9.5.3. SUBROUTINE – FORTRAN CODE

Fortran subroutine has been coded to perform creep calculations & evolution of internal state variables and integration with Abaqus. Separate Fortran codes are written for different cases like system of units undertaken such as “mm-s-MPa-N” or “mm-ms-GPa-kN” and nature of material constants such as

unique solution, least square regression solution, robust weighted least square solution, etc. A sample subroutine is discussed here for detailed line by line understanding of how the code works internally.

```

C Subroutine for Creep analysis using Theta Projection Method
C Updated 20thApr2023 by VaradhaYamunan KK
C Material constants derived for MAR-M-247 using Least Square regression
C Units: Stresses in MPa, Forces in N, lengths in mm, time in s
C
*USER SUBROUTINE
  SUBROUTINE CREEP(DECRA,DESWA,STATEV,SERD,EC,ESW,P,QTILD,TEMP,
1 DTEMP,PREDEF,DPRED,TIME,DTIME,CNAME,LEXIMP,LEND,COORDS,NSTATV,
2 NOEL,NPT,LAYER,KSPT,KSTEP,KINC)
C
  INCLUDE 'ABA_PARAM.INC'
C
  CHARACTER*80 CMNAME
C
  DIMENSION DECRA(5),DESWA(5),PREDEF(*),DPRED(*),TIME(3),STATEV(*),
1 COORDS(*),EC(2),ESW(2)
C
  DOUBLE PRECISION A1,B1,C1,D1,A2,B2,C2,D2,A3,B3,C3,D3,A4,B4,C4,D4,
1 TH1,TH2,TH3,TH4,EB,HC,RC,WC,H,R,W,T1,T2,T3,T4,HCxEB,Z,STRESS,F,
2 dQTILD, STRESSJUMP,AF,BF,CF,DF
C
  PARAMETER one=1.0d0
  PARAMETER asmall=1.0d-27
C
  DO I=1,5
    DECRA(I)=0.0d0
    DESWA(I)=0.0d0
  ENDDO
C
  LEND=0
C
C MATERIAL CONSTANTS FOR THETA COEFFICIENTS
C
  A1= -7.70321580436d1
  B1= 1.48084207363d-1
  C1= 6.13214943858d-2
  D1= -1.2808609245d-4
C
  A2= -2.40641962371d1
  B2= -7.3896127230d-2
  C2= 6.24080436984d-3
  D2= 8.17151244698d-5
C
  A3= 6.943287593830d1
  B3= -1.9324700471d-1
  C3= -6.4261048607d-2
  D3= 1.67588895002d-4
C
  A4= -1.21452609335d2
  B4= 1.34389489531d-1
  C4= 8.74332920112d-2
  D4= -9.8105992025d-5
C
C MATERIAL CONSTANTS FOR FRACTURE STRAIN
C
  AF= -2.88170858d+01
  BF= 3.57331943d-02
  CF= 2.22331983d-02
  DF= -3.11971782d-05
C
C CORRECTION FOR STRESS SINGULARITY DUE TO ELEMENT DAMAGE
C
  dQTILD = QTILD-STATEV(5)
C
  IF(STATEV(5).EQ.0.0d0) GO TO 1
  IF(dQTILD.EQ.0.0d0) GO TO 1
C
  STRESSJUMP = ABS(dQTILD/STATEV(5))

```

```

C
  IF(STRESSJUMP.GT.1.0d0) THEN
    STRESS = ABS(QTILD-dQTILD)
    GO TO 2
  ENDIF
C
  1 STRESS = QTILD
C
C DEFINE LOWER & UPPER LIMITS OF STRESS
C
  IF((STRESS.LE.10.0d0).OR.(STRESS.GE.1.4d3)) THEN
    DECRA(1)=asmall
    STATEV(4)=Z+DECRA(1)
  RETURN
  ENDIF
C
C THETA CALCULATIONS
C
  2 TH1=EXP(A1+(B1*STRESS)+(C1*TEMP)+(D1*TEMP*STRESS))
  TH2=EXP(A2+(B2*STRESS)+(C2*TEMP)+(D2*TEMP*STRESS))
  TH3=EXP(A3+(B3*STRESS)+(C3*TEMP)+(D3*TEMP*STRESS))
  TH4=EXP(A4+(B4*STRESS)+(C4*TEMP)+(D4*TEMP*STRESS))
C
C FRACTURE STRAIN TO DEFINE ELEMENT DELETION
C
  F=EXP(AF+(BF*STRESS)+(CF*TEMP)+(DF*STRESS*TEMP))
C
  IF(F.LT.1.0d-2)THEN
    F=1.0d-2
  ENDIF
C
C CONSTITUTIVE EQUATIONS
C (WITH APPROXIMATIONS TO PREVENT MATHEMATICAL SINGULARITY)
C
  EB=(TH1*TH2)+(TH3*TH4)
C
  IF(EB.eq.0.0d0) THEN
    EB=asmall
  ENDIF
C
  HC=(TH2/EB)
C
  RC=(HC)*(TH3*TH4)
C
  IF(TH3.eq.0.0d0) THEN
    TH3=asmall
  ENDIF
C
  IF(TH2.eq.0.0d0) THEN
    TH2=asmall
  ENDIF
C
  WC=(one/TH3)
C

C STATE VARIABLES DECLARATION
C
  H=STATEV(1)
  R=STATEV(2)
  W=STATEV(3)
  Z=STATEV(4)
C
C CREEP STRAIN INCREMENT CALCULATION
C
  DECRA(1) = (EB*(one+H+R+(W*RC/(TH2)))*DTIME)
C
  IF(DECRA(1).LT.0.0d0) THEN
    DECRA(1)=asmall
  ENDIF
C
  Z=EC(1)
C
C CALCULATION OF DECRA(2) & DECRA(5) FOR IMPLICIT INTEGRATION
C

```

```

IF(LEXIMP.EQ.1) THEN
C
DECRA(2) = ((((-HC*EB)*(one+H+R+W))+RC+((RC*WC/HC)*
1(one+H+R+((RC*W)/(HC*EB)))))*DTIME)/
2(one+H+R+(RC*W/(HC*EB)))
C
T1 = B1+(D1*TEMP)
T2 = B2+(D2*TEMP)
T3 = B3+(D3*TEMP)
T4 = B4+(D4*TEMP)
C
DECRA(5) = (((T1+T2*(one+LOG(one+H+R)))*(EB-(RC/HC))*(one+H+R))+*
1((T3+T4*(one+LOG(one+H+R+W)))*(RC/HC)*(one+H+R+W)))*DTIME
C
ENDIF
C UPDATING STATE VARIABLES
C
3 STATEV(1) = H-((one+H+R)*HC*EB*DTIME)
STATEV(2) = R+(RC*DTIME)
STATEV(3) = W+((one+W)*(WC*RC/HC)*DTIME)
STATEV(4) = Z+DECRA(1)
STATEV(5) = STRESS
C
IF (STATEV(4).GE.F) THEN
    STATEV(4)=0.0d0
ENDIF
C
4 RETURN
END

```

#### 9.5.4. SUBROUTINE – EXPLANATION

Fortran code for user subroutine created for creep analysis using Theta projection method is discussed in this section. ‘C’ denotes comments which are not compiled and only for explanation purposes. Fortran is not case sensitive and codes in small cases or capital letters are read as same. For readability, explanations are provided in between the codes and the actual Fortran code is attached in the next section. It is best practice to start the first section of code with titles, updated date, coder name and the other important data for future references.

```

C Subroutine for Creep analysis using Theta Projection Method
C Updated 20thApr2023 by VaradhaYamunan KK
C Material constants derived for MAR-M-247 using Least Square regression
C Units: Stresses in MPa, Forces in N, lengths in mm, time in s
C
*USER SUBROUTINE
    SUBROUTINE CREEP(DECRA,DESWA,STATEV,SERD,EC,ESW,P,QTILD,TEMP,
1 DTEMP,PREDEF,DPRED,TIME,DTIME,CMNAME,LEXIMP,LEND,COORDS,NSTATV,
2 NOEL,NPT,LAYER,KSPT,KSTEP,KINC)

```

Subroutine named “CREEP” along with all variables used in the subroutine are declared in the brackets. These are the standard variables for any creep subroutine in Abaqus and may not be altered. The numbers in 6<sup>th</sup> digit of second and third lines indicate a line break. Fortran allows only 66 digits in a line. If we need to write more than 66 characters in a line, it can be written in next line with a reference number or character in the 6<sup>th</sup> digit as shown above. All code should be written from the 7<sup>th</sup> digit. Line reference for go to commands can be provided in the 4<sup>th</sup> digit.

```
INCLUDE 'ABA_PARAM.INC'
```

The file “ABA\_PARAM.INC” is called upon. This file has the instructions to call the compiler to compile the subroutine and linker to act as an interface for exchange of input and output data in and out of Abaqus.

```
CHARACTER*80 CMNAME
```

Declares the material name as character datatype with maximum of 80 digits. ‘CMNAME’ denotes the name of the material as given in Abaqus.

```
DIMENSION DECRA(5),DESWA(5),PREDEF(*),DPRED(*),TIME(3),STATEV(*),
1 COORDS(*),EC(2),ESW(2)
```

Declares the dimension of arrays used in the subroutine. Number in the brackets indicate the number of columns in the array. For example DECRA(5) in this declaration denotes that there are 5 columns in the array namely DECRA(1), DECRA(2), DECRA(3), DECRA(4) and DECRA(5). Asterisk \* is mentioned in the brackets if the size of array is not known.

```
DOUBLE PRECISION A1,B1,C1,D1,A2,B2,C2,D2,A3,B3,C3,D3,A4,B4,C4,D4,
1 TH1,TH2,TH3,TH4,EB,HC,RC,WC,H,R,W,T1,T2,T3,T4,HCxEB,Z,STRESS,F,
2 dQTILD, STRESSJUMP,AF,BF,CF,DF
```

Declares variables used in the subroutine as ‘double precision’ datatype. Double precision datatype allows 8-byte floating point with 17 digits including decimal point and sign. Constants are expressed with a ‘d’ indicating double precision. For example, 0.24567 is written as 2.4567d-1

```
PARAMETER one=1.0d0
PARAMETER asmall=1.0d-27
```

The value ‘1’ is declared as a parameter of double precision datatype as calculations can be performed only with values of similar datatypes. For example, 1+3.0d2 is calculated as 3.01E2 where ‘E’ denotes the 4-byte datatype “REAL” which only has 7 digits and hence precision is lost. “asmall” is a small value  $1 \times 10^{-28}$  declared as a parameter and will be used to prevent numerical singularity, i.e., when ‘0’ appears in denominator in calculations, this small number replaces the ‘0’ to avoid infinity.

```
DO I=1,5
DECRA(I)=0.0d0
DESWA(I)=0.0d0
ENDDO
```

Initializing the values of DECRA(1) to DECRA(5) and DESWA(1) to DESWA(5) as zero. This clears any stray value during start of the increment.

```
LEND=0
```

LEND = 0 denotes the subroutine is called at the start of increment

If LEND = 1 was mentioned, subroutine will be called at the end of increment

```
C MATERIAL CONSTANTS FOR THETA COEFFICIENTS
```

```
A1= -7.70321580436d1
B1= 1.48084207363d-1
C1= 6.13214943858d-2
D1= -1.2808609245d-4
```

```
A2= -2.40641962371d1
```

```
B2= -7.3896127230d-2
C2= 6.24080436984d-3
D2= 8.17151244698d-5
```

C

```
A3= 6.943287593830d1
B3= -1.9324700471d-1
C3= -6.4261048607d-2
D3= 1.67588895002d-4
```

C

```
A4= -1.21452609335d2
B4= 1.34389489531d-1
C4= 8.74332920112d-2
D4= -9.8105992025d-5
```

The 16 material constants derived from creep curves are declared in double precision datatype format. 17 digits including decimal places, sign, ‘d’ and powers are allowed. Values with digits 17 digits will result in omission of any digit which may result in serious calculation errors. It is recommended to use at least 8 to at most 12 significant figures for a good accuracy.

#### C MATERIAL CONSTANTS FOR FRACTURE STRAIN

```
AF= -2.88170858d+01
BF= 3.57331943d-02
CF= 2.22331983d-02
DF= -3.11971782d-05
```

Fracture strain constants to calculate fracture strain for given stress and temperature which will be used for element deletion. If creep strain crosses the calculated strain, element is deleted. Logic for this is given later in the code.

#### C CORRECTION FOR STRESS SINGULARITY DUE TO ELEMENT DAMAGE

```
C
dQTILD = QTILD-STATEV(5)
C
IF(STATEV(5).EQ.0.0d0) GO TO 1
IF(dQTILD.EQ.0.0d0) GO TO 1
C
STRESSJUMP = ABS(dQTILD/STATEV(5))
C
IF(STRESSJUMP.GT.1.0d0) THEN
STRESS = ABS(QTILD-dQTILD)
GO TO 2
ENDIF
C
1 STRESS = QTILD
C
```

“STRESS” is a variable which will be used for the calculation of Theta coefficients. Initially value of stress is set to be equal to QTILD which is the Von Mises stress calculated by Abaqus at that integration point in that increment. As, stress is not constant with time during analysis, it is set to be equal to a state variable which is STATEV(5). The above segment of code is written to prevent calculation error due to stress singularity which occurs due to excessive deformation or element deletion as area reduces in some region resulting in value of QTILD which is the stress jumping high or low suddenly. This high stress values results in high creep strain which in turn increases stress further. The above logical loops smoothen these sudden stress-jumps.

Initially STATEV(5) will be zero and analysis starts with STRESS = QTILD later in the code, STATEV(5) is set equal to STRESS. In the next increment if QTILD which is the Von Mises stress calculated

by Abaqus may increase or decrease due to straining. “dQTILD” is a variable declared to measure the amount of increase or decrease in stress at a point between two successive increments. This is done by subtracting the value of stress in previous increment which was retained by STATEV(5) from QTILD which is the stress value at the start of current increment as  $dQTILD = QTILD - STATEV(5)$

If there is no stress change, code proceeds with STRESS = QTILD. If there is change in stress, extent of change is measured by the variable “STRESSJUMP” which is set equal to the absolute value of ratio of change in stress to original stress. High value of stress jump may indicate stress singularity or excessive deformation and affects creep calculation. If stress jump is greater than 100%, creep calculation is proceeded with original (lower) stress (in previous increment) by subtracting the change in stress (dQTILD) from the increased stress (QTILD).

This above section of code may be omitted if stress singularity or high strains are not expected in the model. The number ‘1’ in last line of the above section indicates address for any “go to” commands and must be the 5<sup>th</sup> character in the line.

```
C DEFINE LOWER & UPPER LIMITS OF STRESS
C
IF((STRESS.LE.10.0d0).OR.(STRESS.GE.1.4d3)) THEN
  DECRA(1)=asmall
  STATEV(4)=Z+DECRA(1)
RETURN
ENDIF
C
```

Above section sets the lower and upper limits of stress for creep calculation. Very high or very low values of stress produces very high or very low creep strain rates which might require very low time increments. Since creep effects are not significant at very low stresses and very high stress results in transient fractures, it is coded that creep strain is not calculated when stress value is not within these bounds, which are assumed to be 10 MPa and 1400 MPa for the scope of analysis.

When stress is less than 10 MPa or greater than 1400 MPa, creep strain increment value is set to be “asmall” which was declared as  $1 \times 10^{-27}$  earlier. The command “RETURN” simply stops the subroutine at that line abruptly and returns whatever output obtained till that line to Abaqus.

```
C THETA CALCULATIONS
C
2 TH1=EXP(A1+(B1*STRESS)+(C1*TEMP)+(D1*TEMP*STRESS))
TH2=EXP(A2+(B2*STRESS)+(C2*TEMP)+(D2*TEMP*STRESS))
TH3=EXP(A3+(B3*STRESS)+(C3*TEMP)+(D3*TEMP*STRESS))
TH4=EXP(A4+(B4*STRESS)+(C4*TEMP)+(D4*TEMP*STRESS))
```

Theta coefficients are calculated as per equation  $\theta_i = e^{a_i + b_i\sigma + c_iT + d_iT\sigma}$ ,  $i = 1 \text{ to } 4$ . Each Theta coefficient is represented as TH1, TH2, TH3 and TH4.

```
C FRACTURE STRAIN TO DEFINE ELEMENT DELETION
C
F=EXP(AF+(BF*STRESS)+(CF*TEMP)+(DF*STRESS*TEMP))
C
IF(F.LT.1.0d-2)THEN
```

```
F=1.0d-2  
ENDIF
```

C

Fracture strain is calculated for given stress and temperature at every integration point. Since this is a regressed formulation, for low stresses and temperatures, the calculated fracture strain value may be very low and element may be deleted at very low strain (% elongation). To prevent this, 1% is set as minimum fracture strain.

```
C CONSTITUTIVE EQUATIONS  
C (WITH APPROXIMATIONS TO PREVENT MATHEMATICAL SINGULARITY)  
C  
    EB=(TH1*TH2)+(TH3*TH4)  
C  
    IF(EB.eq.0.0d0) THEN  
        EB=asmall  
    ENDIF  
C  
    HC=(TH2/EB)  
C  
    RC=(HC)*(TH3*TH4)  
C  
    IF(TH3.eq.0.0d0) THEN  
        TH3=asmall  
    ENDIF  
C  
    IF(TH2.eq.0.0d0) THEN  
        TH2=asmall  
    ENDIF  
C  
    WC=(one/TH3)  
C
```

Constitutive equations for creep given by (R.W.Evans, 1984) as explained in section 9.4. are coded. Relation between internal variables and the Theta coefficients as per equation (5) are defined here. EB is variable for instantaneous creep strain rate  $\dot{\epsilon}_0$ . HC is the hardening coefficient  $\hat{H}$ . Since EB appears in the denominator in calculation of HC, it is set to be ‘asmall’ if it is zero, to prevent numerical singularity. RC is the recovery coefficient  $\hat{R}$  and WC is the damage coefficient  $\hat{W}$ . Since TH3 appears in denominator, it is set as ‘asmall’ if it is zero.

```
C STATE VARIABLES DECLARATION  
C  
    H=STATEV(1)  
    R=STATEV(2)  
    W=STATEV(3)  
    Z=STATEV(4)
```

C

Hardening is declared as state variable (1). Recovery is declared as state variable (2). Damage is declared as state variable (3). Z is a variable declared as state variable (4) which will be useful for element deletion, as declared later in the code.

```
C CREEP STRAIN INCREMENT CALCULATION  
C  
    DECRA(1) = (EB*(one+H+R+(W*RC/(TH2)))*DTIME)  
C  
    IF(DECRA(1).LT.0.0d0) THEN
```

```
DECRA(1)=asmall
```

```
ENDIF
```

```
C
```

```
Z=EC(1)
```

DECRA(1) is the deviatoric equivalent creep strain increment  $\Delta\bar{\varepsilon}^{cr}$  which is calculated in terms of internal variables by time integration of equation (8) in section 9.3. as

$$\partial\varepsilon = \dot{\varepsilon}_0 \left[ 1 + H + R + \frac{\hat{R}}{\hat{H}\dot{\varepsilon}_0} W \right] \times \partial t$$

To prevent calculation errors, this is set to be ‘asmall’ when it goes less than or equal to zero. The variable Z is set to be equal to Equivalent creep strain at the start of increment EC(1)

```
C CALCULATION OF DECRA(2) & DECRA(5) FOR IMPLICIT INTEGRATION
```

```
C
```

```
IF (LEXIMP.EQ.1) THEN
```

```
C
```

```
DECRA(2) = ((((-HC*EB)*(one+H+R+W))+RC+((RC*WC/HC)*  
1(one+H+R+((RC*W)/(HC*EB)))))*DTIME)/  
2(one+H+R+(RC*W/(HC*EB)))
```

```
C
```

```
T1 = B1+(D1*TEMP)  
T2 = B2+(D2*TEMP)  
T3 = B3+(D3*TEMP)  
T4 = B4+(D4*TEMP)
```

```
C
```

```
DECRA(5) = (((T1+T2*(one+LOG(one+H+R)))*(EB-(RC/HC))*(one+H+R))+  
1 ((T3+T4*(one+LOG(one+H+R+W)))*(RC/HC)*(one+H+R+W)))*DTIME
```

```
C
```

```
ENDIF
```

```
C
```

DECRA(2) is the rate of change of deviatoric equivalent creep strain increment with respect to equivalent creep strain  $\partial\Delta\bar{\varepsilon}^{cr}/\partial\bar{\varepsilon}^{cr}$ . As per equation (17), DECRA(2) can be given as below:

$$\frac{\partial(\Delta\varepsilon)}{\partial\varepsilon} = \frac{\left[ -\hat{H}\dot{\varepsilon}_0 [1 + H + R + W] + \hat{R} + \left( \frac{\hat{R}\hat{W}}{\hat{H}} \right) \left( 1 + H + R + \frac{\hat{R}}{\hat{H}\dot{\varepsilon}_0} W \right) \right] \times \partial t}{1 + H + R + \frac{\hat{R}}{\hat{H}\dot{\varepsilon}_0} W}$$

DECRA(5) can be calculated by differentiating equation (18) w.r.t. stress as follows:

$$\begin{aligned} \frac{\partial(\Delta\varepsilon)}{\partial\sigma} = & \left\{ [(b_1 + d_1 T) + (b_2 + d_2 T)\{1 + \ln(1 + H + R)\}] \left( \dot{\varepsilon}_0 - \frac{\hat{R}}{\hat{H}} \right) (1 + H + R) \right. \\ & \left. + [(b_3 + d_3 T) + (b_4 + d_4 T)\{1 + \ln(1 + H + R + W)\}] \left( \frac{\hat{R}}{\hat{H}} \right) (1 + H + R + W) \right\} \times \partial t \end{aligned}$$

Above equation can be simplified by assigning variables T1, T2, T3 and T4 for the terms as,  $T_i = b_i + d_i T$ ;  $i = 1$  to 4. Both DECRA(2) and DECRA(5) are to be used only for implicit creep integration and hence the flag LEXIMP=1 is given as the condition for the loop.

```
C UPDATING STATE VARIABLES
```

```
C
```

```
3 STATEV(1) = H-((one+H+R)*HC*EB*DTIME)  
STATEV(2) = R+(RC*DTIME)  
STATEV(3) = W+((one+W)*(WC*RC/HC)*DTIME)
```

```

STATEV(4) = Z+DECRA(1)
STATEV(5) = STRESS

```

C

The state variables H, R & W has to be updated at the end of calculations for before they are passed on to next increment. For small time increment  $\partial t$ , C the state variables hardening-STATEV(1), recovery-STATEV(2) and damage-STATEV(3) are calculated from equation (13), (14) and (15) as below:

$$H_{t+\partial t} = H_t - (\hat{H}\dot{\varepsilon}_0[1 + H + R]) \times \partial t$$

$$R_{t+\partial t} = R_t + (\hat{R} \times \partial t)$$

$$W_{t+\partial t} = W_t + \left[ \frac{\hat{W}\hat{R}}{\hat{H}} \times (1 + W_t) \right] \times \partial t$$

Earlier in the code, the variable Z is assigned to equivalent creep strain value at the start of increment EC(1). It is updated as the sum of creep strain at the start of increment and the incremental creep strain calculated during the increment. Variable Z which is  $STATEV(4) = \varepsilon_t^{cr} + \Delta\varepsilon^{cr}$ . “Stress” value for theta calculation is assigned as the STATEV(5). This is to pass on the current value of stress to next increment to identify any stress jump or stress singularity discussed earlier.

```

IF (STATEV(4).GE.F) THEN
  STATEV(4)=0.0d0
ENDIF

```

If State variable 4 which is the cumulative equivalent creep strain at that increment is greater than the fracture strain value calculated in the beginning the value of state variable 4 is set to be “zero”. This “zero” indicates elemental damage and the corresponding element will be deleted by Abaqus.

```

4 RETURN
END

```

The compiler returns all the output values from the Fortran code to Abaqus. The output values are equivalent creep strain increment and State variables which are hardening, recovery and damage at that node or integration point. The compiling is ended by the “end” command. The solver progresses to next node or integration point in the model and calls the user subroutine along and feeds the inputs for Fortran code like Von Mises stress, Temperature, current values of state variables H, R and W. The Fortran code is run on that nodal point and outputs are again returned to Abaqus.

Similarly, the subroutine is called on all nodal points and values of creep strain, H, R, W & Z are calculated for all nodal points in the model for the time increment. Abaqus solver continues to calculate the stiffness matrix & displacement of all nodal points and checks for convergence. If the solution converges, the increment is ended. If the solution did not converge, the same increment is repeated in the next iteration with lesser time increment. The procedure is repeated till the end of all creep steps for given creep time.

If the solution did not converge for more than 5 successive iterations, Abaqus solver terminates the analysis with an error which can be read from the message file.



## VIII. RESULTS AND DISCUSSION

### 10.CODE VALIDATION – TEST CASES

To validate the Fortran code for its accuracy in prediction of creep strain through Theta Projection Method, following test cases are run in Abaqus using the subroutine and the results are compared with experimental data.

- Test case 1 - 2D Plane stress state – Rectangular plate
- Test case 2 - 2D Plane stress state – Validation with alternate material
- Test case 3 - 3D Triaxial stress state – Rectangular bar
- Test case 4 - Sector with uniform temperature
- Test case 5 - Sector with temperature field
- Test case 6 - Gas turbine blisk sample
- Test case 7 - Gas turbine blisk with modified temperature & fracture

GH-4169 superalloy material is used in test case 2 which is to validate curve-fitting, constants calculation and analysis procedures whereas, MAR-247 superalloy is used in other test cases. The test cases are explained in the upcoming sections.

#### 10.1. TEST CASE 1 - RECTANGULAR PLATE

##### 10.1.1. TEST CASE 1 – ANALYSIS DATA

- Dimension : 100 mm x 50 mm x 1 mm thick
- Density :  $8.54 \times 10^{-9}$  ton/mm<sup>3</sup>
- Young's Modulus : 1,60,000 MPa
- Poisson's Ratio : 0.16
- Mesh size : 10 mm global, biased larger at loaded edge

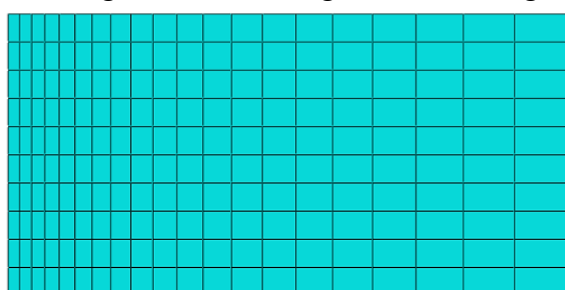
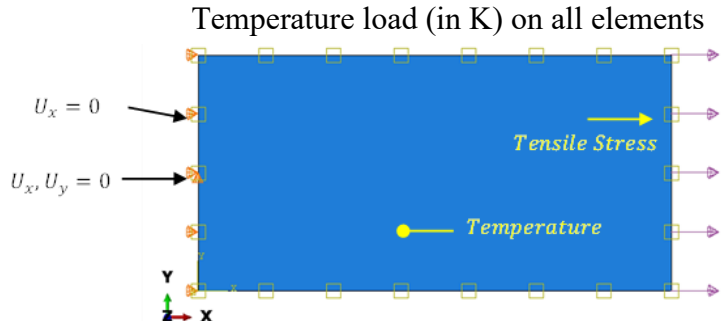


Figure 10.1.1 - Mesh - Test case 1

- Element type : Standard, Linear, Plane stress Quad CPS4

Reduced integration disabled for accuracy

- Boundary conditions<sup>15</sup> : Fixed at one edge ( $U_x = 0$ )  
 $(U_y = 0)$  at midpoint node
- Loads : Tensile Stress (in MPa) at free edge



**Figure 10.1.2 - Boundary condition - Test case 1**

- Steps : General static step (at. 298K) for '0.01 sec'  
Visco step (with test temp. & stress for test time)
- NL Geometry : ON for both static and visco steps
- Incrementation : Initial = 0.01 s  
Minimum =  $1 \times 10^{-12}$  s  
Maximum = 600 s
- Creep error tolerance :  $1 \times 10^{-6}$  to 0.01;

*Note:* In some cases where creep strain rate increases steeply, tertiary analysis is defined in a separate Visco step with much lower time increment (~60s or even 1s) and loose creep error tolerance (0.1) to avoid computational difficulties.

- Creep time integration : 'Explicit /Implicit' or 'Explicit'

*Note:* 'Explicit' time integration runs faster and smooth but gives inaccurate results at higher stresses.  
'Explicit /Implicit' time integration runs iteratively and slow, but gives more accurate results.

- Solution stabilization : Dissipated energy fraction  $2 \times 10^{-4}$  with adaptive strain energy ratio of 0.05
- Equation matrix storage : 'Unsymmetric'
- Solution technique : Full Newton

---

<sup>15</sup> Boundary conditions as per "The Standard NAFEMS Benchmarks," October 1990 TNSB, Rev. 3

- Extrapolation technique: None
- Field output for static step : Default + Nodal temperature (NT)
- Field output for visco step : Default + Nodal temperature (NT) + Equivalent Creep strain (CEEQ) + Solution Dependent Field Variables (SDV)

Same analysis settings as above are followed in the other test cases too unless specified.

### 10.1.2. TEST CASE 1 – RESULTS

#### A. Von Mises Stress - 800°C and 550 MPa

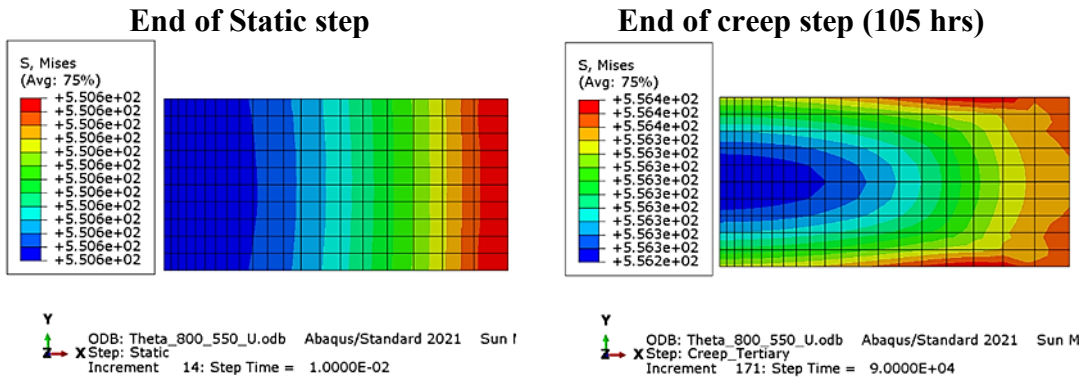
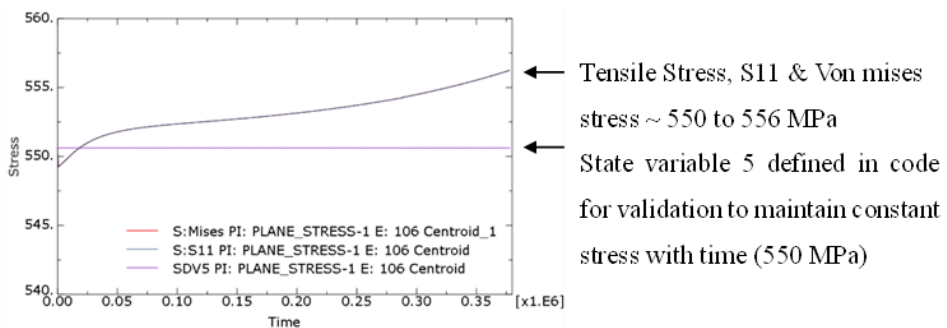


**Figure 10.1.3 - Von Mises Stress - Rectangular Plate - 800 degC & 550 MPa**

Von Mises stress at the end of static step is uniform (550 MPa) throughout whereas at the end of creep step (105 hours), both the magnitude and distribution of stress varies slightly (556 MPa) between the loaded edge and the fixed edge. This is due to the effect of plastic strain which results in thinning of the plane stress elements which results in decrease in cross sectional area perpendicular to load direction.

#### B. Stress – Time History



**Graph 10.1.1 - Stress Vs Time - Rectangular Plate - 800 degC & 550 MPa**

We can observe sudden decrease in stress initially and then gradual increase with time due to creep strain that deforms the mesh elements resulting in decrease or increase in area. This is an effect of geometrical non-linearity.

Even though stress increase or stress relaxation due to plastic creep strain is a practical phenomenon, the aim of this test case analysis is to simulate the experimental conditions and compare the results with

experimental creep data. Uniaxial tensile creep test is done at constant stress condition. Hence, for validation purposes, stress in the analysis has to be constant and code is modified accordingly.

### C. Equivalent Creep Strain – At the end of creep step (105 hrs)

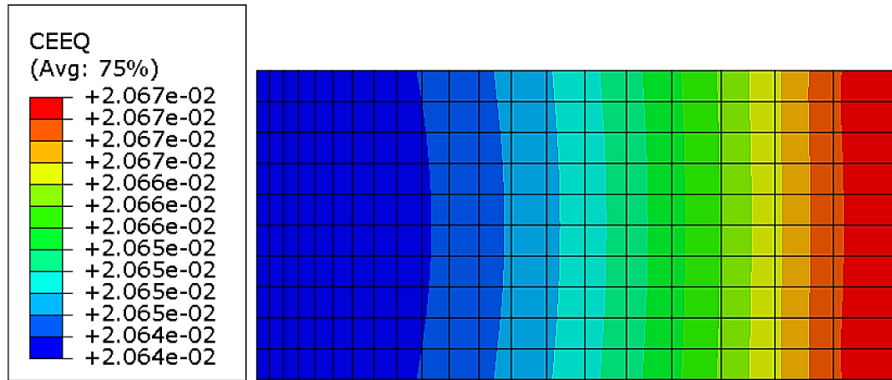
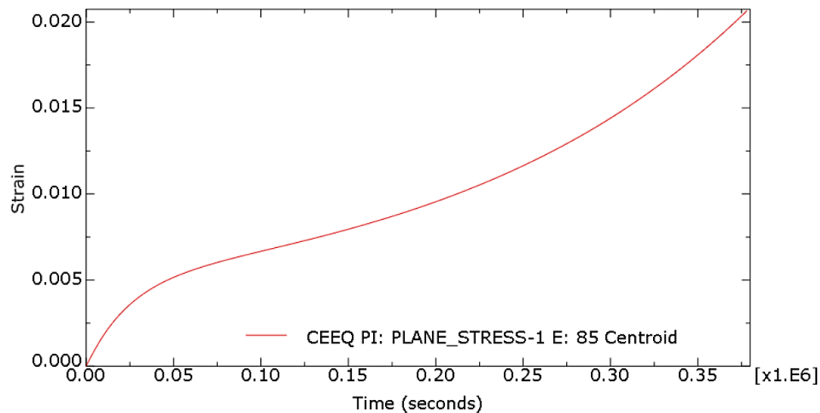


*Figure 10.1.4 – Equiv. creep strain - Rectangular Plate - 800 degC & 550 MPa*

Equivalent creep strain which is the uniaxial creep strain for plane stress condition is almost uniform throughout the plate. Slightly higher strain along the loaded edge is due to slightly higher stress as discussed previously.

### D. Equivalent Creep Strain vs. Time



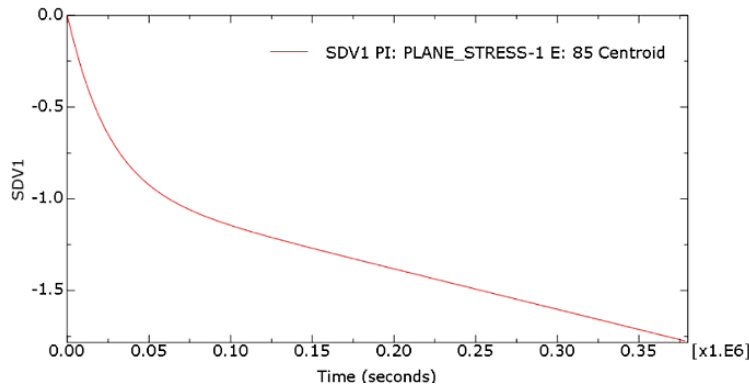
Above creep curve is the result of creep analysis done in Abaqus using Theta projection method

*Graph 10.1.2 - Creep strain Vs Time - Rectangular Plate - 800 degC & 550 MPa*

through our user subroutine. The shape of creep curve as well as the values at different times matches with the experimental data and clearly show expected behaviour in primary, secondary and tertiary stages.

This validates that the user subroutine is working properly and able to predict creep behaviour accurately as expected. It also indicates the accuracy of Theta Projection Method in capturing all stages of creep.

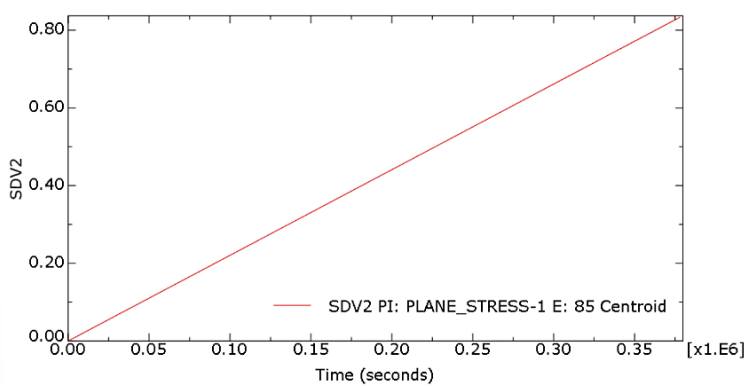
## E. Hardening (Solution dependent variable 1)



*Graph 10.1.3 - Hardening - Rectangular Plate - 800 degC & 550 MPa*

Hardening is prominent in the primary stage and the rate of hardening decreases steeply till the secondary stage and then gradually decreases.

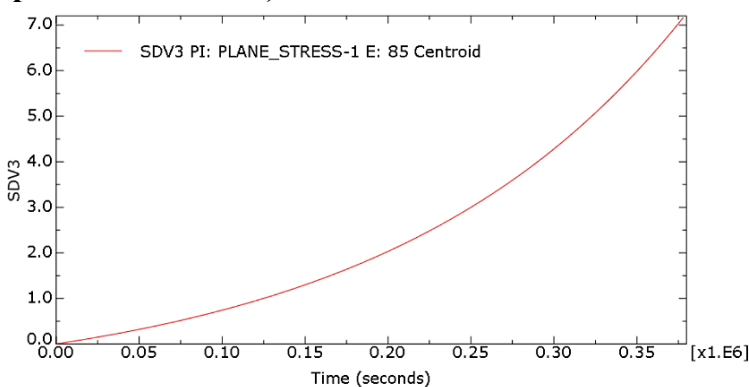
## F. Recovery (Solution dependent variable 2)



*Graph 10.1.4 - Recovery - Rectangular Plate - 800 degC & 550 MPa*

Rate of recovery is independent of strain and hence varies linearly with time.

## G. Damage (Solution dependent variable 3)

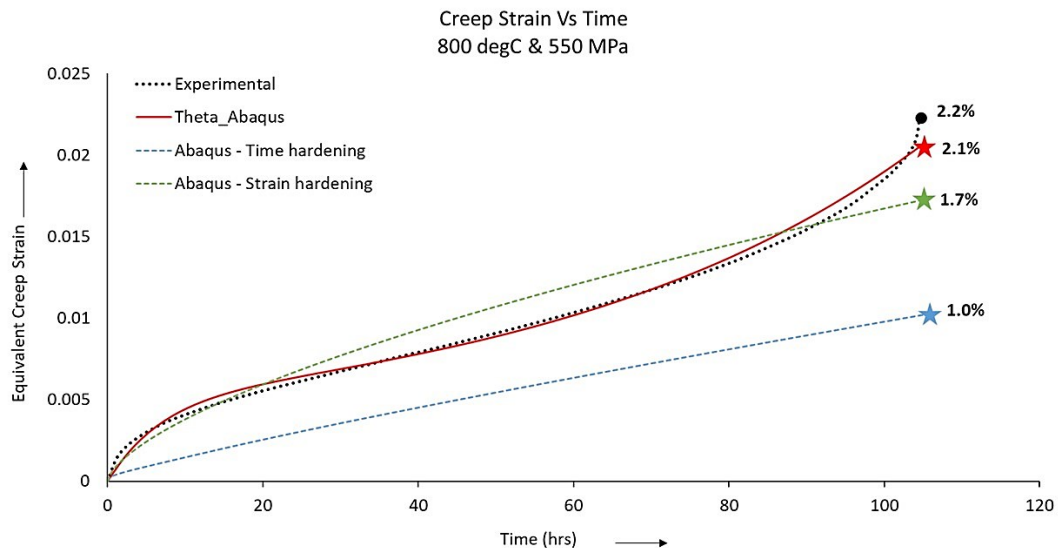


*Graph 10.1.5 - Damage - Rectangular Plate - 800 degC & 550 MPa*

Rate of damage increases exponentially with time and is very significant in the tertiary stage as it is dependent on creep strain rate.

Analysis result of all the internal variables show expected behavior and indicate the robustness of the user-subroutine.

### 10.1.3. COMPARISON WITH POWER LAW CREEP

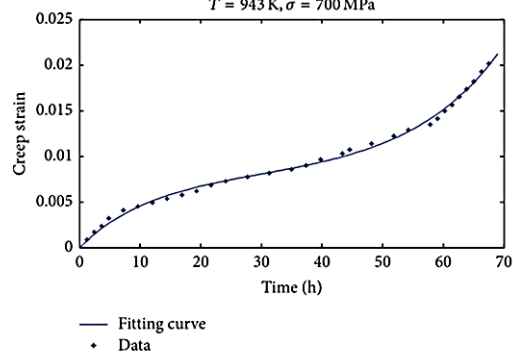
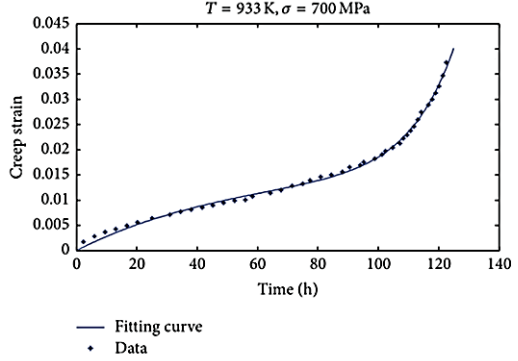
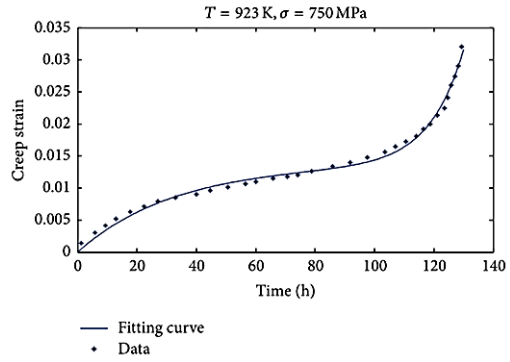
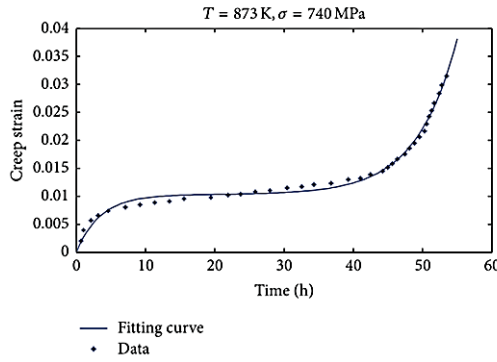


*Graph 10.1.6 - Creep Strain Result - Comparison with power law*

To compare the results of Theta projection method and power law creep models, Abaqus simulation is carried out on same model at same load conditions – 800 degC and 550 MPa stress by using Power law creep models. As expected, power law models did not capture the tertiary creep whereas Theta projection model using the subroutine capture all stages of creep as well as closely match the experimental results.

## 10.2. TEST CASE 2 – PROCEDURE VALIDATION

As the creep curves are taken from research journals and digitized to get the Theta values, there may be some error in the process. To validate the observations made, a second set of creep curves of a different material grade (GH-4169) is taken and same process is repeated. Experimental creep curves for the material are taken from (Donghuan Liu, 2014), as below:



### *Graph 10.2.1 - Experimental Creep Curves - GH-4169*

Temperature dependent material properties for the material GH-4169 are as follows:

*Table 10.2.1 - Mechanical Properties - GH-4169*

Elastic modulus of GH4169 with different temperatures.					
T/°C	25	400	500	650	750
E/GPa	205	175.5	168.5	142	130.5
Poisson's ratio of GH4169 with different temperatures.					
T/°C	25	300	400	500	600
$\mu$	0.321	0.329	0.339	0.344	0.355
				650	750
				0.361	0.381

Theta coefficients are arrived from the creep curves using the same procedure as explained in section 9.1. and material constants are calculated from the Theta coefficients as per the procedure explained in section 9.2.

Material constants are calculated using Least square regression of 4 equations & 4 unknowns. The results are as follows:

**Table 10.2.2 - Material constant results - GH-4169**

Material	GH4169 EA										
Last update	14th Feb 2023	(From Matlab CurveFit Tool)									
Temp (deg C)	Stress (MPa)	Theta 1	Theta 2	Theta 3	Theta 4	Ln(Th1)	Ln(Th2)	Ln(Th3)	Ln(Th4)		
600	740	1.032E-02	7.805E-05	2.468E-06	4.705E-05	-4.5736715	-9.4581609	-12.912102	-9.9642997		
650	750	1.384E-02	8.433E-06	2.552E-07	2.392E-05	-4.2801923	-11.683358	-15.181218	-10.640796		
660	700	1.595E-02	5.468E-06	6.543E-06	1.837E-05	-4.1382964	-12.116598	-11.937115	-10.904792		
670	700	7.952E-03	2.296E-05	1.267E-04	1.883E-05	-4.8343318	-10.681757	-8.9736885	-10.880059		
	a	1.35E+03	-3.33E+03	-5.79E+03	-2.94E+02	-					
	b	-1.84E-06	4.55E-06	7.85E-06	4.02E-07		m <sup>2</sup> N <sup>-1</sup>				
	c	-1.45E+00	3.56E+00	6.26E+00	3.03E-01		K <sup>-1</sup>				
	d	1.97E-09	-4.89E-09	-8.52E-09	-4.29E-10		m <sup>2</sup> N <sup>-1</sup> K <sup>-1</sup>				
	a	1345.751	-3329.313	-5786.073	-294.469	-					
	b	-1.83564192	4.54760867	7.85378312	0.40179526		mm <sup>2</sup> N <sup>-1</sup>				
	c	-1.44903832	3.56403980	6.25688181	0.30281397		K <sup>-1</sup>				
	d	0.00197062	-0.00488651	-0.00851506	-0.00042906		mm <sup>2</sup> N <sup>-1</sup> K <sup>-1</sup>				
											FOR FORTRAN CODE

### 10.2.1. VERIFICATION OF THETA COEFFICIENTS:

To validate the accuracy and robustness of the material constant calculation procedure, theta values are re-computed using the material constants and compared with the actual theta values derived from curve fitting. The accuracy of material constant results is very good (Average deviation less than 0.0014%).

**Table 10.2.3 - Material constants verification summary**

Temp (deg C)	Stress (MPa)	Theta 1	Theta 2	Theta 3	Theta 4	Deviation % from actual			
						-0.00000001%	0.000000003%	0.0000002%	0.0212540%
600	740	1.032E-02	7.805E-05	2.468E-06	4.706E-05	-0.00000001%	0.000000003%	0.0000002%	0.0212540%
650	750	1.384E-02	8.433E-06	2.552E-07	2.392E-05	-0.00000002%	-0.0000003%	-0.0000005%	-0.0000001%
660	700	1.595E-02	5.468E-06	6.543E-06	1.837E-05	-0.00000002%	-0.0000001%	0.0000002%	-0.0000001%
670	700	7.952E-03	2.296E-05	1.267E-04	1.883E-05	-0.00000004%	-0.0000003%	-0.0000004%	-0.0000005%

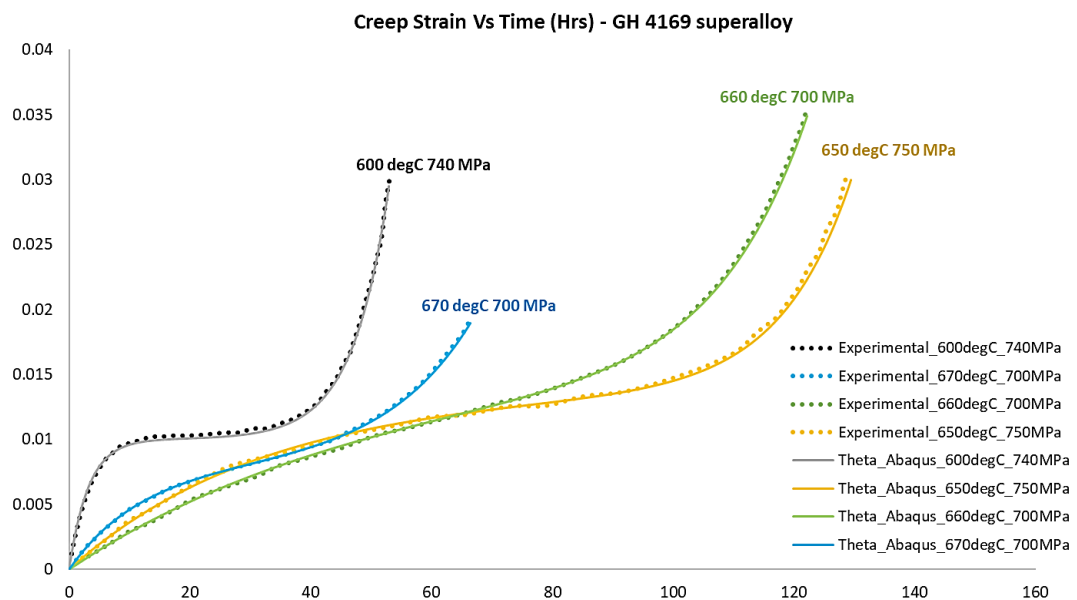
### 10.2.2. TEST CASE 2 – ANALYSIS DATA

- Material grade : GH-4196 superalloy
- Dimension : 100 mm x 50 mm x 1 mm thick
- Density :  $8.54 \times 10^{-9} \text{ ton/mm}^3$
- Young's Modulus : 1,75,000 MPa
- Poisson's Ratio : 0.339
- Mesh, boundary conditions & other analysis settings are same as test case – 1.

### 10.2.3. TEST CASE 2 – RESULTS

Behaviour of Stress, Creep strain & internal variables are very similar to that of test case 1. As the purpose of this test case is to validate the material calculation procedure and check the accuracy of creep strain results, four different creep analysis are performed in Abaqus using the subroutine at four of the design points (load conditions) taken as input for material constant calculation from the experimental creep curves. The results are compared with the experimental data as below:

Abaqus results are accurately matching the experimental creep curves taken for material constants



*Graph 10.2.2 - Creep curve - GH-4169 - Experimental Vs Theta projection results*

calculation. This validates the robustness of Theta coefficient and material constant calculation procedures for different material data.

Accuracy and robustness of the Theta projection model as well as constant calculation procedures for interpolated and extrapolated load conditions are discussed in the later sections.

## 10.3. TEST CASE 3 - RECTANGULAR BAR

To validate the subroutine in 3D triaxial stress state where the Poisson's effect is considerable and the elements have extra degree of freedom than plane stress condition, analysis is done on a rectangular bar as explained below.

### 10.3.1. TEST CASE 3 – ANALYSIS DATA

#### Boundary conditions

- As per “The Standard NAFEMS Benchmarks,” October 1990 TNSB, Rev. 3
- Triaxial stress state with uniaxial tensile load
- Three orthogonal faces have one fixed DOF as shown
- Tensile stress is applied on face opposite to face with  $U_x = 0$
- Temperature is applied on all nodes

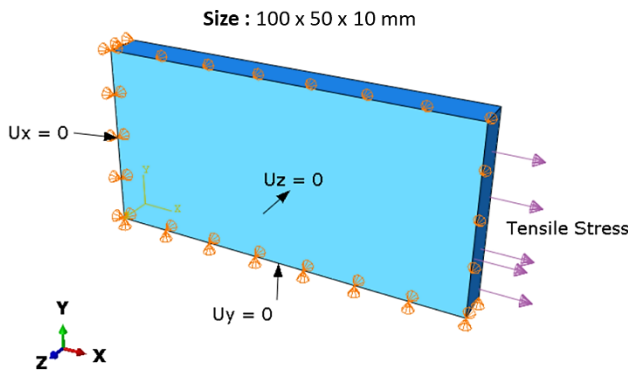


Figure 10.3.1 - Boundary conditions - Test case - 3

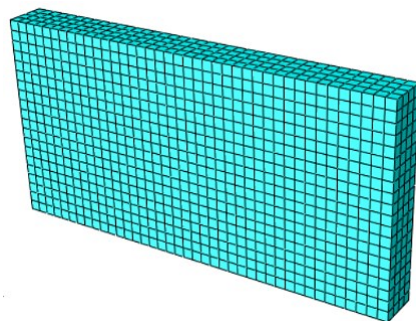


Figure 10.3.2 - Mesh - Test case - 3

#### Mesh

- Standard linear 3D stress brick elements C3D8 of size 5 mm
- Reduced integration is turned off to avoid approximations
- Mesh compiles to all basic quality metrics

#### Time step for creep

- Initial time increment is  $1 \times 10^{-3}$  seconds
- Min and max time increment values are  $1 \times 10^{-8}$  s and 600 seconds
- Creep increment error tolerance of 0.01 to  $1 \times 10^{-4}$  and automatic time increment damping factor is 0.02

### 10.3.2. TEST CASE 3 – RESULTS

All results are discussed for analysis done at 800 degC and 550 MPa.

## A. Von Mises Stress

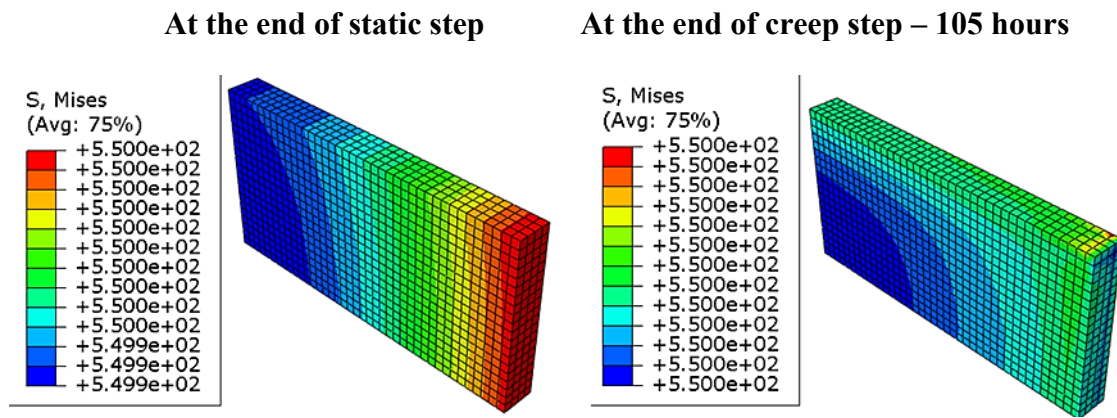
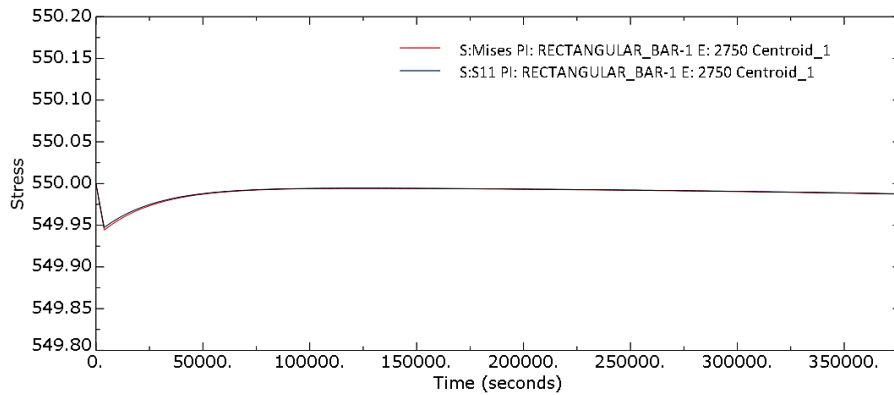


*Figure 10.3.3 - Von Mises Stress - Test case 3 - Rectangular bar*

Contour plot of Von Mises stress shows uniform stress across the model. Stress variation due to geometric non-linearity is minimized due to larger thickness of model relative to the strain values.

## B. Time History of Stress



*Graph 10.3.1 - Stress History - Test case - 3 - Rectangular Bar*

Von mises stress is equal to the applied uniaxial stress. Initially stress reduces slightly due to elastic strain and then gradually increases due to plastic strain. Stress behaviour is similar to plane stress condition.

## C. Equivalent creep strain at the end of creep step

Creep strain contour plot at the end of 104 hours is shown. Equivalent creep strain is uniform throughout the model at all times due to uniform stress.

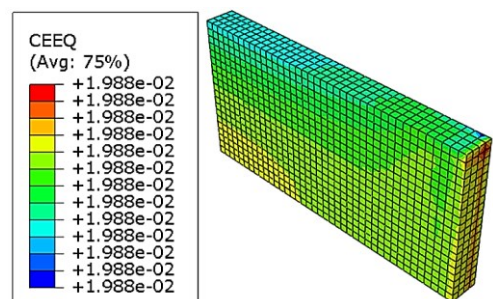
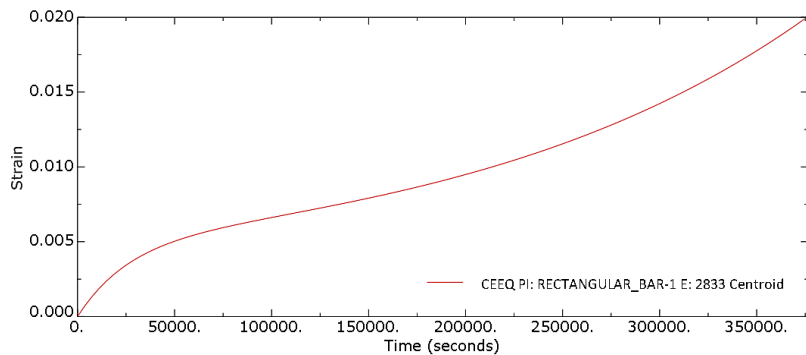


*Figure 10.3.4 - Equivalent creep strain – Rectangular bar - 800degC & 550MPa*

#### D. Equivalent Creep Strain Vs. Time

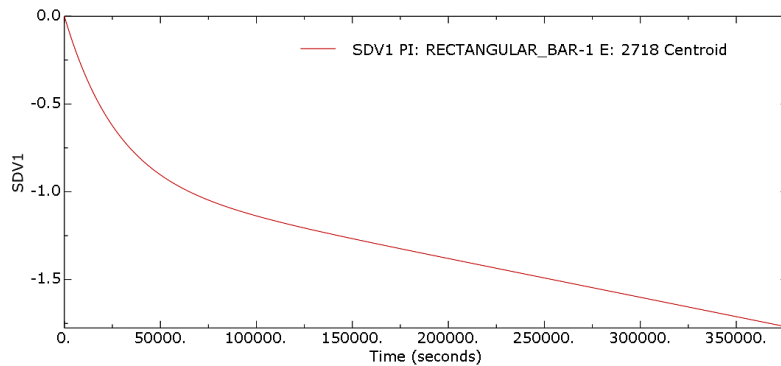


*Graph 10.3.2 - Creep strain Vs Time - Rectangular Bar - 800 degC & 550 MPa*

Creep curve results show that the subroutine is capturing all the primary, secondary and tertiary creep stages clearly and the creep strain values are matching the experimental results as well.

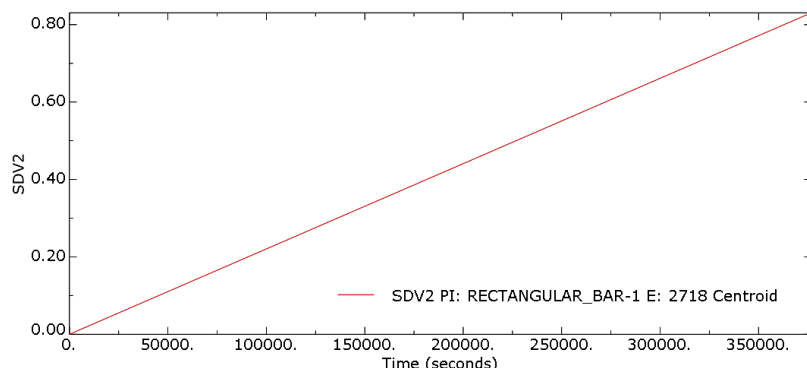
Above results validate the effectiveness of subroutine for 3D triaxial stress state.

#### E. Hardening (Solution dependent variable 1)



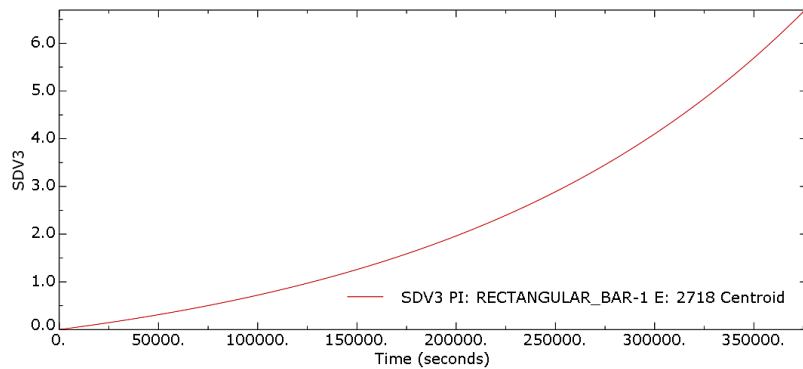
*Graph 10.3.3 - Hardening - Rectangular bar - 800 degC & 550 MPa*

#### F. Recovery (Solution dependent variable 2)



*Graph 10.3.4 - Recovery - Rectangular bar - 800 degC & 550 MPa*

## G. Damage (Solution dependent variable 3)



**Graph 10.3.5 - Damage - Rectangular bar - 800 degC & 550 MPa**

All internal state variables show expected behaviour similar to test case 1.

## 10.4. TEST CASE 4 – SECTOR

Subroutine is validated for cyclic symmetric model with rotational body force (centrifugal force) is applied as angular velocity (RPM), which is close to gas turbine blade boundary conditions.

### 10.4.1. TEST CASE 4 – ANALYSIS DATA

#### Boundary conditions

- Cylindrical co-ordinate system defined with R along radial, Theta along and Z along thickness
- Cyclic symmetry interaction about Z axis – 24 no of sector (15 deg each)
- Inner face has all translational DOF fixed
- Temperature is applied on all nodes
- Rotational body force (centrifugal) applied on all nodes as angular velocity

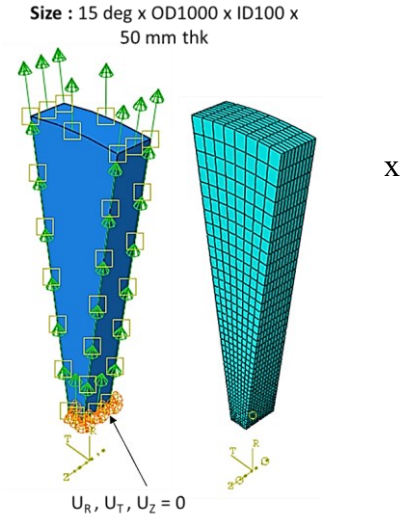


**Figure 10.4.1 - Boundary conditions and Mesh - Test case 4 - Sector**

#### Mesh

- Standard linear 3D stress brick elements C3D8 of global size 20 mm biased to 5 mm size on inner side
- Reduced integration is turned off to avoid approximations
- Mesh compiles to all basic quality metrics

#### Time step for creep

- Initial time increment is  $1 \times 10^{-8}$  seconds
- Minimum and maximum time increment values are  $1 \times 10^{-12}$  s and 600 s.
- Creep increment tolerance of  $1 \times 10^{-4}$  to 0.01 and automatic damping factor is 0.02

Note: As initial strain rates are high at the inner face, iterative equation solver with smaller time increment gives better convergence and hence it is used.

### 10.4.2. BOUNDS FOR APPLIED LOAD

Material constants for MAR-247 are derived from a particular range of stress and temperature (800–950°C and 300 – 600 MPa) and extrapolation errors increase as we move out of this range. Plane stress analysis solution converged only within analysis bounds of (600–1000°C and 100 – 900 MPa).

For sector with rotational body force, initial stresses are high on the inner face and low on the outer face. Such larger stresses produce very high initial values of Theta, H, R, W resulting in high strain rate and excessive distortion of elements. Solution may not converge. To model a sector with reasonable dimensions where the stresses are within our analysis range, calculations<sup>16</sup> for stress components are done in prior.

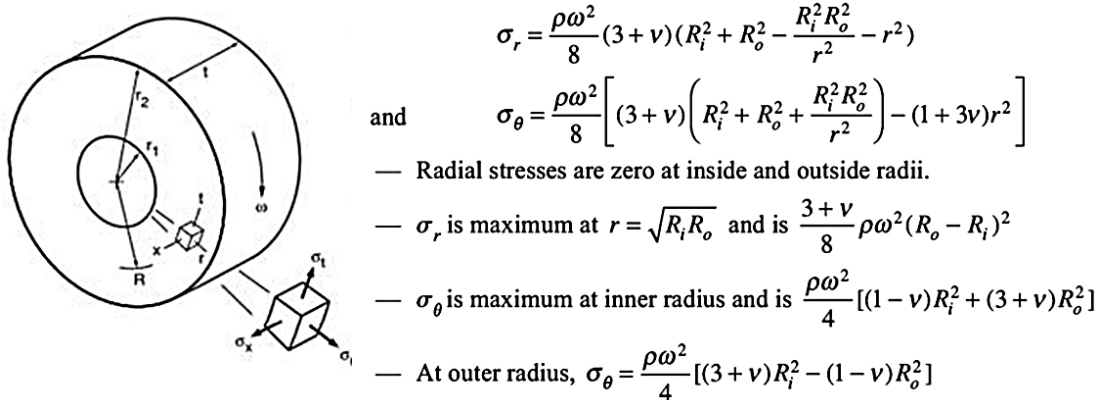


Figure 10.4.2 - Radial and hoop stress components in a hollow disc

Table 10.4.1 - Stresses in hollow rotating disc Vs RPM

#### Bounds for stresses in rotating disc

Radius, $R_o$	0.5	m
Radius, $R_i$	0.1	m
Critical radius, $r$	0.22	m
Density	8540	kg/m <sup>3</sup>
Poisson's ratio	0.16	

RPM	Angular velocity (rad/s)	At inner radius	At $r = 0.09$ m
		Max Tangential stress (Mpa)	Max Radial stress (MPa)
10000	1047	1869	592
9000	942	1514	479
8000	838	1196	379
7000	733	916	290
6000	628	673	213
5000	524	467	148

Below are dimensions & rotational velocities for which stresses are in the analysis range

It is better to avoid both temperature and stresses going out of analysis bounds

<sup>16</sup> "Strength of materials" by S.S. Ratan

### 10.4.3. TEST CASE 4 – RESULTS

Results are discussed for analysis done at 800 deg C & 10,000 RPM

#### A. Von Mises Stress

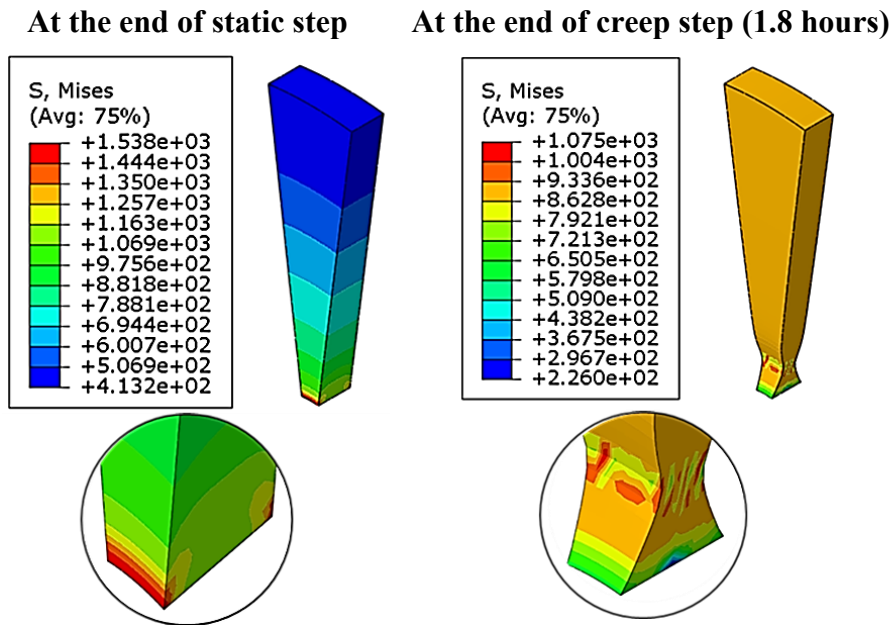


*Figure 10.4.3 - Von Mises Stress - Test case - 4 - Sector*

Contour plot of Von mises stress shows highest stresses on the inner side of the sector and stress decreasing gradually towards the outer side.

At the end of creep step, highly strained elements near the inner surface show very high stresses whereas stresses have reduced on the edges of inner face. This behavior can be explained by reduction in radial stress as the component strains in radial direction due to creep. In the process, lateral and hoop stresses increase in magnitude all over.

#### B. Stress components at the end of static step

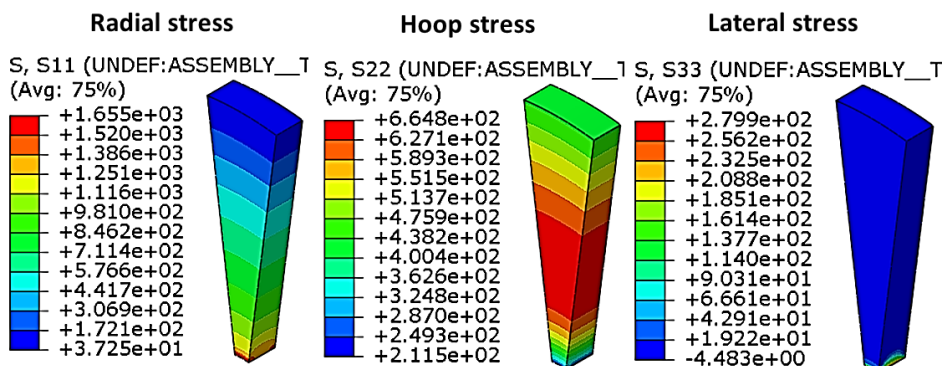


*Figure 10.4.4 - Stress components before creep - Test case 4 - Sector*

Radial stresses are maximum at the inner side where as hoop stresses are maximum at the middle region. Lateral stresses are present only on the inner face as it is fixed.

### C. Stress components at the end of creep step (1.8 hours)

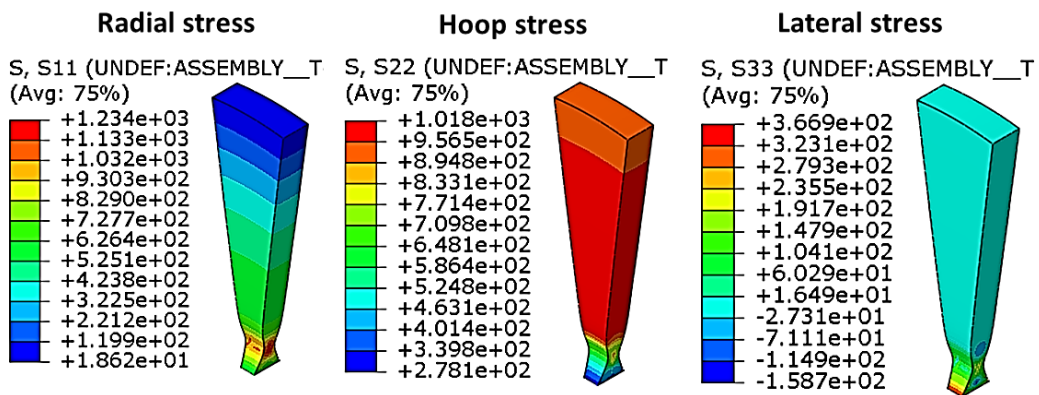
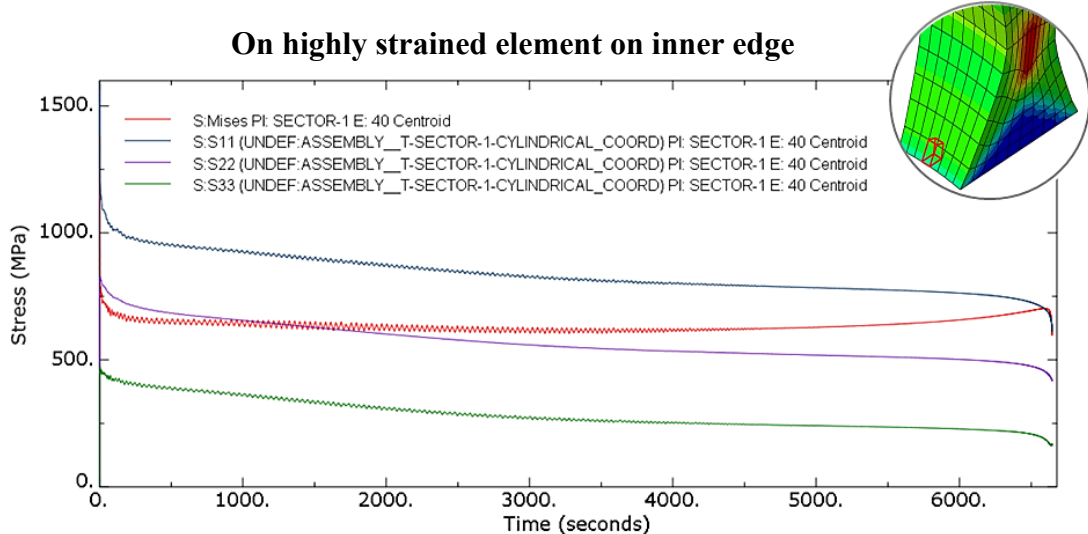


**Figure 10.4.5 - Stress components after creep - Test case 4 - Sector**

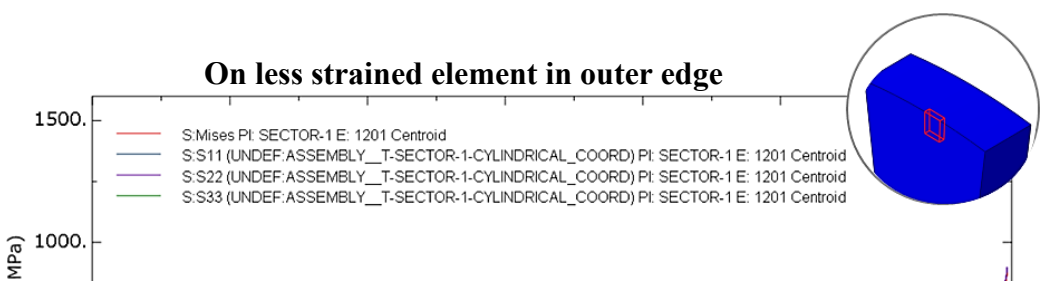
After creep of 1.8 hours, radial stresses have reduced whereas hoop stress and lateral stresses have increased throughout the model. This is due to the effect of higher creep strain along radial direction (radial growth). Elements near the inner surface are highly deformed due to higher Von-Mises stresses. Even though Von-Mises stresses were maximum on the inner surface at the end of static step, elements on the inner surface have strained resulting in some stress relaxation. Elements just above the inner surface are subject to increasing hoop stresses and therefore increased Von-Mises stress at the end of creep step.

### D. Stress components – Time history



**Graph 10.4.1 - Stress components Vs Time - on high strain element**

Both radial & hoop stresses are high at inner edge initially. Lateral stress is present as inner edge is fixed on Z direction also. All stress components decrease with time as creep strain increases. Stresses fall rapidly at the end as the element distort excessively. Small fluctuations are due to residual force correction by the solver as there are convergence issues due to high strain rates.



**Graph 10.4.2 - Stress components Vs Time - on low strain element**

Radial & transverse stresses are almost zero on the outer edge. Von mises stress is almost equal to the hoop (tangential) stress. Stresses increase due to compressive creep strain and progress smoothly as there are no residual force correction.

#### E. Equivalent creep strain at the end of creep step:

Creep strain is more in the inner region as von mises equivalent stresses are large. Due to the higher tensile creep strains in the inner side, elements in the outer surfaces experience compressive radial creep. Analysis was continued as long as convergence is obtained by the solver.

At a maximum creep strain of 11% in the inner side, analysis aborted as creep rate increases steeply and solution started to diverge.

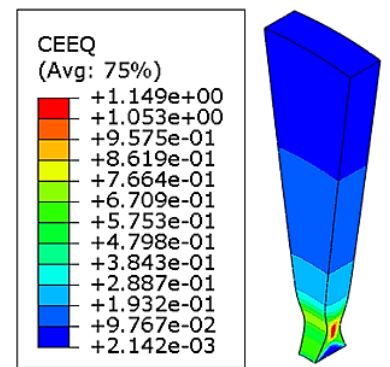


**Figure 10.4.6 - Equivalent creep strain – Sector - 800 degC & 10,000 RPM**

#### F. Creep Strain Components

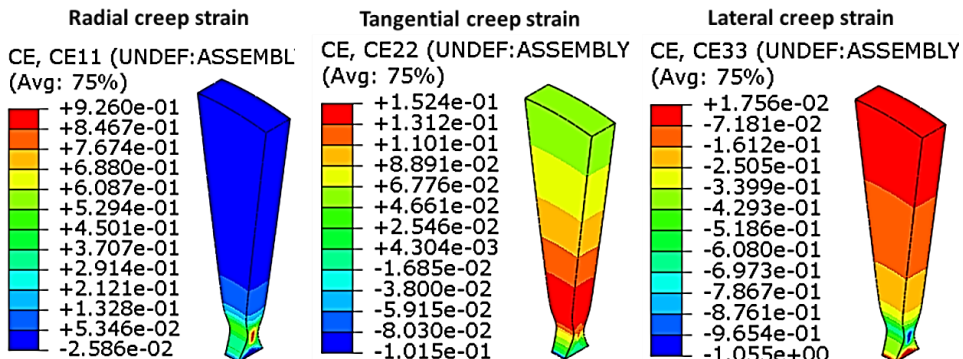
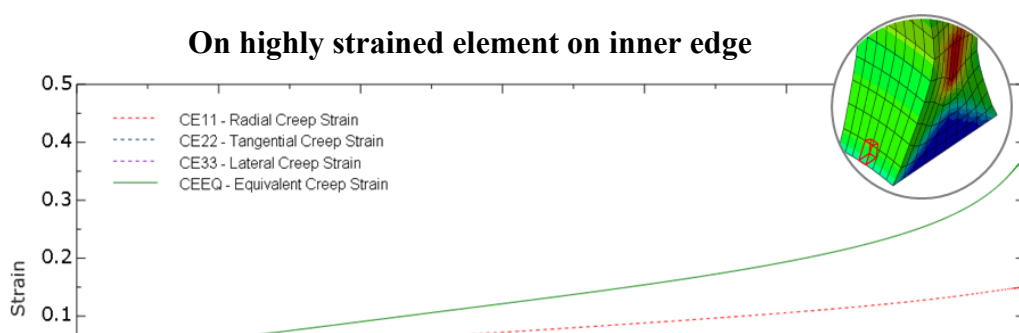


**Figure 10.4.7 - Creep Strain Components - Sector - 800 degC & 10,000 RPM**

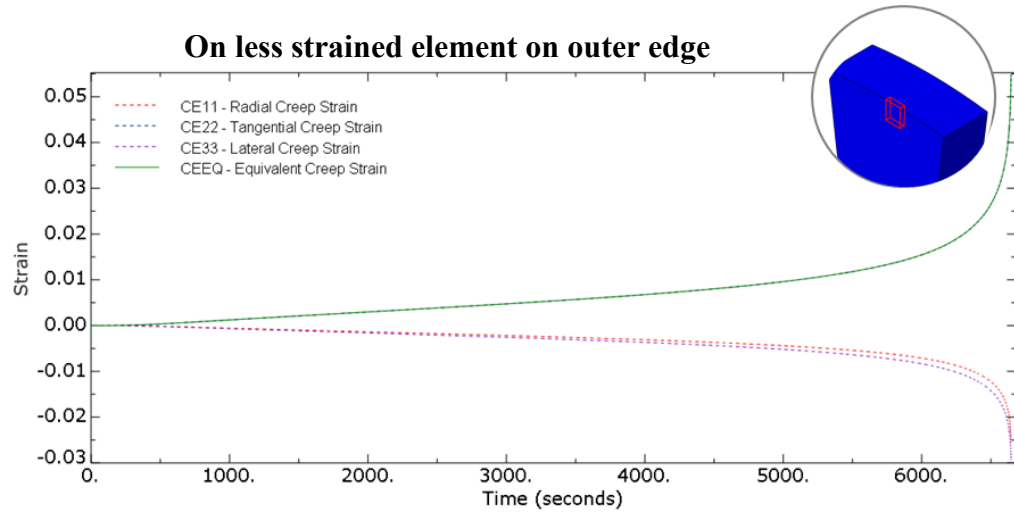
Radial component of creep strain is much higher than other components, in line with the calculated theoretical stress value. Both tensile and compressive strains are observed due to the boundary condition and differential strain rates at different region. Components of creep strain give us an idea of nature of strain.

#### G. Creep strain components Vs Time



**Graph 10.4.3 - Sector - Creep strain components Vs time – High strain element**

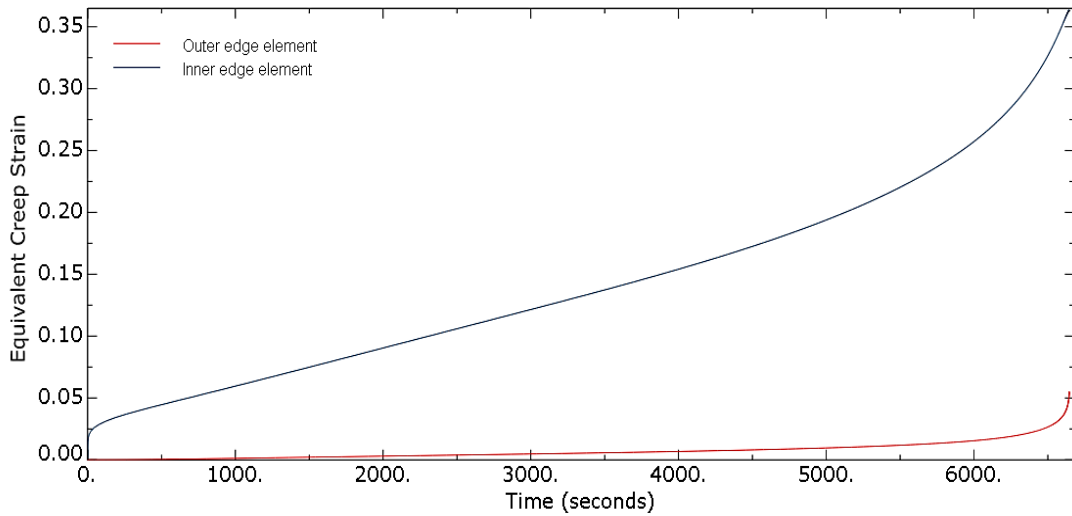
All primary, secondary & tertiary regions are captured. Radial & lateral strains (~0.15) are more than tangential strain (0.005). Lateral creep strain is compressive.



**Graph 10.4.4 - Creep strain components Vs time – Low strain element**

Equivalent creep strain is almost equal to the tangential creep strain. Both lateral radial creep strains are compressive.

## H. Equivalent creep strain – Element on outer & inner faces

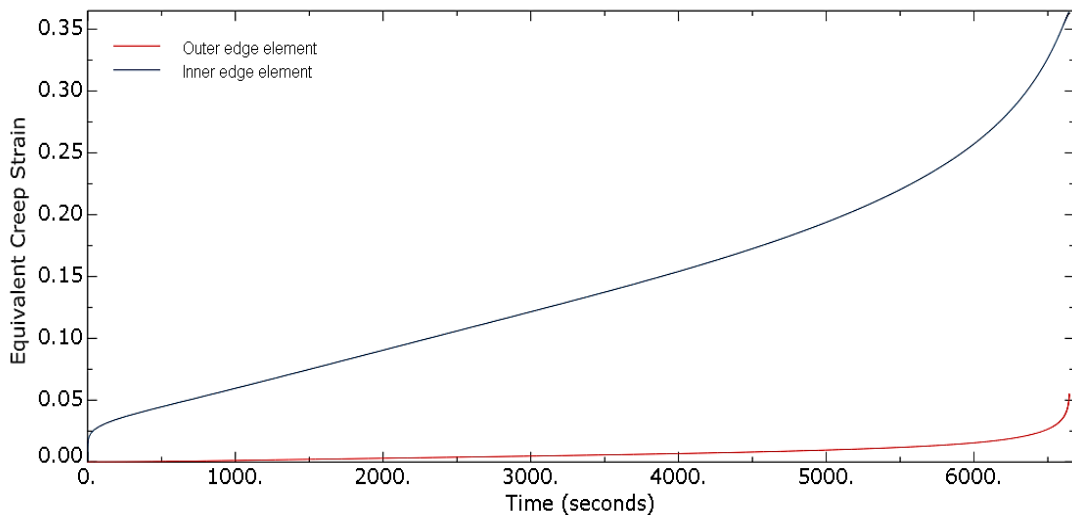


Graph 10.4.5 - Creep curve result - Elements on outer & inner faces

**Inner edge element:** Inner edge element shows high primary creep rate due to high initial stress. Creep rate reduces gradually with stress as strain increases. Lower tertiary rate is observed as stress is gradually reduced due to tensile strain.

**Outer edge element:** Outer edge element shows smaller primary creep rate due to lower initial stress. Higher tertiary rate is observed as the stress increases due to higher compressive strain.

## I. Hardening factor (Solution dependent variable 1)

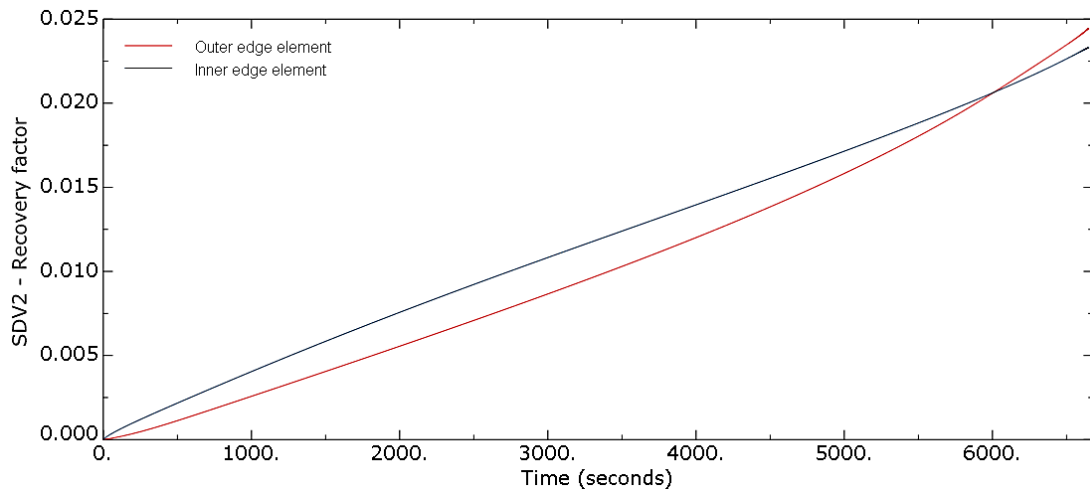


Graph 10.4.6 - Hardening behaviour - Element on inner & outer faces

**Inner edge element:** High initial rate of hardening is observed due to higher creep strain rate. Lower & decreasing tertiary rate of hardening is due to the reducing stresses.

**Outer edge element:** Almost constant rate of hardening due to steady creep strain rate.

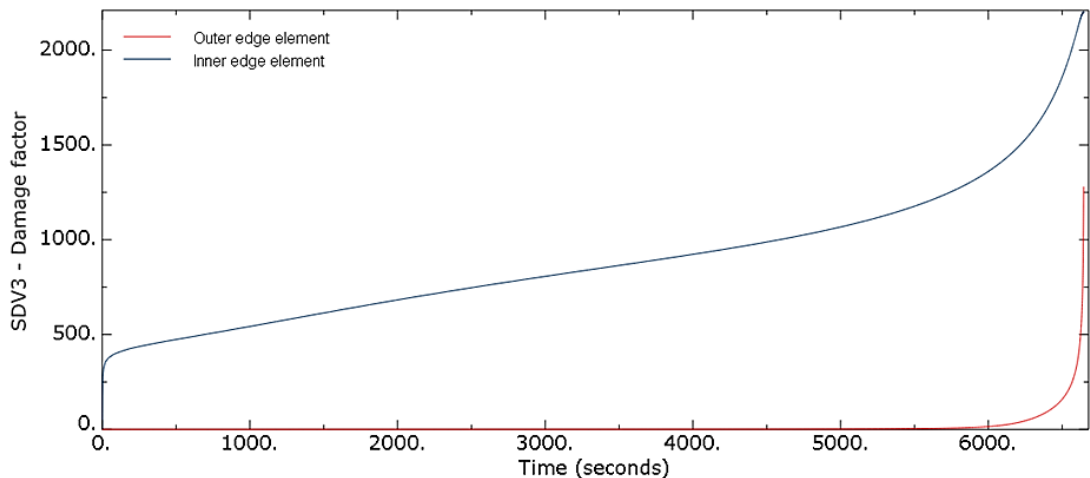
## J. Recovery factor (Solution dependent variable 2)



Graph 10.4.7 - Recovery behaviour - Element on inner & outer faces

Both inner and outer elements show similar rate of recovery as softening is independent of creep strain rate.

## K. Damage factor (Solution dependent variable 3)



Graph 10.4.8 - Damage behaviour - Elements on inner & outer faces

**Inner edge element:** Higher initial damage is observed due to high initial creep rate and stress. Gradual rate of tertiary damage is due to lower tertiary hardening rate.

**Outer edge element:** Lower initial damage is observed due to low initial creep rate and stress. Steep tertiary rate of damage is due to high tertiary creep strain rate (added effect of compressive creep strain due to inner elements).

Damage can be visualized by specifying element deletion criteria in the subroutine. Here, fracture strain is manually given in the code as the criteria.

## L. Damage visualization

The creep strain results shown here are only indicative and for testing the sub-routine. Practically when creep strain in any grain exceeds the fracture strain value, cracks develop and may result in either grain boundary separation and cleavage or stress redistribution around crack depending upon location of crack, grain size and micro-structure.

To visualize damage, code is revised for element deletion based on a given limit of equivalent creep strain. Below are the results for sector at 800 deg C and 10,000 RPM showing elements getting deleted when creep strain of all connected nodes reaches a value of 0.5.

Very high stresses may develop adjacent to deleted elements and solver may face computational difficulties. Code is revised to correct such stress singularity issues for analysis to continue. Mesh size should be very fine and time increment must be kept small ( $\sim 1$  s or less) to facilitate this damage visualization.

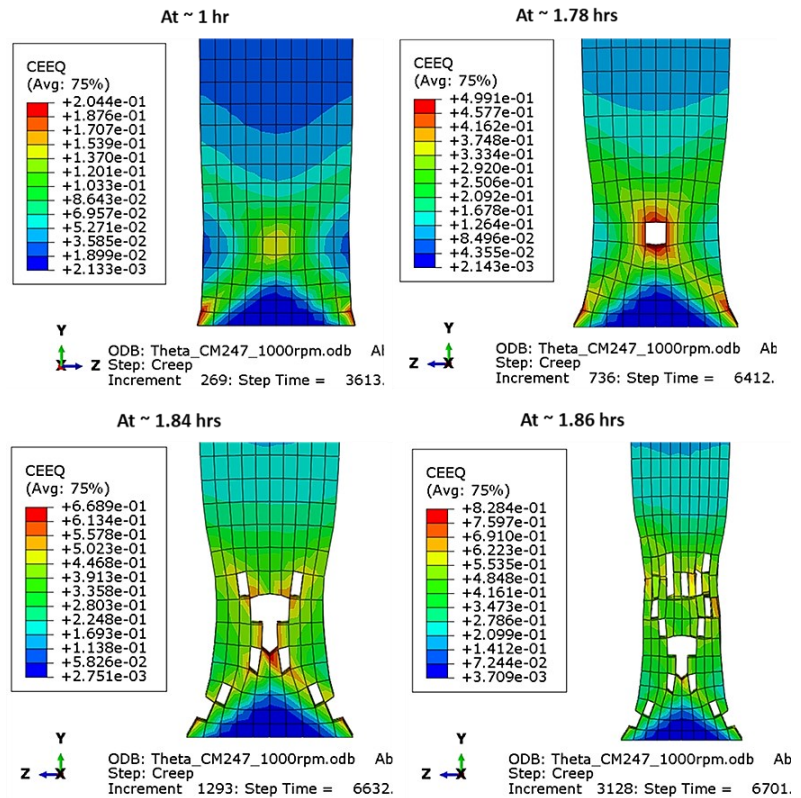
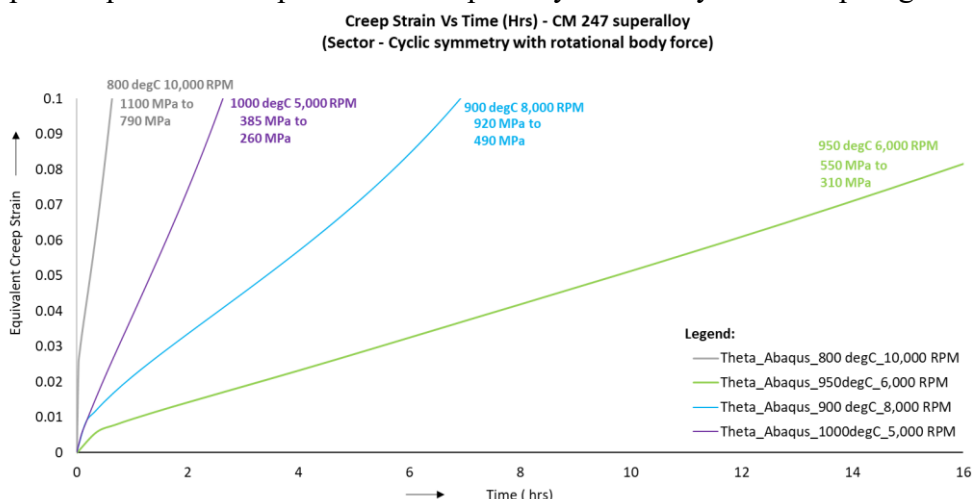


**Figure 10.4.8 - Damage - Element deletion exceeding fracture strain**

## M. Creep strain Vs RPM

The analysis is carried out at different temperature and stress conditions and the results are as follows:

The graph of equivalent creep strain shows primary and steady state creep stages as well as variation



of creep curves for increasing temperature and RPMs. Comparison with experimental data cannot be made as

**Graph 10.4.9 - Creep Strain Vs RPM - Sector**

Von Mises stress is maintained constant in uniaxial creep test where as in our test case, triaxial stress state is applied and hence Von mises stress reduces due to straining of elements in one direction

Von Mises stress at initial state and after reaching 10% creep strain is mentioned next to each creep curve for our understanding. The graph shows the temperature and stress dependence of creep strain.

## 10.5. TEST CASE 5 – SECTOR + TEMPERATURE FIELD

In a uniform temperature analysis, creep strain rate of any element depends only on stress. Since radial stresses are maximum at the inner face, elements nearby inner face experience higher creep rate and fail earlier than other elements. This phenomenon holds true at all rotational speeds (RPM).

In an analysis with different temperatures at different region, we cannot expect the inner face elements (where stresses are higher) to creep at faster rate and fail. This is because of the combined effect of temperature and stress on creep strain rate.

With temperature field as shown (800 degC at inner dia. to 1000 degC at outer dia.), different analyses are done at different RPM to validate this combined effect of stress and temperature on creep strain rate.

### 10.5.1. TEST CASE 5 – ANALYSIS DATA

Model geometry, boundary conditions and analysis data are same as test case 4 except that temperature field is applied as shown in Figure 10.5.1. Young's modulus and Poisson's ratio are defined for each temperature in material properties.

Analysis is carried out at different RPMs and the results are discussed in the next section.

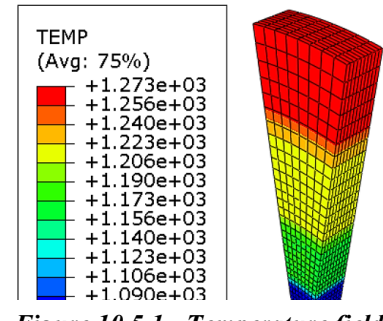
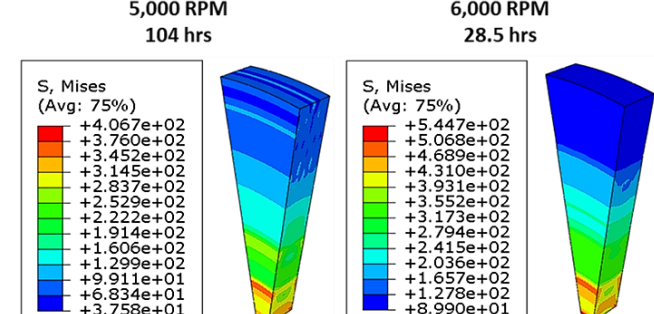


Figure 10.5.1 - Temperature field for test case 5

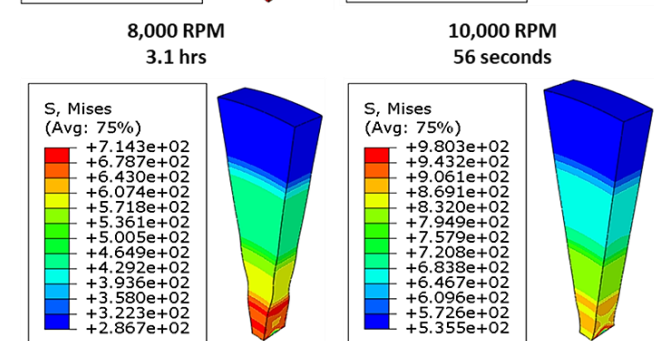
### 10.5.2. TEST CASE 5 – RESULTS

#### A. Von Mises Stress distribution

At different RPMs, Von Mises stress differs, but the stress distribution across the model remains similar – higher stress at inner side to lower stress at outer side



#### B. Creep strain distribution



Creep strain distribution is different at different RPMs even though stress distribution is similar at all RPMs. This validates the combined effect of stress and temperature on strain rate

Elements at the inner dia. show higher creep at higher RPM as stresses are very high, even though temperature is lesser. Elements at the middle show higher creep when RPM is reduced as

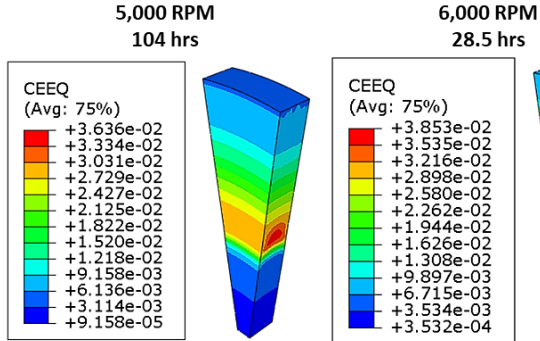


**Figure 10.5.2 - Creep strain distribution - 5000 & 6000 RPM**

'temperature  $\times$  stress' value is higher even though stress is lower. Elements on the outer dia. show lower creep at all RPMs as both temperature and stress values are lower

**Figure 10.5.3 - Von Mises Stress distribution - Test case 5**

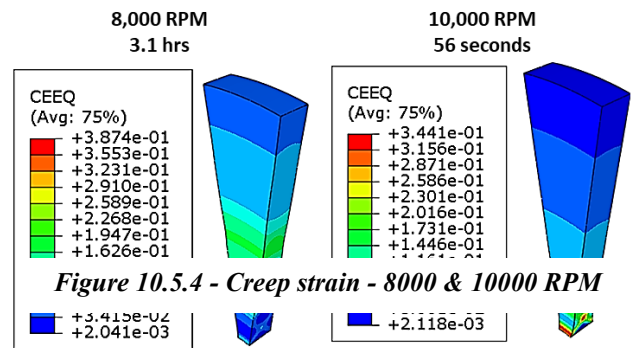
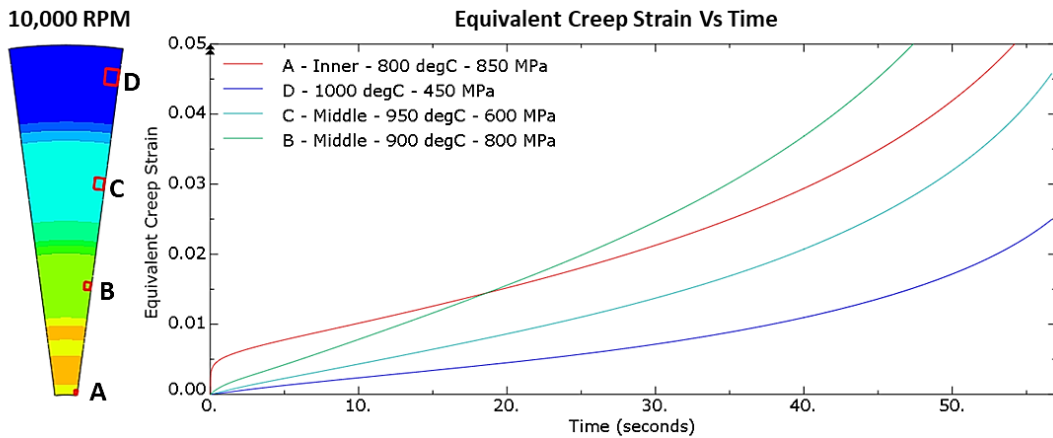


**Figure 10.5.4 - Creep strain - 8000 & 10000 RPM**

### C. Creep strain Vs Time

Four different elements are chosen, one from each temperature region and equivalent creep strain Vs Time is plotted at different RPMs.

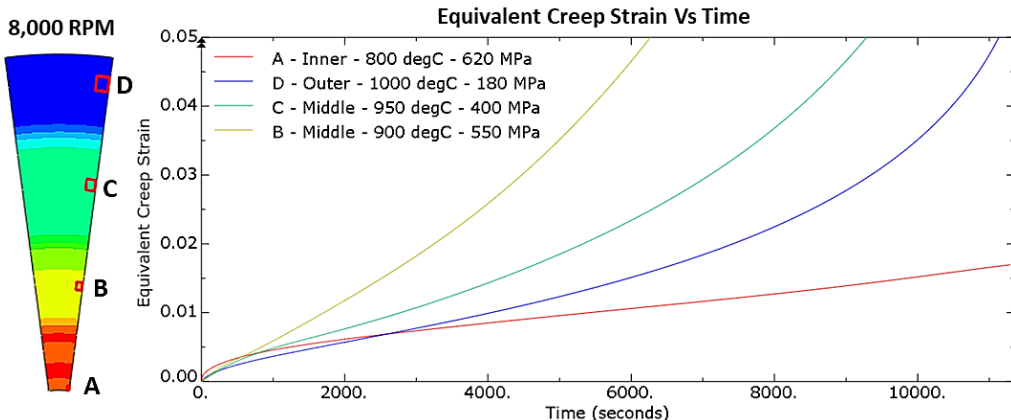
#### Case 1 – 10,000 RPM



Graph 10.5.1 - Creep strain Vs Time - Sector - 10000 RPM

- Element A, on the inner dia. shows high primary rate but low tertiary creep rate.
- Element B, on the middle shows low primary creep rate but high tertiary creep rate.
- Element D, on the outer dia. shows lowest primary and tertiary creep rates.

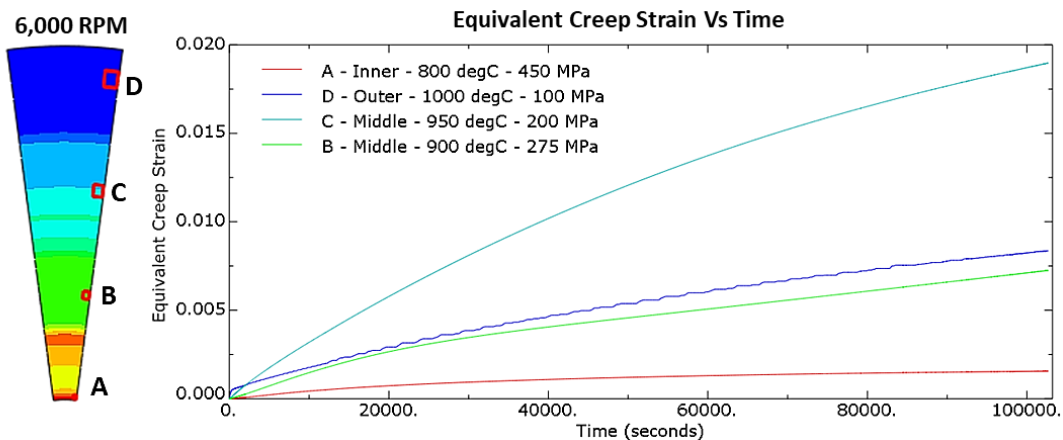
#### Case 2 – 8000 RPM



Graph 10.5.2 - Creep strain Vs Time - Sector - 8000 RPM

- Element A, on the inner dia. shows high primary rate but lowest tertiary creep rate
- Element B, on the middle shows low primary creep rate but high tertiary creep rate
- Element D, on the outer dia. shows low initial and tertiary creep rates

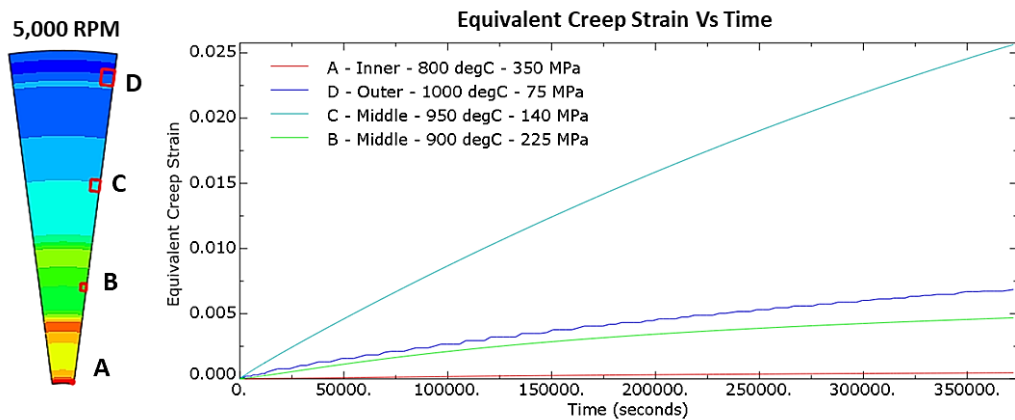
### Case 3 – 6000 RPM



*Graph 10.5.3 - Creep strain Vs Time - Sector - 6000 RPM*

- Element A, on the inner dia. shows lowest primary rate and steady state creep rates
- Element C, on the middle shows low primary rate but highest steady state creep rate
- Element D, on the outer dia. shows highest primary creep rate but moderate steady state creep rate

### Case 4 – 5000 RPM



*Graph 10.5.4 - Creep strain Vs Time - Sector - 5000 RPM*

- Element A, on the inner dia. shows lowest primary and steady state creep rates
- Element C, on the middle shows high primary and steady state creep rate

Combined effect of stress & temperature on creep rate at different locations in the model is evident from the above results. Difference in creep behavior at different locations for different RPM is also observed.

Behaviour of all internal state variables are similar to that of the previous test case.

## 10.6. TEST CASE 6 – TURBINE BLISK

A sector of sample turbine blisk is modelled and creep analysis using Theta projection user subroutine is carried out with only centrifugal force and arbitrary temperature field.

### 10.6.1. TEST CASE 6 – ANALYSIS DATA

#### Geometry:

- Hub : OD 440 mm x ID 180 mm
- Blade tip OD : 720 mm
- Blade span : 141 mm;
- Chord length : 120 mm at base & 150 mm at tip
- Thickness : 6 mm to 3 mm on root; 4 mm to 1.5 mm on tip
- Camber : 11 mm on root; 20 mm on tip
- Incidence angle : 4 deg on root & 20 deg on tip
- Arbitrary aero foil profiles & dimensions, not as per any standard
- Fillets removed for better mesh quality
- Partitioned as shown for better mesh transition & to apply temperature field

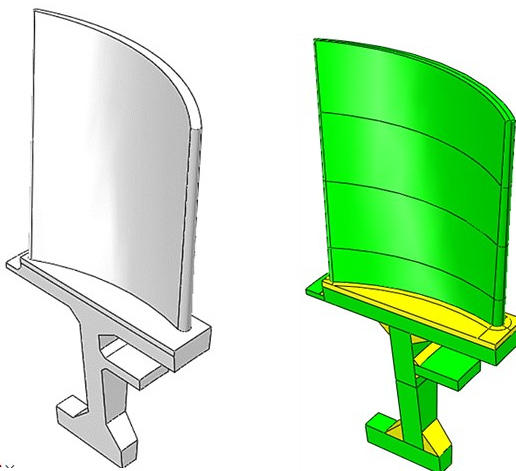


*Figure 10.6.1 - Turbine blisk Geometry & Partition for meshing*

#### Boundary conditions:

- Cylindrical co-ordinate system defined with R along radial, Theta along x and Z along thickness directions
- Cyclic symmetry interaction about Z axis – 45 no. of sectors (8 deg each)
- Inner face has all translational DOF fixed
- Temperature is applied uniformly in different region as shown (700 degC at bottom - 1000 degC at top)

- Rotational body force (centrifugal) applied on all nodes as angular velocity

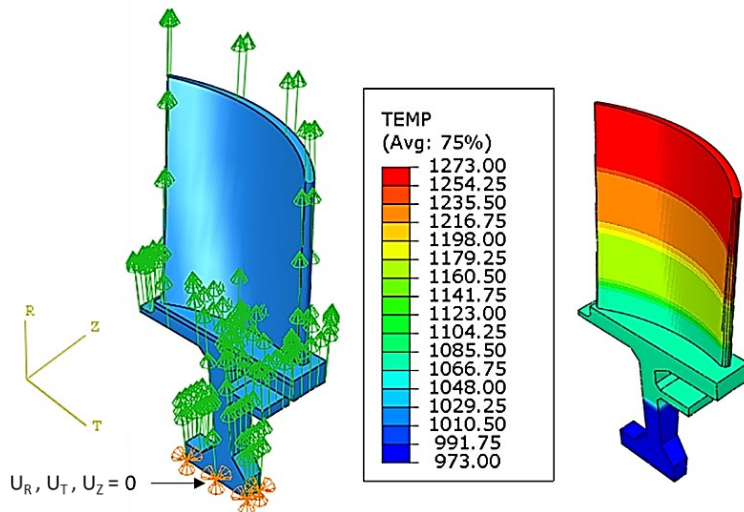


*Figure 10.6.2 - Boundary conditions - Turbine blisk*

### Mesh:

- Element types: Standard linear 3D stress C3D8 brick and C3D6 wedge elements
- Global size 4 mm and minimum size 0.5 mm
- 4 elements across blade thickness & 6 elements across curved edges
- Reduced integration option is turned off to avoid any calculation errors due to approximation
- Element deletion option is selected with max degradation of 1
- Total of 13862 elements complying to all basic quality metrics, as shown below:



*Figure 10.6.3 - Mesh - Turbine blisk*

```

Part: Turbine_blink_new
Hex elements: 13687
  Min angle on Quad Faces < 10: 0 (0%)
  Average min angle on quad faces: 79.84.  Worst min angle on quad faces: 29.69
  Max angle on Quad faces > 160: 0 (0%)
  Average max angle on quad faces: 100.38.  Worst max angle on quad faces: 155.98
  Aspect ratio > 10: 0 (0%)
  Average aspect ratio: 2.88.  Worst aspect ratio: 9.95
  Geometric deviation factor > 0.6: 0 (0%)
  Average geometric deviation factor: 0.00486.  Worst geometric deviation factor: 0.0739
Wedge elements: 175
  Min angle on Tri Faces < 5: 0 (0%)
  Average min angle on tri faces: 39.01.  Worst min angle on tri faces: 5.99
  Min angle on Quad Faces < 10: 0 (0%)
  Average min angle on quad faces: 82.44.  Worst min angle on quad faces: 50.91
  Max angle on Tri faces > 170: 0 (0%)
  Average max angle on tri faces: 88.82.  Worst max angle on tri faces: 160.71
  Max angle on Quad faces > 160: 0 (0%)
  Average max angle on quad faces: 97.51.  Worst max angle on quad faces: 129.48
  Aspect ratio > 10: 0 (0%)
  Average aspect ratio: 2.62.  Worst aspect ratio: 8.60
  Geometric deviation factor > 0.6: 0 (0%)
  Average geometric deviation factor: 0.00145.  Worst geometric deviation factor: 0.00396
Number of elements : 13862.  Analysis errors: 0 (0%).  Analysis warnings: 0 (0%)

```

*Figure 10.6.4 - Mesh quality metrics - Turbine blisk*

### Material properties:

- CM-247 superalloy with density  $8540 \text{ kg/m}^3$

- Young's modulus & Poisson's ratio are specified for temperature range as shown
- Total no. of state variables is 5 and variable 4 controls the element deletion
- Creep law is specified as “User-defined”
- Solid, homogeneous sections are assigned to the model

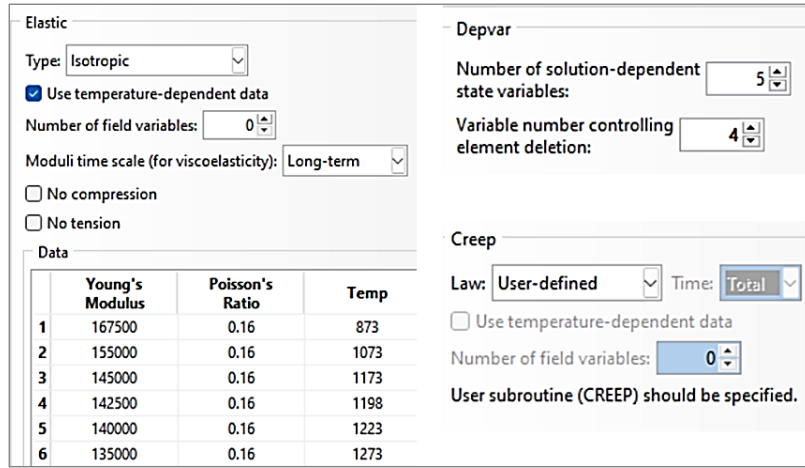
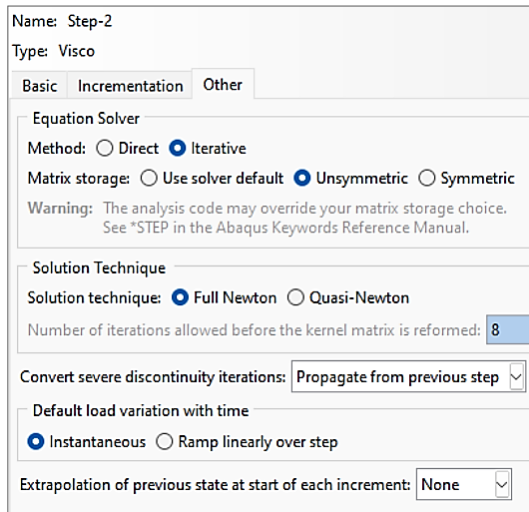


Figure 10.6.5 - Material properties - inputs in Abaqus

#### Analysis Steps:

- Static procedure for 0.01 seconds with NL Geom “On”
- Initial & min time increment of 0.001s and max of 0.0025s for static step
- Visco step with Initial time increment of  $1 \times 10^{-20}$  s, min. of  $1 \times 10^{-35}$  s and maximum of 600 s.
- Creep increment error tolerance of  $1 \times 10^{-4}$  to 0.001
- Creep integration method is “Explicit/Implicit”
- Direct solver & default matrix storage for static step
- “Iterative solver” with “unsymmetric” matrix storage for visco step
- “Extrapolation of previous step at the start of increment” option is turned off (None)

Note: If initial strain rates are high, even smaller initial time increment and lesser creep increment error tolerance is to be used to continue analysis



**Figure 10.6.6 - Creep analysis - solution settings**

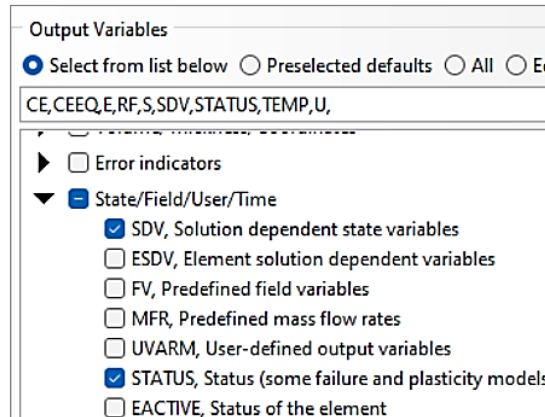


**Figure 10.6.7 - Field output settings**

## Field outputs

- In addition to default values, below outputs may be requested on visco steps
  - Nodal Temperature (NT) - (for both static & visco steps)
  - Creep strain components (CE) & Equivalent creep strain (CEEP)
  - Solution dependent state variable (SDV) & STATUS – to visualize internal variables (Hardening, recovery & damage)

## Job settings

- A job is created for analysis for each load case (each RPM)
- Fortran code (.for) file of the user subroutine is attached as shown
- “Full” nodal output precision is requested as variables data types are declared as double precision in the subroutine code

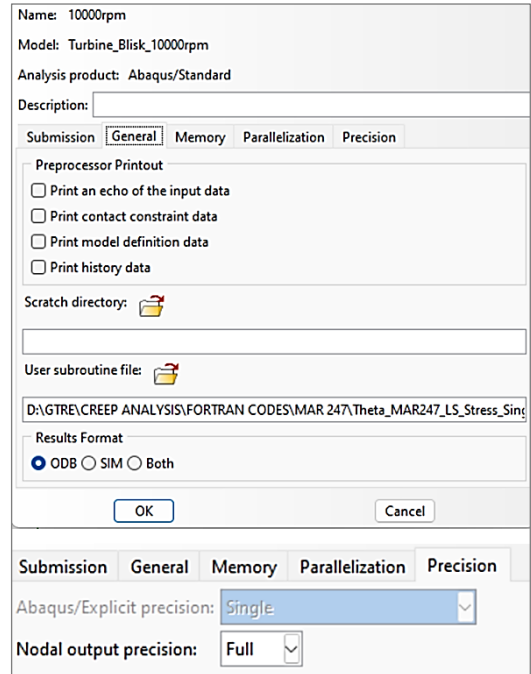


**Figure 10.6.8 - Job settings**

## 10.6.2. TEST CASE 6 – RESULTS – 10,000 RPM

### A. Von Mises Stress – 10,000 RPM

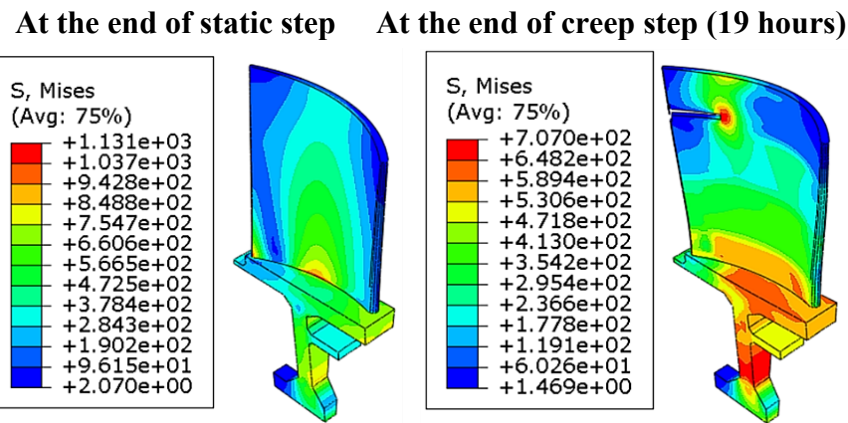


Figure 10.6.9 - Von Mises Stress distribution - Turbine blisk - 10,000 RPM

Initially, maximum stress of 1131 MPa is observed on some high stress concentration areas at the root of the blade. Stresses are relaxed after 2 hrs due to straining of elements. High stress concentration is seen at crack tips after 11 hrs due to damage.

### B. Stress components – 10,000 RPM

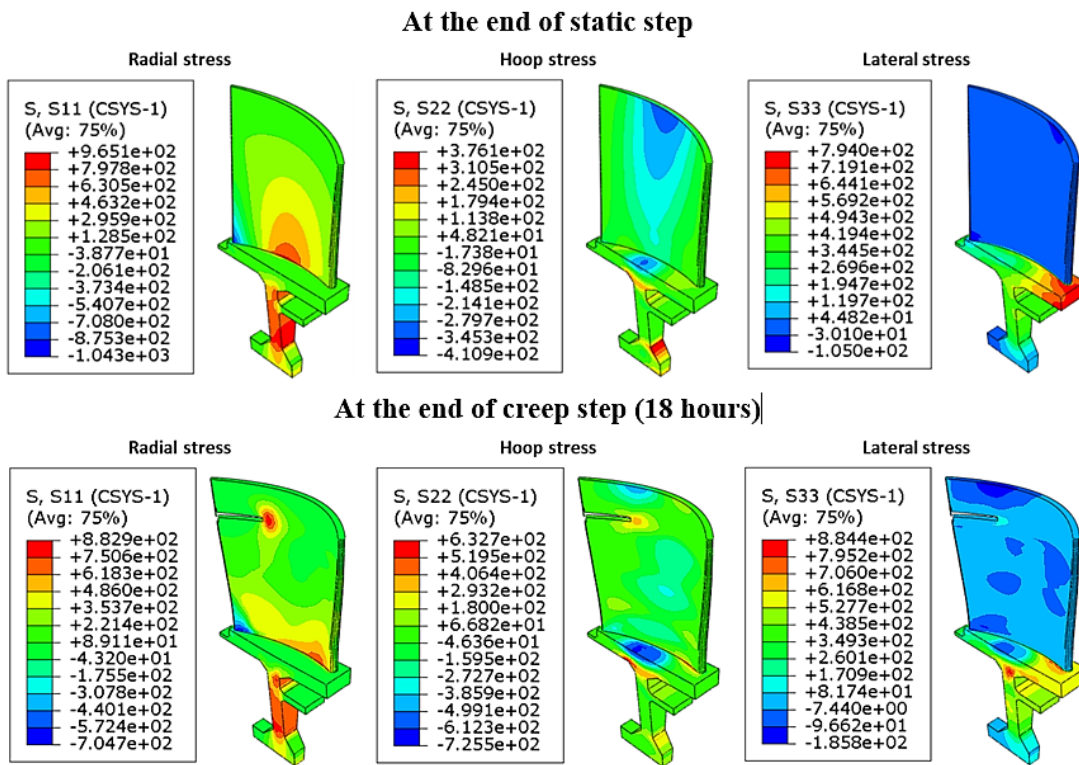
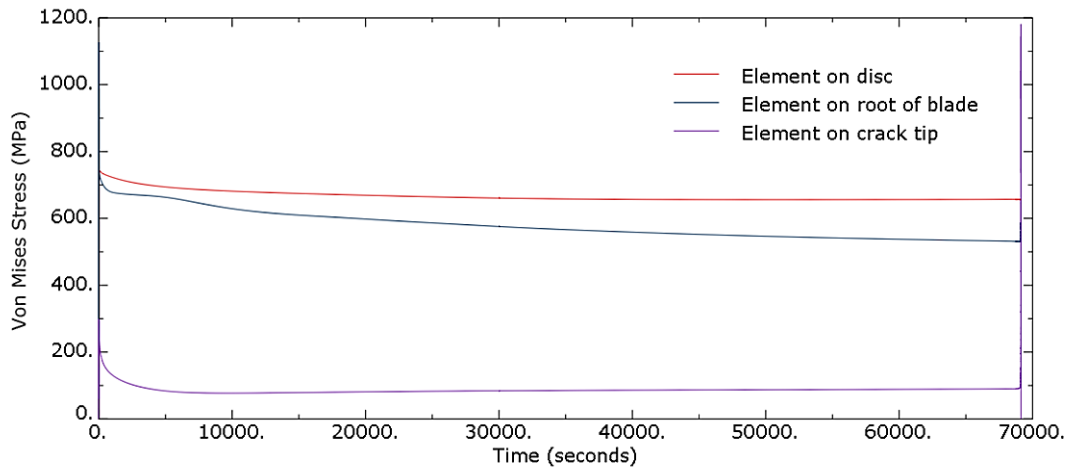


Figure 10.6.10 - Stress components before & after creep damage

Radial stresses have reduced due to creep deformation (radial growth) and blade displacement whereas hoop stresses & lateral stresses have increased at the end of creep step. High concentration of radial stress is seen at the crack tip.

### C. Stress – Time history – 10,000 RPM

Variation of Von Mises stress with respect to time is plotted for 3 elements, one element on the root of the blade where initial stress was maximum, one element on the hub where the stress was maximum during creep stage and one element on the crack tip where high stress concentration was observed due to damage.



**Graph 10.6.1 - Von Mises Stress - Time history**

- Even though initial stress was higher on the root of the blade, stress has decreased due to deformation.
- Since the inner face of the disc is only fixed for all degree of freedom, blade has displaced a little in transverse and lateral directions which relieves the stresses just after the static step.
- Element on the crack tip shown sudden steep increase in stress due to damage and immediately goes to zero due to element deletion indicating fracture.

## D. Total deformation and components – 10,000 RPM

Total deformation includes both elastic and plastic deformation (creep). Magnitude of total deformation and its components are shown below.

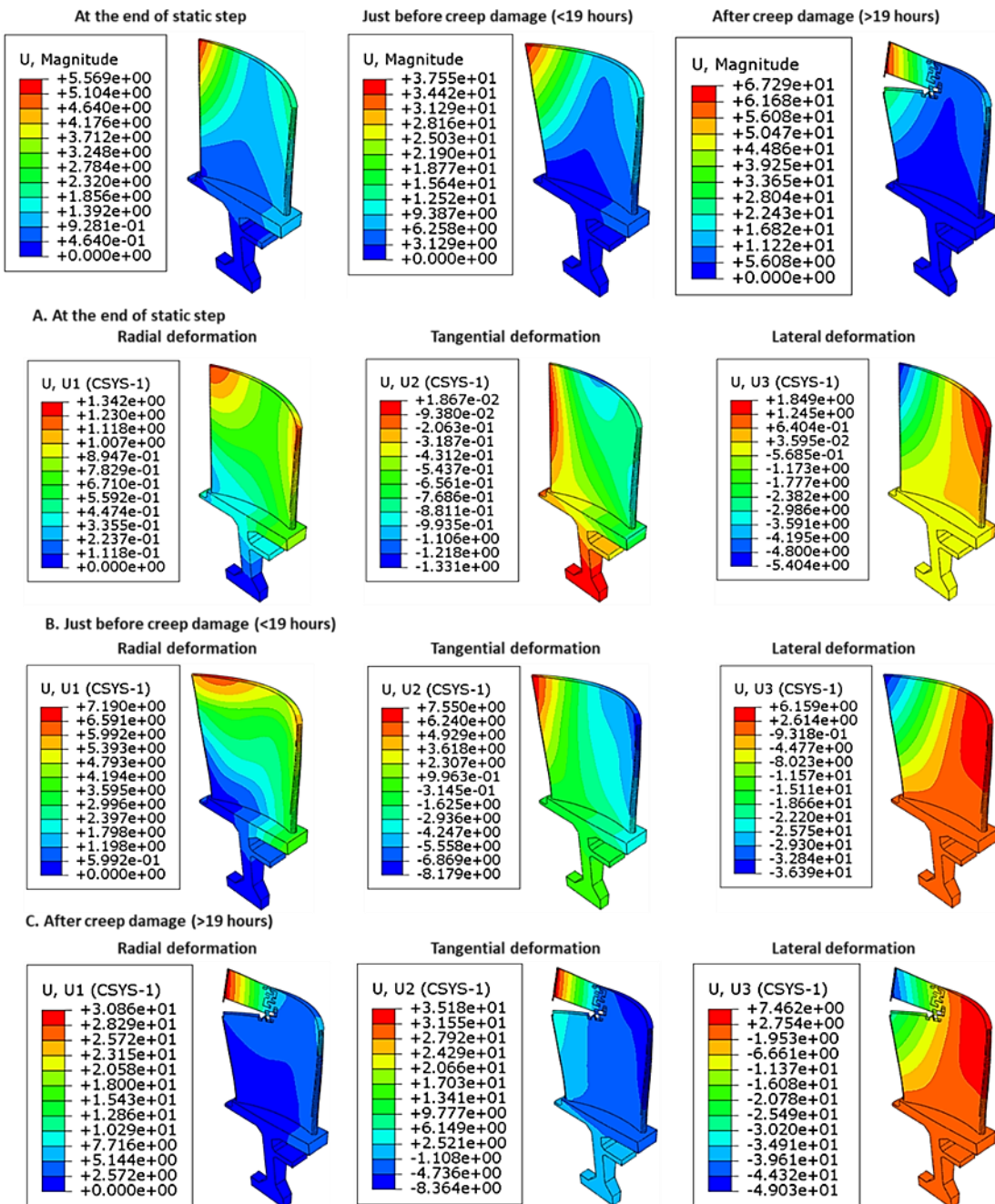


Figure 10.6.11 - Deformation before and after creep damage

Initially at the end of static step, radial and lateral deformation is high. All components of deformation are higher in the tertiary stage and increase rapidly after creep damage as the element connectivity is lost around crack.

## E. Equivalent creep strain – 10,000 RPM

Contour plot of equivalent creep strain at the end of creep step (19 hours) indicating damage is shown below.

Even though stresses are higher at the root of the blade and disc, since temperature is higher towards the tip of the blade, creep strain is higher at the tip of the blade. Fracture strain of 10% is specified for element deletion.

## F. Creep strain components

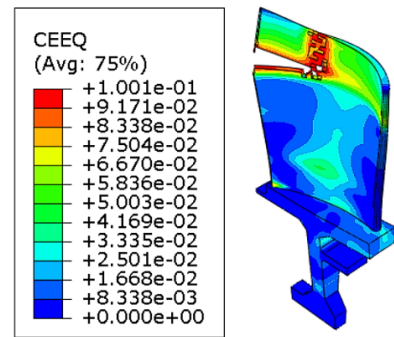


Figure 10.6.12 - Equivalent creep strain - 10,000 RPM - 19 hours

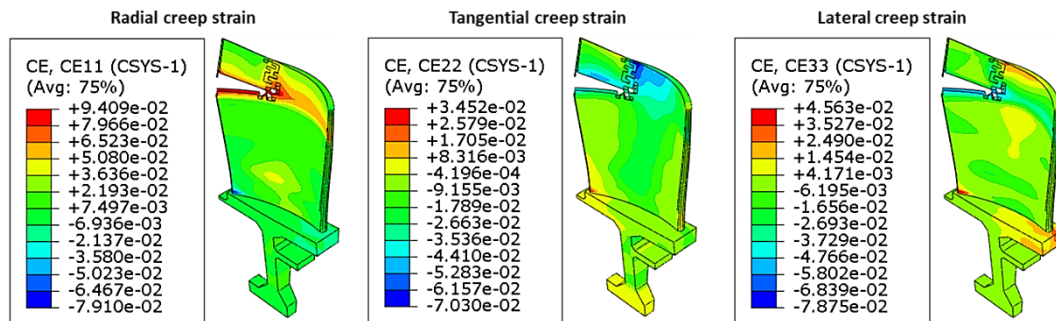
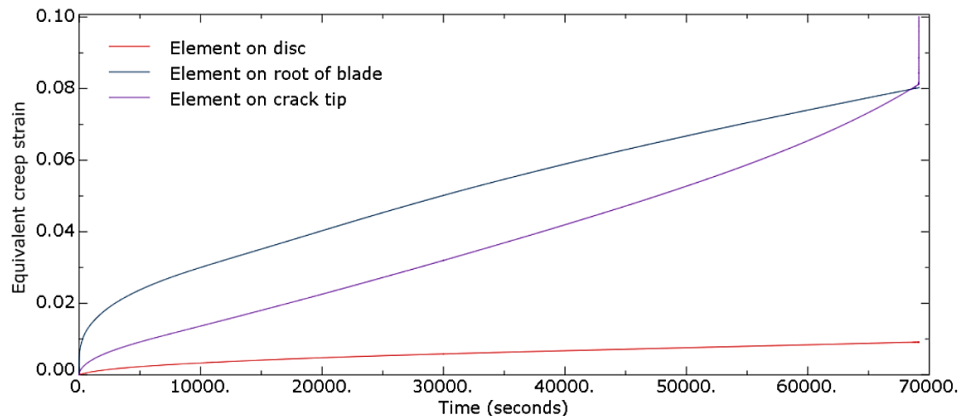


Figure 10.6.13 - Creep strain components - 10,000 RPM - 19 hours

Radial component of creep strain is higher than other components. Tangential and lateral strains are predominantly compressive while radial strains are mostly tensile due to the direction of centrifugal stresses. Radial creep strain at the root of the blade is compressive as the radial stresses are compressive whereas tangential and lateral creep strains at the root of blade are tensile along respective axes.

## G. Equivalent creep strain Vs Time



Graph 10.6.2 - Creep curve results - 10,000 RPM

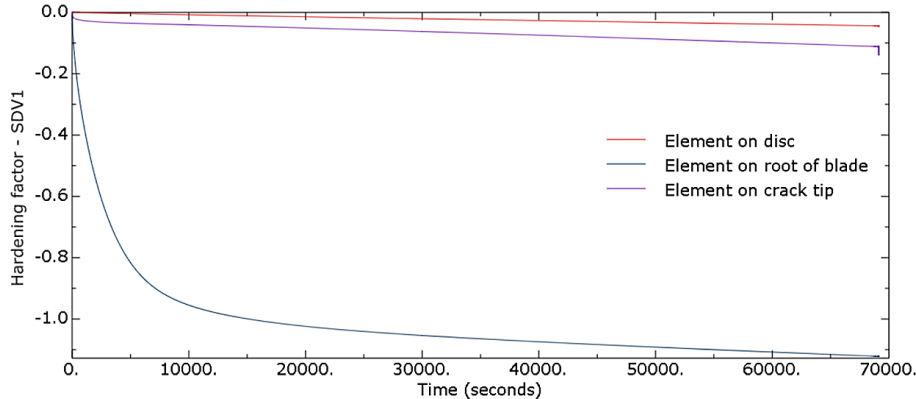
Creep curve results show the primary and secondary creep stages clearly for elements on the disc and root of the blade.

Element on the disc shows lower creep rate in spite of higher stresses due to lower temperature. Element on the root of the blade shows higher primary and steady state creep as the stresses are higher as well as temperature is relatively higher (~800 deg C). This results in higher rate of strain hardening and reduction in further strain rate. Element near the tip of blade shows lower primary rate due to low stresses but higher steady state and steep tertiary creep rate due to the effect of higher temperature (~1000 deg C). This is

analogous to forming of metals at higher temperature and lower stresses which results in plastic deformation without hardening the material.

At the end of creep step (19 hours), creep strain on the element near the tip of blade quickly rises to more than 10% leading to damage and fracture.

#### H. Hardening factor (Solution dependent variable 1)

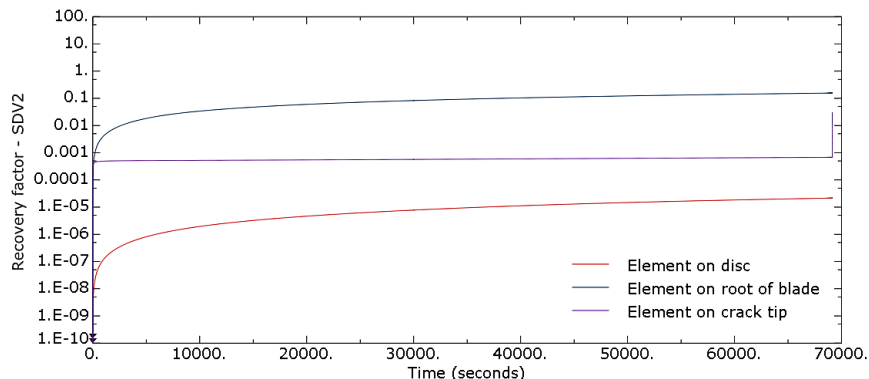


**Graph 10.6.3 - Hardening curve - Turbine blisk - 10,000 RPM – 19 hours**

Higher negative values indicate higher hardening factor. Rate of hardening is higher in the primary stages of element on the root of blade due to high stress & temperature and exponentially decreases as the material strains. Rate of hardening of element on disc is low as both temperature and stress are low. Rate of hardening of element near tip of blade is low but gradually increases as the temperature is high. At the end of 19 hours, hardening factor steeply increases due to high stress concentration during damage.

#### I. Recovery factor (Solution dependent variable 2)

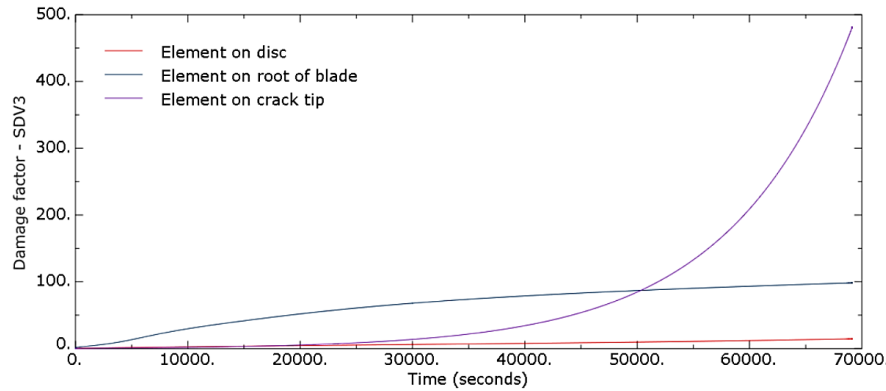
Recovery curve is plotted in logarithmic scale to show large variation in the values.



**Graph 10.6.4 - Recovery curve - Turbine blisk - 10,000 RPM – 19 hours**

Element on disc and element on root of blade show similar linear recovery rates as recovery is independent of strain rate. Also, the slope of log curve (recovery coefficient) which is the scaling factor is high for these two elements as seen apparently from the smooth and gradual scaling in the primary stage. The element near the tip of blade shows very steep primary scaling (low recovery coefficient) due to low temperature. Fracture is also indicated by steep increase in recovery after 19 hours.

## J. Damage factor (Solution dependent variable 3)



**Graph 10.6.5 - Damage curve - Turbine blisk - 10,000 RPM – 19 hours**

Element on the disc shows lower damage rate throughout due to low creep strain rate. Element on the root of blade shows gradually increasing damage due to higher creep strain rate. Element near the tip of blade shows lower primary damage but exponentially increasing damage till fracture.

### 10.6.3. CREEP LIFE ESTIMATION – CASE 1

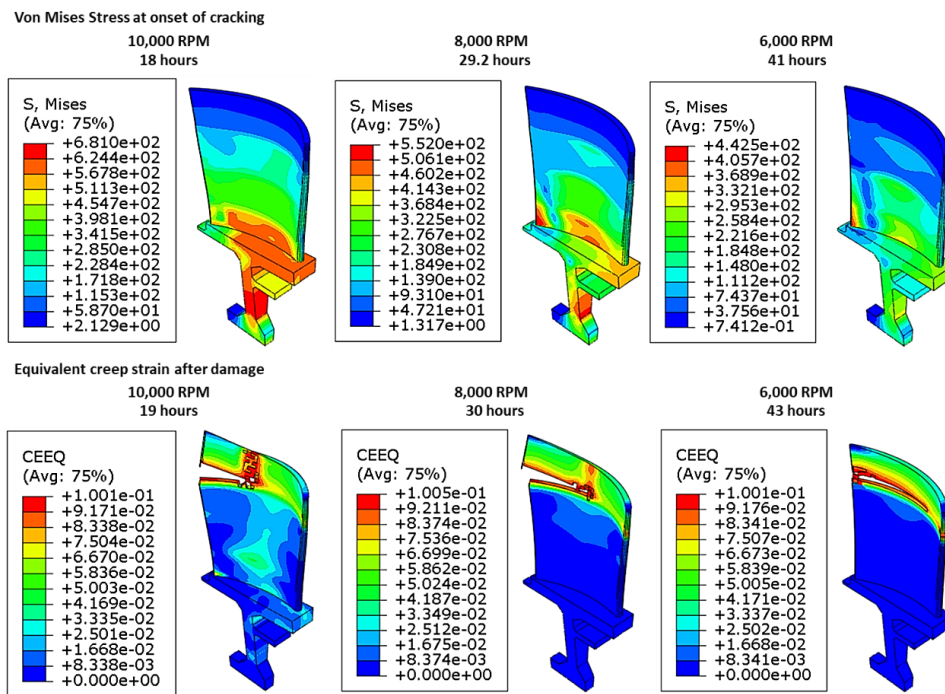


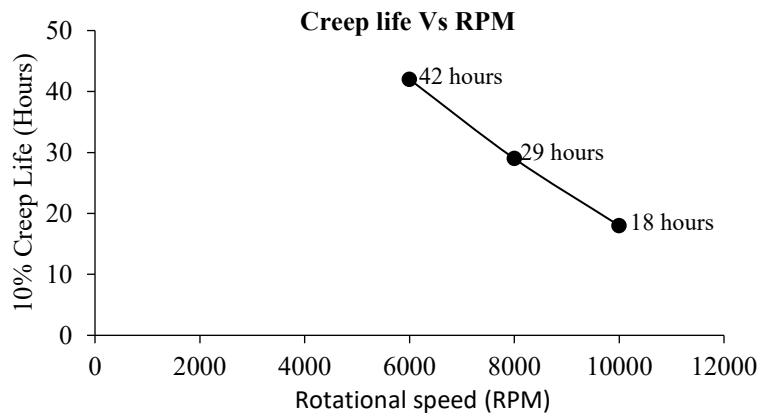
**Figure 10.6.14 - Stress & Creep strain - at different RPMs**

Contour plots of Von Mises stress at the onset of damage and equivalent creep strain after damage is shown in the above figure for different rotational speeds (RPMs). Fracture strain is prescribed as 10% creep strain over which elements are deleted indicating damage and crack.

It is observed that the stress and creep patterns are similar as the analysis is carried out at same temperature fields. The magnitude of creep strain and time to onset of crack varies a little.

Time to fracture (10% creep strain) can be considered as a criterion for strength life of the blade. Considering this, creep life of gas turbine blisk can be directly taken from the analysis results as 18 hours for 10,000 RPM above which cracks start to appear in the material. As stresses decrease with decrease in rotational speeds, 10% creep life is observed to increase to 29.2 hours for 8,000 RPM and 41 hours for 6,000 RPM.

The results of time to onset of fracture (10% creep strain) are plotted at different RPMs. The graph shows quasi-linear relationship between creep life and RPM. Also, the predicted creep life and the fracture patterns do not vary much for different RPMs because at 1000degC along the tip of blade, creep strain rates are very high leading to early fracture at all RPM cases. Also, fracture strain is chosen arbitrarily as 10% which is impractical. Since creep input was only available for 950 degC for material constant calculation, at 1000 degC even for smaller stresses, high initial strain is evident due to high error in extrapolation and there is a need to reduce the same statistically to improve accuracy, which is taken care by using Robust weighting scheme for material constants calculation and discussed in later sections.



**Graph 10.6.6 - Creep Life Vs RPM**

Stiffness life for 2% creep strain can also be directly read from the analysis results by measuring the minimum time at which prescribed percentage of elements (usually 40%) reach a creep strain value of 2%. As shown below, creep strain result of 10,000 RPM case is displayed but only those elements over 2% creep strain are colored.

Even though percentage of elements over 2% creep strain is less than 40% till the end of analysis time, fracture strain has exceeded in a number of elements and stiffness life method may not be suitable for our analysis conditions, as the expected life for 10,000 RPM would be more than 19 hours whereas the material has already fractured.

Stiffness life would be very useful in low creep rate cases with uniform as well as low stress and low temperature conditions where elements do not reach fracture strain for a very long time and analysis can be terminated earlier when 40% of the elements reach prescribed 2% creep strain.

Other life parameters like Larson – Miller parameter, Monkman Grant life for onset of tertiary, etc. can be calculated from the analysis results to project results to other load cases for design envelope & optimization studies. However, since creep analysis using Abaqus user subroutine is simpler, we can perform the analysis and obtain creep life at different load conditions and the life extrapolation parameters would not be necessary.

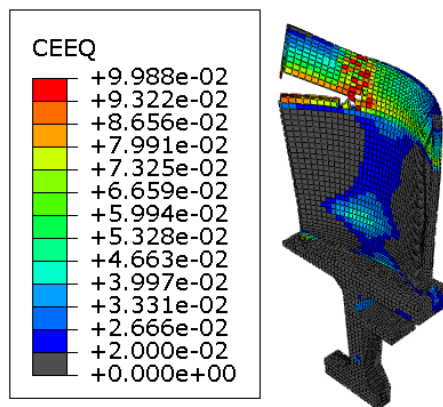


**Figure 10.6.15 - Result showing only 2% creep strain elements - 10,000 RPM**

## 10.7. TEST CASE 7 – TURBINE BLISK CASE 2

The results of time to creep rupture were not satisfactorily modelled in Test case 6 due to the limitations of high stresses and temperature causing very high initial strain rates and rupture causing termination of analysis with most of the elements still below 1% creep strain. Hence, analysis of a new test case with below modifications is carried out to solve the respective modelling difficulties:

- Robust weighting scheme for least square regression has been adopted for improving extrapolation accuracy, the procedure is explained in later sections
- Temperature distribution is modified closer to practical situation for wider stress – temperature combinations with maximum temperature 950 deg C instead of 1000 deg C to prevent high initial strain rates & fracture
- “GPa-ms-kN-mm” system of units is adopted to prevent numerical values of Theta coefficients or internal state variables from going very high or very low which caused difficulties in convergence in previous case modelled with “MPa-s-N-mm” units. (Abaqus cannot handle numerical values less than  $1 \times 10^{-28}$  and greater than  $1 \times 10^{28}$  and any value beyond this range causes numerical overflow).
- To improve range capability of analysis, creep data for 800 degC 10 MPa and 800 degC 1200 MPa has been extrapolated from the curve-fitted Theta coefficients artificially before calculating material constants, whose procedure is discussed in later section
- Empirical model for fracture strain developed by Evans M is adopted for element deletion

### 10.7.1. TEST CASE 7 – ANALYSIS DATA

Geometry and boundary conditions are the same as for turbine blisk described in Test case-6 except for temperature distribution with minimum 600 degC to 950 degC as shown. 1 mm fillet is added at the root for reduce stress concentration and mesh flow. The units of temperature are in kelvin.

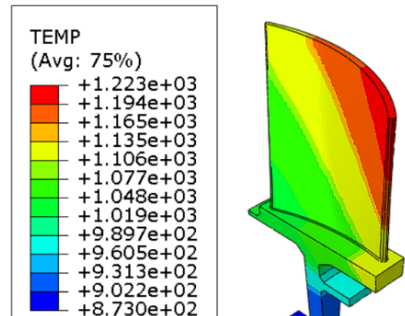


*Figure 10.7.1 - Temperature field -  
Test case 7*

#### Mesh:

- Element types: Standard linear 3D stress C3D8 brick and C3D6 wedge elements
- Global size 6 mm and minimum size 0.5 mm
- 2 elements across blade thickness
- 4 elements across curved edges
- Reduced integration option is turned off to avoid any calculation errors due to approximation
- Element deletion option is selected with max degradation of 1
- Total of 7055 elements complying to all basic quality metrics, as shown below:



*Figure 10.7.2 - Mesh  
- Test case 7*

```
Part: Turbine_bdisk_new
Hex elements: 6542
  Min angle on Quad Faces < 10: 0 (0%)
  Average min angle on quad faces: 80.05, Worst min angle on quad faces: 37.33
  Max angle on Quad faces > 160: 0 (0%)
  Average max angle on quad faces: 99.84, Worst max angle on quad faces: 146.90
  Aspect ratio > 10: 0 (0%)
  Average aspect ratio: 2.00, Worst aspect ratio: 5.68
  Geometric deviation factor > 0.6: 0 (0%)
  Average geometric deviation factor: 0.00760, Worst geometric deviation factor: 0.245

Wedge elements: 513
  Min angle on Tri Faces < 5: 0 (0%)
  Average min angle on tri faces: 41.60, Worst min angle on tri faces: 29.51
  Min angle on Quad Faces < 10: 0 (0%)
  Average min angle on quad faces: 79.34, Worst min angle on quad faces: 47.28
  Max angle on Tri faces > 170: 0 (0%)
  Average max angle on tri faces: 79.93, Worst max angle on tri faces: 113.41
  Max angle on Quad faces > 160: 0 (0%)
  Average max angle on quad faces: 100.58, Worst max angle on quad faces: 129.71
  Aspect ratio > 10: 0 (0%)
  Average aspect ratio: 3.29, Worst aspect ratio: 5.70
  Geometric deviation factor > 0.6: 0 (0%)
  Average geometric deviation factor: 0.0302, Worst geometric deviation factor: 0.244
Number of elements : 7055, Analysis errors: 0 (0%), Analysis warnings: 19 (0.269313%)
```

*Figure 10.7.3 - Quality metrics - Test case 7*

There are 19 warnings for elements along fillet for short edge (0.86 mm) which can be neglected.

#### Material properties:

- CM-247 superalloy with density  $8540 \text{ kg/m}^3$
- Young's modulus & Poisson's ratio are specified for temperature range as shown
- Total no. of state variables is 5 and variable 4 controls the element deletion

- Creep law is specified as “User-defined”
- Solid, homogeneous sections are assigned to the model

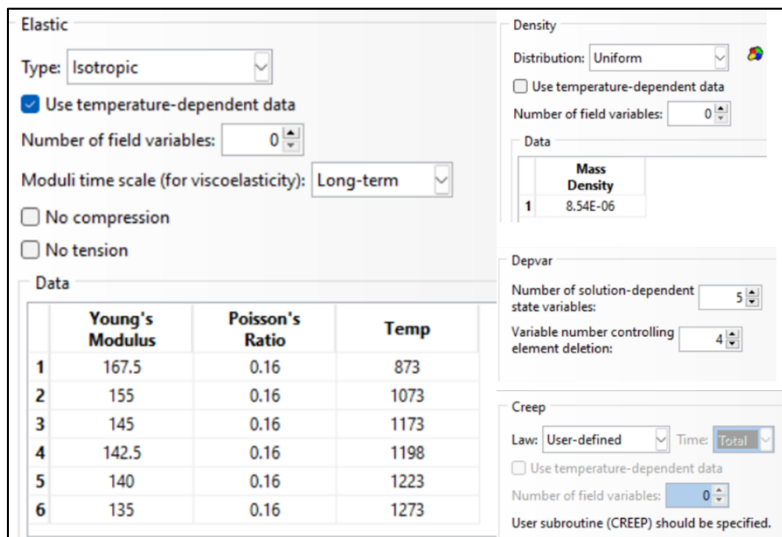


Figure 10.7.4 - Material Properties - Test case 7

### Analysis Steps:

- Static procedure for  $1 \times 10^{-6}$  millisecond with NL Geom “On”
- Initial & min time increment of  $1 \times 10^{-8}$  ms and max of  $5 \times 10^{-7}$  ms for static step
- Visco step with Initial time increment of 0.01 ms, minimum of  $1 \times 10^{-20}$  ms and maximum of  $60 \times 10^3$  ms.
- Creep increment error tolerance of  $1 \times 10^{-4}$  to 0.01
- Creep integration method is “Explicit/Implicit”
- Direct solver & default matrix storage for static step
- “Direct” or “Iterative solver” with “unsymmetric” matrix storage for visco step
- “Extrapolation of previous step at the start of increment” option is turned off (None)

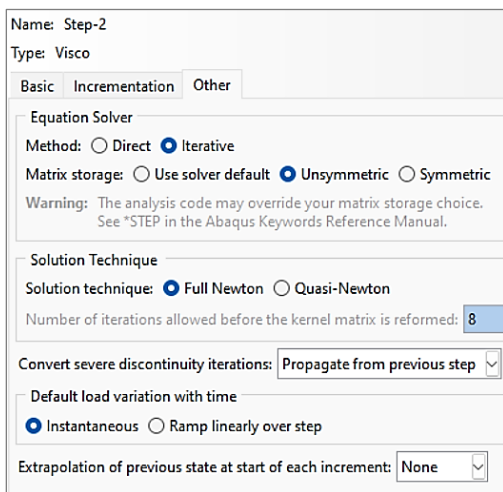


Figure 10.7.5 - Creep analysis - solution settings

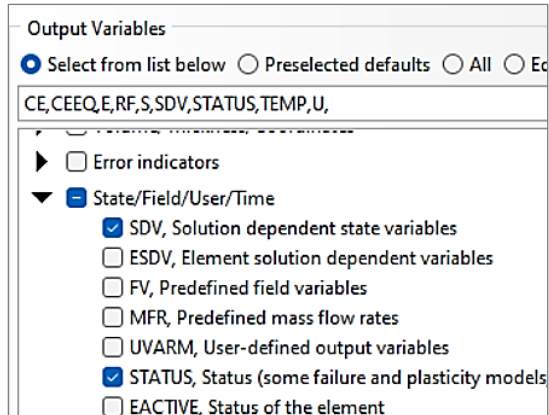


Figure 10.7.6 - Field output settings

*Note:* If initial strain rates are high, even smaller initial time increment and lesser creep increment error tolerance is to be used to continue analysis

## Field outputs

- In addition to default values, below outputs may be requested on visco steps
  - Nodal Temperature (NT) - (for both static & visco steps)
  - Creep strain components (CE) & Equivalent creep strain (CEEP)
  - Solution dependent state variable (SDV) & STATUS – to visualize internal variables (Hardening, recovery & damage)

## Job settings

- A job is created for analysis for each load case (each RPM)
- Fortran code (.for) file of the user subroutine is attached as shown
- “Full” nodal output precision is requested as variables data types are declared as double precision in the subroutine code

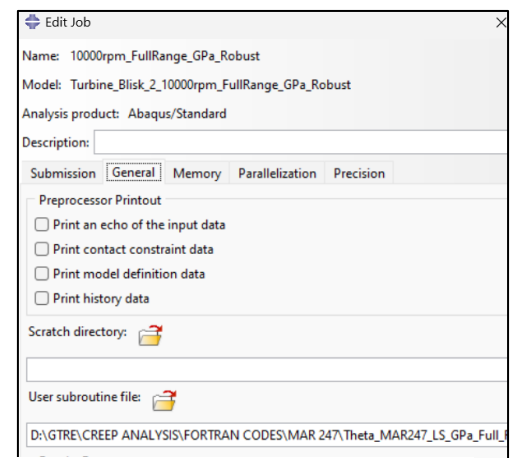
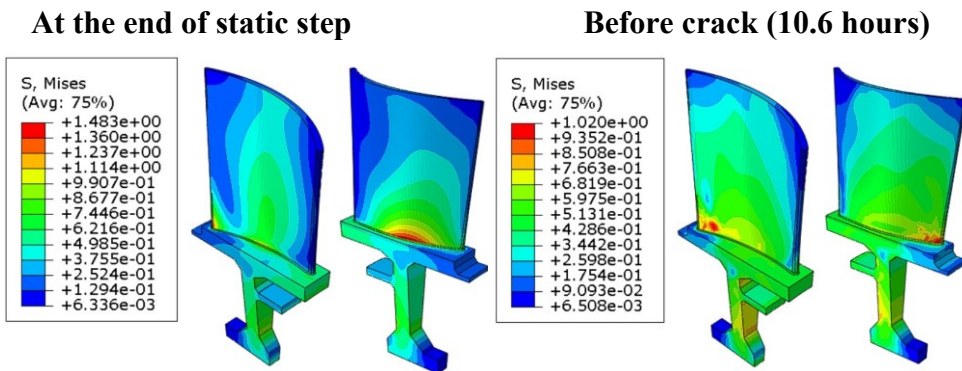


Figure 10.7.7 - Job settings - Test case 7

## 10.7.2. TEST CASE 7 – RESULTS – 10,000 RPM

### A. Von Mises Stress – 10,000 RPM



*Figure 10.7.8 - Von Mises Stress - Test case 7*

Maximum initial stress of 1483 MPa is observed at the root on the suction side & high stress concentration is seen on trailing edge of the blade. Stresses are relaxed due to high initial creep strain & displacement and max stress falls to around 1000 MPa at the root near the trailing edge.

### B. Stress components – 10,000 RPM

Radial stresses have reduced due to blade displacement (deformation) whereas hoop stresses & lateral stresses have increased due to creep deformation (radial growth) towards the end of creep step. (Units in GPa)

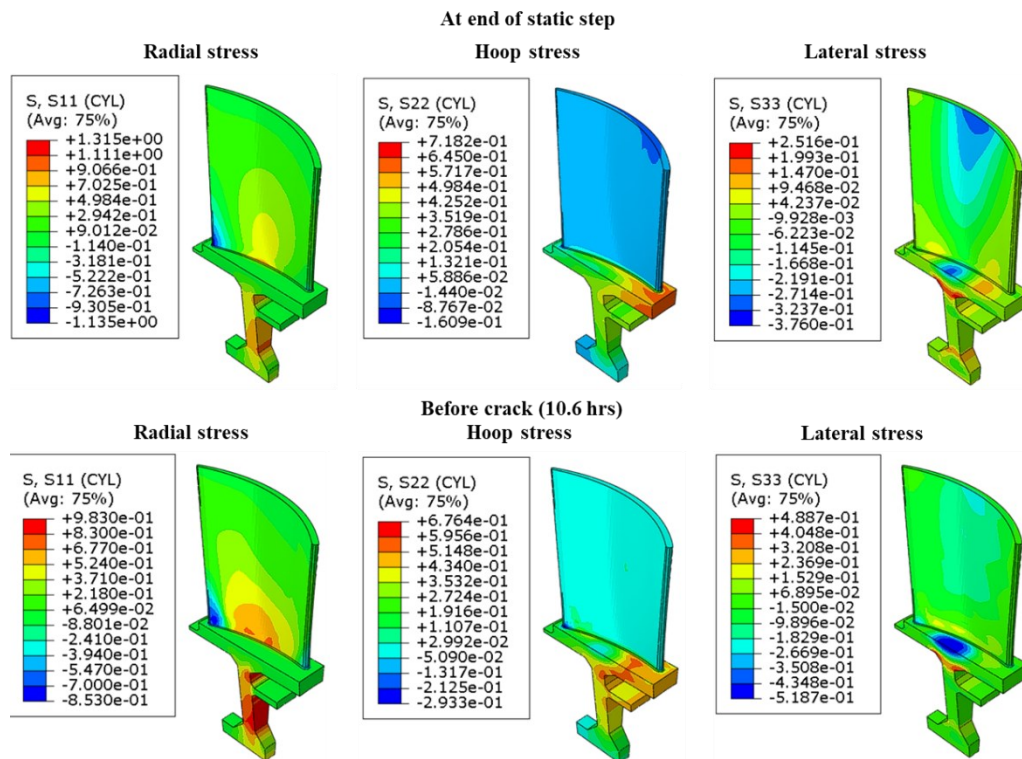
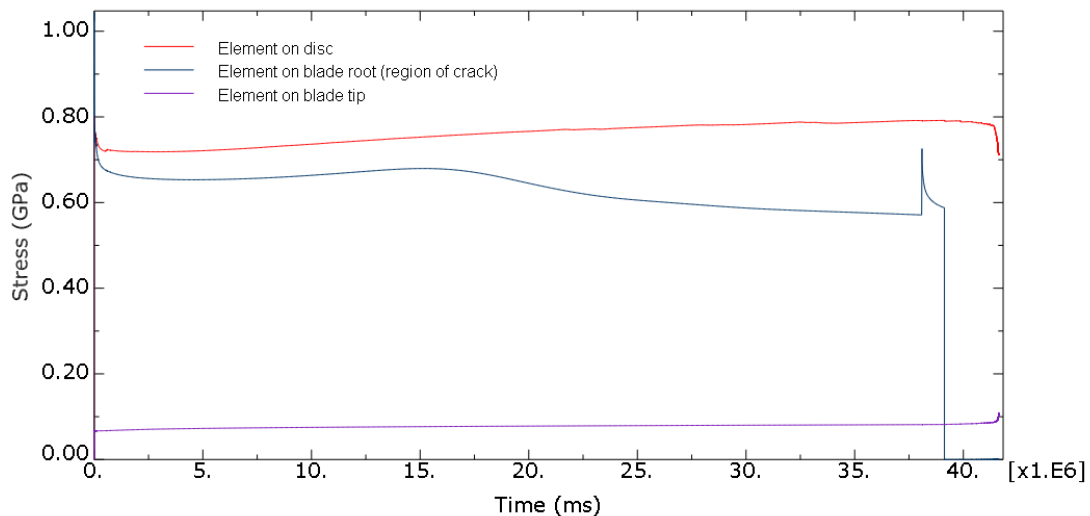


*Figure 10.7.9 - Stress components - Test case 7*

### C. Stress – Time history – 10,000 RPM

Variation of Von Mises stress with respect to time is plotted for 3 elements, one element on the disc of the blade where initial stress was maximum, one element on the blade tip where stresses are low and one element on the root of blade where high stress concentration was observed leading to crack after 11 hrs due to damage.



**Graph 10.7.1 - Time history of Von Mises Stress**

- Even though initial stress was higher on the root of the blade, stress has decreased due to deformation.
- Since the inner face of the disc is only fixed for all degree of freedom, blade has displaced a little in transverse and lateral directions which relieves the stresses just after the static step.
- Element on the crack tip shown sudden steep increase in stress due to damage at around 10.6 hours and goes to zero due to element deletion indicating fracture at 11.6 hours.

## D. Total deformation and components – 10,000 RPM

Total deformation includes both elastic and plastic deformation (creep). Magnitude of total deformation and its components are shown below: (units in mm)

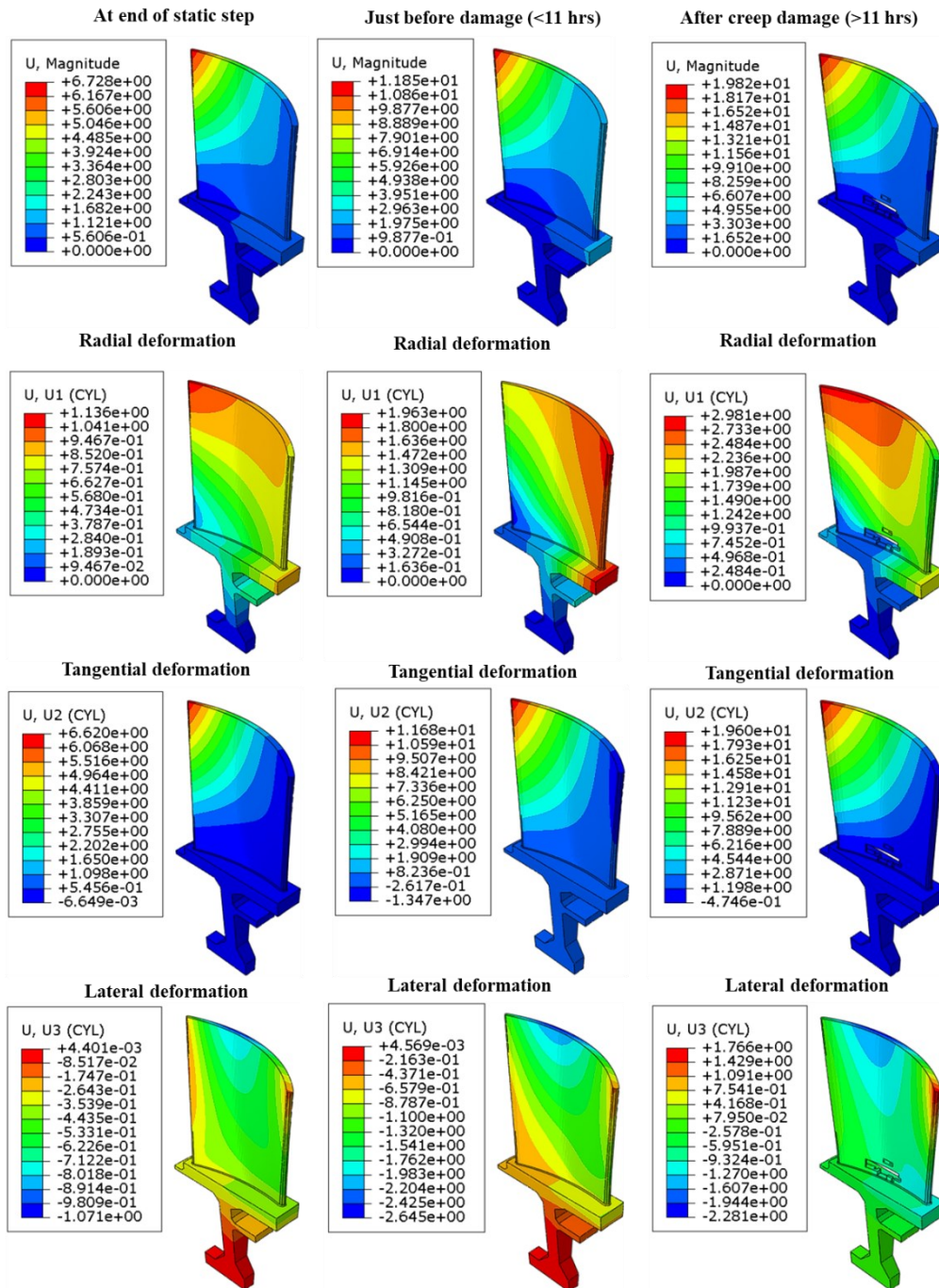


**Figure 10.7.10 - Deformation before & after creep damage**

Initially at the end of static step, radial and lateral deformation is high. All components of deformation are higher in the tertiary stage and increase rapidly after creep damage as the element connectivity is lost around crack.

## E. Equivalent creep strain – 10,000 RPM

Contour plot of equivalent creep strain at 10.6 hours before crack initiation is shown.

Creep strain is higher at the root of the blade due to higher stress and temperature. Even though stress concentration was higher on the trailing edge corner at root, stress relaxation due to creep deformation led to small reduction in creep rate.

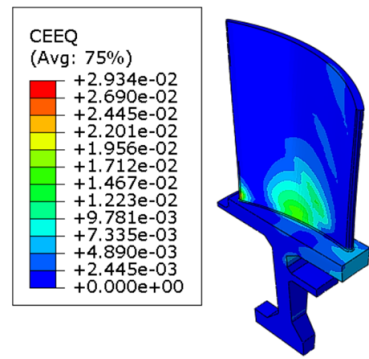


**Figure 10.7.11 - Equivalent creep strain - 10,000 RPM – 10.6 hours**

## F. Creep strain components

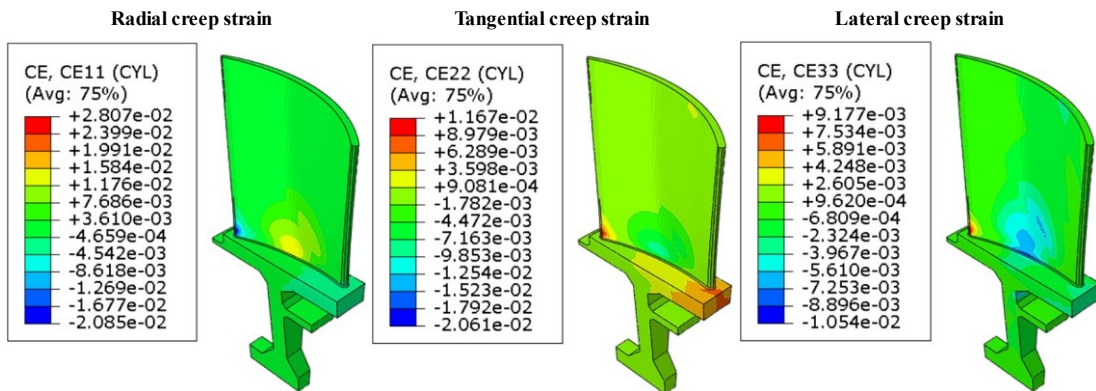
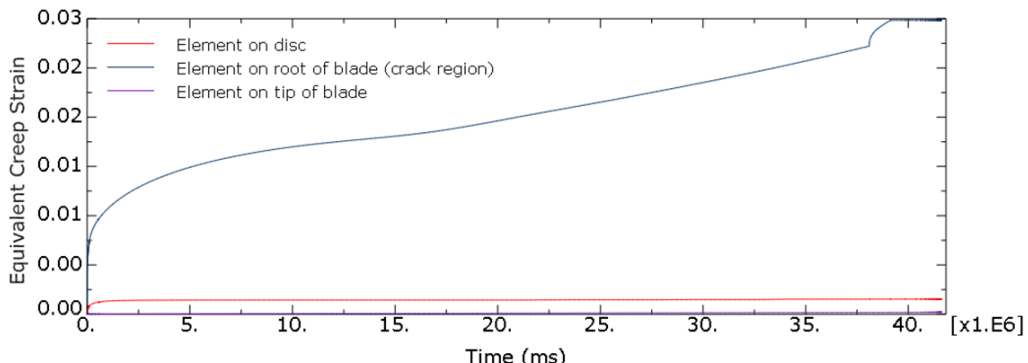


**Figure 10.7.12 - Creep strain components - 10,000 RPM – 11 hours**

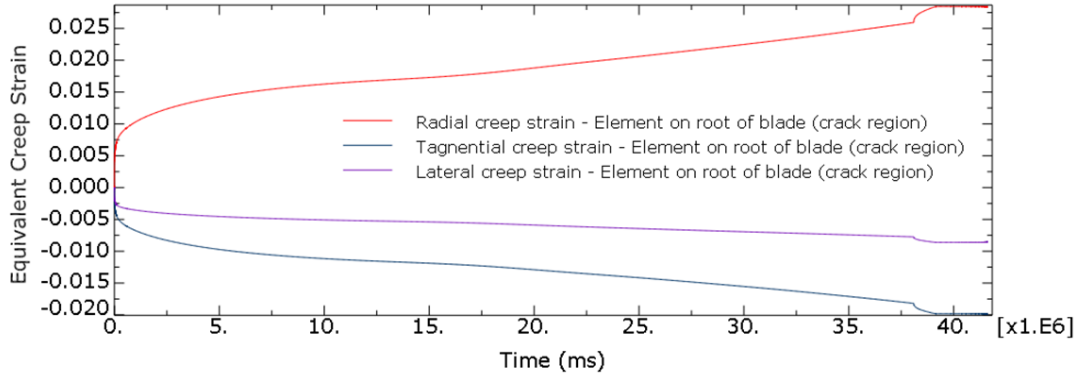
Radial component of creep strain is higher than other components. Tangential and lateral strains are predominantly compressive while radial strains are mostly tensile due to the direction of centrifugal stresses. Radial creep strain at the root of the blade is compressive as the radial stresses are compressive whereas tangential and lateral creep strains at the root of blade are tensile along respective axes.

## G. Time history of creep strain



**Graph 10.7.2 - Creep curve results - 10,000 RPM**

Element on root of blade shows higher primary, secondary and steep tertiary creep strain rate leading to fracture at the end of 11.5 hours. Elements on disc and tip of blade show lower primary creep strain rate and very low secondary creep strain rate till the end of analysis.



**Graph 10.7.3 - Time history of creep components**

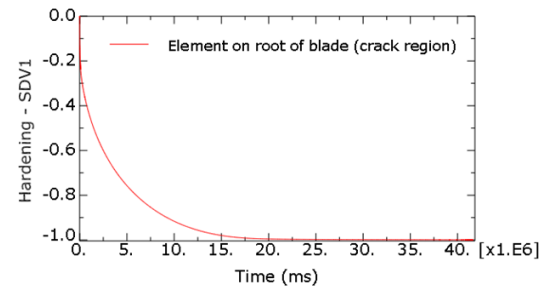
Creep strain components of element on root of blade shows high primary and secondary strain rate of radial and tangential components. Radial creep strain is tensile (towards the tip) whereas lateral & tangential creep strains are compressive along their respective axes.

## H. Hardening factor (Solution dependent variable 1)

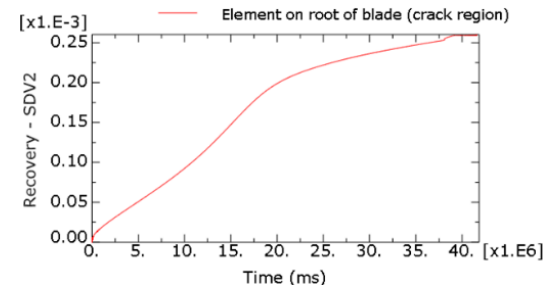
Rate of hardening decreases gradually and reaches a constant minimum in the secondary stage for an element on the root of blade. The saturation after 5 hours indicates no further resistance to creep deformation which lead to increase in creep rate and damage subsequently.

## I. Recovery factor (Solution dependent variable 2)

Rate of recovery is almost constant till tertiary stage and reduces further to minimum till crack due to stress relaxation from tertiary stage.



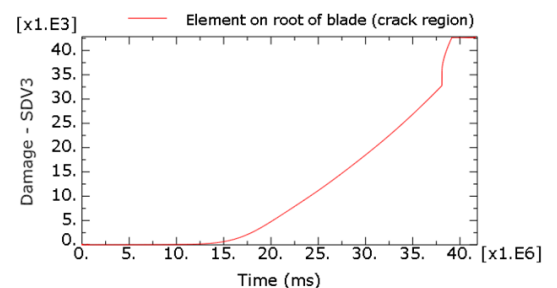
**Graph 10.7.4 - Hardening curve**



**Graph 10.7.5 - Recovery curve**

## J. Damage factor (Solution dependent variable 3)

Rate of damage is low in primary stage. After hardening variable reaches the saturation, damage variable gradually increases till tertiary stage (10.6 hrs) at uniform rate and steeply increases till fracture (11.6 hrs).



**Graph 10.7.6 - Damage curve**

### 10.7.3. CREEP LIFE ESTIMATION – CASE 2

Contour plots of Von Mises stress at the onset of damage and equivalent creep strain after damage is shown in the above figure for different rotational speeds (RPMs). Fracture strain is prescribed as 10% creep strain over which elements are deleted indicating damage and crack.

Creep life can be measured in terms of time taken for crack initiation which is the beginning of creep

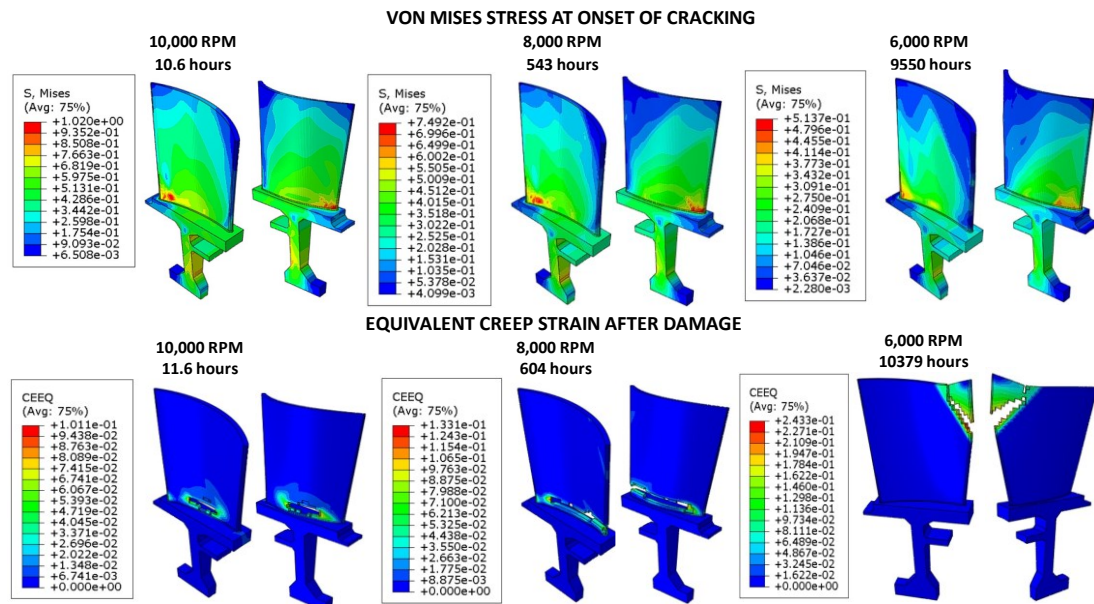
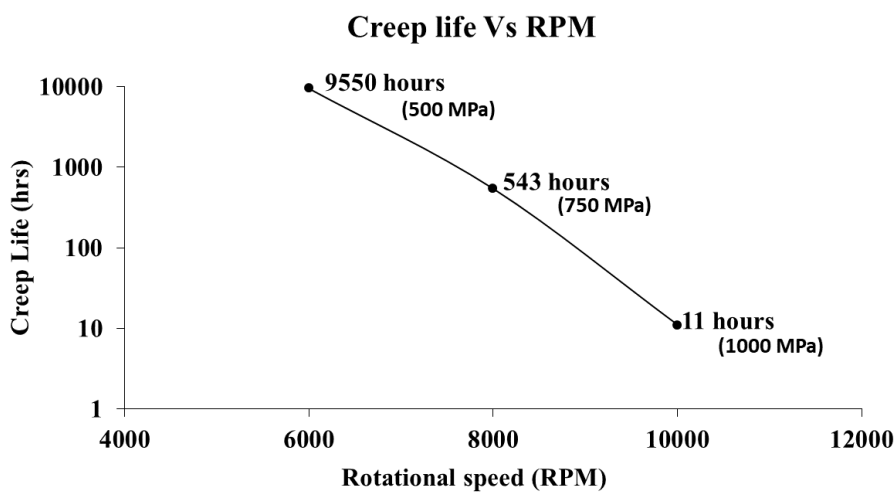


*Figure 10.7.13 - Stress & Creep strain - at different RPMs*

rupture of first element in the model Considering this, creep life of gas turbine bisk can be directly taken from the analysis results as 10.6 hours for 10,000 RPM above which cracks start to appear in the material. As stresses decrease with decrease in rotational speeds, creep life is observed to increase to 543 hours for 8,000 RPM and 9550 hours for 6,000 RPM.



*Graph 10.7.7 - Creep Life Vs RPM - Test case 7*

The results of times to onset of fracture at different RPMs are plotted. The graph shows an exponential relationship between creep life and RPM. Logarithm of creep life in hours shows a quasi-linear relationship with rotational speeds.

This is reasonable by the fact that centrifugal stresses increase with square of rotational speed and creep strain or creep life is exponentially related to the maximum stresses in the model for a given temperature distribution.

Details such as time to onset of crack, equivalent creep strain, damage, etc. can be directly read from the analysis results of Abaqus. Contour plot of creep strain & damage provides a good scope for design optimization for improved creep life.

Other life parameters like Larson – Miller parameter, Monkman Grant life for onset of tertiary, etc. can be calculated from the analysis results to project results to other load cases for design envelope & optimization studies. However, since creep analysis using Abaqus user subroutine is simpler, we can perform the analysis and obtain creep life at different load conditions and the life extrapolation parameters would not be necessary.

## **11. ACCURACY & ROBUSTNESS OF MODEL**

### **11.1. ERRORS IN CREEP PREDICTION**

Following errors (variances) are possible in our creep prediction method:

#### **A. Errors in measured creep data (Experimental errors):**

- Between variation - Differences in creep curves at same load conditions measured in different specimens & different machines
- Within variation - Error in creep measurement in a single specimen at single load condition in single machine)
- Heteroscedasticity – variation of “within variances” of different creep curves
- Autocorrelation of errors – Interdependence of variances of different Theta values on each other. Variances can be assumed to be random variables only if there is no autocorrelation.

#### **B. Errors in curve fitting & constants calculation:**

- Propagation of “within variation” from creep curve to regressed curve & Theta values.
- Autocorrelation of errors – Interdependence of variances of different Theta values on each other. Variances can be assumed to be random variables only if there is no autocorrelation

#### **C. Error Reduction Techniques**

- Regressing minimum of 4 different creep curves for each load condition using least square method minimizes ‘between variations. This requires more experimental data which is not in the scope of this project
- Determining the probabilistic model of the heteroscedasticity function (distribution function of random error that is present in different creep curves)
- Minimizing autocorrelation of errors in each creep curve through taking in account of covariance of Theta coefficients while regressing the curves to find the Theta coefficients
- Applying robust weighting scheme for regression of creep curves for Theta coefficient calculation takes care of heteroscedasticity and autocorrelation of errors.

## 11.2. ANALYSIS OF VARIANCES

Every experimental creep curve can be represented in terms of four Theta coefficients as Theta projection equation with random error (variance) for every datapoint, as below:

$$\varepsilon_n = \theta_1(1 - e^{-\theta_2 t_n}) + \theta_3(e^{\theta_4 t_n} - 1) + \vartheta_n$$

Least square method works by starting with an initial guess  $\hat{\theta}_n$  for all of the Theta coefficients and finding the variances  $\hat{\vartheta}_n$  at every datapoint and then iteratively changing the Theta coefficients values till sum of squares of variances  $\sum \vartheta_n^2$  is minimum.

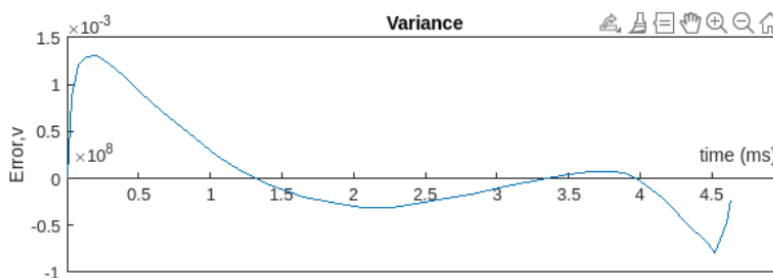
This process continues till the sum of squares of variances (SSE) reach a prescribed minimum value or forward – backward iterative function tolerance reaches a minimum or Theta values which gives a minimum SSE on a prescribed number of iterations is chosen

Since this is an overdetermined system with large number of equations (datapoints) and lesser variables (4 Theta coefficients), many sets of solutions are possible. Upon fixing one Theta value, all other 3 Theta values are changed iteratively to obtain a solution and variances are calculated at every datapoints. The procedure can be repeated by fixing a different Theta value and changing the other values. In this way, that solution set for which SSE is minimum can be considered as the final solution.

### 11.2.1. AUTOCORRELATION

Accuracy of arrived solution depends on the accuracy of initial guesses since direction of iteration depends heavily on convergence of solution for a given initial estimate. Since one of the Theta values is fixed and other Theta values are arrived iteratively in the process, there is also a strong autocorrelation of errors because of which the error function  $\vartheta_n$  cannot be considered as random error.

Autocorrelation of errors can be visualized by plotting variances with respect to time. For example, plot of variances of curve fitting the experimental creep curve at 800 degC 500 MPa condition is shown. The graph shows a low frequency oscillation pattern. This means, error at time ‘t’ and error at time ‘t-1’ can be related by an autocorrelation function.



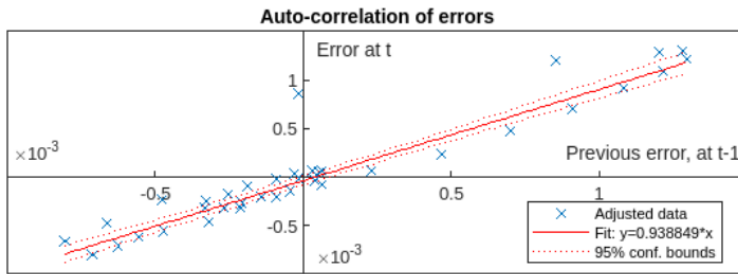
Graph 11.2.1 - Variances Vs Time

To find the nature of autocorrelation, error value at time ‘t’ is plotted against error value at its previous datapoint ‘t-1’. As shown, there exists a linear relationship between errors which progresses along all

datapoints. This is called ‘first order autocorrelation’. Second order autocorrelation can be found by plotting error value at time ‘t’ against ‘t-2’th datapoint. Similarly, ‘ $n^{th}$ ’ order autocorrelation could be present and can be modelled as,

$$\vartheta_i = \rho_1 \vartheta_{i-1} + \rho_2 \vartheta_{i-2} + \dots + \rho_n \vartheta_{n-1}$$

where,  $\rho_n$  is the  $n^{th}$  order autocorrelation coefficient



**Graph 11.2.2 - Auto-correlation of errors**

This autocorrelation of errors exists in the curve fitting process and has to be removed or minimized to treat variances as random.

### 11.3. ROBUST CURVE FITTING

Errors in regression often result in huge deviation between actual and predicted creep curves in extrapolation. In order to effectively reduce the regression errors, a robust weighting scheme was suggested by (Evans M. , 2002) and the same is adopted which takes care of heteroscedasticity and autocorrelation of errors.

Assuming first order autocorrelation in all creep curves, the autocorrelation coefficient  $\rho$  can be calculated as:

$$\rho = \frac{\sum_{i=2}^n \vartheta_i \vartheta_{i-1}}{\sum_{i=1}^n \vartheta_i^2}$$

Since error or variance at each data point has a component related to error at previous data point related by the linear autocorrelation function, subtracting this linear autocorrelation function from each data point removes the autocorrelation of errors ( $\vartheta_i - \rho \vartheta_{i-1}$ ). Resulting variance can now be treated as a random variable.

Variance of first order autocorrelated errors can be calculated as,

$$\sigma^2 = \left( \frac{1}{n-1-m} \right) \sum_{i=2}^n (\vartheta_i - \rho \vartheta_{i-1})^2$$

where, n is the number of data points

m is the number of Theta coefficients (In our case, m=4)

Correlation between the regressed Theta values can be minimized by using a sensitivity matrix  $\chi$  with 4 columns and ‘n’ rows whose elements are the derivatives of Theta projection equations with respect each Theta coefficient.

$$\chi_{m,n} = \frac{\partial}{\partial \theta_m} [\theta_1(1 - e^{-\theta_2 t_n}) + \theta_3(e^{\theta_4 t_n} - 1)]$$

Sensitivity matrix for Theta coefficients is given as,

$$\chi = \begin{bmatrix} (1 - e^{-\theta_2 t_1}) & \theta_1 t_1 (1 - e^{-\theta_2 t_1}) & (1 - e^{-\theta_4 t_1}) & \theta_3 t_1 (1 - e^{-\theta_4 t_1}) \\ (1 - e^{-\theta_2 t_2}) & \theta_1 t_2 (1 - e^{-\theta_2 t_2}) & (1 - e^{-\theta_4 t_2}) & \theta_3 t_2 (1 - e^{-\theta_4 t_2}) \\ \vdots & \vdots & \vdots & \vdots \\ (1 - e^{-\theta_2 t_n}) & \theta_1 t_n (1 - e^{-\theta_2 t_n}) & (1 - e^{-\theta_4 t_n}) & \theta_3 t_n (1 - e^{-\theta_4 t_n}) \end{bmatrix}$$

Theta values used in above matrix are the Theta values estimated from least square regression. This sensitivity matrix can be used to estimate the covariance of Theta values. Variances of the regressed Theta coefficients which is free from auto-correlation can be found using the covariance matrix as follows

$$Var(\hat{\theta}_m) = (\chi' m \chi_m)^{-1} \Omega_m (\chi' m \chi_m)^{-1}$$

Where,

$\chi_m$  -  $m^{th}$  row of the sensitivity matrix,  $\chi' m$  - transpose of  $m^{th}$  row

$\Omega_m$  -  $m^{th}$  row of autocorrelation matrix defined by (Newey W, 1987)

$$\Omega_m = \sum_{i=1}^n \vartheta_i^2 (\chi_{(i,m)} \chi'_{(i,m)}) + \sum_{l=1}^L \sum_{i=l+1}^n \left( \frac{l}{L+1} \right) \vartheta_i \vartheta_{i-1} [(\chi_{(i,m)} \chi'_{(i-1,m)}) + (\chi_{(i-1,m)} \chi'_{(i,m)})]$$

Where, L is the maximum lag which is the order of autocorrelation to be taken for consideration. L is taken here as 8.

### 11.3.1. ROBUST CURVE FITTING – MATLAB CODE

The entire mathematical procedure explained in previous section has been coded into a MATLAB program as shown below:

```

1 % Clear any previous stray data
2 clear;
3 clc;
4
5 % Experimental data - Time in 'ms' and creep strain (absolute values)
6 exp_data=[0 0.0000E+00
7 2960523.555 1.0105E-03
8
9 ...
10 ...
11
12 460065652.3 1.5150E-02
13 463618402.9 1.6213E-02];
14
15 t=exp_data(:,1);
16 e=exp_data(:,2);
17
18 % Count of datapoints
19 n=length(t);
20
21 % Plot of experimental data
22 figure(1)
23 plot(t,e)
24 title('Creep curve');
25 legend('Experimental');
26 xlabel('time (ms)');
27 ylabel('strain,epsilon')
28 hold on
29
30 % Least Square regression (Curvefit)
31 e_calc=@(Th, t) Th(1)*(1-exp(-Th(2)*t)) + Th(3)*(exp(Th(4)*t)-1);
32 Th0=[7.815E-03 5.897E-09 4.125E-08 2.653E-08];
33 options = optimoptions('lsqcurvefit','Algorithm','trust-region-reflective',...
    'MaxFunctionEvaluations',20000,'MaxIterations', 20000,'StepTolerance',1e-12);
34 lb=[0 0 0 0];
35 ub=[1 1 1 1];
36 Th_fit = lsqcurvefit(e_calc, Th0, t,e,lb,ub,options);
37 % Display regressed result of Theta coeffecients
38 format long
39 Th_fit
40
41

```

Initial guess for Theta values

Lower & Upper bound for Theta values

```

42 % Plot of regressed (calculated creep strain Vs Time) curve
43 e_calc=Th_fit(1)*(1-exp(-Th_fit(2)*t)) + Th_fit(3)*(exp(Th_fit(4)*t)-1);
44 plot(t,e_calc)
45 legend('Experimental');
46
47 % ANALYSIS OF VARIANCE (ERRORS)
48
49 for i=1:length(t)
50     t(i)=t(i);
51     %Calculation of variance (errors) in each datapoint
52     v(i,1)=[e(i)-e_calc(i)];
53     %Calculation of preceding error for auto-correlation
54     ch1(i)=1-exp(-Th_fit(2)*t(i));
55     ch2(i)=Th_fit(1)*t(i)*exp(-Th_fit(2)*t(i));
56     ch3(i)=(exp(Th_fit(4)*t(i))-1);
57     ch4(i)=Th_fit(3)*t(i)*exp(-Th_fit(4)*t(i));
58 end
59
60 % Sensitivity Matrix chi
61 chi=[ch1';ch2';ch3';ch4'];
62
63 % Plot of variance (errors) with time
64 figure(2)
65 tiledlayout(2,1)
66 nexttile
67 plot(t,v)
68 ax = gca;
69 ax.XAxisLocation = 'origin';
70 title('Variance');
71 xlabel('time (ms)');
72 ylabel('Error,v')
73
74 % Autocorrelation of errors (1st order)
75 for k=2:n
76     v_pr(k,1)=v(k-1);
77 end
78
79 % Autocorrelation coefficient, rho
80 rho=(sum(v.*v_pr))/(sumsq(v));
81 nexttile
82 mtl = fitlm(v_pr,v,'poly1',RobustOpts='bisquare');

```

OUTPUT

```

83 %Plot of autocorrelation of errors
84 plotAdded(mdl)
85 ax = gca;
86 ay = gca;
87 ax.XAxisLocation = 'origin';
88 ay.YAxisLocation = 'origin';
89 title('Auto-correlation of errors');
90 xlabel('Previous error, at t-1');
91 ylabel('Error at t')
92 rho2=mdl.Coefficients{"x1","Estimate"};
93
94 % Standard deviation of errors, sigma
95 v_ac=(v-(rho*v_pr));
96 sigma=sqrt(sumsq(v_ac)/(n-5));
97
98 % Correlation matrix of Theta coefficients, omega
99 Var=zeros(4,4);
100
101 for ii=1:n
102     X(ii,:)=1-exp(-Th_fit(2)*t(ii)),Th_fit(1)*t(ii)*exp(-Th_fit(2)*t(ii)),
103     (exp(Th_fit(4)*t(ii))-1, Th_fit(3)*t(ii)*exp(-Th_fit(4)*t(ii)));
104 end
105
106 for jj=1:n
107     S_0(jj,1)=((v(jj))^2*X(jj,:)*X(jj,:));
108 end
109
110 for l=1:8
111     for kk=(l+1):n
112         q(l)=1/9;
113         S_1(kk,1)=(q(l)*v(kk)*v(kk-1)*((X(kk,:)*X(kk-1,:)))+(X(kk-1,:)*X(kk,:)));
114     end
115 end
116
117 autocorr=sum(S_0)+sum(S_1);
118
119 format long
120 Var=(inv((X'*X))*autocorr*(inv((X'*X)))
121

```

*Figure 11.3.1 - MATLAB code for Robust curve fitting*

Inputs to the MATLAB code are the experimental creep strain – time datapoints, initial guess values and bounds for Theta coefficients. Convergence and speed of solution depends on the accuracy of initial guesses. Reasonable initial guess values can be taken from ordinary curve fitting using MATLAB CurveFit or any other literature.

Since Theta coefficients are purely exponential functions of material constants, negative values are not possible. Hence lower bounds for theta values are set as 0. Upper bounds can be given loosely based on reference values from literature.

The MATLAB code gives the regressed (calculated) Theta coefficients and variances of regressed solution as results as shown below:

**Figure 11.3.2 - Robust CurveFit output from MATLAB code**

The diagonal elements in the output covariance matrix are the variances of regressed Theta coefficients and represent how accurately these regressed values fit the curve. Large variance represents poor fit for that particular Theta value whereas smaller variance represents a good fit of that particular Theta value. These variances are used for determining weights for material constants calculation. Non-diagonal elements represent the covariance between different Theta coefficients and are not useful for our scope of work.

The same procedure is followed to get Theta coefficients and their variances of all available experimental creep curves at different stress and temperature conditions.

### 11.3.2. ROBUST CURVE FITTING - RESULTS

Output of Theta coefficients and their corresponding variances (diagonal elements of variance matrix) are summarized below:

**Table 11.3.1 - Robust curve fitting results**

			(From Matlab CurveFit Tool)				(From Matlab code - results)			
Temp (K)	Stress (GPa)	T*S (kNK/mm <sup>2</sup> )	Theta 1	Theta 2	Theta 3	Theta 4	Var(Th1)	Var(Th2)	Var(Th3)	Var(Th4)
1073	0.01	1.073E+01	4.666E-04	7.057E-13	7.275E-07	4.175E-15				
1073	0.5	5.365E+02	7.815E-03	6.250E-09	4.125E-08	2.653E-08	1.962E+06	9.204E-06	2.154E-05	2.304E+06
1073	0.55	5.902E+02	9.962E-03	1.356E-08	5.213E-08	3.350E-08	1.618E+06	1.062E-04	2.074E-05	2.652E+07
1073	0.6	6.438E+02	1.015E-02	8.238E-08	6.952E-08	1.929E-07	2.778E+05	7.650E-04	2.880E-05	7.174E+07
1073	1.2	1.288E+03	1.724E-01	1.279E-02	1.267E-05	1.567E-03				
1173	0.2	2.346E+02	2.194E-03	6.079E-09	3.606E-04	6.540E-10	5.134E+05	2.895E-06	5.095E+01	1.920E-05
1173	0.25	2.933E+02	4.194E-03	6.119E-09	3.680E-04	2.114E-09	1.710E+05	2.569E-07	1.790E+01	7.105E-05
1173	0.3	3.519E+02	9.927E-03	6.171E-09	3.758E-04	5.469E-09	8.814E+07	5.308E-03	5.979E+03	3.876E+00
1223	0.3	3.669E+02	1.056E-02	8.329E-08	3.013E-03	3.403E-08	4.563E+06	6.409E-05	3.5500E+03	4.834E-03
1223	0.4	4.892E+02	1.757E-02	2.084E-07	7.772E-03	2.021E-07	8.220E+09	5.036E+02	1.489E+07	2.797E+03
1223	0.45	5.504E+02	2.212E-02	2.329E-07	9.835E-03	4.104E-07	5.595E+12	1.895E+03	4.171E+09	2.200E+03

Theta values for 800 degC at 10 MPa & 1200 MPa arrived through linear extrapolation of  $\ln(\theta)$  as discussed in later section are also added for material constant calculation to improve range.

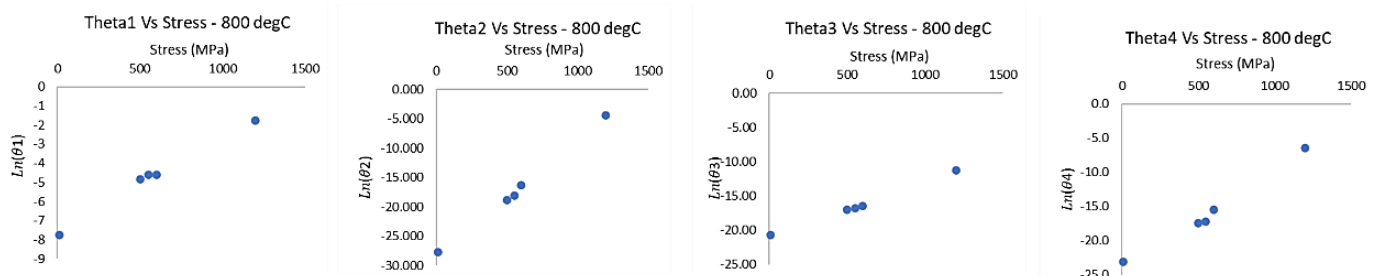
## 11.4. IMPROVING RANGE OF ANALYSIS

Since Von Mises stresses in our model can be as low as 1 MPa and high as 1400 MPa and experimental creep data is not available for such low and high stresses, regressing with a small range of input creep curves and extrapolating to very low and very high stresses results in very low or very high values (or order  $10^{-28}$ ) which may cause numerical instabilities for the Fortran code and Abaqus.

To improve the stress range of analysis with fewer experimental data, creep curves for very low & very high stresses can be generated artificially by extrapolating the Theta coefficients of known stresses. Theta coefficients and its variances for each experimental creep curve is obtained by the robust curve fitting method discussed before.

The reliability of the Theta values can be checked visually by plotting  $\ln(\theta)$  against  $\sigma$  and  $T$  for different test conditions and the graph should show linear relationship, as shown below. If any particular value outliers from the trend, robust curve fitting of that particular creep curve is revisited with initial guess of Theta values modified to follow the trend of  $\ln(\theta)$  Vs stress graph.

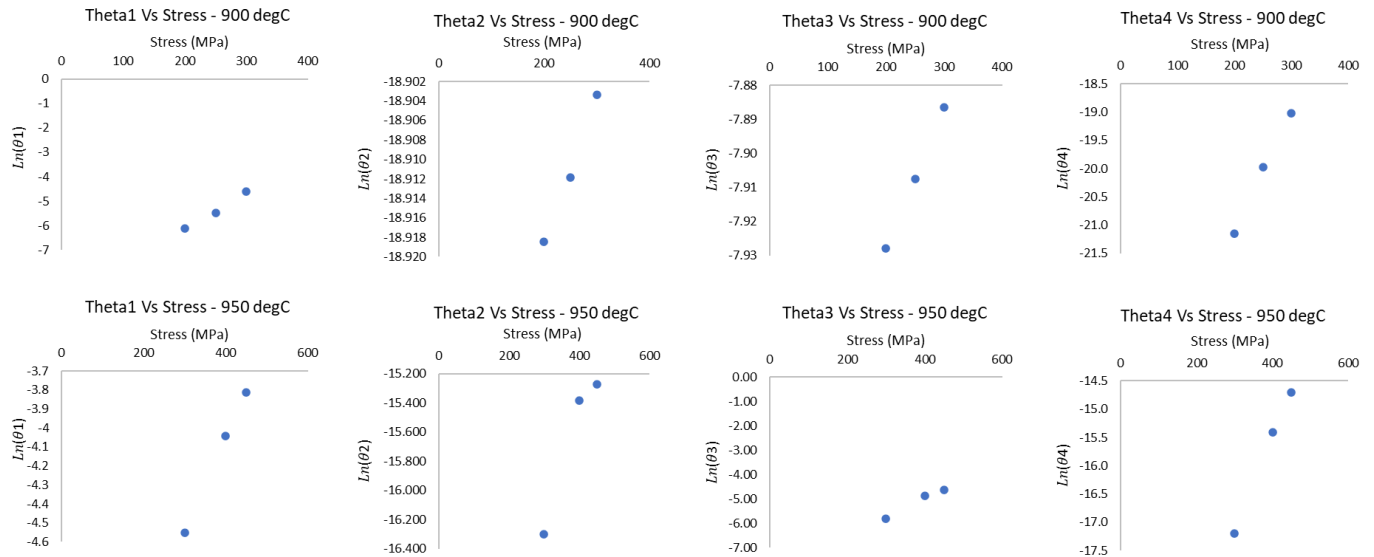
As an example, case, we have arrived the Theta values for 800 degC at 500 MPa, 550 MPa and 600 MPa stresses by regressing experimental data. But Von Mises stresses in our model can be as low as 1 MPa and high as 1400 MPa and experimental creep data is not available for such low and high stresses. Deriving material constants with Theta values for 500 MPa to 600 MPa and extrapolating it to 1400 MPa or 10 MPa can result in very huge or very low strain values which causes termination of analysis due to convergence issues in Abaqus.



Graph 11.4.1 - Theta coefficients Vs Stress at 800 degC

Using the slope of  $\ln(\theta)$  Vs  $\sigma$  curve for 500 MPa to 600 MPa stress range as shown above, we can extrapolate and find Theta values at one low and one high stress conditions (say 10 MPa & 1200 MPa). This way, we can verify that Theta values do not cross the numerical limits (or order  $10^{-28}$ ) for such low / high stresses.

It is also safe to include these artificially arrived high & low stress Theta values in our material constant calculation to improve the range of analysis and reduce numerical difficulties. Trend of Theta values for different stress and temperature conditions of our reference material MAR-247 are shown below:



**Graph 11.4.2 - Theta coefficients Vs Stress at 900 and 950 degC**

The coefficients calculated for other cases show a good log-linear relationship and can be relied upon.

## 11.5. ROBUST WEIGHTING SCHEME

Variances of the four Theta coefficients can be obtained from the diagonal elements of Covariance matrix  $Var(\hat{\theta}_m)$  calculated before. The resulting Theta coefficients and its variances are more reliable and unbiased as autocorrelation of errors and co-variances between regressed Theta coefficients has been taken care. Since this variance represents the reliability of the regressed Theta coefficient, it can be considered as a weighting parameter.

$$Var(\ln(\theta_{ij})) = \frac{Var(\theta_{ij})}{\theta_{ij}^2}$$

Since accuracy of Theta values is inversely proportional to their variances, Weights for each Theta value can be calculated as,

$$w_{ij} = \frac{\theta_{ij}^2}{Var(\theta_{ij})}$$

Expression for material constant a, b, c and d in terms of stress & temperature is as follow:

$$\ln(\theta) = a + b\sigma + cT + d\sigma T$$

Each term in the above expression can be weighted based on the inverse of variances, as calculated in the above step

$$w_{ij} \times \ln\theta_{ij} = (w_{ij} \times a) + (w_{ij} \times b\sigma_j) + (w_{ij} \times cT_j) + (w_{ij} \times d\sigma_j T_j)$$

Material constants can be calculated by the same least square regression procedure, but with the above equation with robust weights. Weights for extrapolated data sets can be taken as average of all other weights calculated from variances of respective Theta coefficients.

Weights calculated for each of 4 theta coefficients for 11 Load cases and the respective weighted  $\ln(\theta)$  values are shown in Table 11.5.1 . Weights, weighted stress, weighted temperature & weighted temp\*stress values for each Theta coefficients are calculated for 11 cases are shown in Table 11.5.2. These will be inputs for material constants calculation.

**Table 11.5.1 - Variances & weights for 11 load cases**

Temp (K)	Stress (GPa)	$T^*S$ (kN/mm <sup>2</sup> )	(From Matlab CurveFit Tool)												(From Matlab code - results)												
			Theta 1	Theta 2	Theta 3	Theta 4	Var(Th1)	Var(Th2)	Var(Th3)	Var(Th4)	weight (Th1)	weight (Th2)	weight (Th3)	weight (Th4)	w_th1*ln(Th1)	w_th2*ln(Th2)	w_th3*ln(Th3)	w_th4*ln(Th4)									
1073	0.01	1.073E+01	4.666E-04	7.057E-13	4.175E-15	4.175E-07	2.154E-05	2.304E-06	9.204E-06	2.154E-05	3.114E-11	4.244E-12	7.901E-09	3.055E-17	-1.1853E-09	-1.3857E-10	-1.37708E-15										
1073	0.5	5.365E+02	7.815E-03	6.250E-09	4.125E-08	2.653E-08	1.962E-06	1.618E-06	1.052E-04	2.074E-05	2.652E+07	6.130E-08	4.233E-12	1.310E-11	-2.8265E-10	-2.19746E-07	-7.28324E-16										
1073	0.55	5.902E+02	9.962E-03	1.356E-08	3.213E-08	3.350E-08	1.350E-08	1.929E-07	2.778E-05	7.650E-04	2.880E-05	7.174E+07	3.712E-10	8.872E-12	1.678E-08	5.190E-17	-1.7035E-09	-1.44714E-10	-2.76611E-07	-8.02378E-16							
1073	0.6	6.438E+02	1.015E-02	8.238E-08	6.952E-08	6.952E-08	1.929E-07	2.778E-05	7.650E-04	2.880E-05	7.174E+07	3.712E-10	8.872E-12	1.678E-08	5.190E-17	-1.7035E-09	-1.44714E-10	-2.76611E-07	-8.02378E-16								
1073	1.2	1.288E+03	1.724E-01	1.279E-02	1.267E-05	1.567E-03	1.279E-02	1.279E-02	1.279E-02	1.279E-02	1.279E-02	1.279E-02	1.279E-02	1.279E-02	1.279E-02	1.279E-02	1.279E-02	1.279E-02	1.279E-02	1.279E-02	1.279E-02	1.279E-02	1.279E-02	1.279E-02	1.279E-02		
1173	0.2	2.346E+02	2.194E-03	6.079E-09	3.606E-04	5.134E-05	2.895E-06	5.095E-01	1.920E-05	9.377E-12	1.2766E-11	2.552E-09	2.227E-14	5.7405E-11	-2.41469E-10	-2.02326E-08	-4.71026E-13										
1173	0.25	2.933E+02	4.194E-03	6.1119E-09	3.658E-04	2.114E-09	1.7110E-05	2.569E-07	1.790E+01	7.105E-05	1.029E-10	1.457E-10	7.567E-09	6.290E-14	-5.63159E-10	-2.75597E-09	-5.98376E-08	-1.25647E-12									
1173	0.3	3.519E+02	9.927E-03	6.1711E-09	3.758E-04	5.469E-09	8.814E-07	5.308E-03	5.979E+03	3.876E+00	1.1138E-12	7.175E-15	2.362E-11	7.717E-18	-5.15712E-12	-1.35630E-13	-1.86273E-10	-1.46815E-16									
1223	0.3	3.669E+02	1.056E-02	8.329E-08	3.013E-03	3.403E-03	4.563E-06	6.409E-05	3.550E+03	4.834E-03	2.445E-11	1.082E-10	2.558E-09	2.396E-13	-1.11246E-10	-1.7653E-09	-1.48458E-08	-4.11937E-12									
1223	0.4	4.892E+02	1.757E-02	2.084E-07	7.772E-03	2.021E-07	8.220E-09	5.036E+02	1.489E+07	2.797E+03	3.755E-14	8.624E-17	4.056E-12	1.460E-17	-1.51765E-13	-1.32671E-15	-1.97013E-11	-2.25083E-16									
1223	0.45	5.504E+02	2.212E-02	2.329E-07	9.8335E-03	4.104E-07	5.595E+12	1.895E+03	4.171E+09	2.200E+03	8.747E-17	2.861E-17	2.319E-14	7.654E-17	-3.33373E-16	-4.37000E-16	-1.07168E-13	-1.12557E-15									

**Table 11.5.2 - Weights, weighted stress & temperature for 11 load cases**

Temp (K)	Stress (GPa)	$T^*S$ (kN/mm <sup>2</sup> )	Theta 1				Theta 2				Theta 3				Theta 4											
			Weighted Stress (Th1) (GPa)	Weighted Temp (Th1) (K)	Weighted $T^*S$ (kN/mm <sup>2</sup> )	Weighted Temp (Th2) (GPa)	Weighted Stress (Th2) (GPa)	Weighted Temp (Th3) (K)	Weighted $T^*S$ (kN/mm <sup>2</sup> )	Weighted Temp (Th3) (GPa)	Weighted Stress (Th3) (GPa)	Weighted Temp (Th4) (K)	Weighted $T^*S$ (kN/mm <sup>2</sup> )	Weighted Temp (Th4) (GPa)	Weighted Stress (Th4) (GPa)	Weighted Temp (K)	Weighted $T^*S$ (kN/mm <sup>2</sup> )									
1073	0.01	1.073E+01	1.545E-10	1.545E-12	1.658E-07	1.658E-09	4.948E-12	4.948E-14	5.310E-09	5.310E-11	1.260E-08	1.260E-10	1.352E-05	1.352E-07	4.159E-17	4.159E-19	4.4635E-14	4.4635E-16								
1073	0.5	5.365E+02	3.114E-11	1.557E-11	3.341E-08	1.670E-08	4.244E-12	4.244E-12	4.554E-09	2.277E-09	7.901E-09	3.951E-09	8.478E-06	4.239E-06	3.055E-17	1.5258E-17	3.2785E-14	1.6395E-14								
1073	0.55	5.902E+02	6.133E-11	3.373E-11	6.580E-08	3.619E-08	1.730E-12	9.514E-13	1.856E-09	1.021E-09	1.310E-08	7.207E-09	1.406E-05	7.733E-06	4.233E-17	2.3285E-17	4.542E-14	2.4993E-14								
1073	0.6	6.438E+02	3.712E-10	2.227E-10	3.983E-07	2.390E-07	8.872E-12	5.323E-12	9.519E-09	5.712E-09	1.678E-08	1.007E-08	1.801E-05	1.080E-05	5.190E-17	3.114E-17	5.569E-14	3.341E-14								
1073	1.2	1.288E+03	1.545E-10	1.854E-10	1.658E-07	1.990E-07	4.948E-12	5.938E-12	5.310E-09	6.372E-09	5.104E-10	2.994E-09	5.104E-06	5.987E-07	4.159E-17	4.991E-17	4.463E-14	5.355E-14								
1173	0.2	2.346E+02	9.377E-12	1.875E-12	2.100E-08	2.200E-09	1.276E-11	2.553E-12	1.497E-08	2.994E-09	2.552E-09	5.104E-10	2.994E-06	2.227E-14	4.455E-15	2.613E-11	5.225E-12									
1173	0.25	2.933E+02	1.029E-10	2.572E-11	1.207E-07	3.017E-08	1.457E-10	3.643E-11	1.709E-07	4.273E-08	7.567E-09	1.892E-09	8.876E-06	2.219E-06	6.290E-14	1.573E-14	7.379E-11	1.845E-11								
1173	0.3	3.519E+02	1.118E-12	3.354E-13	1.312E-09	3.935E-10	7.175E-15	2.152E-15	8.416E-12	2.525E-12	2.362E-11	7.086E-12	2.771E-08	8.312E-09	7.717E-18	2.315E-18	9.052E-15	2.716E-15								
1223	0.3	3.669E+02	2.445E-11	7.334E-12	2.990E-08	8.970E-09	1.082E-10	3.247E-11	1.324E-07	3.972E-08	2.558E-09	7.673E-10	3.128E-06	9.384E-07	2.396E-13	7.187E-14	2.930E-10	8.789E-11								
1223	0.4	4.892E+02	3.755E-14	1.502E-14	4.593E-11	1.837E-11	8.624E-17	3.450E-17	1.055E-13	4.219E-14	4.056E-12	1.622E-12	4.961E-09	1.984E-09	1.460E-17	5.841E-18	1.786E-14	7.143E-15								
1223	0.45	5.504E+02	8.747E-17	3.936E-17	1.070E-13	4.814E-14	2.861E-17	1.288E-17	3.499E-14	1.575E-14	2.319E-14	1.043E-14	2.836E-11	1.276E-11	7.654E-17	3.444E-17	9.360E-14	4.212E-14								

### 11.5.1. ROBUST WEIGHTING – MATLAB CODE

A MATLAB code is developed for estimating material constants using Robust weights using the procedure described above.

**Figure 11.5.1 - MATLAB code for Robust weighted regression**

### 11.5.2. ROBUST WEIGHTING - RESULTS

16 material constant values calculated by regressing weighted values of 11 load cases using the MATLAB code are presented below:

**Table 11.5.3 - Material constants - Robust weighted**

Material MAR-M247 EA				(From Matlab CurveFit Tool)				(From Matlab code - results)				
Temp (deg C)	Stress (N/mm <sup>2</sup> )	Temp (K)	Stress (GPa)	T*S (kN/mm <sup>2</sup> )	Theta 1	Theta 2	Theta 3	Theta 4	Var(Th1)	Var(Th2)	Var(Th3)	Var(Th4)
800	10	1073	0.01	1.073E+01	4.666E-04	7.057E-13	7.275E-07	4.175E-15				
800	500	1073	0.5	5.365E+02	7.815E-03	6.250E-09	4.125E-08	2.653E-08	1.962E+06	9.204E-06	2.154E-05	2.304E+06
800	550	1073	0.55	5.902E+02	9.962E-03	1.356E-08	5.213E-08	3.350E-08	1.618E+06	1.062E-04	2.074E-05	2.652E+07
800	600	1073	0.6	6.438E+02	1.015E-02	8.238E-08	6.952E-08	1.929E-07	2.778E+05	7.650E-04	2.880E-05	7.174E+07
800	1200	1073	1.2	1.288E+03	1.724E-01	1.279E-02	1.267E-05	1.567E-03				
900	200	1173	0.2	2.346E+02	2.194E-03	6.079E-06	3.606E-04	6.540E-10	5.134E+05	2.895E-06	5.095E+01	1.920E-05
900	250	1173	0.25	2.933E+02	4.194E-03	6.119E-09	3.680E-04	2.114E-09	1.710E+05	2.569E-07	1.790E+01	7.105E-05
900	300	1173	0.3	3.519E+02	9.927E-03	6.171E-09	3.758E-04	5.469E-09	8.814E+07	5.308E-03	5.979E+03	3.876E+00
950	300	1223	0.3	3.669E+02	1.056E-02	8.329E-08	3.013E-03	3.403E-08	4.563E+06	6.409E-05	3.550E+03	4.834E-03
950	400	1223	0.4	4.892E+02	1.757E-02	2.084E-07	7.772E-03	2.021E-07	8.220E+09	5.036E+02	1.489E+07	2.797E+03
950	450	1223	0.45	5.504E+02	2.212E-02	2.329E-07	9.835E-03	4.104E-07	4.595E+12	1.895E+03	4.171E+09	2.200E+03
a				-1.2238E+01	-1.0944E+02	-1.1486E+02	-5.1069E+01	-	mm <sup>2</sup> kN <sup>-1</sup>			
b				-1.4702E+01	1.3953E+02	5.7466E+01	-1.8660E+01	mm <sup>2</sup> kN <sup>-1</sup>	K <sup>1</sup>			
c				4.3243E-03	7.5217E-02	9.1503E-02	2.1483E-02	K <sup>1</sup>	mm <sup>2</sup> kN <sup>-1</sup> K <sup>-1</sup>			
d				1.8322E-02	-1.1110E-01	-5.1127E-02	3.5991E-02	mm <sup>2</sup> kN <sup>-1</sup> K <sup>-1</sup>				

## 11.6. ACCURACY – MATERIAL CONSTANTS

To check the accuracy of material constants derived by different methods, % deviation between the input Theta coefficients from curve-fitting and Theta coefficients calculated from material constants are studied

### 11.6.1. ACCURACY – UNIQUE SOLUTION

Result of comparison of curve fitted Theta values and Theta values calculated from material constants with unique solution method (matrix inversion) is summarized below:

*Table 11.6.1 - Accuracy - Unique solution*

Temp (deg C)	Stress (MPa)	Theta 1	Theta 1	Theta 3	Theta 4	Deviation % in calculated Theta values from input Theta values			
800	500	3.677E-03	8.455E-06	1.848E-02	5.053E-07	76%	25%	-9511131%	4512%
800	550	5.142E-03	3.673E-05	2.216E-03	5.440E-06	-0.00000002%	0.00000043%	0.00000005%	0.00000022%
800	600	7.190E-03	1.596E-04	2.659E-04	5.857E-05	-0.00000004%	0.00000002%	0.00000002%	-0.00000001%
900	200	5.216E-03	4.297E-06	1.025E-03	8.172E-07	10856%	10244713%	-20788871%	333%
900	250	3.966E-03	1.436E-05	2.217E-03	1.466E-06	105%	7972079%	-28897949%	147%
900	300	3.015E-03	4.800E-05	4.795E-03	2.629E-06	-0.00000040%	-0.00000001%	-0.00000004%	-0.00000016%
950	300	5.339E-03	2.158E-03	3.515E-05	6.949E-04	13%	-460%	14993%	-2304%
950	400	1.678E-03	1.855E-02	2.964E-03	3.724E-04	1175%	-11221%	152%	-84%
950	450	9.411E-04	5.437E-02	2.722E-02	2.726E-04	0.00000002%	0.00000002%	0.00000002%	-0.00000004%

The results show a very good accuracy (deviation %  $\sim 10^{-8}$ ) at 4 input conditions as highlighted, but large deviation % (order of  $10^2 - 10^8$ ) at interpolated / extrapolated conditions.

This method is suitable only for analysis at highlighted 4 input test conditions and the applications can be creep test simulation, piping or structural simulation with uniform stresses.

Since the results shown large deviation for interpolated or extrapolated conditions, using Unique solution material constants will give very inaccurate creep results for Turbine blade applications as a large range of stress & temperature values are observed across different areas of a turbine blade.

### 11.6.2. ACCURACY – LEAST SQUARE SOLUTION

Result of comparison of curve fitted Theta values and Theta values calculated from material constants using Least square regression with 9 experimental creep curves & 2 extrapolated creep curves is summarized below:

*Table 11.6.2 - Accuracy - Least square solution*

Temp (K)	Stress (GPa)	T*S (kNK/mm <sup>2</sup> )	Theta 1	Theta 2	Theta 3	Theta 4	Deviation % in calculated Theta values from input Theta values			
1073	0.01	1.0730E+01	1.264E-03	2.123E-10	6.385E-05	5.971E-12	-171%	-29983%	-8676%	-142901%
1073	0.5	5.3650E+02	4.131E-03	1.240E-08	3.543E-05	1.894E-09	43%	20%	-3989%	962%
1073	0.55	5.9015E+02	4.662E-03	1.877E-08	3.336E-05	3.409E-09	10%	96%	6543%	60%
1073	0.6	6.4380E+02	5.261E-03	2.843E-08	3.142E-05	6.135E-09	37%	461%	715%	864%
1073	1.2	1.2876E+03	2.244E-02	4.136E-06	1.528E-05	7.090E-06	-30%	-223%	-316%	-728%
1173	0.2	2.3460E+02	2.843E-03	4.027E-08	1.284E-03	2.450E-09	-30%	61%	-256%	-275%
1173	0.25	2.9325E+02	2.984E-03	6.496E-08	1.401E-03	3.978E-09	-174%	-53%	-30%	-149%
1173	0.3	3.5190E+02	3.133E-03	1.048E-07	1.529E-03	6.458E-09	-4%	-118%	214%	-146%
1223	0.3	3.6690E+02	3.474E-03	6.985E-07	8.903E-03	3.863E-08	75%	-83%	-69%	-33%
1223	0.4	4.8920E+02	3.561E-03	1.935E-06	1.227E-02	9.183E-08	405%	-920%	-44%	111%
1223	0.45	5.5035E+02	3.605E-03	3.221E-06	1.441E-02	1.416E-07	-284%	1595%	89%	92%

The table shows that least square solution constants are slightly less accurate at all stress or temperature values than unique solution constants with average deviation % less than  $10^4$  except at first test condition (800degC - 10 MPa) whose Theta values are extrapolated and added for better range of analysis.

But the deviation in interpolation & extrapolation are relatively smaller than unique solution constants.

Least square solution constants are suitable for turbine blades with reasonable accuracy at wider test conditions. Accuracy of creep prediction can be further improved by robust weighting.

### 11.6.3. ACCURACY – ROBUST SOLUTION

Result of comparison of curve fitted Theta values and Theta values calculated from material constants using Robust weighted least square regression with 9 experimental creep curves & 2 extrapolated creep curves is summarized below:

*Table 11.6.3 - Accuracy - Robust weighting*

Temp (deg C)	Stress (GPa)	Theta 1	Theta 2	Theta 3	Theta 4	Deviation % in calculated Theta values from input Theta values			
800	0.01	5.2679E-04	4.0699E-13	5.8496E-08	8.2984E-13	-13%	73%	1144%	-19774%
800	0.5	5.9780E-03	8.6050E-09	2.0980E-07	1.4656E-08	31%	-38%	-409%	81%
800	0.55	7.6596E-03	2.3774E-08	2.3900E-07	3.9754E-08	30%	-75%	-358%	-19%
800	0.6	9.8141E-03	6.5681E-08	2.7227E-07	1.0783E-07	3%	25%	-292%	79%
800	1.2	1.9213E-01	1.2988E-02	1.3008E-06	1.7107E-02	-11%	-2%	874%	-992%
900	0.2	3.0035E-03	3.8758E-09	3.2513E-04	6.4777E-10	-37%	57%	11%	1%
900	0.25	4.2176E-03	6.1442E-09	2.8683E-04	2.1035E-09	-1%	0%	28%	0%
900	0.3	5.9223E-03	9.7401E-09	2.5305E-04	6.8306E-09	68%	-58%	49%	-25%
950	0.3	9.6772E-03	7.9096E-08	1.1405E-02	3.4310E-08	9%	5%	-278%	-1%
950	0.4	2.0912E-02	1.1406E-07	6.8747E-03	4.3313E-07	-19%	83%	13%	-114%
950	0.45	3.0741E-02	1.3696E-07	5.3373E-03	1.5389E-06	-39%	70%	84%	-275%

The results show slightly lesser accuracy than unique solution constants but better accuracy than ordinary least square regression solution constants with average deviation % less than  $10^3$  in all cases except at first test condition (800degC - 10 MPa) whose Theta values are extrapolated and added for better range of analysis.

Robust weighted Least square solution constants are best suitable for turbine blades with reasonable accuracy at all test conditions and interpolated / extrapolated range.

### 11.7. ACCURACY – CREEP PREDICTION

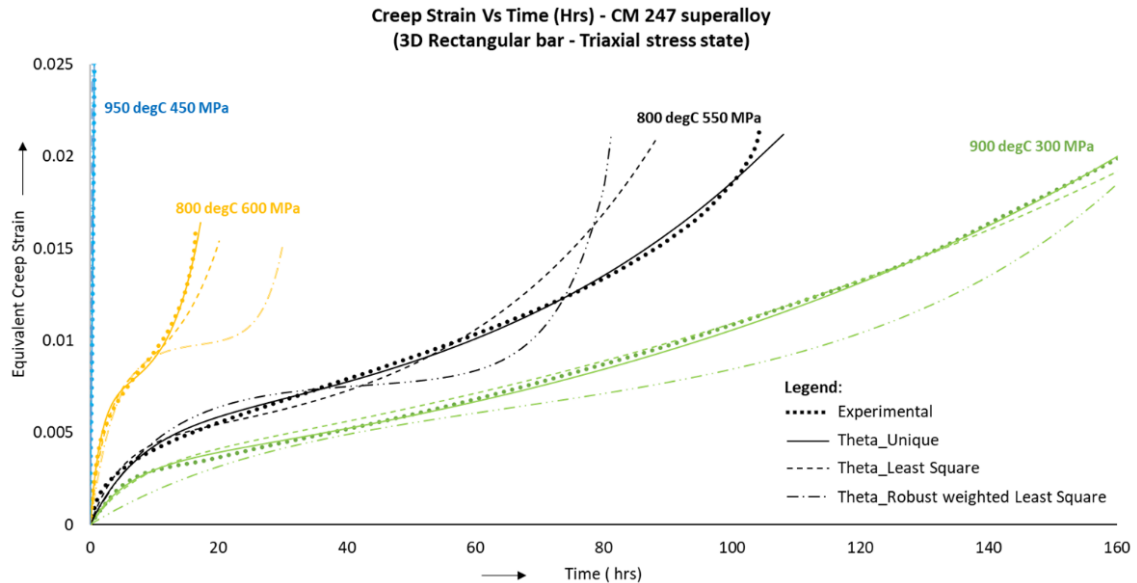
Accuracy of the creep prediction model is checked by comparing the analysis results with experimental data. Since we are considering only certain load conditions as inputs in our material constants calculation, the accuracy of results may decrease at other interpolated / extrapolated load conditions.

The load conditions considered as inputs for material constant calculation are referred to as “design points” and the results at other load conditions are calculated by the subroutine using Theta projection method. Accuracy of the results obtained from subroutine through analysis in Abaqus at design points, interpolated and extrapolated loads are discussed here.

#### 11.7.2. ACCURACY AT DESIGN POINTS

Abaqus results are matching the experimental creep curves taken for material constants calculation

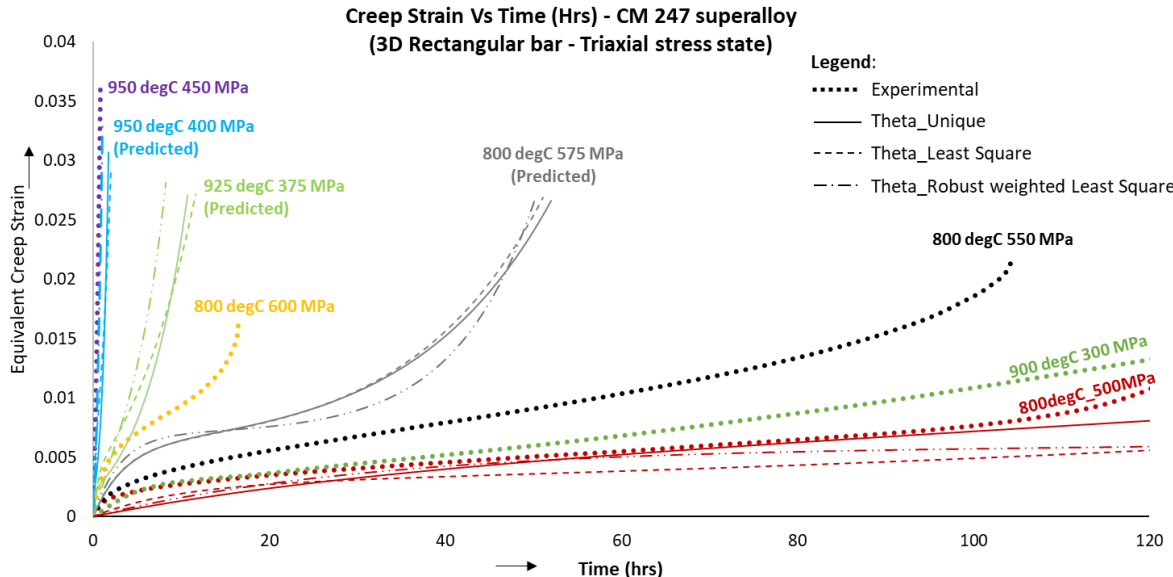
- Unique solution gives the best accurate results at 4 design points taken for material constants calculation, till tertiary stage.
- Ordinary least square & Robust weighted least square solutions vary by ~10-20 hours from experimental data



*Graph 11.7.1 - Accuracy at design points*

### 11.7.3. ACCURACY AT INTERPOLATED LOADS

- Interpolation results are satisfactory, but not very accurate as at design points
- For small interpolation ( $\sim 50$  MPa), unique solution results are satisfactory. Ordinary & robust least square results are also appreciable

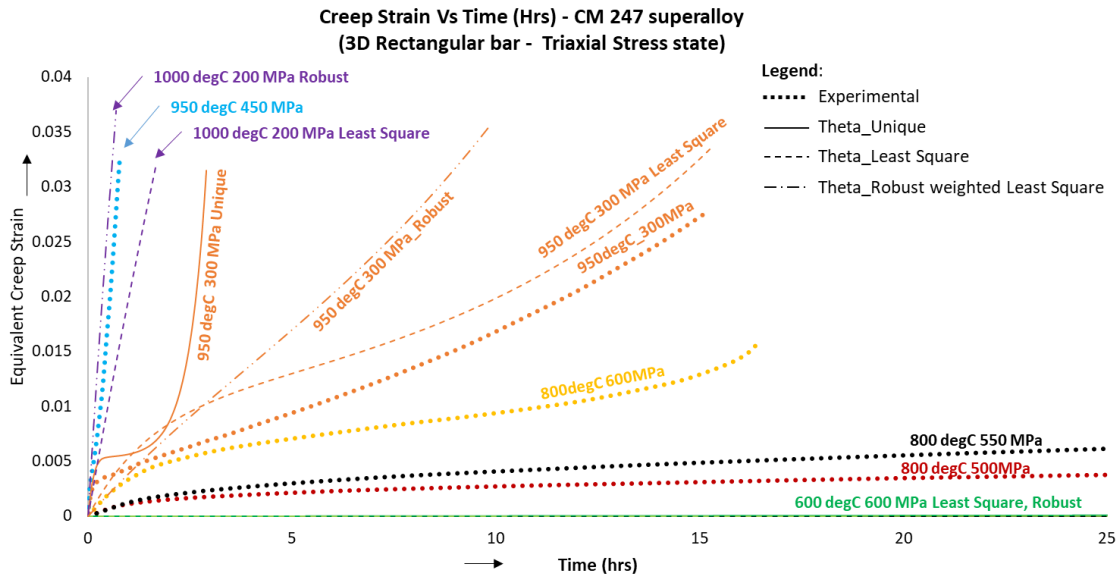


*Graph 11.7.2 - Accuracy at interpolated loads*

### 11.7.4. ACCURACY AT EXTRAPOLATED LOADS

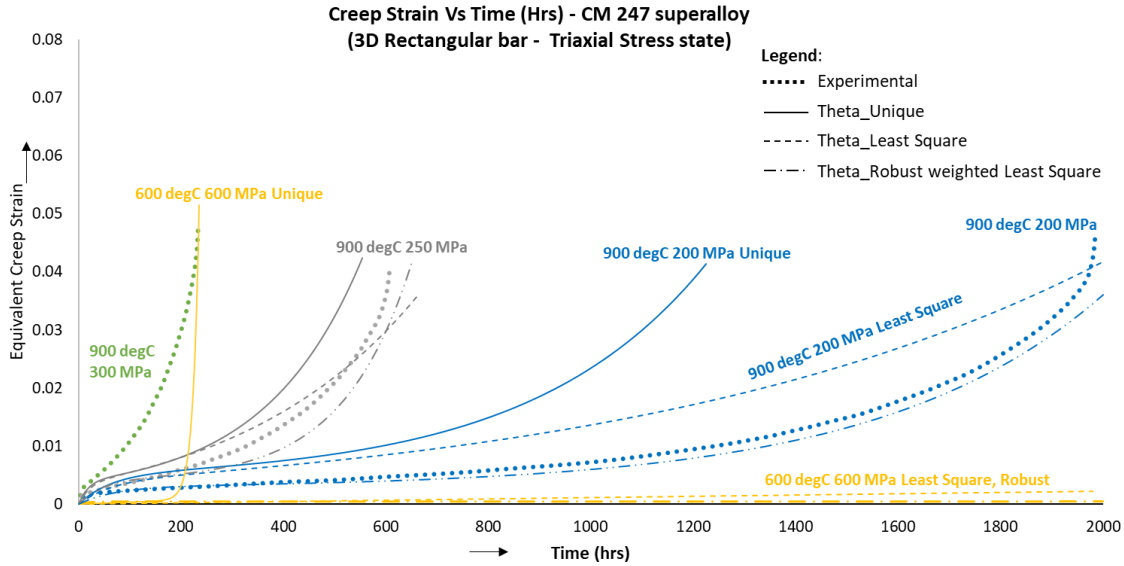
Accuracy of subroutine at load conditions extrapolated out of load range taken as input in material constant calculation depends on analysis time and magnitude of strain. Since error is cumulative and the Theta values are exponentially related to the material constants, small error in material constants result in very large deviation in extrapolation at higher and lower stress / temperature conditions. This errors also grows in time.

For smaller strain and smaller analysis times, results of both ordinary and robust weighted least square regressed constants are satisfactory whereas unique solution results are very poor. Unique and least square constants are giving different results with least square solution being more accurate.



**Graph 11.7.3 - Accuracy for short time extrapolation**

Since error increases with time and accumulates with strain, accuracy of subroutine for larger creep time and strain is found to be less as shown below:



**Graph 11.7.4 - Accuracy for long time extrapolation**

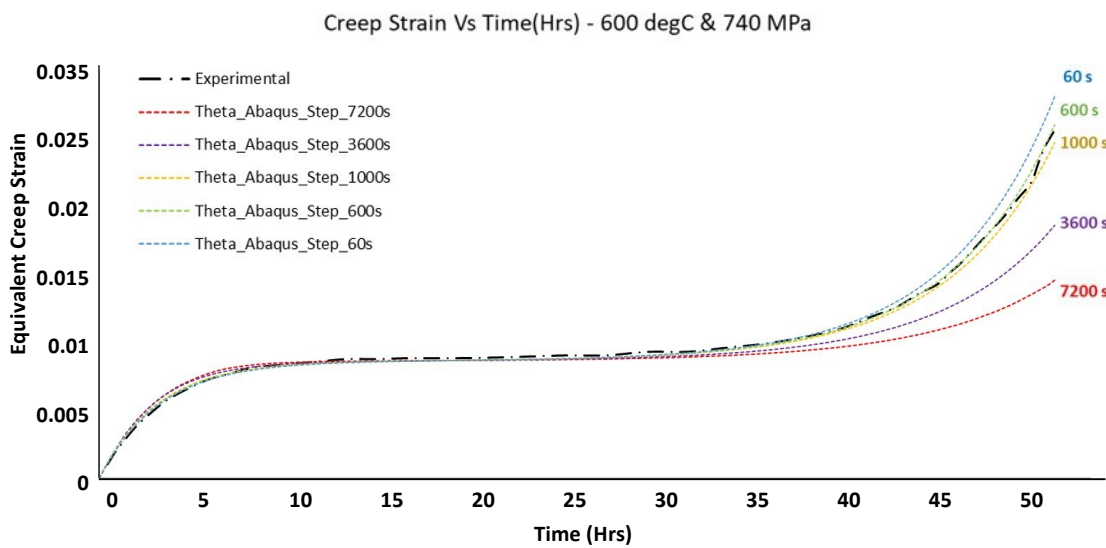
- Unique solution results are very inaccurate (order of magnitude of 100-1000 hours) for long time extrapolation
- Loads taken for constant calculation is 800–900°C and 300 – 600 MPa. The results of both unique & least square are far apart & inaccurate for all the test cases far from our design loads
- Robust least square method gives consistently satisfactory results for both long time as well as long range extrapolation

## 11.8. EFFECT OF TIME INCREMENT ON ACCURACY

There is always a small error in Theta values calculated from material constants and the actual theta values computed by curve fitting the creep curves (experimental). This initial error in creep computation grows with time.

A sample analysis with same boundary conditions but different time increments is done on a 2D rectangular plate with GH-4169 material and the results are as follows:

- Higher time increments give lower accuracy – due to progressive (multiplication) effect of initial error
- Lower time increments also gives slightly lower accuracy due to higher number of increments required (cumulation of error)



Graph 11.8.1 - Effect of time increment size on accuracy

It is observed from the sample analysis that a time increment of 600 seconds gives the results very close to the experimental results and the error grows with any higher or lower time increment. Hence, the optimum time increment size for a given analysis should be calculated by trial-and-error method before justifying the accuracy of the results.

## IX. FUTURE WORK

As the developed Fortran code satisfies all the objectives for the scope defined for the project, the following are the possible extensions that could be planned.

- Creep analysis of gas turbine blade under actual working conditions with
  - ✓ Actual temperature distribution with cooling (coupled thermo-mechanical creep)
  - ✓ Aerodynamic pressure loads with RPM loads to be ramped as per actual speed profiles to model recovery during creep relaxation

- Effect of thermal barrier coatings on creep damage & the reverse effect of creep on coating life could be studied
- Effect of Creep – Fatigue interaction has to be studied and the possibility of integrating creep damage variable with fatigue damage variable has to be explored to predict the combined effect of creep and fatigue.
- The project could be extended to model the effect of pre-strain and presence of initial damage on blades to effectively evaluate the remaining useful life fraction.

## X. CONCLUSION

This research work presented in this thesis is an attempt to address the inadequacy of existing CAE tools in modelling all stages of creep and visualizing damage. Different interpretations of advanced continuum damage mechanics methods were studied and Theta projection method was selected. The constitutive equations given by (R.W.Evans, 1984) prove useful to model creep in terms of the internal variables hardening, recovery and damage. With all these insights, a new user subroutine was developed and tested for a variety of test cases for validation of results.

When the results of creep analysis done using the subroutine are compared with experimental data, it is apparent that creep prediction of gas turbine components could be done with reasonable accuracy using robust weighted least square regressed material constants through the subroutine. When compared to the existing built-in creep models in CAE tools, the proposed method shows the following advantages:

- All Stages of Creep are modelled
- Internal state variables Hardening, Recovery (Softening) and Damage are visualized
- Creep fracture strain, Time to creep fracture and onset of cracking data are visualized
- Visualize critical regions of Creep
- Reliable results at interpolated and extrapolated stress conditions

Damage visualization also offers a good insight on understanding crack initiation and propagation. With this, we can observe high creep areas in the model and improve the design and working load envelope of gas turbine components for best creep life at the design stage itself.

## XI. REFERENCES

1. Agustín Jose Torroba, O. K.-M. (2014). Investment casting of nozzle guide vanes from nickel-based superalloys. *Integrating Materials and Manufacturing Innovation*.
2. Bong Min Song, J. Y. (2007). Creep model based on Theta projection and Omega method for predicting creep behaviour of alloy 718. *Trans Tech Publications*.
3. C.M.Omprakash, A. K. (2013). Prediction of creep curves of high temperature alloys using Theta projection concept. *6th International conference on creep, fatigue and creep-fatigue interaction*.
4. Calvin M. Stewart, A. P. (2010). Analytical Method To Determine The Tertiary Creep Damage Constants Of The Kachanov-Rabotnov Constitutive Model. *Proceedings of the ASME 2010 International Mechanical Engineering Congress & Exposition, IMECE2010*. Vancouver, British Columbia, Canada: ASME.
5. D. L. May, A. P. (2013). The application of the norton-bailey law for creep prediction through power law regression. *Turbine Technical Conference and Exposition*. ASME Turbo Expo 2013.
6. D.R. Hayhurst\*, F. V.-T. (2003). Constitutive equations for time independent plasticity and creep of 316 stainless steel at 550 8C. *International Journal of Pressure Vessels and Piping*, 97-109.
7. Domen Sergua, M. F. (2010). Creep Damage Calculation for Thermo Mechanical Fatigue. *Journal of Mechanical Engineering*.
8. Donghuan Liu, H. L. (2014). Numerical Simulation of Creep Damage and Life Prediction of Superalloy Turbine Blade. *Mathematical Problems in Engineering, Volume 2015 Article ID: 732502*.
9. Evans, M. (2002). The application of a new and robust weighting scheme for establishing theta projection parameters to 1CrMoV rotor steel. *The Journal of Strain Analysis for Engineering Design 2002 37: 169*.
10. Evans, R. W. (1982). *Recent advances in creep and fracture of engineering materials and structures*. Swansea: Pineridge Press.
11. Evans, R. W. (1988). Statistical scatter and variability of creep property estimates in Theta projection method. *Materials Science and Technology, Institute of Metals*.
12. Evans, R. W., & Wilshire, B. (1985). *Creep of metals and alloys*.
13. Evans.M. (2011). A new statistical framework for the determination of safe creep life using Theta projection technique. *J Mater Sci*.
14. Gifkins, R. C. (2006). Diffusional Creep Mechanisms. *Journal of the American Ceramic Society 51(2)*, 69 - 72.
15. Harrison, D. W. (2007). Application of the Theta projection method to creep. *Abaqus UK Regional User Meeting*.

16. J.P. Rouse, W. S. (2013). Comparative assessment of several creep damage models for use in life prediction. *International Journal of Pressure Vessels and Piping*, 81-87.
17. K. Harris, G. E. (1984). MAR M 247 Derivatives - CM 247 LC DS alloys, CMSX Single crystal alloys properties and performance. *Fifth International Symposium on Superalloys*. The Metallurgical Society of AIME.
18. Li, Y. D. (1996). A new creep lifetime prediction method: the C-project concept . *Int. J. Pres. Vrs. d Piping* 69, 161-167.
19. M.I.M Ahmad, J. S. (2011). Characterization of creep behavior using power law model in copper alloy. *Journal of Mechanical Engineering and Sciences*.
20. Marie Kvapilova, J. D. (2018). Creep behaviour and life assessment of a cast nickel – base superalloy MAR – M247. *De Gruyter*, 592.
21. Ming Song, T. X. (2018). A modified theta projection model for the creep behaviour of creep-resistant steel. *International Journal of Pressure Vessel and Piping*.
22. Mingchen Huoa, Y. Y. (2021). A new creep constitutive relationship for high temperature alloys. *International Journal of Mechanical Sciences* 194.
23. Mohammad Shafinul Haque, C. M. (2019). *International Journal of Pressure Vessels and Piping*, 1-9.
24. Newey W, W. K. (1987). A simple positive semi-definite heteroscedasticity and autocorrelation consistent covariance matrix. *Econometrica*, 55.
25. Peng Yu, W. M. (2020). A modified Theta projection model for creep behavior of RPV steel 16MND5. *Journal of Material Science & Technology*.
26. R Rajendran, V. P. (2012). Dynamic elastic properties of aero-engine metallic isotropic materials. *Journal of Materials: Design and applications*.
27. R.W.Evans. (1984). A constitutive model for the high-temperature creep of particle hardened alloys based on the Theta projection method. *The Royal Society*.
28. Ramkumar Oruganti, M. K. (2012). A New Approach To Modeling Of Creep In Superalloys. *Superalloys 2012: 12th International Symposium on Superalloys*. TMS (The Minerals, Metals & Materials Society).
29. S G R Brown, R. W. (1984). Creep Strain and Creep life prediction for the Cast Nickel based superalloy IN-100. *Materials Science and Engineering*.
30. Seongin Moon, J.-M. K. (2021). Modified Theta projection model-based constant-stress creep curve for alloy 690 Steam generator tube material. *Nuclear Engineering and Technology*.

31. Tom H. Hyde, B. S. (2013). Analysis and Design of a Small, Two-Bar Creep Test Specimen. *J. Eng. Mater. Technol.* volume 135, issue 4, 135(4).
32. Veronica Gray, M. W. (2015). Development and Assessment of a New Empirical Model for Predicting Full Creep Curves. *Materials*.
33. W David Day, A. P. (2014). Life Fraction Hardening applied to a modified Theta Projection Creep model for a Nickel based Superalloy. *Turbine Technical Conference and Exposition - Proceedings of ASME Turbo Expo 2014*. Dusseldorf, Germany: ASME.
34. William Harrison, M. W. (2017). Advanced Methods for Creep in Engineering Design. In M. S. Tomasz Tanski, *Creep* (pp. 221-238). IntechOpen.
35. Xiao-feng Guo, (2022). An improved creep damage mechanics model and its application to evaluate creep strain design codes for hot outlet manifold in steam reformer furnace. *International Journal of Pressure Vessels and Piping*.
36. DS Simulia - Abaqus documentation
37. MATLAB documentation